M-PM-G7

PROTEIN INTERACTIONS WITH VISCOUS COSOLVENTS : LIGAND ESCAPE RATE *versus* ROTATIONAL BROWNIAN DIFFUSION

((D. Lavalette, C. Tetreau, and M. Tourbez))
INSERM U350,Institut Curie, 91405-Orsay France.

The rate of ligand escape from respiratory proteins such as Myoglobin or Hemerythrin is characterized by a reciprocal power-law dependence on viscosity ($k \sim \eta^{-p}$, with $p < 1$), at variance with Kramers' theory which predicted that p=1. This has been attributed to partial screening of the solvent friction by the protein matrix.
Recently we have shown that the exponent p is a function of the cosolvent's molecular weight, suggesting that direct protein-solvent interactions rather than bulk viscosity are affecting local protein motions. We now show that the protein rotational correlation time (ϕ), though characterizing a large scale motion of the molecule as a whole, is also best described by $\phi \sim \eta^{q}$. Deviations of the Stokes-Einstein equation become apparent in the viscosity range 1-70 cP when the cosolvent's molecular weight exceeds about 5 kD. The molecular weight dependence of q is similar, though distinct from that of p.

M-PM-G8

THE ROLE OF SERUM ALBUMIN IN PORPHYRIN METABOLISM. A FLUORESCENCE STUDY. ((R. Galantai, E. Balog, F. Tolgyesi, J. Fidy)) Institute of Biophysics Semmelweis University of Med. Budapest (Spon. by J. Fidy)

The translocation of carboxylic porphyrins within cells has been studied by a model system in 10mM TRIS buffer at pH7.4. Unilamellar liposomes of L-α-phosphatidylcholine, dimyristoyl (DMPC) +5% L-α-phosphatidyl-DL-glycerol, dimyristoyl (DMPG) of 60nm size have been prepared by a sonication technique. The size of the liposome has been detected by dynamic light scattering, and was found to be stable under experimental conditions. Mesoporphyrin (MP) IX has been selected as carboxylic porphyrin because of its higher solubility in organic or aqueous solutions and precautions have been taken to avoid the formation of aggregates. The binding of the porphyrin to liposomes, to human serum albumin (HSA) and to HSA-liposome complexes have been compared on the basis of fluorescence spectroscopy, anisotropy decay and fluorescence lifetime measurements where the signal originated either from MP or from the single tryptophan of HSA. The time resolution of the data has been limited to decay times above 1ns, as a time domain technique with a ns flashlamp as excitation source has been used. The fluorescence parameters indicated that MP binds both to liposomes and to HSA with high affinity as shown by the association constants. When the binding of MP to liposome-HSA complexes have been studied, a preference for binding to HSA has been demonstrated. The transport of MP from the liposome to HSA through the aqueous phase could be excluded.

DNA/RNA/NUCLEIC ACIDS

M-Pos1

WHAT ARE THE MAIN FACTORS DETERMINING THE STRUCTURE OF THE IONIC ATMOSPHERE OF NUCLEIC ACIDS? ((Vitaly Buckin[1], Besik I. Kankiya[2], Victor Morozov and Luis A. Marky[1])) [1]Department of Chemistry, New York University, New York, NY 10003, USA; [2]Scientific Center of Radiobiology and Radiation Ecology, Georgian Academy of Sciences, Tbilisi 380003, Republic of Georgia.

We have used a combination of high precision ultrasonic velocity, density spectroscopy, and scanning microscopy techniques to investigate the changes in hydration upon substitution of sodium for magnesium ions in the ionic atmosphere of single-, double- and triple-stranded DNA and RNA molecules. This substitution results in a positive compressibility and volume effects that reflect a dehydration of the whole counterion-polymer system. For RNA and DNA double helices containing A•U or dA•dT base pairs, the absolute values of compressibility and volume effects correspond to outer-sphere complexes. This means that the dehydration of Mg^{2+} in the ionic atmosphere of these duplexes is small and that Mg^{2+} keeps its coordinated water. In the case of duplexes with dG•dC base pairs, poly(A) and poly(U) single strands, the inner-sphere type of Mg^{2+} binding is observed. Relative to a duplex, we did not find significant differences in the hydration parameters of the triple helix ionic atmosphere. Furthermore, the highest dehydration effect was observed for single stranded polymers, in spite of their lower linear charge density. These results suggest that the local structure of the nucleic acid ionic atmosphere is mainly determined by short range forces, including ion-water and nucleic acid-water interactions. The long range electrostatic interactions responsible for the condensation of counterions do not show significant influence on the local structure of the ionic atmosphere. Supported by Grant GM-42223 from the NIH.

M-Pos2

APPARENT CHARGE MEASUREMENTS OF DEOXYOLIGONUCLEOTIDES.
((John Wooll[1], Jonathan B. Chaires[2], Thomas M. Laue[1])) Department of Biochemistry and Molecular Biology, The University of New Hampshire, Durham, NH 03857. Department of Biochemistry, The University of Mississippi Medical Center, Jackson, MS 39216

The apparent charges (Q_{app}) of 20-residue-long single-, double - and triple-stranded DNA oligonucleotides were estimated from steady-state electrophoresis (SSE) and free-boundary electrophoretic mobilities. For both methods, measurements were made with varying field strengths, K^+ concentrations and oligonucleotide concentrations. Q_{app} from SSE decreases strongly with increasing oligonucleotide concentration, whereas Q_{app} from electrophoretic mobility is much less sensitive to the oligonucleotide concentration. With increasing field strength the magnitude of Q_{app} from SSE approaches the Q_{app} estimated from electrophoretic mobility.
This work was supported by grants NSF BIR 9314040 and NCI CA 35635

M-Pos3

SODIUM CONDENSATION AROUND DNA OLIGOMERS FROM MD SIMULATIONS. ((Nina Pastor and Harel Weinstein)) Dept. of Physiology and Biophysics, Mount Sinai School of Medicine, New York, NY 10029.

To be able to account for the effect of counterions in the formation of protein-DNA complexes, we have explored sequence dependent structural and dynamic properties of DNA on sodium condensation, and the influence of "end effects" on these properties. We have carried out molecular dynamics (MD) simulations with the CHARMM potential of 8 DNA dodecamers of different sequences and 2 decamers of the same sequence, one simulating a free decamer, the other simulating an infinite helix. The systems include explicit waters and enough sodium ions to ensure electroneutrality (no added salt condition, at an ionic strength of 0.36M), with periodic boundary conditions. The simulation times were >500 ps, without any constraints other than SHAKE applied to hydrogen containing bonds. We have studied the required equilibration times for the sodium population, and have followed the distribution of sodium atoms around the DNA, both globally and as a function of axial position along the DNA. From these simulations, we estimate the Manning radius to be very close to 5Å, in striking concordance with the estimated Debye length for the ionic strength in the simulated systems. The [Na+] within a 5Å shell around the free DNA is ~0.7M, in agreement with the Grand Canonical Monte Carlo estimates (Olmsted, M.C. *et al.* (1989) *P.N.A.S. USA* **86**, 7766-7770) for oligomers of such length. The contribution of "end effects" will be obtained from the comparison of the sodium distributions around the infinite helix and the free DNA.

Supported by a grant from the Association for International Cancer Research and by a Fulbright/CONACyT (Mexico) scholarship (to NP).

M-Pos4

Molecular Dynamics Simulation Of B-DNA With Explicit Counter-ions Using The CHARMM Force-field

(Aswin Dinakar, G. Ravishanker, D.L. Beveridge) Department Of Chemistry, Wesleyan University, Middletown, CT 06459.

Results from a nanosecond molecular dynamics study of the dodecamer CGCGAATTCGCG with explicit counter-ions and TIP3P waters will be presented. The focus of this study will be to show how the presence of counter-ions affect the fine structure of DNA. The use of protocols such as force-shifted function and ewald summation on the structure of DNA will be presented. The structure of ions and their correlated motions will be examined in this work. The current simulations will be compared with other simulations from our lab using other force-fields.

M-Pos5

THE EFFECT OF IONIC STRENGTH AND SUPERHELICAL STRESS ON THE TORSION CONSTANT OF SUPERCOILED DNAS

((Bryant S. Fujimoto, Jeffrey J. Delrow, James B. Clendenning, Lu Song, and J. Michael Schurr)) Department of Chemistry, Box 351700, University of Washington, Seattle, WA 98195

Recent cryo-electron microscope studies suggest that closed circular DNA becomes so tightly interwound that it is laterally contacted along almost its entire length when either (i) the ionic strength is increased from 5mM to 100mM at native superhelix density, or (ii) the superhelix density is increased from zero to native at 0.1 M ionic strength. If such a lateral association actually occurs in solution, the measured value of the apparent torsion constant should be substantially increased. A previous study by Selvin et al. (1992) indicated a rather large decrease in torsion constant of a supercoiled DNA with increasing ionic strength. We present results for dependence of the measured torsion constant on both superhelix density and the ionic strength. The measured torsion constants for zero and native superhelix densities in 0.1 M NaCl are very similar as are the measured torsion constants for native supercoiled DNAs in 20mM and 110mM ionic strength. There is no evidence in our measurements for any significant lateral association of native supercoiled DNAs in 0.1 M ionic strength.

M-Pos6

OBSERVATION OF EARLY STAGES OF COLLAPSE DURING CONDENSATION OF PLASMID DNA BY HEXAAMMINE COBALT (III).

((C.G. Baumann, S. He and V.A. Bloomfield)) Department of Biochemistry, University of Minnesota, St. Paul, MN 55108

Plasmid DNA condensed by hexaammine cobalt (III) forms compact, multimolecular particles with a toroidal shape similar to that released from lysed bacteriophage heads. At low DNA concentrations (1-10 μg/ml) near the critical hexaammine cobalt concentration required for condensation, the initial rate of collapse (time [t] ≥ 15 sec after manual mixing) appears insensitive to DNA concentration. We suggest a nucleation-limited condensation mechanism exists whereby stable "critical nuclei" must form during an early rate-limiting nucleation step. We have constructed a continuous-flow apparatus according to a published design [Feng, H.-P. *et al.*, *Biochemistry* 32:7824 (1993)] allowing early stages of DNA condensation (t ≥ 1 sec after mixing) to be studied by total intensity light scattering and transmission electron microscopy (TEM). Early collapsed structures (t = 1-10 sec after mixing) observed by TEM are toroidal with an average radius of ~150 Å. Particle sizes determined from light scattering intensity correlate well with the above TEM results. The dimensions of the initial toroidal particles appear insensitive to DNA monomer length, and thus may represent the aforementioned "critical nuclei". The independence of particle dimensions from DNA monomer length suggests that a minimum number of base pairs are required for stable nucleus formation. Extension of these approaches will allow the influences of DNA concentration, length and topology on nucleation to be determined.

M-Pos7

HYDRATION ANALYSIS OF DNA BASES: A MOLECULAR DYNAMICS STUDY OF THE DNA DUPLEX d(CGCAAATTTGCG)$_2$ AND d(CGCGAATTCGCG)$_2$ IN AQUEOUS SOLUTION USING AMBER 4.1

((K. J. McConnell, M. A. Young, G. Ravishankar, D. L. Beveridge)) Wesleyan University, Molecular Biophysics Program, Department of Chemistry Middletown, CT 06459

In our current study we present a detailed study of the water structure around nucleic acid bases as observed in the molecular dynamic simulations of d(CGCAAATTTGCG)$_2$ and d(CGCGAATTCGCG)$_2$ duplexes. Both simulations were carried out using AMBER4.1 and the Cornell 1994 force field, with explicit TIP-3P water and Na^+ counter ions. The calculation used periodic boundary conditions and the Particle Mesh Ewald method in a TPN ensemble with no restraints on the DNA, water, or ions for run lengths up to 1ns. The resulting trajectories are analyzed for the water structure around each of the four nucleic acid bases as well as for the DNA structure. The geometries of the water position are calculated for the first shell of hydration. A detailed description of the ion atmosphere and hydration and for each of the base atoms with respect to hydrogen bond angle and distance is presented and compared to crystallographic studies. Also the change in hydration as a function of groove width will be discussed.

M-Pos8

WATER INDUCED ENTHALPY - ENTROPY COMPENSATION ON DRUG INTERCALATION TO DNA.

(João Ruggiero Neto and Marcio F. Colombo) Dept. of Physics- UNESP- S. José do Rio Preto, 15.054.000 - BRAZIL (Spon. by M.F.Colombo)

The induced effect water activity on the actinomycin D (actD) intercalation to DNA has been studied using osmotic stress methods. The binding isotherms and constants, obtained by spectrophotometric titration, showed that the solutes which are excluded from the drug and DNA surfaces induced higher binding levels of intercalation on DNA. They also revealed a second class of binding sites which are not accessed in the absence of co-solvents. It was, also, observed that the binding constants vary linearly with water activity when these variables were plotted on logarithmic scales. From these latter plots we determined the number of water molecules released on drug binding (Δn_w), which is proportional to the co-solvent molecular weights or molecular volumes. This linkage between the hydration and free energy changes on binding with solute molecular volumes suggests that the entropic gain upon releasing Δn_w to the bulk on drug binding is a source for the higher drug intercalation levels observed in the presence of these co-solvents. At moderate ionic strength (phosphate buffer 0.001 M 150 mM NaCl) and in the absence of co-solvents, the actD intercalation presents an unfavorable enthalpy contribution, $\Delta H_{van'tHoff}$ = +1.8 kcal/mol. Our hypothesis is that the entropic contributions resulting from the exclusion of the co-solvent could compensate for this positive enthalpy, making the binding energetically more favorable. To test this hypothesis we measured the van'tHoff enthalpy of the intercalation in the presence of different concentrations of sucrose. We found that $\Delta H_{van'tHoff}$ decreased linearly with the increase of sucrose concentration and, consequently, with the Entropy increase of dissolving Δn_w water molecules in the sucrose solution. For instance, $\Delta H_{van'tHoff}$ measured in 30% (W/V) sucrose equals - 8.0 kcal/mol, a values usually observed in the intercalation of other drugs to DNA. These data seems to emphasize the importance of water and of non-ideality of the cellular medium on the control of drug to DNA affinity.

Financial support: FAPESP, CNPq AND PADCT

M-Pos9

EFFECT OF SELECTIVE CYTOSINE METHYLATION AND HYDRATION ON THE CONFORMATIONS OF DNA TRIPLE HELICES CONTAINING A TTTT LOOP STRUCTURE BY FT-IR SPECTROSCOPY.

((L-S. Kan[a], S.-B. Lin[b], Y. Fang[c], C. Bai[c], Y. Wei[c])) [a]Institute of Chemistry, Academia Sinica, [b]Institute of Medical Technology, National Taiwan University, Taipei, [c]Institute of Chemistry, Chinese Academy of Sciences, Beijing, China.

5-Methylcytosines (mC's) have been introduced into triplex forming oligonucleotides and shown to extend the pH range over acidic pH (Tsay, *et al.*, (1995) J. Biomol. Str. Dyn., 13, 1235). We here present results obtained by FT-IR spectroscopy concerning the conformation of the hairpin triplex (5'-d(TC)$_3$T$_4$(CT)$_3$ ([CC]) + 5'-dA(GA)$_2$G ([AG6])) as a function of the selective substitution of cytosines by mC's in the host strand. Namely, cytosines are substituted by mC's in either the 3'-pyrimidine portion ([CM]) or the 5'-pyrimidine portion ([MC]) or in both ([MM]) of the host strand. The order of pK values, *i.e.*, [MM]·[AG6] (6.2) > [MC]·[AG6] (6.0) > [CM]·[AG6] (5.7) > [CC]·[AG6] (5.2) > single-stranded oligopyrimidines (4.6), indicating that cytosine methylation expands the pH range compatible with the hairpin triplex formation regardless of whether the substitution is in the 5'-pyrimidine (Hoogsteen) portion or in the 3'-pyrimidine (Watson-Crick) portion. IR spectra recorded in D_2O and H_2O solutions revealed that cytosine methylation does not significantly influence the conformation of triplex DNA in solution, *i.e.*, all the four triplexes accept a similar sugar conformation, and predominately take on a S-type sugar pucker with a relative proportion of two S-type sugars for one N-type. (supported by NSC)

M-Pos10

INTERACTION OF CROSS-LINKED LEXITROPSINS WITH POLY [d(AT)]•POLY [d(AT)].

((Karen Alessi[1], Michelle Alonso[1], Luis A. Marky[1], Yong-Huang Chen[2], and J. William Lown[2])) [1]Department of Chemistry, New York University, New York, NY, USA; and [2]Department of Chemistry, University of Alberta, Edmonton, Alberta, Canada.

The new structural binding motif of lexitropsins, in which two ligands lie in the minor groove of B-DNA in an antiparallel side-by side fashion, has increased the number of possibilities of recognizing specific sequences of DNA. We use a set of lexitropsins consisting of two tripyrrolecarboxamide strands covalently linked by a chain of 2 to 12 methylene groups to investigate the effect of the poly methylene chain length on DNA binding. Specifically, we used a combination of isothermal titration calorimetry (ITC) and temperature-dependent spectroscopy techniques to determine standard thermodynamic profiles ($\Delta G°$, ΔH and ΔS) for the interaction of these stapled-lexitropins to poly [d(AT)]•poly [d(AT)]. The increase in thermal stability of the saturated lexitropsin-DNA complex relative to the free polymer yielded binding affinities, K_b, ranging from 10^6 to 10^8; this corresponds to $\Delta G°$ terms of -8.8 kcal/mol to -11.8 kcal/mol. ITC binding isotherms indicate binding of each ligand to 3-4 dA•dT base pairs and exothermic enthalpies of -8.8 kcal/mol to -15.4 kcal/mol. However, as a function of the number of methylene groups, the $\Delta G°$ values were most favorable for ligands with 4 to 8 methylene groups, for which 5 and 8 resulted in more favorable binding heats. The overall results will be discussed in terms of the actual binding mode, specific molecular interactions and the contribution of the hydrophobic linker. Supported by Grant GM-42223 from the NIH (L.A.M) and The Natural Sciences and Engineering Research Council of Canada (J.W.L.).

M-Pos11

FLUORESCENCE LIFETIME AND ANISOTROPY OF TOMAYMYCIN-DNA ADDUCTS. ((W. J. Walczak, Q. Chen and M. D. Barkley)) Department of Chemistry, Louisiana State University, Baton Rouge, LA 70803.

We explore the fluorescence lifetime and anisotropy decay of tomaymycin bound to guanine in various DNA adducts. Lifetime properties are explained in terms of an anomeric effect on the dipole moments of bases surrounding the bound guanine. The anisotropy decay data are fitted to the predicted non-exponential decay model for twisting and bending motions of a semi-flexible rod. The angle that the emission transition dipole of tomaymycin makes with the DNA helix allows fluorescence anisotropy decay to report predominantly on DNA bending motions. We extract the persistence length, the torsional rigidity, the radius of the helix and the orientation of the transition dipole of the drug with respect to the DNA helix from these measurements. The behavior of these parameters with DNA base pair composition is determined. Natural calf thymus DNA, poly(dAdG) poly(dTdC) (1000±50 bp), poly(dGdC) poly(dGdC) (950±100 bp), and the linearized plasmid pSP65 (3005 bp) were studied in this work. Supported by NIH grant GM35009.

M-Pos12

THERMODYNAMICS OF NON-CANONICAL BASE-PAIR AND LOOP STACKING INTERACTIONS OF CENTROMERE SEQUENCES. ((Dionisios Rentzeperis[1], Jenelle Holder[1], Luis A. Marky[1], and Angel E. Garcia[2])) [1]Department of Chemistry, New York University, New York, NY 10003; [2]Theoretical Biology and Biophysics Group, T-10, MS K710, Los Alamos National Laboratory, Los Alamos, NM87545.

The sequence d(AATGG) is found in the DNA of human centromeres. In solution, repeats of this sequence fold into single-stranded double hairpin molecules that are stabilized by unusual base-pair stacks (AA/GT, TG/AA, and GG/AG) and GGA triplet loops. We have used a combination of temperature-dependent UV absorption and differential scanning calorimetry techniques to evaluate the thermodynamic contribution of these base-pair stacks and tri-loops by investigating the melting behavior of $d(AATGG)_n$ with n = 4 or 6 and four related mutants (with n = 4) containing single or multiple substitutions in the stem or loops. In 10 mM sodium phosphate buffer at pH 7.0, all six molecules melt in monophasic transitions, with transition temperatures, T_m, independent of strand concentration, characteristic of monomolecular processes. We obtained $dT_m/d\log[Na^+]$ values of 8.0-15.2°C, which correspond to counterion releases that are proportional to the length of stems with 7 and 12 base pairs. Standard thermodynamic profiles at 20°C reveal that the favorable free energy of forming these ordered structures results from the characteristic partial compensation of favorable enthalpies with unfavorable entropies. Substitution of a dG•dG for a dC•dG between dA•dG base pairs yielded a hairpin with similar stability and enthalpy while the substitution of dG for dT in the loops resulted in a less stable hairpin with a lower transition enthalpy. Supported by Grant GM-42223 from the NIH.

M-Pos13

THERMODYNAMIC CHARACTERIZATION OF A FAMILY OF DNA DUPLEXES WHICH CONTAIN THE CANONICAL AND SELECTIVELY MODIFIED ECORI BINDING SITES.

((Danuta Szwajkajzer and Kenneth J. Breslauer))
Department of Chemistry, Rutgers University, New Brunswick, New Jersey 08855-939

We have used a combination of spectroscopic and calorimetric techniques to characterize thermodynamically the consequences of systematically altering the canonical GAATTC EcoRI binding site within a family of 17-mer DNA duplexes. Each "mutant" differs by a single or double purine substitution for adenine, alterations which result in one or two Watson-Crick hydrogen bonds being deleted in the "mutant" relative to the "wild type" duplex. Our data reveal that deletion of any hydrogen bond results in duplex destabilization, with the magnitude of this destabilization being dependent on the position and the number of the added purine residues, as well as the nature of the neighboring base pairs. Theses results are discussed in the contex of the binding studies of Jen-Jacobson and coworkers (Jen-Jacobson, 1991; Lesser, 1990; 1992) in which the same 17-mer duplexes were used as targets for EcoRI.

M-Pos14

NMR CHARACTERIZATION OF AN INTRAMOLECULAR TRIPLEX CONTAINING A NOVEL CYTOSINE BASE. ((D.M. Noll, G. Bi, C.-Y. Huang, P.S. Miller and A.F. Miller)) Johns Hopkins Univ., Baltimore, MD 21205 (Spon. by M. Lavilla)

UV melting and 1D and 2D proton NMR were used to characterize an oligodeoxyribonucleotide, d-TCTXTC(T)$_4$CTGTCT(T)$_4$AGACAG (**I**, C is 5-MeC) which contains N^4-(6-amino-2-pyridinyl)deoxycytidine (X) and is designed to form an intramolecular triplex having two C$^+$•G•C, three T•A•T and a single X•G•C triad. Absorbance (260 nm) *versus* temperature studies show typical hypochromicity changes consistent with triplex formation. Thus two transitions are observed at pH 6.5 (0.1 M sodium chloride, 20 mM magnesium chloride, 50 mM MOPS). The first (Tm 30°C) is due to melting of the Hoogsteen and the second (Tm 61°C) melting of the Watson-Crick domain of **I**. The 1D proton NMR of **I** shows well resolved resonances between 8.0 and 16.4 ppm which correspond to imino and amino resonances of the base triads. The temperature dependence of these resonances is consistent with the UV melting behavior of **I**. The 2D proton NMR NOESY spectrum (200 ms mixing time) has allowed assignment of the exchangeable imino and amino protons in the five canonical base triads. Resonances attributable to X suggest that this base occupies a position within the major groove of the triplex. This observation is consistent with dimethylsulfate alkylation experiments which show protection of N-7 of G13. These results suggest that X may be a useful base analog for targeting a C•G interruption of an otherwise pyr•pur tract in duplex DNA. (Supported by NIH GM27512).

M-Pos15

DOES *TATA* MATTER? ((Nina Pastor and Harel Weinstein)) Dept. of Physiology and Biophysics, Mount Sinai School of Medicine, New York, NY 10029. (Spon. by Marc Glucksman)

The binding of the TATA box-binding protein (TBP) to the TATA sequence promoter is considered essential for eukaryotic basal transcription. TBP binds in the minor groove of DNA, causing an unprecedented distortion of the DNA helix (Kim,Y. *et al.* (1993) *Nature* **365**, 512-520; Kim,J.L. and Burley,S.K. (1994) *Nature Struct. Biol.* **9**, 638-653); TBP inserts Phe residues at TA steps and at AG (or AA) steps, and unwinds the DNA, most notably at the central base pair of the TATA box. To gain insight into the role of the TATA sequence in determining the specificity of the DNA substrates of TBP, we have chosen 8 DNA dodecamer sequences, 7 of which are either known, or expected to bind to TBP, and studied their solution structure and dynamics in molecular dynamics (MD) simulations with the CHARMM potential. The system includes explicit waters, one sodium ion/phosphate, and periodic boundary conditions. The total simulation time for each dodecamer was >500 ps. We report a comparison of the structural parameters of these dodecamers with the structural parameters of DNA in the crystal structures of two TBP/DNA complexes. The overall degree of unwinding and bending, and the width of the grooves, describe the characteristics of the various dodecamers from a whole molecule perspective. All the dodecamers are unwound compared to B-DNA, but they retain sequence specific features. A local property of the various sequences is the extent of kinking in the structure of the steps where TBP inserts the Phe residues; the AG steps tend to roll so as to open the minor groove, in a manner that would facilitate the observed insertion of Phe residues at these steps.
Supported by a grant from the Association for International Cancer Research and by a Fulbright/CONACyT (Mexico) scholarship (to NP).

M-Pos16

NUCLEOTIDE OCCURRENCE DISTRIBUTIONS IN DNA CODING SEGMENTS. ((T.Castrignano', A.Colosimo, S.Morante, V.Parisi, G.C.Rossi)) Dip. di Fisica, 2° Universita' di Roma, Via della Ricerca Scientifica, 1- 00137 Roma - Italy. (Spon. by L.Castellani)

Identifying peculiar deviations in the occurrence frequency distributions of oligonucleotides, with respect to what can be a priori expected, is of the utmost importance in biology. Differences between expected and actual distributions can in fact confirm the existence of specific biological mechanisms related to them and/or suggest that certain oligopeptides may belong to the class of "DNA signal sequences". The approach we have eleborated is innovative in at least two aspects: i) the analysis of the genomic data is carried out in the light of the observation that the distribution of the four nucleotides along the coding parts of the genoma is biased by a well defined "reading frame"; ii) the "experimental" numbers found by counting the occurrences of the various oligonucleotide sequences are appropriately corrected for the many kinds of mistakes and redundancies present in the genetic Data Bases. A significative further improvement of our approach is represented by the fact that, in order to decide whether or not the (corrected) "experimental" value of the occurrence frequency of a given oligonucleotide is within statistical expectations, a measure of the strength of the selective pressure, having acted on it in the course of the evolution, is assigned to the sequence, by taking into account both the value of the "experimental" occurrence frequency of the sequence and the magnitude of the probability that this number might be the result of statistical fluctuations. If the strength of the selective pressure evaluated in this fashion turns out to be sufficiently large, the corresponding sequence will be considered to be statistically and biologically interesting.

M-Pos17

IS THERE AN ERROR CORRECTING CODE IN THE BASE PAIR SEQUENCE OF DNA?

((L. S. Liebovitch, Y. Tao, A. T. Todorov, and L. Levine))
Center for Complex Systems
Florida Atlantic University, Boca Raton FL 33431

ISBN book numbers, driver's licenses, credit cards, and UPC product codes use error check codes, where some digits are functions of other digits, to detect errors in transmission. We developed a method to test if the base pair sequence in DNA uses a similar digital error correcting code to protect the fidelity and transmission of genetic information. We coded the 4 bases as 0,1,2,3 and used the Gauss-Jordon method, modified for modulus 4, to test if some bases are linear combinations of other bases. We did not find such a simple error correcting code in the lac operon or the gene for cytochrome c.

Supported by NIH EY6234.

M-Pos18

DETECTION OF DNA HELICAL FLUCTUATIONS MANIFESTED BY THE BINDING OF ANTP(C39S) HOMEODOMAIN OR ANTP FULL-LENGTH PROTEIN. ((E.V. Bobst*, R.S. Keyes*, D. Resendez-Perez#, W. Gehring#, and A.M. Bobst*)) *Department of Chemistry, University of Cincinnati, Cincinnati, Ohio 45221, and #Biozentrum der Universität Basel, CH-4056 Basel.

A model system has been developed for examining the binding effect of the Antp(C39S) homeodomain (HD) (MW 7,817) and the Antp full-length protein (MW 42,800) on a cognate 26mer containing a two-atom-tethered spin-labeled thymidine analog downstream from the binding site. EPR spectra were acquired for both the free 26mer and the corresponding protein-bound complexes. The spectra were analyzed according to a motional model that separates the dynamics into global contributions from macromolecular tumbling and internal contributions from diffusion of the spin-labeled base. Previous work indicated that the two-atom-tethered DUMTA can be described by the dynamic cylinder model where the global tumbling is characterized by hydrodynamic correlation times and the internal motion is quantified by an order parameter (Keyes, R.S. and Bobst, A.M. *Biochemistry 34*, 9265 (1995)). Binding of either HD or full-length protein causes a similar line shape change. This is unexpected since the two proteins differ significantly in their molecular volumes which should result in complexes with considerably different global tumbling rates. Gel mobility shift assays for determining the dissociation constant of the DNA complexed with either HD or full-length protein gave similar values in the same binding mixture. Therefore, it is proposed that an additional relaxation process becomes apparent when either the HD or the full-length protein binds to the same target sequence. This process is intermediate to the slower global tumbling and the faster base dynamics. The observed intermediate relaxation may be due to helical fluctuations that are manifested by the binding event. Supported in part by NIH GM 27002.

M-Pos19

THERMODYNAMIC CHARACTERISTICS OF OLIGONUCLEOTIDES WITH 2-AMINOPURINE BASE PAIRED WITH A, C, G, AND T. ((S.M. Law[1], R. Eritjas[2], M.F. Goodman[3], and K.J. Breslauer[1])). [1]Dept. of Chemistry, Rutgers University, Piscataway, NJ, 08855; [2]Dept. of Biological Sciences, USC, Los Angeles, CA, 90089; and [3]European Molecular Biological Laboratories, Heidelberg, Ger. 69117. (Spon. by C. A. Gelfand)

The nucleotide 2-aminopurine (Ap) promotes A•T to G•C transitions in prokaryotes and bacteriophages. This event involves incorporation of C opposite Ap, which occurs at a higher frequency than the incorporation of C opposite A. At present, it is not known if this increased incorporation frequency correlates with differences in stability between an A•C and an Ap•C base pair, or whether other interactions with the DNA polymerases are controlling. To probe this question, we have used a combination of spectroscopic and calorimetric techniques to characterize the thermodynamics of six 11-mer duplexes containing common flanking sequences and the following variable central base pairs (bp): A•T, A•C, Ap•T, Ap•C, Ap•A, and Ap•G. Analyses and interpretation of the optical data suggests the relative stability of the central base pairs to be A•T ≥ Ap•T > Ap•C > Ap•A > Ap•G > A•C. Calorimetric measurements also demonstrate enhanced stability for the Ap•C duplex relative to the A•C duplex. These results suggest that during incorporation, base discrimination by DNA polymerases may be dictated by the stability of the newly formed base pair.

M-Pos20

BINDING SPECIFICITY OF METHYLPHOSPHONATE OLIGONUCLEOSIDES FOR DNA TARGETS DETERMINED BY CAGE. ((T.L. Trapane and P.O.P. Ts'o)) Biochemistry, Johns Hopkins SHPH, Baltimore, MD 21205.

An electrophoresis system, "constant activity gel electrophoresis" (CAGE), is being developed which enables determination of the binding affinity between a nonionic methylphosphonate oligomer (MPO) and negatively-charged nucleic acid targets. Gels are constructed in which the electrophoretically immobile MPO is incorporated directly into the polyacrylamide matrix at fixed concentrations within defined regions. When a radioactively-labeled DNA oligomer is electrophoresed into a region of the gel that contains an activity of MPO high enough to support binding, the mobility of the charged molecule will be decreased accordingly. This method allows determination of concentration-dependent binding constants, $K_a = K_d^{-1}$, at isothermal conditions. The ability of the CAGE method to determine relative binding constants for interactions of a single MPO probe with the four phosphodiester "target" oligomers from the *ras* gene (below) is examined.

MPO probe	$^{3'}$CGGCCGCACCTCCTC-d$^{5'}$	K_d (μM)
complementary target	$^{5'}$d-GCCGGCCTGGAGGAG$^{3'}$	0.04
central mismatch	$^{5'}$d-GCCGGCCA**G**GAGGAG$^{3'}$	2.0
penultimate mismatch	$^{5'}$d-GCCGGCCTGGAGG**T**G$^{3'}$	0.2
scrambled sequence	$^{5'}$d-GGCAGCGGACGTCGG$^{3'}$	>>10

These experiments, carried out at 52°C, show that CAGE analysis can afford relative binding affinities of MPO's for complementary and mismatched target sequences. [Supported by Genta, Inc.]

M-Pos21

CONFORMATIONAL CHARACTERISTICS OF DOUBLE HELICAL NUCLEIC ACID STRUCTURES CONTAINING PEPTIDE NUCLEIC ACIDS COMPLEXED WITH A-, B-, AND Z-DNA BACKBONES. (A. R. Srinivasan and Wilma K. Olson, Department of Chemistry, Wright-Rieman Laboratories, Rutgers, the State University of New Jersey, New Brunswick, New Jersey 08903

A detailed theoretical analysis has been carried out to investigate the conformational characteristics of Watson-Crick hydrogen bonded PNA (peptide nucleic acid) •DNA double helical nucleic acid structures. A constrained molecular modeling method [1] developed in our laboratory has been applied to predict the DNA backbones and the PNA structures are identified using a slightly modified approach. The base-pair arrangements found in the fiber models of A- and B-DNAs [2] and the d(CGCGCG)$_2$ Z-DNA single crystal structure [3] are used as starting skeletals to build the relevant backbone conformations. Extended investigations have also been carried out with starting base-pair planes having different helical twist angles and relative translations. Low energy PNA backbones are obtained for the A- and B-DNA base-pair arrangements, but not for the *zig-zag* Z-DNA structure. Also, the introduction of PNA backbones in A-DNAs is found to have a profound effect on increasing the diameter of the double helix. The implications of these results are analyzed in the light of recent NMR studies of PNA•DNA and PNA•RNA complexes. (Supported by USPHS Grant GM20861.)

[1] A. R. Srinivasan and W. K. Olson, *J. Biomol. Str. & Dyn.*, **4** (1987) 895.
[2] R. Chandrasekaran and S. Arnott in: *Landolt-Börnstein Numerical Data and Functional Relationships in Science and Technology, Group VII/1b, Nucleic Acids*, ed. W. Saenger (Springer-Verlag, Berlin, 1989) p. 31.
[3] A. H. -J. Wang, G. J. Quigley, F. J. Kolpak, G. van der Marel, J. H. van Boom and A. Rich, *Science* **211** (1981) 171.

M-Pos22

Antisense DNA· RNA Pairing Initiated By A Loop-Strand Interaction. (Jing Li, Kang Hoon Nam, Roger M. Wartell, School of Biology, Georgia Institute of Technology, Atlanta, Georgia 30332, U.S.A)

Several functionally important RNA duplexes are initiated by the interaction of an RNA loop with a complimentary RNA strand. This complex is followed by unwinding of an intramolecular RNA duplex and the formation of a bimolecular RNA duplex. We have examined the ability of DNA hairpins to form DNA•RNA duplexes initiated by DNA loop-RNA strand pairing. Two DNA hairpins were synthesized with identical 5 nucleotide loops and either a 10 bp stem or a 9 bp stem with a central G-G mismatch. Their T_m 's were 71°C and 55°C respectively in 0.1 M Na^+. A 75 nt RNA target strand was synthesized as a runoff transcript from a modified pGEM7Zf(+) plasmid. The transcript contained 25 nt sequence from HIV genome that includes 10 consecutive pyrimidines. The sequence of the loop and one strand of the hairpin stems was complimentary to the 15 nt region of the RNA containing the pyrimidine stretch. The interaction between the hairpins and the 75 nt RNA was examined by PAGE and RNaseH degradation. Titration of the hairpin DNAs with the RNA strand at 25°C decreased the intensity of the free DNA bands in the gel. RNase H degradation experiments also showed that the target RNA was digested after incubation with either hairpin molecule at 25°C. RNase H digestion of the RNA strand was more rapid with the hairpin containing the G•G mismatch. No significant RNA degradation was detected when DNA oligomers containing non-complimentary sequences were employed. The results suggest that DNA hairpin molecules can form site specific RNA·DNA duplexes through strand exchange initiated by a loop-strand complex.

M-Pos23

STABILITIES OF DUPLEX RNA WITH SINGLE BASE PAIR CHANGES AND MISMATCHES MEASURED BY TGGE. ((Jian Zhu and Roger M. Wartell)) School of Biology, Georgia Institute of Technology, Atlanta GA 30332.

The thermal stabilities of long RNA duplexes with base pair substitutions and mismatches were investigated by temperature gradient gel electrophoresis (TGGE). Seven homologous plasmids with base pair differences within the first melting domain of a 333bp region were used. In separate PCR reactions, a T7 promoter was attached to each end of the 333bp region. The resulting transcription templates were then used to generate different sense and antisense ssRNA. These RNA products were annealed to form homologous 339bp dsRNA differing from each other by single or double base pair substitutions and mismatches at specific sites. The relative stabilities of these duplexes were determined using TGGE. RNA fragments containing G·C to A·U transition and A·U to U·A transversion were distinguishable. Compared to homoduplexes, RNA duplexes carrying a single mismatch were destabilized by up to 8°C and those with a double mismatch were destabilized by 10°C or more. UV-melting studies showed that the RNA duplexes contained three melting domains as expected from RNA melting theory. All possible base pair substitutions and mismatches were introduced into the first melting domain within the nearest neighbor environment: (GXU) · (AYC) with X, Y=A, U, C, G. General consistency was shown between the order of stabilities of both substitutions and mismatches and the hierarchy given by the nearest neighbor free energies determined from RNA oligomer data. In addition, TGGE was shown to be effective at distinguishing small differences at the ends of PCR amplified DNA not detected by conventional PAGE.

M-Pos24

mRNA IRON RESPONSIVE ELEMENT STABILITY AND NMR STRUCTURE STUDY. ((L.G. Laing and K. B. Hall)) Department of Biochemistry and Molecular Biophysics, Washington University School of Medicine, St. Louis, Missouri 63110

We are primarily interested in how RNA and proteins interact to control gene expression. The iron responsive system is one of only a few known examples of a eukaryotic post-transcriptional control pathway, involving unique RNA sequences (IRE, iron responsive elements) in the 5' and 3' untranslated regions (UTR) of the mRNA of proteins involved in iron uptake and storage. These IRE sequences are the sites for direct interaction with the iron responsive factor protein (IRF). The IREs adopt a stemloop structure which we are working to describe. Our model of the IRE system, a 34 nucleotide RNA oligomer, has been divided into its two component secondary structures, a 16 nucleotide hairpin and 18 nucleotide helical duplex. We will show that the 34 nucleotide element melts in two two-state transitions. The terminal hairpin model, consisting of a six nucleotide loop and five base pair stem, has been studied most extensively as its sequence is a key feature of the IRF protein interaction. We will present thermodynamic data for several loop sequences which show a very stable hairpin for each sequence. The description of the structure by NMR suggests that many six nucleotide loops may adopt similar structures.

M-Pos25

STRUCTURAL FEATURES OF RNA MOLECULES INVOLVED IN *trans*-SPLICING REACTIONS. ((Nancy L. Greenbaum*, Ishwar Radhakrishnan*, Dinshaw J. Patel+, and David Hirsh*)) *Department of Biochemistry and Molecular Biophysics, Columbia University, NY, NY 10032, and +Cellular Biophysics and Biochemistry Program, Memorial Sloan Kettering Cancer Institute, NY, NY 10021.

Trans-splicing involves the ligation of two independent RNA molecules into a single transcript, and is a required process in the maturation of precursor mRNAs of nematodes and trypanosomes. All known spliced leader (SL) RNAs, which donate a short spliced leader to a separate pre-mRNA transcript, are thought to fold into secondary structures containing three stem loops. The solution structure of a 26-nucleotide RNA fragment of the first stem loop of the SL1 RNA of *C. elegans* containing the base paired splice site and a nine nucleotide hairpin loop has been determined by distance-restrained molecular dynamics calculations using data from homonuclear and heteronuclear NMR spectra. The well-defined loop is stabilized by base stacking and hydrogen bonding interactions; the structure reveals a deep pocket formed by a bulged adenine at the base of the loop. The proximity of the pocket to the splice site, which is located in the helical stem immediately adjacent to the loop, suggests that it may be a docking site for protein or RNA in the *trans*-splicing process. The spliced leader itself, i.e., the first 22 nucleotides of the SL1 RNA, has been shown by homonuclear and heteronuclear NMR studies to fold into a distinctly different conformation from that of the same sequence prior to splicing.

M-Pos26

CHARACTERIZATION OF INDIVIDUAL NUCLEIC ACID POLYMERS WITH AN ION CHANNEL. ((J.J. Kasianowicz†, E. Brandin‡, D. Branton‡, and D.W.Deamer#)) † NIST, ‡ Harvard U., # UC Santa Cruz.

We show that single channels of *S. aureus* α-toxin in a lipid bilayer can be used to characterize the size (length) and concentration of polymers such as single stranded DNA and RNA. Addition of size-selected samples of poly[U] to the sub phase bathing one side of the bilayer causes well-defined and substantial reductions (blockades) in the open channel current when the applied potential is correctly polarized, and sufficiently high, to drive the anionic polymer into the channel. The lifetimes of the channel blockades are proportional to the polymer length and inversely proportional to the applied potential. Double stranded DNA causes virtually no channel blockades, presumably because the α-toxin channel is too narrow to admit the double stranded molecule. Experiments with poly[dT] show that the number of blockades per unit time is directly proportional to the polymer concentration. As expected, when long strands of poly[U] are enzymatically hydrolyzed by RNAase, the initial increase in the number of poly[U] hydrolysis products results in a striking increase in the blockade rate. Our results suggest that the oligonucleotides traverse the α-toxin channel as individual, extended molecules which, because of their negligible contribution to the ionic current, reduce the channel conductance. Supported by the NAS/NRC (JJK), and the NSF.

M-Pos27

COMPUTER SIMULATION OF STEADY STATE ELECTROPHORESIS AND DIFFUSION. ((T.P. Moody and T.M. Laue)) Dept. of Biochemistry and Molecular Biology, Univ. of New Hampshire, Durham NH 03824. (Spon. By T.M. Laue)

In conjunction with experiments looking at the electrophoresis and diffusion of various macromolecules in a rectangular cell, a computer program was written that simulates such experiments. The basis of the program is that given certain characteristics of a molecule, such as its frictional coefficient and its charge, its behavior when an electric field is placed across the cell should be predictable if the flux due to diffusion and the flux due to electrophoresis during sufficiently short time intervals are calculated for a sufficient number of subdivisions of the cell. Starting with a concentration distribution chosen by the user, a simulation generates output files giving the mass concentration versus position within the cell. Each file represents the concentration distribution at some time after the start of the simulation. The program can not only be used to simulate some of the systems that are likely to be encountered in actual experiments, but can also be used to see what happens when some of the various characteristics that a system might have are taken to extremes that would probably not be encountered otherwise. For example, in a simple system containing a charged macromolecule that does not self-associate, simulated electrophoresis results in an exponential mass concentration distribution at the steady state. This conforms with expectations and actual observations. If the same macromolecule is then modeled as a monomer dimer equilibrium in which, due to counter-ion condensation, the charge of the dimer is much different from twice that of the monomer, simulation demonstrates that the concentration gradient at the steady state should not be exponential. Grant acknowledgments: NSF BIR-9314040, NSF DIR-9002027 and NSF DIR-8914571.

M-Pos28

EMPIRICAL DISPERSION FUNCTIONS FOR SEPARATIONS OF DNA BY STATIC FIELD GEL ELECTROPHORESIS. ((John C. Sutherland and Kiley Reynolds)) Biology Department, Brookhaven National Laboratory, Upton, NY 11973.

The dispersion function (the relationship between velocity and molecular length) of DNA in an electrophoretic gel is an observable that is used both in studies of the mechanism of separation and in applications that require determination of the length of DNA molecules migrating with an observed velocity. Simple log-linear and log-log representations of dispersion functions are adequate within a limited range of length-velocity space, but fail for the extremes of lengths that can be separated by a given electrophoretic system. Southern [Analyt. Biochem. **100**, 319-323 (1979)] showed that an offset hyperbolic dispersion function, which includes three experimentally determined constants, greatly improves accuracy at the length extremes. Several groups have shown that experimental fits, as judged by χ^2, are improved further by raising one of the experimental variables in Southern's equation to an arbitrary power, thus resulting in four experimentally determined fitting parameters. We measured dispersion functions each of which is based on several hundred DNA length classes (bands) separated in polyacrylamide gels. Images of the electrophoretic pattern were recorded in finish-line mode with a LI-COR (Lincoln NB) automated sequencer. We show that our data can be described by the equation $\left(\frac{L}{L_\infty}\right)^p = \frac{t - t_0}{t_\infty - t}$, where t is the time of arrival at the detector of molecules of length L, t_0 and t_∞ are the times of arrival of molecules of "zero" and "infinite" length respectively, and L_∞ is the length of DNA molecules at $t = (t_0 + t_\infty)/2$. The four fitting constants: t_0, t_∞, L_∞, and p, were determined by the Levenberg-Marquardt algorithm. Reasonable fits to the data can be achieved **only** for $p \neq 1$. Thus, the exponential form of the equation is **required** to describe the migration of the DNA in this system.

Supported by OHER/DOE and a CRADA with LI-COR Corp.

M-Pos29

RIBOSE-LINKED SULFOINDOCYANINE CONJUGATES OF ATP: Cy3-EDA-ATP AND Cy5-EDA-ATP. ((J.F. Eccleston, K. Oiwa*, M.A.Ferenczi, M. Anson, J.E.T. Corrie, A. Yamada*, H. Nakayama* & D.R. Trentham)) Nat. Inst. Med. Res., London NW7 1AA, U.K., *KARC, Communications Research Laboratory, Kobe 651-24, Japan.

Indocyanine dyes are promising fluorophores for single molecule studies of myosin triphosphatase activity (Funatsu *et al., Nature*, 1995, **374**, 555). Two ribose-modified fluorescent analogues have been synthesized by conjugating 2'(3')-*O*-[*N*-(2-aminoethyl)carbamoyl]ATP with succimidyl esters of the sulfoindocyanine carboxylic acids, Cy3.29.OH and Cy5.29.OH (Mujumdar *et al., Bioconjugate Chem.*, 1993, **4**, 105). Purified analogues were characterized by absorbance and fluorescence spectrophotometry, mass spectroscopy and hplc. Interaction of Cy5-EDA-ATP with rabbit skeletal myosin subfragment 1 (S1) and acto-S1 was studied by stopped-flow techniques. The rate constants of the binding of Cy5-EDA-ATP to S1 and acto-S1, the dissociation of Cy5-EDA-ADP from S1, and the turnover of Cy5-EDA-ATP by S1 were all within a factor of two of those of ATP (or ADP). The Cy5-EDA-ATPase of acto-S1 gave a K_m for F-actin of 19 μM and a k_{cat} of 7.1 s^{-1} compared to 6.7 s^{-1} for ATP. Where tested, the kinetics of Cy3-EDA-ATP and Cy5-EDA-ATP were identical. Permeabilized fast-twitch rabbit muscle fibers at 20°C developed isometric force in the presence of 0.5 mM Cy5-EDA-ATP, and shortened when the load was reduced to zero. The maximal shortening velocity with 0.5 mM Cy5-EDA-ATP was 10% of that with 0.5 mM ATP.

M-Pos30

MICROSCOPIC OBSERVATIONS OF Cy3-EDA-ATP AND Cy5-EDA-ATP BINDING TO MYOSIN FILAMENTS *IN VITRO*. ((K. Oiwa[1], M. Anson[2], A. Yamada[1], J.F. Eccleston[2], J.E.T. Corrie[2], M.A.Ferenczi[2], D.R. Trentham[2] & H. Nakayama[1])) [1]Kansai Advanced Research Center, Iwaoka, Kobe 651-24, Japan., [2]National Institute for Medical Research., Mill Hill, London NW7 1AA, U.K.

Fluorescent ATP analogues, Cy3-EDA-ATP and Cy5-EDA-ATP, where sulfoindocyanine dyes are attached to the ribose ring (Eccleston *et al., this volume*) have been applied to *in vitro* motility assays and to single molecule triphosphatase studies on fast-twitch skeletal muscle proteins. 1 μM and 3μM Cy5-EDA-ATP supported translation of actin at 25 °C over heavy meromyosin at 0.32 and 0.41 $\mu m \cdot s^{-1}$ respectively, comparable to velocities under similar conditions expected from ATP. Synthetic myosin filaments, length 2.6±0.6 μm, immobilized on a quartz surface were observed at analogue concentrations from 0.2-50 nM as uniformly-bright fluorescent images in the microscope with evanescent-wave laser excitation. On displacing Cy5-EDA-ATP with excess ATP, filament fluorescence decayed exponentially with rate constant 0.047±0.022 s^{-1}. At 50 pM Cy3-EDA-ATP discrete fluorescent spots were seen on the filaments, with lifetimes up to 100 s. In further analysis of these single molecule events power spectral densities of intensity fluctuations in individual filament fluorescence were computed from time sequences of digitized images and fitted to a Lorentzian model with corner frequency 0.018 Hz. This indicates that observations of fluorescence from these molecules while bound to myosin filaments follow a simple stochastic process with half-lifetime 9 s.

M-Pos31

CROSS-LINKING OF THE ACTO-MYOSIN S-1 COMPLEX AT THE HYDROPHOBIC BINDING INTERFACE ((R. Bertrand and R. Kassab)). CRBM-CNRS, INSERM U 249, Montpellier, France. (Spon. M. Le Maire)

The complex of Ni (II) and the tripeptide Gly-Gly-His was recently shown to catalyze, in the presence of monoperoxyphtalic acid, a highly specific protein-protein cross-linking *via* an oxidative radical pathway involving mainly aromatic side-chains and not at all nucleophilic residues [Brown *et al.* (1995) Biochemistry **34**, 4733]. We have taken advantage of this unprecedented cross-linking system to directly and selectively probe in solution the structure and functioning of the strong, hydrophobic and stereospecific acto-S-1 interaction interface in comparison with its atomic model which predicts the occurrence of aromatic amino acids at the contact sites of both actin and S-1. Following verification of the structure of the Ni (II)-peptide chelate and of its oxidized active form by mass spectrometry, rigor complexes of F-actin and S-1 or proteolytic S-1 derivatives were readily cross-linked under various controlled conditions and without apparent alteration of the acto-S-1 recognition. Only two covalent adducts were formed and were identified by specific immunochemical reactions. One included actin and the central 50 K heavy chain fragment ; the other one contained actin and the C-terminal 20 K fragment and its production depended on the attachment of the latter fragment to the 50 K-20 K junction. The mapping of the cross-linked sites in both species is in progress. The data point to the general usefulness of this cross-linking approach to directly study the hydrophobic binding interface of motor proteins in complexes with actin filaments or microtubules.

M-Pos32

FLUORESCENCE ENERGY TRANSFER DISTANCES WITHIN THE CHICKEN SKELETAL MYOSIN REGULATORY DOMAIN. ((Lakshmi D. Saraswat and Susan Lowey)) Rosenstiel Research Center, Brandeis University,Waltham, MA 02254.

The regulatory domain (RD), or neck region of the myosin head, consists of two classes of light chains that stabilize an α-helical segment of the heavy chain. RD from chicken skeletal muscle myosin was prepared in *E. coli* by coexpression of a 9-kDa heavy chain fragment with the essential light chain (ELC). Recombinant regulatory light chain (RLC), wildtype or mutant, was added separately to reconstitute the complex. Purified RD migrated as a single homogeneous peak by gel filtration and sedimentation velocity. The affinity of RD for divalent cations was determined by measuring the change in fluorescence of heavy chain tryptophans (-WPW-) upon addition of calcium or magnesium. The single endogenous tryptophan of the RLC was replaced by phenylalanine, and the ELC contains no tryptophans. The complex bound divalent cations with high affinity, similar to the binding data reported for native myosin. The intrinsic fluorescence of the two tryptophans was used as a donor to measure the resonance energy transfer (RET) distance to a single IAEDANS-labeled cysteine at position 2 on the RLC. Dansylated Cys2 could also serve as a donor by preparing RLC with a second cysteine at position 79 which was labeled with an acceptor probe. These RET distances (R=25-30 Å), together with a previous distance of 30 Å from Cys2 to Cys155 (Wolff-Long et al., J.Biol.Chem. in press) suggest that the N-terminus of the RLC, which includes the phosphorylatable serine, is unlikely to modulate myosin's activity by a direct interaction with residues in the C-terminus.

M-Pos33

STRUCTURAL EXPLANATIONS FOR THE ANGULAR DISTRIBUTION OF SPIN PROBES IASL AND MSL IN MYOSIN ((J. David Lawson*, †Ed Pate, Ralph G. Yount*, and Ivan Rayment¥)) *Department of Biochemistry and Biophysics, Washington State University, Pullman, WA 99164. †Department of Mathematics, Washington State University, Pullman, WA 99164. ¥Department of Biochemistry and Institute for Enzyme Research, University of Wisconsin, Madison, WI, 53705.

We have modeled the electron paramagnetic resonance (ESR) spin labels IASL and MSL into the nulceotide-free chicken skeletal myosin subfragment 1 (S1) crystal structure. The spin labels were modeled as covalently bonded to the reactive sulfhydryl, Cys-707 (SH1), which sits at the bottom of a ~10 Å deep pocket (the SH1 pocket). Molecular dynamics simulations were then performed on both the IASL-S1 and MSL-S1 models. The angular distributions in the preliminary simulations were compared to the fiber axis according to the S1•actin rigor structure proposed by Rayment et al (1993. *Science 261*: 58-65). The angular distribution of IASL with respect to actin was centered at 69° with a full width at half maximum of ~22°. The angular distribution of MSL was centered at 86° with a full width at half maximum of ~19°. These results compare to the experimental values of 68° and 82° for IASL and MSL respectively, both with full widths at half maximum of ~15° (Thomas and Cooke. 1980. *Biophys. J.* 32: 891-906). The simulations reveal that the main reason for the difference between the orientation of IASL and MSL is due to the steric interactions of the groups which link the nitroxide spin probes to SH1. The iodoacetamide linking group of IASL sits lower in the SH1 pocket than the bulkier maleimide linking group of MSL, thus causing IASL and MSL to be oriented within the pocket differently. Further molecular dynamics simulations are currently being conducted on spin-labeled S1 with nucleotide bound. This work was supported by NIH grants DK05195 (R.G.Y) and AR39643 (E.P.) and by a NIH Biotechnology Training grant GM08336 (J.D.L.). E. Pate is an AHA Established Investigator.

M-Pos34

MOLECULAR SIMULATIONS OF THE "BACK DOOR" IN MYOSIN ((J. David Lawson*, Ralph G. Yount*, and Ivan Rayment†)) *Dept. of Biochemistry and Biophysics, Washington State Univ., Pullman, WA 99164. †Dept. of Biochemistry and Institute for Enzyme Research, Univ. Wisconsin, Madison, WI, 53705.

Myosin, the molecular motor responsible for muscle contraction, has recently been identified as a possible "back door" enzyme (Yount et al. 1995. *Biophys. J. 68*: 44s-49s). The back door (a secondary entrance/exit to the active site) is evident in the recently solved crystal structure of truncated *Dictyostelium* S1 complexed with the ATP analog ADP•BeF_X (Fisher et al. 1995. *Biochemistry 34*: 8960-72). In this structure, the BeF_X group can be observed through an opening (the back door) at the base of the major cleft in the 50 kDa fragment. The glycine-rich P-loop and the highly conserved residues Lys-185, and Arg-238 frame the back door. Movements of any of these residues, especially P-loop residue Ser-181, could easily expand the opening allowing the cleaved γ-phosphate (Pi) to leave without displacing the bound ADP. This is important since the cleaved Pi is buried deep within the nucleotide binding pocket and can not exit the active site through the "front door" unless ADP leaves first. Thus, this mechanism explains several previous experimental observations which indicate that Pi can leave the active site while ADP remains bound. In the present work we conduct molecular dynamics simulations of the chicken skeletal S1 crystal structure active site and back door regions. These simulations, run with Mg•ADP•Pi in the active site, indicate that the side chains which frame the back door are quite mobile under the influence of thermal motion. This may enable the back door to "breathe" and thus allow the orthophosphate product of ATP cleavage to escape through this opening. This work was supported by NIH grants DK05195 (R.G.Y.) and AR35186 (I.R.) and by a NIH Biotechnology Training grant GM08336 (J.D.L.).

M-Pos35

MYOSIN HEAVY CHAIN SEQUENCE VARIATIONS IN THE MOTOR DOMAIN DETERMINE THE ATPASE TURNOVER RATES OF MOLLUSCAN MYOSINS. ((C.L.Perreault, V.N. Kalabokis, A.G. Szent-Györgyi)) Brandeis University, Waltham, MA 02254
(Spon. by E. Marder)

ATPase activities of *Placopecten* catch muscle myosin are 2-3 fold lower than those of striated. To determine which subunits may be responsible for the different enzymatic properties of these myosins, we cloned and sequenced the cDNA encoding the essential light chain (ELC), regulatory light chain (RLC) and heavy chain (HC) of *Placopecten* catch and striated muscle myosins. The ELC was identical in catch and striated myosins, therefore, this subunit cannot account for the different activities. We found 3 different RLC isoforms, 2 in catch and 1 in striated (*cf Patinopecten*; Miyanishi *et al., J. Biochem.*, 1985). However, hybrids with the expressed recombinant RLC isoforms indicated that ATPase activity was independent of the particular RLC isoform. Sequences of the HC of striated myosin (1941 amino acids) and catch myosin (1951 amino acids) revealed 2 isoforms that differ only in 5 small regions due to the alternative RNA splicing of a single HC gene. Three spliced regions are within the motor domain, 1 is at the S2 hinge, the last is a non-helical tailpiece in catch HC only. S1 activity reflected the differences observed in the parent myosins. Actin-activated ATPase of S1 indicated a lower V_{max} of catch compared to striated (8 versus 20 s^{-1}) and only little change in actin affinity. These data indicate that the different ATPase activities of catch and striated myosins are due to HC sequence variations within the motor domain. (Supported by NIH Grant AR15963 and MDA.)

M-Pos36

PREPARATION AND PROPERTIES OF SINGLE-HEADED SCALLOP MYOSIN. ((V. N. Kalabokis, P. Vibert, M. York, and A. G. Szent-Gyorgyi)) Brandeis University, Waltham, MA 02254. (Spon. by C. Cohen).

Single-headed scallop myosin was prepared by digesting scallop myosin with papain and separated from rods and undigested myosin by hydrophobic interaction chromatography. The purified product was shown to be single-headed myosin by (i) its electrophoretic analysis under native and denaturing conditions and (ii) its shape in electron micrographs which shows the presence of only one domain to which the rod is attached. Single-headed myosin and myosin had similar specific activities per active site. Calcium sensitivity (% inhibition of ATPase on removal of calcium) of single-headed scallop myosin ranged 60-70% both in the presence and absence of actin. This sensitivity is lower than that of the undigested myosin fraction (~85% sensitivity). The Ca^{2+}-dependence of ATPase activity paralleled Ca^{2+}-binding which showed the presence of a single site that binds Ca^{2+} with an association constant of 1.2×10^7 M^{-1}. The Ca^{2+}-dependence of ATPase activity of single-headed myosin is in sharp contrast to that of intact myosin which is activated by Ca^{2+} in a highly cooperative fashion. (Supported by NIH Grant AR15963 and MDA.)

M-Pos37

BINDING OF Ca^{2+} AND NUCLEOTIDES BY SCALLOP MYOSIN AND ITS PROTEOLYTIC FRAGMENTS HMM AND S1. ((V. N. Kalabokis and A. G. Szent-Gyorgyi)) Brandeis University, Waltham, MA 02254

Binding studies with scallop HMM were carried out with a highly regulated HMM preparation (Ca^{2+}-sensitivity > 90%) which was prepared by tryptic digestion of scallop myosin and separated from unregulated molecules by anion exchange chromatography. The preparation contained two major heavy chain fragments and both essential light chain and regulatory light chain.

The binding of Ca^{2+} and nucleotides to regulated scallop myosin and scallop HMM is interdependent in contrast to the unregulated scallop S1. In the presence of nucleotides (ADP or AMP-PNP) scallop myosin and scallop HMM bind Ca^{2+} cooperatively while in the absence of nucleotides both specific Ca^{2+}-binding sites bind Ca^{2+} independently. Binding of ADP or AMP-PNP by scallop myosin and scallop HMM is cooperative in the absence of Ca^{2+} and non-cooperative in the presence of Ca^{2+}. Ca^{2+} and nucleotides bind antagonistically to scallop myosin and scallop HMM but do not influence their respective binding to the unregulated scallop S1. The simplest explanation for these observations is that the Ca^{2+} and nucleotides binding sites interact through contacts among the myosin subunits which are strenghtened by nucleotides and weakened by Ca^{2+}. (Supported by NIH Grant AR15963 and MDA.)

M-Pos38

SMOOTH MUSCLE MYOSIN LONG S1 BUT NOT SHORT HMM MOVES ACTIN FILAMENTS INDEPENDENTLY ON PHOSPHORYLATION. ((Masataka Sata, Motoi Matsuura, Mitsuo Ikebe)) Department of Physiology, University of Massachusetts Medical Center, Worcester, MA 01655.

To investigate the mechanism of smooth muscle myosin regulation, we produced truncated smooth muscle myosin heavy chains containing various lengths of S2 portions using baculovirus expression system (FEBS letters 363 (1995) 246-250). Nondenaturing gel electrophoresis and gel filtration studies revealed that SM1153 (Met^1-Glu^{1153}) exists as a heavy chain dimer whereas SM944 (Met^1-Ser^{944}) exists as a monomer when co-expressed with essential and regulatory light chains. While SM1153 was properly regulated by phosphorylation, SM944 was active in phosphorylated (P) and dephosphorylated (DP) states. However, the sliding velocity of SM944 was only half of that of phosphorylated SM1153. Actin activated ATPase activity (nmol/mg/min) and sliding velocity of actin filaments (μm/s) at 25 °C in an *in vitro* motility assay were as follows.

	SM1153		SM944	
	P	DP	P	DP
ATPase activity	53 ± 12	1.4 ± 0.2	48 ± 5	52 ± 6
Sliding Velocity	0.59 ± 0.11	0	0.27 ± 0.04	0.27± 0.05

Conclusion: The two-headed structure of smooth muscle myosin is crucial for proper phosphorylation-dependent regulation. Supported by NIH.

M-Pos39

SEQUENCE DETERMINANTS FOR A MYOSIN HINGE. ((M.J. Redowicz, D.C. Rau*, E.D. Korn, and J.A. Hammer III)) *LBM, NIDDK AND LCB, NHLBI, NIH, Bethesda, MD 20892.

Electron micrographs of *Acanthamoeba* myosin II (MII) reveal a single flexible site or hinge in its otherwise rigid rod-like tail. At the corresponding position in the sequence is a stretch of ~25 residues that are nonhelical, are devoid of the hydrophobic heptad repeat, and contain a helix-breaking proline. Measurements made using electric birefringence (EB) on minifilaments (MF) are consistent with an average bend of 20° at this site. We have now expressed as GST fusion proteins the wild type MII rod, a mutant rod in which the proline has been changed to an alanine, and a mutant rod in which the entire hinge region has been deleted. These proteins were purified to homogeneity, the GST moiety was removed, and the flexibilities and bend angles of the assembled rod molecules were assessed by EB. MF made with the wild type rod exhibited the same bend identified previously in native MII MF. MF made with the deletion mutant, on the other hand, were completely inflexible. Interestingly, MF made with the point mutant were no longer bent, although they did retain considerable flexibility. These results confirm that the flexibility resides entirely within the hinge domain, and indicate that while hinge residues other than the proline confer significant flexibility, the proline is required for the normal bend to occur. The creation of MII molecules that possess variable degrees of flexibility should reveal the role that the hinge plays in the MF-based regulation of MII.

M-Pos40

Ca^{++}-REGULATION AND MYOFIBRILLAR STRUCTURE IN HUMAN CARDIOMYOPATHIC HEARTS. ((S.S. Margossian, P.A.W. Anderson, P. Norton, J.B. Caulfield, P.D. Chantler, H.S. Slayter)) Alb Med Col, Albany, NY 12208; Duke U Med Ctr, Durham, NC; U Alabama, Birmingham, AL; Royal Vet Col, London, UK; Dana-Farber Can Inst, Boston, MA.

A significant change in myofibrillar structure during idiopathic dilated cardiomyopathy (IDC) is the proteolysis of myosin LC2, TnT and TnI as reported (SSM et al., 1992) and since confirmed (Corbett et al., 1995). The breakdown is mediated by a neutral protease, mekratin, active during IDC. The protease was purified from ventricular tissue and the increased purity and activity monitored by SDS-PAGE and casein zymograms. An internal tryptic peptide was coupled to KLH in order to raise polyclonal antibodies against it. The effect of the protease on myofibrillar activity is seen in both thin and thick filaments: in thick filaments there is a continuous cleavage of LC2 with consequential changes in myosin assembly and enzymatic activity. In thin filaments, degradation is evidenced by breakdown products of troponin, primarily TnT but also TnI, and a shift in TnT isoform expression is also seen in some patients. Ca^{++}-binding measurements with myofibrils indicate a shift to a higher Ca^{++} requirement in IDC samples, while a reduced Ca^{++}-sensitivity is observed by a decrease in the inhibition of MgATPase activity in the presence of EGTA. Thus, IDC appears to be characterized not only by structural and functional alterations within the muscle proteins of the heart, but also, a genetic element inducing preferential expression of one of the troponin T isoforms in some individuals.

M-Pos41

PARTIAL cDNA SEQUENCE OF THE NEUTRAL PROTEASE MEKRATIN AND PROBING HUMAN CARDIOMYOPATHIC HEART RNA. ((J.C. Holt, J.B. Caulfield, P. Umeda, H.S. Slayter, L. Martino, J.A. Melendez, S.S. Margossian)) Rhône-Poulenc Rorer, King of Prussia, PA; U Alabama, Birmingham, AL; Dana-Farber Can Inst, Boston, MA; Alb Med Col, Albany, NY 12208. (Spon. by J.E. Estes)

Using sequences of two internal peptides obtained from a purified hamster protease responsible for cleavage of myosin LC2 and troponin subunits during idiopathic dilated cardiomyopathy (IDC), degenerate oligonucleotide probes were constructed for RTPCR to obtain a cDNA fragment of the protease. The resulting cDNA fragment was comprised of 150 base pairs and its nucelotide and corresponding amino acid sequences were determined. Probes for human heart myosin ELC and RLC were also generated by a similar approach using control human cardiac RNA. In order to determine (1) the level of expression of the protease and (2) the degree of expression of LC1 and LC2 and their ratios in control and IDC hearts, RNA prepared from two control individuals and three IDC cases were probed by Northern blots. In the case of the protease, total ventricular tissue extracts from control and IDC samples were also analyzed by Western blots using a polyclonal antibody raised against one of the internal protease peptides coupled to KLH. The results suggest a possible decrease in the level of expressed mRNA for one of the light chains, LC2, in IDC hearts. A decrease in LC2 was also observed and reported earlier during IDC, due to proteolysis catalyzed by the neutral protease, mekratin, active in IDC hearts.

M-Pos42

A COMPARATIVE STUDY OF NONMUSCLE MYOSIN HEAVY CHAINS A AND B DURING EMBRYONIC DEVELOPMENT IN *XENOPUS LAEVIS*. ((N. Bhatia-Dey, M.A. Conti and R.S. Adelstein)) NHLBI, NIH, Bethesda, MD 20892-1762.

Nonmuscle myosin IIs are a distinct class of myosins that are thought to participate in diverse cellular processes such as cytokinesis and cell shape changes. Earlier we had reported the cDNA cloning and partial characterization of nonmuscle myosin heavy chain B (MHC-B) from *Xenopus laevis* (Bhatia-Dey et al., *Proc. Natl. Acad. Sci.* **90**, 2856, 1993). We now report that the MHC-B transcripts are evenly distributed throughout the embryo in blastula, gastrula, and early neurula stages. In the late neurula the transcripts begin to localize in the anterior part of the embryo and in differentiated somites. As development proceeds the transcripts become concentrated in differentiated somites. In swimming tadpoles they are localized in differentiated somites, developing eye, branchial arches, and brain. We also isolated the cDNAs for a closely related but distinct isoform representing *Xenopus* nonmuscle myosin heavy chain A (MHC-A). A probe including part of the rod and 3' UTR of *Xenopus* MHC-A detects 2 transcripts by Northern analysis: i) a 7.5 kb transcript which is present at a similar level from unfertilized eggs to stage 40 and ii) an 8.3 kb transcript that is first detected at stage 15, peaks at stage 25-30 and is barely detected by stage 47. In adult tissues a single 7.5 kb transcript is detected for both MHC-A and MHC-B isoforms. Currently we are trying to understand the role of these myosin isoforms during *Xenopus* embryogenesis.

M-Pos43

EFFECT OF METAL IONS ON THE CONFORMATION OF MYOSIN S1-NUCLEOTIDE COMPLEXES: A CD STUDY. ((K. Ajtai[1], Y.M. Peyser[2] and A. Muhlrad[2])) [1]Mayo Clinic & Foundation, Rochester, MN 55905 and [2]Hebrew University, Jerusalem 91120, Israel.

The predominant intermediate of the myosin (M) catalyzed ATP hydrolysis is the M**.MgADP.Pi complex, which can be stabilized by substituting Pi with phosphate analogs (PA), such as vanadate (Vi), beryllium or aluminum fluoride (BeF_x, AlF_x). We compared the structure of the S1.MgADP.Pi, S1.MgADP and S1.MgADP.PA complexes in the vicinity of aromatic residues by recording their near uv CD spectra and studied the effect of Mg substitution on their conformation. The CD spectra of S1.MgADP and S1.MgADP.BeF_x resembles that of S1.MgADP.Pi, while the spectrum of S1.MgADP.AlF_x is similar to that of S1.MgADP, which may indicate structural similarities between the relevant complexes. Mg was substituted with Fe^{2+}, Mn^{2+}, Ni^{2+}, Co^{2+} or Ca^{2+}. All these metals (Me) support the formation of the S1-nucleotide complexes (Peyser et al., 1994, Biophys. J. 66:A75). The S1.MeADP.Pi and S1.MeADP spectra are similar to each other in the presence of all metals with the exception of Mg, which points to the specific role of Mg in the conformational change occurring upon dissociation of Pi. The spectra of the S1.MeADP.Vi and S1.MeADP.BeF_x complexes depend on the nature of the metal present. In the CD spectra of the S1.Me.ADP.Vi complexes a new peak appears in the 330-350 nm region corresponding to the absorption peak of Vi, which shows that Vi becomes chiral upon binding to the active site. This peak is also metal ion dependent. The results indicate the structural significance of the specific coordination of the divalent cations to the active site residues of myosin. Supported by NIH R01AR 39288, AHA 930 06610 and the Mayo Foundation.

M-Pos44

MOLECULAR GENETIC EXPRESSION AND CHARACTERIZATION OF CHICKEN BRUSH BORDER MYOSIN I. ((F. Wang, M.A. Conti, H. Jiang, E.V. Harvey, and J.R. Sellers)) Laboratory of Molecular Cardiology, NHLBI, NIH, Bethesda, MD 20892-1762. (Spon. by M.D. Pato)

We have co-expressed full-length chicken brush border myosin I heavy chain (BBMI cDNA clone was a gift from K. Collins and P. Matsudaira) along with calmodulin as light chains (CaM virus was a gift from C. Montell and A. Kreuz) in the Baculovirus/Sf9 cell system using pVL1393 as the transfer vector. Soluble myosin I was extracted from the infected cells using ATP and high speed centrifugation. The expressed BBMI binds to actin in an ATP-dependent manner, a property we used to aid in purification. An antibody raised against the carboxyl terminal 14 amino acids of the BBMI heavy chain sequence was used to immunoprecipitate BBMI or capture BBMI for *in vitro* motility studies. The expressed myosin I translocates actin filaments at a rate indistinguishable from that of tissue-purified myosin I. The movement of actin filaments by the expressed BBMI is inhibited by Ca^{++} and by tropomyosin, which is characteristic of BBMI purified from tissue. We are currently expressing a carboxyl terminal, FLAG-tagged, BBMI heavy chain for further studies, and we are investigating the structure/function relationships of myosin I by introducing various point mutations.

M-Pos45

CONFINED MOVEMENT OF ACTIN FILAMENTS ON HMM ADSORBED BY POLYMETHYL METHACRYLATE FILM TRACKS ((H. Suzuki & S. Mashiko)) Kansai Adv. Res. Center, C.R.L., Kobe 651-24, Japan (Spon. by A. Yamada)

In the most of the *in vitro* motility assay systems, actin filaments moved on myosin-coated glass surface in the random direction because of uniformly and randomly distributed myosin molecules on the surface. We had previously proposed in order to control the moving direction another system in which actin filaments moved linearly on myosin-coated PTFE ridges. This system, however, included two weaknesses; the velocity of actin movement on the PTFE substrate was slower than that on a siliconized glass and parallel running tracks was the only pattern to be made. We have developed a new *in vitro* system where actin filaments moved on tracks of polymethyl methacrylate (PMMA) made by lithography. PMMA was obtained from Tokyo Ohka Kogyo Co. (OEBR-1000) and thin film of PMMA was prepared by spin casting at 4000 rpm for 90 s from the ethyl cellosolve acetate solution on a cover slip. After baking at 170 °C for 20 min, the film was irradiated with deep UV through a mask which contained various patterns such as concentric circles. The films were developed and then baked at 170 °C for 20 min. This procedure produced tracks of PMMA, whose heights were about 500 nm and widths were about 1 μm. HMM molecules were adsorbed on the tracks and actin filaments moved on the tracks in the presence of ATP. The mean velocity on PMMA tracks was and about 4.5 μm/s (25 °C) and was faseter than that on a PTFE ridges.

M-Pos46

STRUCTURAL TRANSITIONS IN RELAXED SKINNED MUSCLE FIBER WHILE CHANGING TEMPERATURE AND IONIC STRENGTH ((S.Malinchik, S.Xu and L.Yu)) NIH, Bethesda, MD 20892.

At room temperature relaxed skinned rabbit psoas fibers produce X-ray diffraction pattern with strong myosin based system of layer lines. Our analysis and fitting by computer modeling of the first six myosin layer lines suggest that the crossbridges form a helix close to the surface and wrap around the thick filament backbone. With temperature decreasing to 4°C the layer lines decrease in intensity considerably and diffuse scattering increases. These data suggest that some fraction of crossbridges becomes disordered (see also Wray,1987; Lowy et al.1991) and ordered fraction of crossbridges decreases. Analysis of the first layer line indicates that the ordered fraction of crossbridges moves radially from the backbone surface and that the mass of the fraction decreases at least by factor of two leading to higher diffuse scattering. On the other hand, lowering of ionic strength, at 4° and 25°C, the axial position of the first layer line shifts toward actin filament spacing. This can be modeled by increasing the number of crossbridges which attach to actin at varied angles, non-stereospecifically.

M-Pos47

BINDING OF RABBIT SKELETAL MUSCLE PHOSPHOFRUCTOKINASE TO THE FILAMENTS FORMED BY SKELETAL MUSCLE MYOSINS FROM GROUND SQUIRREL AT DIFFERENT STAGES OF HIBERNATION. ((N.A.Lukoyanova, S.N.Udaltsov, Z.A.Podlubnaya)) ITEB RAS, Pushchino Moscow region, 142292 Russia. (Spon. by A.Orlova)

We have previously shown the capability of phosphofructokinase (PFK) to bind both to reconstituted myosin filaments and thick filaments from rabbit skeletal muscle (Freydina *et al.*, JMRCM, 1986, 7, 481). Here we present data on changes in PFK-binding to the filaments formed by myosins isolated from skeletal muscles of active (Act), hibernating (Hib) and arousing (Ar) ground squrrels *Citellus undulatus*. Because there are data on the identity of PFK-properties from euthermic and hibernating animals (Hachimi *et al.*, Comp.Biochem.Physiol., 1992, 102b, 507) we used PFK from rabbit skeletal muscle in binding assays. PFK-binding to myosin was tested by sedimentation under the same conditions. PFK-binding to Act-myosin and to Ar-myosin appeared higher by 1.5 times than to Hib-myosin. We concluded that the changes in PFK-binding are due to the changes in myosins and it is consistent with our previous data on the structural properties of myosins from ground squirrels at different states.

M-Pos48

DOMAIN ANALYSIS OF MYOSIN-BINDING PROTEINS C AND H (MyBP-C AND MyBP-H) OF CHICKEN SKELETAL AND CARDIAC MUSCLE. ((T. Alyonycheva,T. Mikawa, D.A. Fischman)). Department of Cell Biology and Anatomy, Cornell University Medical College, 1300 York Avenue, New York, NY 10021 (Spon: D.A. Fischman)

Although present in all vertebrate striated muscle, the functions of MyBP-C and MyBP-H (C and H protein) remain ill-defined. In our laboratory full length cDNAs encoding chicken and human skeletal MyBP-H and MyBP-C have been isolated and sequenced. All are members of a protein family characterized by repetitive Immunoglobulin (Ig) C2 and fibronectin (Fn) type III motifs. We have shown before that the major myosin-binding domain of chicken fast-type MyBP-C resides in a 14kDa C-terminal chymotryptic peptide containing a single Ig C2 repeat. In this report, we have extended the domain analyses to cardiac MyBP-C and skeletal muscle MyBP-H. Limited α-chymotryptic digestion of cardiac MyBP-C generated three peptides, similar in size to those of skeletal MyBP-C: ~100, 40 and 15kDa. Tryptic digestion of MyBP-H produced two peptides: 50 and 14kDa. Partial amino acid sequences of these peptides revealed that the 15 and 14kDa fragments contain the C-terminal amino acid regions of cardiac MyBP-C and skeletal MyBP-H, respectively. All fragments were analyzed for myosin binding by a sedimentation assay. Only the 14 and 15kDa peptides exhibited high affinity binding to myosin. We conclude that the predominant myosin binding site in all three proteins resides within an homologous, C-terminal Ig C2 domain. We have also analyzed the binding reactions between the skeletal and cardiac MyBPs and the corresponding skeletal or cardiac myosin filaments. Both proteins and their C-terminal peptides exhibit saturable binding to myosin but there is higher limiting stoichiometries with the homologous isoform partners. Hill and Scatchard plots showed strong positive cooperativity for binding skeletal and cardiac MyBP-C and skeletal MyBP-H to both skeletal and cardiac myosin. The number of binding sites per mole of myosin for skeletal MyBP-H, cardiac and skeletal MyBP-C was ~3, 2.5 and 2, respectively. (Supported by NIH AR32147, HL45458, and the MDA.)

M-Pos49

LARGE SCALE PURIFICATION OF NATIVE THICK FILAMENTS FROM SKELETAL MUSCLE. ((M.E. Rodgers and J.S. Davis)) Department of Biology, Johns Hopkins University, Baltimore, MD 21218.

Preparation of sufficient quantities of pure native thick filaments for physical studies requires complete separation from contaminating thin filaments. Using previous methods, it was only feasible to prepare small quantities of rather pure material [Trinick, J.A. (1982) *Meth. Enzymol.* 85:17-20]. We have developed a simple procedure for large scale purification of native thick filaments. As in earlier methods, psoas muscle tissue was briefly homogenized in relaxing buffer to obtain a suspension of thick and thin filaments. After centrifugation to remove debris, bacterial expressed gelsolin fragment Fx-45 [Yu, et al. (1991) *J. Biol. Chem.* 266:19269-75, Granzier, H.L.M and Wang, K. (1993) *Biophys. J.* 65:2141-59] was added in slight excess over the actin monomer concentration to depolymerize the thin filaments. Optimal separation of native thick filaments from depolymerized thin filament proteins was obtained by chromatography on a Sephacryl S-500 gel filtration column. Assay of the column fractions indicated complete separation of thick filaments from contaminating thin filament proteins. Electron microscopy of the native thick filament fractions showed intact thick filaments alone. No thin filaments were seen in the numerous fields examined. This method is simple, inexpensive and easily scaled for purification of large amounts of native thick filaments. Supported by NIH grant AR-04349 to JSD.

E-C COUPLING I

M-Pos50

FUNCTIONAL DOMAINS OF THE DIHYDROPYRIDINE RECEPTOR (DHPR) α_1 SUBUNIT II-III LOOP: "ACTIVATOR" DOMAIN. ((R. El-Hayek[1], and N. Ikemoto[1,2])). 1, Boston Biomed. Res. Inst.; 2, Dept. Neurology, Harvard Med. Sch., Boston, MA.

A synthethic peptide corresponding to the residues Thr^{671}-Leu^{690} of the rabbit skeletal muscle DHPR α_1 subunit II-III loop (Peptide A) activated ryanodine binding to the RyR and induced Ca^{2+} release from SR (El-Hayek et al. 1995, *J. Biol. Chem.* **270**, 22116-22118). This suggested that this sequence represents the putative Activator domain of the II-III loop, whose binding to the RyR triggers E-C coupling. To further characterize the function of this domain, we investigated both $[Ca^{2+}]$- and dose-dependences of Peptide A binding to triads and peptide-induced activation of RyR conformational change and SR Ca^{2+} release. In the presence of 2 μM [^{3}H]Peptide A (peptide A-cys-[^{3}H] N-ethyl maleimide), at 0 μM Ca^{2+}, ≈ 130 pmoles ligand were bound per mg triad without producing conformational change and Ca^{2+} release. Upon increasing $[Ca^{2+}]$ to 1 μM, however, 2 μM peptide activated both conformational change in the RyR (increase in the MCA fluorescence) and Ca^{2+} release. This activation depended upon an additional Ca^{2+}-dependent peptide binding characterized by a B_{max} value of 50 pmol/mg and $K_{assoc.} = 8.1 \times 10^5\ M^{-1}$. Furthermore, the dose-dependence of activation of conformational change and Ca^{2+} release showed a close parallelism to that of peptide binding. We propose that the binding of one Activator domain of the loop to each RyR subunit is involved in the activation of both RyR conformational change and SR Ca^{2+} release. (Supported by NIH and MDA)

M-Pos51

FUNCTIONAL DOMAINS OF THE DIHYDROPYRIDINE RECEPTOR (DHPR) α_1 SUBUNIT II-III LOOP: "BLOCKER" DOMAIN. ((N. Ikemoto[1,2], B. Antoniu[1], and R. El-Hayek[1])). 1, Boston Biomed. Res. Inst.; 2, Dept. Neurology, Harvard Med. Sch., Boston, MA.

A synthethic peptide corresponding to the residues Glu^{724}-Pro^{760} of the rabbit skeletal muscle DHPR α_1 subunit II-III loop (Peptide C) blocked Peptide A-induced SR Ca^{2+} release, suggesting that this region of the loop may work as a Blocker (El-Hayek et al. 1995, *J. Biol. Chem.* **270**, 22116-22118). Here we report that (a) Peptide C produced a small but significant decrease in the fluorescence intensity of the RyR-bound MCA probe, and (b) T-tubule polarization also produced a decrease in the RyR-MCA fluorescence. Since the RyR-MCA fluorescence increases upon depolarization of the primed triad (Yano et al. 1995, *J. Biol. Chem.* **270**, 3017-3021), the fluorescence decrease reported here would represent a mechanism prerequisite to the subsequent depolarization-induced activation. Preincubation of triads with Peptide C produced a partial inhibition of polarization-induced MCA fluorescence decrease. We synthetized a new chimeric Peptide C in which the Glu^{726}-Pro^{742} sequence, reported as the critical determinant of the skeletal muscle-type Ca^{2+} transient (Nakai et al., 1995, *Biophys. J.* **68**, A372), had been replaced with the cardiac type sequence. Interestingly, this chimeric peptide produced no change in the MCA fluorescence. We propose that upon T-tubule polarization the blocking domain binds to the RyR, inducing a low MCA fluorescence state; upon depolarization, the blocker domain is removed. This de-blocking allows the activator domain to bind to the RyR, which induces an activating conformational change in RyR and SR Ca^{2+} release. (Supported by NIH and MDA).

M-Pos52

CLONING OF *JUNCTIN*, A MAJOR CALSEQUESTRIN (CSQ) BINDING PROTEIN OF JUNCTIONAL SARCOPLASMIC RETICULUM (SR). ((Lin Zhang, Annelise Jorgensen, and Larry Jones)) Krannert Institute of Cardiology, Indiana University School of Medicine, Indianapolis, IN 46202 and University of Toronto, Toronto, Ontario M5S IA8

Previously we identified a protein of apparent Mr = 26,000 as the major CSQ binding protein in cardiac and skeletal muscle junctional SR vesicles (Mitchell, R.D., *et al.* (1988) *J. Biol. Chem.* **263**, 1376). We have now purified the 26-kDa CSQ binding protein from canine cardiac SR vesicles and determined its complete primary structure by cDNA cloning. The cDNA insert encodes a polypeptide of 210 amino acids. The protein is composed of three domains: a short N-terminal domain located in the cytoplasm; a single transmembrane region; and a large intralumenal domain that comprises the bulk of the molecule and contains 55% charged residues. Significant homologies are noted with aspartyl β-hydroxylase and triadin. The same gene is expressed in cardiac and skeletal muscle tissues. The CSQ-binding activity of the 26-kDa protein and its codistribution with ryanodine receptors strongly suggest that the protein plays an important role in the organization and/or function of triad/dyads. We have named this protein *JUNCTIN*, based on its localization to the junctional membrane in heart and skeletal muscle.

M-Pos53

JUNCTIN, THE 26kd CALSEQUESTRIN BIND PROTEIN LOCALIZES TO JUNCTIONAL SR. A.O. Jorgensen*, W. Arnold*, C. Thompson* and L.R. Jones+ - *Dept. of Anat. and Cell Biology, U. of Toronto, Toronto M5S 1A8 Canada and +Dept. of Med. Krannert Inst. of Cardiology, Indianapolis, Indiana 46202.

Corbular (c) SR and junctional (j) SR in cardiac muscle have previously been identified as potential Ca^{2+} storage/release sites by demonstrating that calsequestrin, the ryanodine receptor (RR) and calcium are very densely distributed in these two specialized domains in situ. To further characterize the composition of the j-SR and c-SR the subcellular distribution of junctin, (J.Biol. Chem. 263, 2376 (1988)) and the RR have been compared in adult canine cardiac myocytes by double immunofluorescence labeling and confocal imaging. In ventricular myocytes junctin codistributes with the RR in discrete foci localized to the center of the I-band where j-SR and c-SR are localized. However, in some atrial myocytes and in Purkinje fibers strongly fluorescent junctin-positive foci are confined to the cell periphery while strongly flourescent RR-positive foci are localized at both the cell periphery and in I-band regions centrally located in these fibers. Because Purkinje fibers and many atrial myofibers lack transverse tubules, these results support the conclusion that junctin is mainly confined to j-SR at to the cell periphery and not detected in the calsequestrin and RR containing corbular SR extending from the network SR in the central regions of these fibers. To test this possibility immunoelectron microscopical studies of canine myocardial fibers are in progress.

Supported by grants from MRC of Canada (AOJ), HSFO (AOJ) and NIH (LRJ).

M-Pos54

IMMUNOLOCALIZATION OF RYANODINE RECEPTORS IN THE DEVELOPING MAMMALIAN HEART. ((S.A. Lewis Carl and D.G. Ferguson)) Department of Anatomy, CWRU, Cleveland, OH 44106.

In previous studies we have determined the subcellular distribution of dihydropyridine receptors (DHPR), ryanodine receptors (RyR) and triadin in adult rabbit ventricle and atrium (Lewis Carl et, al., J. Cell Biol., 129:673). The localization of the DHPR and the RyR has also been examined in the developing chick myocardium (Sun et al., J. Cell Biol., 129:659).

In the present study, we have immunolocalized the RyR in developing mammalian hearts (fetal day 18, newborn, early postnatal, and adult rat) using laser scanning confocal microscopy. As early as fetal day 18, clusters of RyR were observed as discrete foci at the cell periphery. In addition, faint cytoplasmic staining was observed in both the atria and ventricle at this age. In the day 1 neonatal heart the RyR was already distributed in a pattern similar to that observed in the adult heart. Discrete subsarcolemmal foci were highly ordered and aligned with brightly stained cytoplasmic striations in both the atrium and ventricle. Previous EM studies of the developing heart have suggested that the dyadic junctional components are not present or organized until 7-10 days after birth. Our data suggests that this view of the development of the EC coupling apparatus in mammalian heart must be re-evaluated.

Supported by NIH HL34779 and the AHA.

M-Pos55

INTERACTION OF THE JUNCTIONAL FOOT PROTEIN OF SKELETAL MUSCLE WITH TRIADIN AND DETERMINATION OF TRIADIN BINDING REGIONS. ((H. Fan, H.K. Motoike, and A.H. Caswell)) Dept of Pharmacology, University of Miami, Miami, FL 33136

Intact triadin binds reversibly to the junctional foot protein (JFP) of skeletal muscle, and its binding affinity with JFP is 40 nM. In order to determine the interacting domains of triadin with JFP, the following triadin fusion peptides have been synthesized: triadin 1 (1-49), 2 (68-389), 2a (68-278), 2a1 (68-163), 2a2 (165-240), 2b (242-389), 2b1 (242-297), 3 (370-706), 3a (370-562), 3b (551-706), 3b1 (551-672), and 3b2 (673-706) (Numbers in parenthesis indicate the corresponding amino acids within triadin). Iodinated JFP was employed to detect its binding to the triadin fusion peptides in Western blot overlay. The most strongly labelled band relative to its density in the Coomassie Blue Stain is triadin 2a, but triadin 2, 3, 3a, 3b and 3b1 are all labelled. No significant binding was detected to triadin 1 and 3b2, representing the N or C terminal 40 amino acids, respectively. This observation suggests that JFP bound strongly to the putative cytoplasmic loop of triadin between amino acids 100 and 270 and more weakly in the putative luminal region between amino acids 270 and 685. Among the domains on triadin 2, the JFP labels strongly to triadin 2a2, 2, 2b but not triadin 2a1 and 2b1. These data indicate that JFP selectively interacts with at least two domains of the triadin molecule.

The interactions of triadin with JFP can be both cytoplasmic and luminal since both of them are intrinsic proteins of the terminal cisternae. It is possible that both the net positive charges and the unique *KKEEK* repeats within triadin molecule may play an important role in binding to select regions of the JFP. Supported by AHA.

M-Pos56

4-CHLORO-M-CRESOL, A SPECIFIC TOOL TO DISTINGUISH BETWEEN MH NORMAL AND MH SUSCEPTIBLE MUSCLE. ((A. Herrmann-Frank, M. Richter and F. Lehmann-Horn)) Department of Applied Physiology, University of Ulm, D-89069 Ulm, Germany.

We have recently shown that 4-chloro-m-cresol (4-CmC) is a potent activator of the skeletal muscle ryanodine receptor (RyR1) isolated from the sarcoplasmic reticulum (SR) of rabbit back muscle (Herrmann-Frank et al., BBA, in press, 1995). To determine if 4-CmC is a suitable tool to distinguish between MH normal and MH susceptible muscle tissue, we examined the effect of 4-CmC on high-affinity [^{3}H]ryanodine binding to SR vesicles and purified solubilized RyR1 isolated from the *longissimus dorsi* of pigs with (MHS) and without porcine stress syndrome. [^{3}H]ryanodine binding was performed in the presence of low salt (0.1 M KCl) and 0.1 μM Ca^{2+}, a concentration we found no differences in activation between normal and MHS vesicles. Under these conditions, 4-CmC increased [^{3}H]ryanodine binding in concentrations up to 750 μM in both tissues. The EC_{50} value was about 193 μM for MHS and 395 μM for nomal SR. This enhanced 4-CmC affinity of MHS vesicles was confirmed when investigating the effects of 4-CmC on [^{3}H]ryanodine binding to the isolated Chaps-solubilized RyR1. The purified RyR1 isolated from MHS muscle also displayed a higher affinity for caffeine compared to the normal receptor. The sensitivity for 4-CmC, however, was found to be 20-30-fold higher than for caffeine.

It is therefore suggested that the RyR1 Arg615Cys mutation is causative for the hypersensitivity of MHS muscle to caffeine and 4-CmC.

M-Pos57

SPHINGOSINE INHIBITION OF [^{3}H]RYANODINE BINDING IS ALTERED IN MALIGNANT HYPERTHERMIA-SUSCEPTIBLE (MHS) PORCINE SKELETAL MUSCLE SARCOPLASMIC RETICULUM. ((R. Betto, G. Salviati, F. Turcato, M. Duca, and A. Teresi)) C.N.R. Unit for Muscle Biology and Physiopathology, Via Trieste 75, 35121 Padova, Italy.

We have previously reported that sphingosine is a potent inhibitor of skeletal and cardiac muscles sarcoplasmic reticulum (SR) ryanodine receptor. This study examines the effect of sphingosine on the [^{3}H]ryanodine binding properties of SR terminal cisterns (TC) membranes from MHS and normal pigs. Sphingosine caused a dose dependent inhibition of [^{3}H]ryanodine binding to both MHS and normal TC membranes, showing similar IC_{50} values (8.5 and 6.3 μM, respectively). However, at pCa 5, sphingosine caused a significantly higher inhibition of the apparent affinity for ryanodine in MHS than in normal TC membranes, whereas no differences were observed in the presence of 10mM ATP. [^{3}H]Ryanodine binding to MHS and normal TC membranes was greatly influenced by both pH and ionic strength. The inhibitory action of sphingosine was optimal at neutral pH and at physiological ionic strength. High KCl concentrations caused a dramatic reduction of sphingosine inhibitory effect on both MHS and normal TC membranes. On the contrary, increasing pH selectively attenuated sphingosine inhibition of the binding to normal TC membranes only, being ineffective in MHS membranes. Present results suggest a possible involvement of sphingosine in the altered behaviour of the MHS mutated ryanodine receptor. (Supported by Telethon Italy 469 and C.N.R.).

M-Pos58

CALMODULIN SENSITIVITY OF MH NORMAL AND MH SUSCEPTIBLE MUSCLE. ((S. O'Driscoll[1,2], A. Herrmann-Frank[1], T.V McCarthy[2] and F. Lehmann-Horn[1])) (1)Department of Applied Physiology, University of Ulm, D-89069 Ulm, Germany and (2)Department of Biochemistry, University College, Cork, Ireland. (Spon. by A. Herrmann-Frank)

The point mutation Arg615Cys of the skeletal muscle ryanodine receptor (RyR1) has been shown to be responsible for porcine stress syndrome, an equivalent to malignant hyperthermia in humans. Studies with isolated vesicles from sarcoplasmic reticulum (SR) revealed that Ca^{2+} release from MH susceptible (MHS) muscle is hypersensitive to Ca^{2+} and caffeine. To determine if an abnormal calmodulin regulation of SR Ca^{2+} release contributes to this hypersensitivity, we investigated the effect of calmodulin on high-affinity [^{3}H]ryanodine binding to SR vesicles from normal and MHS skeletal muscle of pigs. In the presence of high Ca^{2+} (pCa=4.3), calmodulin inhibited [^{3}H]ryanodine binding in concentrations between 10 nM and 10 µM, with no differences between normal and MHS vesicles. In the absence of Ca^{2+} (500 µM EGTA), calmodulin activated [^{3}H]ryanodine binding more strongly in MHS vesicles. Significant differences between normal and MHS tissue were observed for calmodulin concentrations between 50 nM and 10 µM. A polyclonal antibody raised against the central region of RyR1 specifically inhibited the activating effect of calmodulin, indicating that this region of RyR1 is a potential binding domain for calmodulin in the absence of Ca^{2+}. The above data suggest that in vivo calmodulin might contribute to the hypersensitivity of MHS muscle to Ca^{2+} and caffeine.

M-Pos59

ROLE OF THE MALIGNANT HYPERTHERMIA LOCUS IN THE GATING OF THE RYANODINE RECEPTOR Ca^{2+} CHANNEL. ((P. Menegazzi, S. Treves, M. Ronjat F. Zorzato)) Lab. BMC, URA 520 CNRS, CEA/CENG, DBMS, 17 rue des Martyrs, 38054 Grenoble Cedex 9, France, Istituto di Patologia Generale, Universita' degli Studi di Ferrara, 44100 Ferrara, Italy (Spon. P. Volpe)

50% of the human malignant hypertermia pedigrees are linked to point mutations in the ryanodine receptor gene, the Gly 341 to Arg being the most frequent missense mutation. RYR-fusion protein containing Gly 341 was used to raise monoclonal antibodies (Ab 419). Epitope mapping demonstrate that the 419 mAb react with a sequence a few residues upstream from the Gly 341. Triads vesicles were incubated 2h at 370C in presence or absence of Ab 419, and then passively loaded with $45Ca^{2+}$. Ca^{2+} release was measured using rapid filtration technique. Ca^{2+} releasing solution contained 25mM MES, 150mM KCl, 2mM EGTA, pH 7 and various concentrations of Ca^{2+} in order to obtain different pCa. Incubation of the vesicles with Ab 419 induced a 5 fold increase of the Ca^{2+} release rate at pCa 8. The effect of Ab 419 decreases when Ca^{2+} release is induced at lower pCa, and almost no effect observed at pCa 4. When Ca^{2+}. release is induced at pCa 5 in the presence of ATP and caffeine, the incubation with Ab 419 does not induce any further acceleration of Ca^{2+} release. These results provide biochemical evidence for the crucial role of the region containing Gly 341 in RyR Ca^{2+} channel gating. **(Supported by Association Francaise contre les Myopathies, M.U.R.S.T 40% and 60%, and Telethon Italy.)**

M-Pos60

HETEROGENEITY OF Ca^{2+} GATING OF SKELETAL MUSCLE RYANODINE RECEPTOR (RyR-1) COMPARED WITH CARDIAC RyR-2. ((Julio A. Copello, Sebastian Barg, Hitoshi Onoue, and Sidney Fleischer)). Department of Molecular Biology. Vanderbilt University. Nashville, TN 37235.

Rabbit skeletal muscle RyR-1 was compared with dog heart RyR-2 with regard to channel heterogeneity. Gating of both channels by Ca^{2+} was studied after incorporation of sarcoplasmic reticulum vesicles into planar lipid bilayers, with Ca^{2+} (trans) as charge carrier. Cytosolic free Ca^{2+} concentrations ($[Ca^{2+}]_i$) were varied from 20 nM to 10 mM, using dibromo-BAPTA as Ca^{2+} buffer. We found a remarkable difference between the complexity of RyR-1 and RyR-2 channel populations. RyR-2 appeared homogeneous with regard to activation by Ca^{2+}, both in the presence of 2 mM Mg^{2+} - 1 mM ATP (2 Mg^2/ATP1; free $[Mg^{2+}]_i$ ~ 1mM) or in the absence of both agents (no Mg^{2+}/ATP present). Most RyR-2 channels were closed at $[Ca^{2+}]_i$ ~ 0.1 µM, and were activated sharply with open probability (P_o) of 0.7-0.99 in the µM $[Ca^{2+}]_i$ range. The Hill coefficient for Ca^{2+} activation (n_H) was ~3 for the average channel. By contrast, RyR-1 showed extensive heterogeneity under comparable conditions. Two main groups of RyR-1 were identified: low activity (LA) channels (~20%), and high activity (HA) channels. LA RyR-1 never reached P_o greater than 0.1. Increasing $[Ca^{2+}]_i$ from 0.1 to 100 µM increased P_o of the average RyR-1 gradually; (n_H ~ 1, EC_{50} ~3 µM). Only HA RyR-1 were activated in the presence of $2Mg^{2+}$/1ATP by $[Ca^{2+}]_i$ (n_H ~ 1, and EC_{50} ~ 5 µM for the average channel), whereas LA RyR-1 remained closed. This heterogeneity in RyR-1 (skeletal muscle) contrasts with the sharp activation in a narrow Ca^{2+} range found with RyR-2 (heart). The differences in Ca^{2+} gating between RyR-1 and RyR-2 could have physiological significance. They may reflect the endogenous steady-state of the RyR in heart vs skeletal muscle, as required for calcium induced calcium release vs depolarization induced calcium release respectively. (NIH Grants HL32711 & H46681)

M-Pos61

PURIFICATION OF DIFFERENT ISOFORMS OF THE CALCIUM RELEASE CHANNEL/RYANODINE RECEPTOR FROM CEREBELLUM BY AFFINITY CHROMATOGRAPHY USING GST/FKBP12 AND GST/FKBP12.6 FUSION PROTEINS ((Hong-Bo Xin, Takashi Kanematsu, Loice Jeyakumar, Hitoshi Onoue and Sidney Fleischer)) Department of Molecular Biology, Vanderbilt University, Nashville, TN 37235

We have developed a new procedure to isolate RyR from skeletal muscle and cardiac muscle by exchanging endogenously bound FKBP on the RyR with the fusion proteins of glutathione-S-transferase(GST)/FKBP and then purifying the RyR using glutathione affinity chromatography (Xin et al. (1995) *Biochem. Biophys. Res. Communs.* 214, 263-270, and Timerman et al. (1995) submitted). In this study, the procedure has been applied to purify and separate RyR-1 and RyR-2 from the same tissue (cerebellum). The methodology is based on the further observation that RyR-2 specifically binds to FKBP12.6, a new isoform of FKBP, whereas RyR-1 binds both FKBP12 and FKBP12.6 with comparable tight affinity (Timerman et al. (1995) submitted). RyR-1 was first isolated from the CHAPS solubilized cerebellar microsomes by GST/FKBP12 exchange and affinity chromatography and then the RyR-2 remaining in the supernatant was purified using GST/FKBP12.6. The results show that a) RyR-1 and RyR-2 like receptors from cerebellum share similar characteristics with the RyR from skeletal muscle and cardiac SR, respectively, as studied by immunoreactivity and radioligand binding studies. (NIH HL32711, HL46681 and Muscular Dystrophy Association to SF)

M-Pos62

EVIDENCE FOR A SECOND TYPE OF FKBP BINDING SITE ON CARDIAC RYANODINE RECEPTOR (RyR-2)

((Sebastian Barg, Julio A. Copello, Hitoshi Onoue, and Sidney Fleischer))
Department of Molecular Biology. Vanderbilt University. Nashville, TN 37235.

The ryanodine receptor from skeletal muscle (RyR-1) is a hetero-oligomer with structural formula (RyR-1 protomer)$_4$(FKBP12)$_4$. Recently, dog heart RyR-2 was found to consist of a similar structural formula, albeit with a novel FKBP isoform (FKBP12.6) instead of FKBP12 (Timerman, Onoue, Xin, Barg, Wiederrecht, and Fleischer, 1995, submitted). In this study we used FKBP12 and FKBP12.6 in an attempt to modulate RyR-2 from dog cardiac sarcoplasmic reticulum (SR), which were incorporated into planar lipid bilayers. Calcium (trans) was used as charge carrier. The SR vesicles and FKBPs were added to the cis side of the bilayer, reflecting the cytosolic face of the channel. FKBP12.6 had no effect on control channels. FKBP12 induced a second open state of approximately two-thirds of the full conductance in a dose dependent manner. The effect was pronounced at physiological concentrations of FKBP12 (~3µM). Positive voltage applied to the cis side increased the frequency of the substates observed, whereas negative voltage decreased it. FKBP12.6 added in excess over FKBP12 did not influence the amount of substates observed. The results suggest that FKBP12 interacts with RyR-2 at a different site from FKBP12.6, and that cytosolic FKBP12 may modulate RyR-2. (Supported in part by NIH HL32711 and HL46681)

M-Pos63

CALCIUM ACTIVATION OF THE SKELETAL MUSCLE RYANODINE RECEPTOR IS INCREASED IN THE PRESENCE OF CHLORIDE. ((B.R. Fruen, P.K. Kane, J.R. Mickelson, and C.F. Louis)) Department of Veterinary PathoBiology, University of Minnesota, St. Paul, MN 55108.

We have examined the mechanism of Cl^--dependent Ca^{2+} release from the sarcoplasmic reticulum (SR) described by Sukhareva *et al.* (*Biophys. J.* 67: 751, 1994). The rate of Ca^{2+}-activated Ca^{2+} release from $^{45}Ca^{2+}$-loaded skeletal muscle SR vesicles was increased ~4-fold in 150 mM KCl *versus* in 150 mM Kpropionate, whereas Ca^{2+}-activated Ca^{2+} release from cardiac SR was similar in the two different salts. Ca^{2+}-activated [^{3}H]ryanodine binding to skeletal muscle SR was also increased ~4-fold when the buffer contained Cl^- instead of propionate, gluconate, or methanesulfonate, indicating that increased Ca^{2+} release in the presence of Cl^- was likely due to increased ryanodine receptor (RYR) channel activity. Activation of Ca^{2+} release and [^{3}H]ryanodine binding to skeletal muscle SR by 5 mM ATP, however, was unaffected by Cl^- (150 mM), suggesting that Cl^- primarily alters Ca^{2+} activation of the RYR channel. The Ca^{2+} activation of [^{3}H]ryanodine binding to the skeletal muscle RYR reconstituted into liposomes was increased ~4.5-fold relative to the Ca^{2+} activation of binding to native SR, with little additional stimulation by Cl^- (150 mM). This suggests that both high Cl^- and reconstitution may activate the RYR by reducing intermolecular interactions that limit Ca^{2+} activation *in situ*. We conclude that in experiments performed with these supraphysiological Cl^- concentrations or with reconstituted RYR protein, (ATP-independent) Ca^{2+} activation of the skeletal muscle RYR is exaggerated in comparison to that exhibited by native membranes at physiological Cl^- (2-10 mM).

M-Pos64

EVIDENCE FOR A SHORT SELECTIVITY FILTER AND SUCROSE BLOCKADE IN THE SKELETAL MUSCLE RYANODINE RECEPTOR/Ca^{2+} RELEASE CHANNEL. ((Ashutosh Tripathy, Le Xu and Gerhard Meissner)) Departments of Biochemistry and Biophysics, and Physiology, University of North Carolina, Chapel Hill, North Carolina, 27599.

Streaming potentials developed across the skeletal muscle ryanodine receptor (RyR)/Ca^{2+} release channel were measured after incorporating purified RyRs in lipid bilayer membranes and imposing osmotic gradients across the membrane by adding sucrose to only one side. When sucrose was added to the lumenal (trans) side the current-voltage (i-v) curves were linear and a streaming potential of 1.46 mV/osmol/kg was recorded. These data are in good agreement with previously published results of streaming potential in cardiac RyR (Tu et al., Biophys. J. 67:2280-2285, 1994). However, when sucrose was added to the cytosolic (cis) side, i-v curves were nonlinear. The conductance (g) appreciably decreased at positive potentials (trans defined as ground), indicating block by sucrose. g_{+40}/g_{-40} was about 0.5. The i-v curves were linear at negative holding potentials. Using this linear portion of the i-v curve a streaming potential of 1.48 mV/osmol/kg was recorded. Similar results were obtained when sucrose was added to the cytosolic side of cardiac RyR incorporated in planar lipid bilayer. The results indicate that the skeletal RyR has a short single-file constriction of < 10 Å which can accomodate at most 3 H_2O molecules. The results further indicate that sucrose, when added to the cytosolic side, can be swept into the channels at positive holding potentials (cation flux from cis → trans) and can act as a blocker in both skeletal and cardiac RyRs. Supported by NIH.

M-Pos65

REGULATION OF SKELETAL MUSCLE RYANODINE RECEPTOR/ CA^{2+} RELEASE CHANNEL BY MONO- AND DIVALENT IONS. ((Gerhard Meissner and Geoffrey Mann)) Department of Biochemistry and Biophysics, University of North Carolina, Chapel Hill, NC 27599

The effects of ionic composition on rabbit skeletal muscle ryanodine-sensitive Ca^{2+} release channel activity were investigated in vesicle-$^{45}Ca^{2+}$ flux and [^{3}H]ryanodine binding measurements. $^{45}Ca^{2+}$ efflux was slow when SR vesicles were loaded in KCl, KMes, cholineCl or cholineMes media and diluted into media containing $<10^{-8}$ M free Ca^{2+} and 5 mM Mg^{2+}. In the presence of 20 μM Ca^{2+}, a 30 -250-fold increase in the $^{45}Ca^{2+}$ efflux rate was observed. The highest efflux rate was measured in cholineCl medium followed by KCl, cholineMes, and KMes medium. The Ca^{2+}-dependence of channel activity was assessed by [^{3}H]ryanodine binding. In the above four media, a bell-shaped Ca^{2+} activation curve was obtained. However, only in cholineCl medium were observed substantial levels of [^{3}H]ryanodine binding at $[Ca^{2+}] < 10^{-8}$ M. Substitution of Cl^- by Mes^- greatly reduced [^{3}H]ryanodine binding levels at all [Ca^{2+}]. Competition studies indicated that ionic composition affects channel activity by at least three different mechanisms: (i) competitive binding of Mg^{2+} and monovalent cations to specific high-affinity Ca^{2+} activation site(s), (ii) binding of divalent cations to low-affinity Ca^{2+} inhibition site(s), and binding of anions to Cl^- activation site(s). Supported by NIH.

M-Pos66

RECTIFICATION OF CARDIAC RYANODINE RECEPTOR CURRENT BY ENDOGENOUS POLYAMINES ((A. Uehara[2], P. Vélez[1], M. Yasukochi[3] and M. Fill[1])) [1]Department of Physiology, Loyola University Chicago, Maywood, IL 60153. [2]Department of Physiology & [3]Laboratory of Human Biology, School of Medicine, Fukuoka University, Fukuoka, JAPAN.

The action of three endogenous polyamines (spermine, spermidine & putrescine) was defined on single purified rabbit cardiac Ca^{+2} release channels (ryanodine receptors, RyRs) incorporated into planar lipid bilayers. In the presence of polyamine, the current-voltage relationship had a characteristic N-shape. Polyamine acted from both sides of the channel and was readily washed out. The degree of polyamine action was dependent on ion current direction and the ion selectivity of the RyR pore. In the presence of different charge carriers (Cs^+, K^+, or Ba^{2+}), polyamine efficacy in the different salts ($Cs^+ > K^+ > Ba^{2+}$) was inversely related to ion selectivity ($Ba^{2+} > K^+ > Cs^+$). These data suggest the polyamines act as permeable cationic blockers of the RyR channel. The apparent half-block concentration (K_B) of spermine at 0 mV was <0.1 mM indicating that the polyamine levels present in muscle are sufficient to alter RyR function. Thus, endogenous polyamine may make the SR Ca^{+2} release process inward rectifying (near 0 mV). Polyamines are also involved in inward rectification of surface membrane K^+ channels. A similar action on diverse types of ion channels suggests that the endogenous polyamines are ubiquitous ion channel modulators.

M-Pos67

ADAPTATION OF CARDIAC RYANODINE RECEPTOR CHANNELS ((P. Vélez, A. J. Lokuta[1], H. H. Valdivia[1], S. Györke[2] and M. Fill)) Departments of Physiology, Loyola University, Maywood, IL 60153, [1]University of Wisconsin, Madison, WI 53706 & [2]Texas Tech University, Lubbock, TX 79430.

Single cardiac ryanodine receptor (RyR) channel activation and adaptation have been defined using flash photolysis of two versatile caged-Ca^{+2} compounds, DM-nitrophen and NP-EGTA. Photolysis induced a fast Ca^{+2} spike at the leading edge of the sustained Ca^{+2} stimulus. It is possible that the spike (< 1 ms) may saturate the RyR Ca^{+2} activation site(s) and that adaptation ($\tau \approx 1300$ ms) simply reflects Ca^{+2} coming off the activation site(s). ***If true, then the channel should respond slowly ($\tau \approx 1000$ ms) to a fast drop in [Ca^{+2}].*** This premise was tested by applying a fast [Ca^{+2}] decrease to channels by photolysis of Diazo-2, a caged-Ca^{+2} chelator. The channels responded rapidly (τ<50 ms) to the [Ca^{+2}] decrease. ***If Ca^{+2} spikes saturate the activation site(s), then Ca^{+2} spikes by themselves should activate and induce adaptation.*** This possibility was tested by adding EGTA to the experimental media. The EGTA attenuated the sustained Ca^{+2} stimulus but did not significantly alter Ca^{+2} spike amplitude or kinetics. The fast Ca^{+2} spike by itself did not activate or induce adaptation. These data demonstrate that adaptation is not a consequence of the fast Ca^{+2} spike. Thus, adaptation is an inherent property of single RyR channels and may be fundamental to intracellular Ca^{+2} signalling in heart. Supported by AHA & NIH (AR41197).

M-Pos68

PARTIAL CHARACTERIZATION OF THE CHANNEL REGION OF RYANODINE RECEPTOR ISOFORMS: AN EVOLUTIONARY PERSPECTIVE. ((John E.Keen, Jens P.C. Franck, Richard L. Londraville, Sarah Polgar and Barbara A. Block)) Hopkins Marine Station, Stanford University, Pacific Grove, CA 93950.

The analysis of natural variation in primary protein structure has been an important tool for discerning the structural and functional domains of ion channels. This approach is particularly useful if the amino acid sequences being compared are from animals with ancient evolutionary divergences. We are investigating the amino acid substitution pattern within the channel region of the ryanodine receptor (RyR) isoforms by obtaining sequence from fish, sharks and a cephalochordate, Amphioxus. A conserved primer pair derived from mammalian sequences was used to amplify a 700 bp region of the blue marlin cardiac ryanodine receptor (RyR2). This product was used to screen a blue marlin cardiac UniZAP cDNA library (Stratagene) which yielded a 2.35 kb clone (MnC1). This clone codes for amino acids 4312-4969 of the corresponding rabbit RyR2 and includes part of the 3' untranslated region. Amino acid alignment of this portion of the molecule using published RyRs (rabbit RyR1, RyR2, and RyR3; human RyR1 and RyR2; frog RyR1 and RyR3) and blue marlin RyR1 identifies 5 RyR2-specific deletions and 18 RyR2-specific amino acid substitutions. Two isoform defining sites were also noted. Using the rabbit RyR2 amino acid designation system, Val^{4608} common to both rabbit and fish RyR2, is replaced by Leu in all RyR1 sequences and by Ile in all RyR3 sequences. Also, Met^{4656} in RyR2 is replaced by Leu and Ile in RyR1 and RyR3 molecules, respectively. Primer pairs derived from the fish RyR1 sequence were used to amplify a RyR message from Amphioxus and shark. The 162 amino acid region aligns with residues 4743-4898 in the rabbit RyR1 sequence. Although the shark and Amphioxus RyR sequences have extensive amino acid substitutions when compared to the corresponding region of published RyR sequences, the overall hydropathicity profile remains similar. This indicates that the region is under selective constraint for protein structure and maintenance of the transmembrane domains.
Research supported by NIH (BAB), BCHSF (JEK) and NSERC (JPCF)

M-Pos69

STOICHIOMETRY AND AFFINITY OF CALMODULIN BINDING TO THE TURKEY SR Ca^{2+}-RELEASE CHANNEL. ((L.-J. Wang and G.M. Strasburg)) Dept. of Food Science & Human Nutrition, Michigan State Univ., East Lansing, MI 48824

Calmodulin (CaM) acts as a partial inhibitor of Ca^{2+} release in muscle by direct binding to the ryanodine receptor. We have previously shown that the stoichiometry of CaM binding to the porcine skeletal muscle ryanodine receptor is approximately 20 mol/mol (5 mol/mol of subunit) and that stoichiometry of binding of CaM is independent of [Ca^{2+}], whereas the affinity of CaM binding varies with [Ca^{2+}] [Yang et al., *Biochemistry* (1994) 33:518]. Turkey skeletal muscle displays 2 Ca^{2+} channel protein isoforms (α and β) whose CaM-binding properties are ambiguous. We have initiated studies to define the role of CaM in regulation of avian SR Ca^{2+} channel proteins by characterizing the stoichiometry and affinity of CaM binding. Wheat germ CaM was derivatized with tetramethylrhodamine maleimide (Rh-CaM); binding of Rh-CaM to the Ca^{2+} channel protein in turkey SR vesicles was determined by fluorescence anisotropy. In the presence of 1 mM EGTA, Rh-CaM bound to the channel protein with a Kd of 9 nM and a Bmax of 56 ± 3 pmol/mg. In the presence of 0.1 mM $CaCl_2$, the Kd of Rh-CaM was 7 nM while the Bmax increased to 84 ± 5 pmol/mg. Ryanodine-binding studies on the turkey SR preparations yielded an average Bmax value of 4.3 pmol/mg. Taken together, these results are consistent with approximately 3 CaM molecules bound per channel protein subunit in the presence of EGTA and 5 CaM molecules bound per subunit in the presence of 0.1 mM $CaCl_2$. Crosslinking studies in the presence of EGTA indicate substantially greater CaM bound to the α subunit than to β. In the presence of 0.1 mM Ca^{2+}, the subunits are crosslinked in approximately a 1:1 ratio, thus suggesting that as [Ca^{2+}] is increased, the additional CaM binding occurs at the β subunit. These results suggest that CaM differentially regulates Ca^{2+} release activity by α and β subunits of avian skeletal muscle.

M-Pos70

EVIDENCE FOR NONIDENTITY OF THE DANTROLENE AND RYANODINE RECEPTORS FROM PORCINE SKELETAL MUSCLE. ((S.S. Palnitkar[1] and J. Parness[1,2])) Depts. Anesthesia[1], Pharmacology[2], & Pediatrics[2], UMDNJ-Robert Wood Johnson Medical School, New Brunswick, N.J. 08901

Dantrolene, a hydantoin derivative, is the only known therapy for malignant hyperthermia (MH), a genetic sensitivity to volatile anesthetics resulting in massive release of intracellular Ca^{2+} and consequent hypercontracture and hypermetabolism of skeletal muscle. The genetic change in the porcine model for MH is linked to an ARG^{615}-CYS change in the gene for the skeletal muscle ryanodine receptor (RYR1), the primary Ca^{2+} release channel in sarcoplasmic reticulum (SR). Dantrolene suppresses the Ca^{2+} release in MH-, as well as in normal skeletal muscle. Though we have recently identified (J.Biol.Chem., *270*, 18465) specific [^{3}H]dantrolene binding sites in porcine skeletal muscle SR which parallel [^{3}H]ryanodine binding in subcellular membrane fractions, the molecular site of dantrolene action is unknown. We report herein on our successful attempts at separating [^{3}H]dantrolene from [^{3}H]ryanodine binding sites by fractionation and selective solubilization techniques. Two separate binding peaks for the two ligands were demonstrated after linear sucrose density gradient centrifugation of heavy SR membranes. Selective solubilization of crude skeletal muscle microsomes with 0.6% CHAPS and 50 mM KCl, followed by linear sucrose density gradient centrifugation, revealed a macromolecular complex with [^{3}H]dantrolene binding activity, devoid of [^{3}H]ryanodine binding activity. This fraction did not contain RYR, as determined by PAGE and dot-blots with both N- and C-terminal specific anti-RYR antibodies. We conclude that the dantrolene and ryanodine receptors are likely separate molecular entities. (Supported by FAER and Dept. of Anesthesia)

M-Pos71

STRUCTURAL STUDIES OF THE SKELETAL MUSCLE Ca^{2+} RELEASE CHANNEL IN DIFFERENT FUNCTIONAL STATES. ((Irina Serysheva+, Elena Orlova*, Michael Schatz*, Andrew Marks#, Marin van Heel*, Wah Chiu+ and Susan Hamilton+)) +Dept. of Biochemistry and Dept. of Molecular Physiology and Biophysics, Baylor College of Medicine, Houston, TX 77030; #Brookdale Center for Molecular Biology and Molecular Medicine, Mount Sinai School of Medicine, NY, NY 10021; *Fritz Haber Institute of the Max Plank Society Faradayweg 4-6, D-14195 Berlin, Germany.

We use electron cryomicroscopy and angular reconstitution techniques to examine the structure of the skeletal muscle Ca^{2+} release channel in different functional states. Our first reconstruction of the Ca^{2+} release channel in the presence of EGTA at 30 Å resolution reveals a transmembrane domain organized around a central channel and an extended cytoplasmic region with a hollow appearance [1]. The subsequent reconstruction of Ca^{2+} release channel in the presence of Ca^{2+} and ryanodine shows structural changes that reflect a functional transition of the channel from closed to open states. It has been shown that the Ca^{2+} release channel purified after solubilization with CHAPS from SR membranes is tightly associated with FK506-binding protein (FKBP12). FKBP12 specifically modulates the activity of the Ca^{2+} release channel and can be dissociated from the channel complex with rapamycin. We have analyzed the structure of the Ca^{2+} release channel in the presence of 100 μM Ca^{2+}, before and after incubation of the channel protein with rapamycin. Preliminary maps suggested structural changes in both the putative membrane spanning and cytoplasmic regions. Our current studies demonstrate that electron imaging and angular reconstitution techniques can detect structural changes in Ca^{2+} release channel in different functional states.

[1] Irina Serysheva *et al.* Nature Struct. Biol. 2, 18-24, 1995.
This work is supported by the NCRR of NIH, W.M. Keck Foundation, R.Welch Foundation, Muscular Dystrophy Association of America and DFG.

M-Pos72

FUNCTIONAL AND BIOCHEMICAL CHARACTERIZATION OF DYSPEDIC MOUSE MUSCLE. ((E.D. Buck*, P.D. Allen#,&, H. T. Nguyen& and I.N. Pessah*)) *Department of Molecular Biosciences, School of Veterinary Medicine, University of California, Davis, CA, #Department of Anesthesia, Brigham & Woman's Hospital, Boston, MA, and &Department of Cardiology, Children's Hospital, Boston, MA

A transgenic mouse which is homozygous for a "knockout" of the RyR1 gene (dyspedic mouse) has a birth lethal phenotype. Whole skeletal muscle homogenates from both dyspedic and newborn (age matched) control mice were prepared by differential centrifugation and assayed for biochemical and functional markers. Equilibrium binding experiments performed with 1 nM [^{3}H]ryanodine reveal saturable and specific binding to control muscle (B_{max} = 0.34 pmol/mg, K_d = 18 nM), but not to dyspedic muscle. Binding experiments performed with [^{3}H]PN200 show a 36% reduction in [^{3}H]PN200 binding in dyspedic muscle with respect to control muscle (B_{max} = 0.42 pmol/mg, K_d = 1.47 nM). Western blot analysis was done to demonstrate the presence or absence of proteins known or thought to be important in normal RyR1 channel complex function. Results indicate that DHPRα1, FKBP12, triadin, calsequestrin, SERCA1 and myosin heavy chain are present in both dyspedic and control mouse muscle. Neither control nor dyspedic muscle expressed RyR2, and only age matched control mouse muscle expressed RyR1. Dyspedic muscle was shown to express RyR3, but this isoform could not be evaluated in normal muscle because of cross reactivity of the RyR3 Ab with RyR1. These result indicate that the proteins which are known to be necessary for normal EC-coupling are present in dyspedic muscle, with the exception of RyR1, and that this model will allow studies of RyR1 structure-function in a normal muscle environment .

M-Pos73

A MOUSE MYOGENIC CELL LINE LACKING EXPRESSION OF RYR-1 AND RYR FUNCTION. ((I.N. Pessah*, T.D. Meloy*, H.T. Nguyen&, J. Galceran& and P.D. Allen#,&)) *Department of Molecular Biosciences, School of Veterinary Medicine, University of California, Davis, CA and #Department of Anesthesia, Brigham & Woman's Hospital, Boston, MA, &Department of Cardiology, Children's Hospital, Boston, MA

CCE ES cells possessing two mutant alleles for the skeletal muscle ryanodine receptor (RyR-1) have been produced and subcutaneously injected into SCID mice to produce RyR-1 (-/-) teratocarcinomas (Allen, P.D. *et al.* Biophys. J. 68:A52). A primary fibroblast cell line was isolated from a RyR-1 (-/-) tumor which exhibited a doubling time of 18-24 h, was not contact growth inhibited, did not change its morphology upon serum withdrawal, and possessed the normal complement of chromosomes. We have infected this clone with a retrovirus containing the cDNA encoding Myo-D and a puromycin selection marker. Several puromycin (2.5 μg/ml) resistant subclones were expanded and examined for their ability to express Myo-D and form multinucleated myotubes upon serum withdrawal. One of these clones (1B5 cells) exhibited uniform expression of Myo-D, myosin heavy chain, and desmin antigens upon differentiation in 5% heat-inactivated horse serum for 6-10 days. The 1B5 myotubes have been shown to express key triadic proteins by western blot analysis, including triadin, calsequestrin, FKBP12, SERCA1, and DHPRα1. Neither RyR-1 nor RyR-2 protein is detectable, however a small amount of RyR-3 protein is detectable. Ratiofluorescence photometric measurements of intracellular Ca^{2+} with fura 2-loaded cells reveal that differentiated 1B5 cells exhibit NO response to caffeine (60 mM) or ryanodine (200 μM), whereas BC_3H1 cells that express RyR-1 respond predictably to these pharmacological agents. The 1B5 cell line provides an invaluable model in which to study RyR-1 structure and function within the environmental context of a mammalian skeletal muscle cell.

M-Pos74

COMPARISON OF SARCOPLASMIC RETICULUM CAPABILITIES IN TOADFISH (Opsanus tau) SONIC MUSCLE AND RAT FAST TWITCH SKELETAL MUSCLE ((J.J.Feher, T.D.Waybright and M.L.Fine)) Virginia Commonwealth University, Richmond VA 23298

The sonic muscle of the toadfish is capable of contracting at frequencies of 300 Hz. Electron microscopy shows a great abundance of the SR in this muscle, but no functional characterization of the capabilities of the SR in this muscle has been reported. We measured the oxalated-supported Ca^{2+} uptake rate and capacity of homogenates of toadfish sonic muscle and rat EDL muscle and determined the number of pump units by titration with thapsigargin, a high-affinity, specific inhibitor of the SR Ca-ATPase. The Ca^{2+} uptake rate averaged 70.9 ± 9.5 μmol min^{-1} g^{-1} tissue for the toadfish sonic muscle and 73.5 ± 3.7 μmol min^{-1} g^{-1} for rat EDL. The capacity for Ca^{2+}-oxalate uptake was 161 ± 20 μmol g^{-1} for toadfish and only 33 ± 2 μmol g^{-1} for rat EDL. Thus, the rates of Ca^{2+} uptake were similar in the two muscles, whereas the toadfish had about 5 times the capacity of the rat EDL. Thapsigargin titration gave 69 ± 4 nmol of Ca-ATPase per g tissue in the toadfish and 42 ± 5 nmol Ca-ATPase per g tissue in the rat EDL. The turnover number, defined as the Ca^{2+} uptake rate divided by the number of pumps, was 1220 ± 298 min^{-1} for toadfish and 1786 ± 230 min^{-1} for rat EDL, $p > .05$. Normally, the rat EDL muscle operates at 37°, while the toadfish sonic muscle operates at ambient temperatures closer to 22°. The Ca^{2+} uptake rate at 22° averaged 42 ± 1 % of the rate at 37°. At these operating temperatures, the toadfish SR is slower than the rat fast twitch SR, yet the toadfish supports more rapid contractions. A likely explanation for this is that the source of activator Ca^{2+} for the toadfish is its extensive SR stores, while relaxation is mediated by parvalbumin rather than by the pumping of the SR.

M-Pos75

SPONTANEOUS Ca^{2+} RELEASE EVENTS IN FROG SKELETAL MUSCLE FIBERS. ((M.G. Klein, H. Cheng, L.F. Santana, Y.-H. Jiang, W.J. Lederer, and M.F. Schneider)) Departments of Biochemistry and Physiology, University of Maryland School of Medicine, Baltimore, MD 21201

Discrete, spontaneous Ca^{2+} release events occur in frog skeletal muscle fibers voltage-clamped to a holding potential of -90 mV (Klein et al, these abstracts). These spontaneous release events are comparable in amplitude and spatio-temporal waveform to unitary release events evoked by small depolarizations. Spontaneous Ca^{2+} release events were also observed in single, depolarized frog fibers using confocal line-scan imaging of fluo-3 fluorescence. Nifedipine (1 μM) had no effect on the frequency or spatio-temporal waveform of spontaneous Ca^{2+} release events, and was used in all subsequent experiments to inactivate voltage sensors not already inactivated by depolarizaion. Caffeine (0.4 mM) caused a 4.1-fold increase in the frequency of spontaneous release events with little effect on their amplitude. Procaine (0.3 mM) abolished all Ca^{2+} release events and waves both in control and in the presence of caffeine. Heparin (20 μg/ml) had no effect on the frequency of spontaneous Ca^{2+} release events. Exposure to elevated Ca^{2+}-internal solution resulted in an increase in the frequency of spontaneous release events. These results show conclusively that spontaneous Ca^{2+} release events can be activated by a voltage-independent mechanism, and are consistent with the idea that the spontaneous release events are caused by Ca^{2+}-induced Ca^{2+} release. Supported by NIH and MDA.

M-Pos76

SR CALCIUM RELEASE DETERMINATION IN QUIN-2 BUFFERED FROG CUT SKELETAL MUSCLE FIBERS. ((S.K. Dey, M.G. Klein, M.F. Schneider)) Dept. of Biological Chemistry, Univ. of Maryland School of Medicine, Baltimore, MD 21201.

Quin-2 fluorescence signals were recorded in −90 mV voltage clamped fibers containing mM concentrations of Quin-2, which suppress the myoplasmic $\Delta[Ca^{2+}]$ during depolarization (Dey et al. Biophy J, 86:A88, 1994). Taking into account the Ca^{2+} binding to Quin and to intrinsic myoplasmic sites and the Ca^{2+} being pumped back to SR, the full rate of Ca^{2+} release from SR can be determined as $R_{rel}=d([Ca\text{-}Quin]+[Ca\text{-}Sites]+[Ca\text{-}Pumped])/dt$. The Ca^{2+} binding to intrinsic myoplasmic sites and the Ca^{2+} pumped back to SR were determined by fitting the Ca^{2+} removal model of Brum et al. (J Physiol, 398:441, 1988) to the decay phases of [Ca-Quin] signals after various pulses. Release waveforms calculated during depolarizing pulses exhibited an early peak followed by a rapid and then a slow phase of decline. The latter is attributed to the depletion of Ca^{2+} from SR. Correction for the Ca^{2+} depletion converted the slow declining phase of release into a maintained steady level and it also slightly raised the peak. Comparable SR calcium content values were obtained from double pulse records using fractional suppression technique (Dey et al. Biophy J, 66:A88, 1994) and from SR depletion correction. Corrected release records were fit by an empirical exponential power function of time, $F(t)=a(1-\exp(-(t-g)/b))^c(d+(1-d)\exp(-(t-g)/f))$, to obtain the peak and steady level. Though the peak as well as the steady level of release gradually decreased with time and increasing [Quin], perhaps due to a gradual run down of charge movement, their ratio did not decrease. The maintained shape of the release waveform indicates either that $[Ca^{2+}]$ feedback is not important in determining the release waveform or that Quin-2 did not effectively buffer $[Ca^{2+}]$ in the immediate vicinity of the regulatory Ca^{2+} binding sites for controlling release. Supported by NIH and MDA.

M-Pos77

Ca^{2+} HOMEOSTASIS IN ADULT MOUSE FAST -TWITCH SKELETAL MUSCLE FIBERS MAINTAINED IN CULTURE. ((Y-W. Liu, S.L. Carroll, M.G. Klein, M.F. Schneider)) Department of Biological Chemistry, University of Maryland School of Medicine, Baltimore, MD 21201

Enzymatically dissociated adult mouse flexor digitorum brevis fibers exhibited regular sarcomere structure for at least 8 days in culture in Minimal Essential Medium (37°C) with normal (1.8 mM) or high (9.0 mM) $[Ca^{2+}]$. After various times in culture, fibers were loaded with fura-2 (30 min in 1.0 μM fura-2AM at room temp) and studied in Ringer's solution with the same $[Ca^{2+}]$ as in culture. Resting $[Ca^{2+}]$ (nM) determined from the fura-2 fluorescence ratio for 380 and 358 nm excitation (K_D = 70 nM) did not change significantly over the 8 day culture period in either normal or high Ca^{2+} medium (35.1 ± 1.3, day 0 compared to 32.6 ± 1.1, day 8 for normal calcium; 30.2 ± 1.4, day 0 compared to 30.3 ± 0.6, day 8 for high calcium) indicating that the fibers did not accumulate Ca^{2+} over the culturing period, even in high Ca^{2+} medium. $[Ca^{2+}]$ transients ($\Delta[Ca^{2+}]$) triggered by external electrical stimulation (100 Hz) were calculated from fluorescence ratio records corrected for non-instantaneous reaction of fura-2 with Ca^{2+} (k_{on} = 3.66 x 10^8 M^{-1} s^{-1}; k_{off} = 26 s^{-1}) for 1, 5, and 10 action potentials. For a single action potential peak $\Delta[Ca^{2+}]$ did not vary considerably from 1 μM even after 8 days in culture in normal or high Ca^{2+}. Interestingly, the rate constants of the decay of $\Delta[Ca^{2+}]$ decreased significantly after 4 days in culture (34 - 47%). The average rate constants of the $\Delta[Ca^{2+}]$ decay also exhibited a stimulation duration dependence which was not affected by 8 days in culture. Effects of the calcium pump inhibitor DBHQ (2.0 μM), which decreased the rate of decay of $\Delta[Ca^{2+}]$ after a single action potential by 10 - 12 fold, and of various other agents on the calcium homeostasis of cultured muscle fibers are being investigated. Supported by NIH and AHA Maryland Affiliate.

M-Pos78

A CROSS-TALK BETWEEN IP3-SENSITIVE AND RYANODINE-SENSITIVE CALCIUM STORES IN GUINEA PIG ILEUM SMOOTH MUSCLE ((Radek Pelc)) University Department of Pharmacology and University Laboratory of Physiology, Parks Road, Oxford OX1 3PT, U.K.

Oscillations in contractile activity of guinea pig ileum smooth muscle strips were observed with the aim to understand interactions between InsP3-sensitive and ryanodine-sensitive calcium stores which we found to be involved in these oscillations. We were able to induce them by ryanodine. Usually they had two components: fast (period of 10 to 15 s) and slow (period of several min). Subsequent application of carbachol resulted in diminishing the fast component while the slow one remained. Carbachol on its own failed to induce such oscillations. Although it was not always possible to detect well pronounced oscillations during ryanodine treatment subsequent application of carbachol triggered them. Apart from ryanodine, caffeine was also able to induce periodic contractions (period of several minutes). We conclude from our results that (1) there is a cross-talk between ryanodine-sensitive and InsP3-sensitive stores and (2) a single pulse of calcium released by carbachol from InsP3-sensitive store can trigger oscillations driven by ryanodine-sensitive store. Correlation is made with the two pool model of cytosolic calcium oscillations (Berridge & Galione 1988).

Berridge M.J. & Galione A., *FASEB J.* 2: 3074-3082 (1988)

M-Pos79

NITRIC OXIDE INCREASES CALCIUM TRANSIENTS AND FORCE PRODUCTION IN SKELETAL MUSCLE FIBERS. ((M.B. Reid, D.G. Allen, J. Lännergren, and H. Westerblad)) Karolinska Institutet, Sweden; Baylor College of Medicine, USA; and University of Sydney, Australia.

Skeletal muscle fibers produce nitric oxide (NO) which modulates excitation-contraction coupling (*Nature* 372:546-548, 1994) by an unknown mechanism. We tested the hypothesis that calcium transients during muscle excitation are sensitive to NO. *Methods.* Single fibers from mouse flexor brevis were mounted in a superfusion chamber, injected with indo-1, and stimulated to contract electrically (0.5 ms pulses, 30-100 Hz) with or without sodium nitroprusside 1-10 mM (SNP), an NO donor. We measured isometric force and intracellular calcium levels ($[Ca^{2+}]_i$) during activation. *Results.* SNP increased $[Ca^{2+}]_i$ and force (20 of 25 trials; $P < 0.05$) in each of 4 fibers tested; washout reversed these changes (18 of 22 trials; $P < 0.001$). SNP augmented $[Ca^{2+}]_i$ by an average of 6.5% (± 1.7 SE) at all stimulus frequencies ($P < 0.002$). Accordingly, changes in absolute $[Ca^{2+}]_i$ were more pronounced during near-maximal tetanic (100 Hz) than submaximal tetanic (30-40 Hz) contractions ($P < 0.0001$). SNP did not alter the $[Ca^{2+}]_i$-force relationship; force therefore was increased most markedly during submaximal tetanic contractions, in which the $[Ca^{2+}]_i$-force relationship is steep. *Conclusion.* NO exposure improves excitation-contraction coupling in this preparation by increasing $[Ca^{2+}]_i$ transients. *Supported by The Karolinska-Baylor Exchange Program, NIH grant #HL-45721, Swedish MRC Project #10842, and the National Health and Medical Research Council of Australia.*

M-Pos80

LOW [ATP] REDUCES DEPOLARIZATION-INDUCED CALCIUM RELEASE IN SKELETAL MUSCLE FIBERS ((V.J. Owen, G.D. Lamb and D.G. Stephenson)) School of Zoology, La Trobe University, Bundoora, Melbourne, 3083, Victoria, Australia.

Using the mechanically-skinned fiber preparation with functional excitation-contraction coupling, we investigated the effects of lowered [ATP] and raised $[Mg^{2+}]$ on the depolarization-induced release of Ca^{2+} from the SR of skeletal muscle. The extent of Ca^{2+} released at various [ATP] and $[Mg^{2+}]$ was quantified by examining the amount of Ca^{2+} remaining in the sarcoplasmic reticulum (SR) after a single depolarization (2-3 seconds) in the presence of 1 mM EGTA. Depolarization released a similar amount of SR Ca^{2+} at both 8 mM and 2 mM ATP, but only approximately 43% of this amount at 0.5 mM ATP. This latter reduction was not reversed by the additional presence of 1.5 mM AMP. At each [ATP], raising the $[Mg^{2+}]$ from 1 to 3 mM independently reduced Ca^{2+} release by a factor of 1.5 to 2. These results show that local decreases of [ATP] close to the release channels, together with the concomitant increase in $[Mg^{2+}]$, can account for the reduced Ca^{2+} release seen in severe fatigue.

M-Pos81

CARDIAC GLYCOSIDES ENHANCE CALCIUM RELEASE FROM THE SARCOPLASMIC RETICULUM OF THE FROG ((L. Csernoch, S. Sárközi, P. Szentesi, L. Kovács)) Dept. Physiol., Univ. Med. Sch., Debrecen, Hungary.

The effects of cardiac glycosides on the rate of release of calcium (Rrel) from the sarcoplasmic reticulum (SR) of the frog was studied using two techniques. Rrel was either determined using actively loaded heavy SR vesicles with the method of Palade (1987, J. Biol. Chem. **262**, 6135) or calculated from the calcium transients measured in cut fibers mounted in a double vaseline gap chamber. In case of the former after the addition of 1 μM ryanodine the vesicles released their calcium content completely. Both digoxin and ouabain were capable of inducing release at the same rate as ryanodine when applied in a 2 μM or 15 μM concentration, respectively. In cut fiber experiments extracellularly applied digoxin, 5 nM, and ouabain, 250 nM, increased the early inactivating peak of Rrel with no significant changes on the steady level at large depolarizations. This effect was neither due to a decrease in the calcium dependent inactivation of the release channels nor to a change in intramembrane charge movement. Unlike caffeine neither cardiac glycoside affected the time-to-peak of the calcium transients evoked by short depolarizing pulses suggesting that the voltage control of Rrel was not lost. These results, taken together with the earlier observations that cardiac glycosides affect the cardiac but not the skeletal type ryanodine receptor (RyR) and that amphibians exhibit both in their skeletal muscle, suggest that in frog the cardiac type RyR is mainly involved in the generation of the inactivating peak of Rrel. Supported by OTKA.

M-Pos82

SARCOPLASMIC RETICULUM LUMENAL Ca^{2+} HAS ACCESS TO CYTOSOLIC ACTIVATION AND INACTIVATION SITES OF SKELETAL MUSCLE Ca^{2+} RELEASE CHANNEL. ((Ashutosh Tripathy and Gerhard Meissner)) Departments of Biochemistry and Biophysics, and Physiology, University of North Carolina, Chapel Hill, North Carolina, 27599. (Spon. by Edward J. Massaro)

In a previous report (*Biophys. J. A356, 1995*) we found that rabbit skeletal muscle sarcoplasmic reticulum (SR) Ca^{2+}-release channels activated by mM ATP in the presence of nM cytosolic (cis) Ca^{2+} and 0.05-10 mM lumenal (trans) Ca^{2+}, exhibited a profound voltage-dependence of activation and gating. We had interpreted our results in terms of a model in which lumenal Ca^{2+} has access to the cytosolic Ca^{2+}-activation and inhibition sites. In this report we provide further experimental support for the above model. We show that cytosolic ATP-activated channel activities decreased as lumenal Ca^{2+} fluxes were reduced by the addition of 1 - 5 mM $BaCl_2$ or $MgCl_2$ to the lumenal side which contained 50 μM Ca^{2+}. Reduction of lumenal Ca^{2+} fluxes at 50 μM trans Ca^{2+} by increasing [KCl] from 0.25 M to 1 M also reduced single channel activities. At 1 M [KCl], channel activities increased as lumenal Ca^{2+} fluxes were increased by raising trans Ca^{2+} from 0.05 to 0.2 mM. These results demonstrate a direct relationship between lumenal Ca^{2+} flux and channel activity. Our results further show that low lumenal Ca^{2+} fluxes (up to ~1.25 pA) activate and higher fluxes inactivate the channel. Cis addition of fast Ca^{2+}-complexing buffer BAPTA removed high Ca^{2+} flux-induced channel inhibition and increased channel activity. Based on the above data we propose that the activation site is located within 4 nm and the inactivation site between 4-8 nm from the channel mouth. Supported by NIH.

M-Pos83

THE Ca^{2+} POOLS RELEASABLE BY CAFFEINE AND VOLTAGE IN SKELETAL MUSCLE. ((N.Shirokova and E.Ríos)) Rush University, Chicago, IL 60612. (Spon. by M.Barany)

Properties of the of voltage- and caffeine-releasable Ca^{2+} pools were studied in skeletal muscle of *Rana pipiens* with a fast flow, computer-operated 2-Vaseline-gap chamber. The chamber was used to combine voltage pulses with "caffeine" pulses (timed extracellular applications of high concentrations of caffeine) while simultaneously recording electrophysiological and optical signals. Release by caffeine was determined from Ca^{2+} transients with the removal method of Melzer at al., 1987. After reaching a maximum of 2.5 mM/s at about 3 s, caffeine-induced Ca^{2+} release terminated spontaneously during a prolonged caffeine application, due to depletion of Ca^{2+} from sarcoplasmic reticulum (SR). Its integral, approximately constant in repeated exposures to 5 or 10 mM caffeine, was interpreted as the total caffeine-releasable content of SR. The average value was 2.9 ± 0.4 mM ($n = 10$) expressed in terms of accessible myoplasmic volume. An estimate of SR Ca^{2+} content releasable by depolarizing pulses was obtained evaluating the depletion of the SR caused by voltage-elicited Ca^{2+} release (Schneider et al., 1987). These estimates, at different times during a caffeine exposure, were identical to the estimates of Ca^{2+} remaining in the caffeine releasable pool. This indicates that the caffeine-releasable and the voltage-releasable Ca^{2+} pools are one and the same. A 500 ms pulse to 10 mV, applied simultaneously with exposure to 10 mM caffeine, resulted in large Ca^{2+} release and, upon repolarization, a reduction in the release flux below the level due to caffeine alone (even though caffeine was still present). This appears to extend to adult muscle the observation by Suda and Penner (1994) of RISC (repolarization-induced stop of caffeine contracture). In our case the effect was negligible for shorter pulses, or pulses to a lower voltage. It was a complete stop of release for pulses > 1.5 s to voltages >0 mV. The effectiveness of the pulse to cause this stop correlated with the cumulative release due to the pulse. When release flux caused by caffeine, depolarizations, or both stimuli combined, was divided by the calcium contents remaining in the releasable pool, an SR Ca^{2+} permeability was obtained. The permeability elicited by caffeine was not affected by depolarizing pulses. Therefore, the mechanism of stop of release, in these cells, was Ca^{2+} depletion. (Supported by NIH and MDA).

M-Pos84

DUAL EFFECT OF Cl^- ON Ca^{2+} RELEASE IN RABBIT SKELETAL MUSCLE SARCOPLASMIC RETICULUM. ((M. Sukhareva and R. Coronado)) Dept. of Physiology., Univ. of Wisconsin, Madison, WI 53706.

Rapid filtration was used to investigate release of passively-loaded $^{45}Ca^{2+}$ in junctional SR equilibrated in 150 mM K-Gluconate or 150 mM Choline-Cl salts. Ca^{2+} release was stimulated by extravesicular micromolar free Ca^{2+} and was blocked by 100 μM neomycin in Cl^--free SR but not in Cl-containing SR. Releases in both solutions were sensitive to 20 μM ruthenium red. At pCa 6, ryanodine stimulated release with ED_{50} ~120 nM in K-Gluconate and ~10 nM in Choline-Cl. [^{3}H]ryanodine binding analysis confirmed stimulation of high affinity binding by Cl^-. Cl^- increased the binding affinity of ryanodine and stimulated a Ca^{2+} sensitive but neomycin insensitive flux component, not mediated by a type 1 (skeletal) ryanodine receptor. (Supported by NIH and MDA).

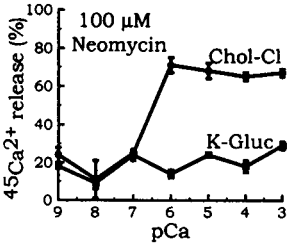

M-Pos85

DIFFERENTIAL EFFECTS OF INACTIVATION ON STIMULATION OF Ca RELEASE IN FROG SKELETAL MUSCLE. ((Elizabeth W. Stephenson)), Department of Physiology, UMD-New Jersey Medical School, Newark, NJ 07103.

The relation between the state of the TT voltage sensor (VS) and Ca release stimuli helps define coupling mechanisms. Low ClO_4^- (perchlorate) shifts the voltage dependence of charge movement and Ca release; it increased Ca release in skinned frog fibers stimulated by submaximal depolarization, but not unstimulated ^{45}Ca efflux (J.Gen.Physiol.93:173,1989). Stimulation by ClO_4^- alone (12 mM) is highly sensitive to the VS state: polarized fibers give large responses but chronically depolarized (inactivated) fibers are refractory (Biophys.J. 68(2):A176,1995; J.Gen.Physiol. 105:17a,1995). The present studies compare responses to SR release channel stimuli, caffeine or free [Mg^{2+}] reduction, between polarized and inactivated fibers. Methods were as described previously, but initial SR Ca was set with 50 nM free [Ca^{2+}], 3 mM $EGTA_T$. Ca release was assayed from normalized isometric force responses. In polarized fibers, 2.5 mM caffeine stimulated large responses with little delay, but 1.5 and 1.0 mM gave no response during ~10s exposure; after inactivation, these subthreshhold levels were effective stimuli with short delays (<3s; <5s). Similarly, sudden decrease in free [Mg^{2+}] from ~800 uM (5 mM Mg_T,5 mM ATP_T) to ~200 uM (3 mM Mg_T) or to ~400 uM (4 mM Mg_T) stimulated large responses in inactivated fibers with short delays (~1s; 4s) but not in polarized fibers during longer exposures (>10s; >20s). Thus Ca release is not refractory to these release channel stimuli in inactivated fibers, but facilitated. These differential effects suggest that ClO_4^- acts by a different mechanism, correlated positively with junctional conformational changes during normal coupling.

M-Pos86

MULTIPLE HETEROGENOUS SPIKES AND BURSTS OF Ca RELEASE AT REST AND DURING ACTIVATION IN ISOLATED SKELETAL MUSCLE FIBERS. ((M. Rozycka, R. Cordoba-Rodriguez and H. Gonzalez-Serratos)) Department of Physiology, University of Maryland, School of Medicine, Baltimore MD. 2101.

Ca^{2+} release from skeletal muscle SR is supposed to be controlled only by the T-tubular membrane potential. This has lead to the assumption that Ca^{2+} release is homogenous along the T-tubular SR. However, other excitable cells where the release is influenced by $[Ca^{2+}]_i$ show substantial calcium fluctuations and large gradients during activation. We have investigated whether there is an unitary Ca^{2+} release at rest and whether during activation the release is homogenous. Gradients and oscillatory bursts in skeletal muscle would indicate an intracellular Ca^{2+} release regulatory mechanism. We have examined skeletal muscle spatial Ca^{2+} distribution by illuminating the fibre on a plane perpendicular to the long axis of the cell and observing along the long axis Ca^{2+} fluorescence (Fluo-3) images. Ten ms video images were taken at 30 frames/sec synchronized with the stimulating pulse. We have found brief narrow Ca^{2+} spikes at rest and broader larger Ca^{2+} burst releases during steady-state tetanus. The bursts form gradients of very significant and slow Ca^{2+} release fluctuations. These gradients and fluctuations are not caused by movement or random photon noise. Caffeine induced a more even distributed Ca^{2+} release without bursts and large gradients. These experiments, which confirm some of our previous results (J. of Muscle and Cell Motility 14, 527,1993), have led us to propose that a similar Ca^{2+} release activation and inactivation mechanism may operate at rest and during activation. This might consist of a Ca-induced Ca-release inhibition produced by the high $[Ca^{2+}]_i$ built in the restricted space surrounding the release channels. Supported by NIH grant NS 17048.

M-Pos87

APPLICATION OF FURA-2 TO DETERMINE VOLTAGE-DEPENDENT Ca^{2+} RELEASE IN FROG AND HUMAN SKELETAL MUSCLE FIBRES. ((A. Struk, G. Szücs, H. Kemmer, F. Lehmann-Horn and W. Melzer)) Dept. of Applied Physiology, University of Ulm, D-89069 Ulm.

Avoiding indicator saturation and using a correction for non-instantaneous Ca binding we used fura-2 (200 μM) in voltage-clamped amphibian and human cut muscle fibres to determine depolarization-induced Ca release. In frog muscle fibres 15 mM internal EGTA was used to reduce the Ca transients in size (Gonzáles & Ríos, J. Gen. Physiol. 102, 373-421, 1993). Measurements with the rapid metallochromic indicator antipyrylazo III showed that free Ca drops within less than 10 ms to a steady level at the end of a depolarization while the fura-2 signal decays exponentially for a longer time. The in-vivo off rate constant of fura-2 was determined as 26 s^{-1} from the relaxation time constants at different Ca concentrations. Together with an in-vivo estimate of the dissociation constant (180 nM) this parameter was used to calculate the time course of free Ca. Subsequently the rate of Ca release was calculated by using the method of Baylor et al. (J. Physiol. 344, 625-666, 1983). The method was also applied to cut muscle fibres dissected from biopsies of human m. vastus lateralis under conditions of low EGTA buffering (0.1 mM) and revealed similar kinetic characteristics of the rate of release as in frog fibres, i.e. an early peak immediately after depolarization, subsequent drop to a lower level and rapid turn-off after repolarization. The procedure may help to identify alterations of voltage-dependent Ca release in muscle diseases.

M-Pos88

MEASUREMENTS OF FREE INTRACELLULAR MAGNESIUM CONCENTRATION ($[Mg^{++}]_i$) USING THE FLUORESCENT INDICATOR MAGINDO-1 IN ISOLATED MOUSE SKELETAL MUSCLE FIBERS.

((*L. Csernoch, #J.C. Bernengo and V.Jacquemond)). Physiologie des Eléments Excitables, CNRS URA 180, Univ. Claude Bernard Lyon1, Villeurbanne, France. *Dept. of Physiology, Univ. Med. School, Debrecen, Hungary. #INSERM U.121, Bron, France. (Spon. by P. Charnet).

Magindo-1 is a ratiometric fluorescent dye which binds magnesium with a reported affinity in the millimolar range, however its use as $[Mg^{++}]_i$ indicator in living cells has yet been poorly documented. Enzymatically isolated mouse skeletal muscle fibers were pressure microinjected with a 1mM magindo-1 containing solution. The $[Mg^{++}]_i$ in individual fibers was estimated from the ratio (R) of the fluorescence measured at 405 and 470 nm upon 335 nm excitation. In vivo calibration was performed with brief applications of 0.1% saponin using external solutions containing no calcium (10 mM EGTA) and various concentration of Mg^{++} (1 to 50 mM). The R value in absence of Mg (Rmin) was obtained from cells that were microinjected with a solution containing (in mM) 60 K-Asp, 60 K_2-ATP, 1 magindo-1 and 10 Hepes (pH 7.2). Using the in vivo calibration parameters, the mean resting $[Mg^{++}]_i$ measured from 42 cells was 0.79 ± 0.07 mM. In order to test whether the dye could be used to detect a change in $[Mg^{++}]_i$, some cells were bathed in presence of a 100 mM Mg containing solution and stimulated by carbachol (Cch) while fluorescence was measured from the endplate area. In 10 cells on which this protocol was tested, transient increases in R were observed in response to Cch applications. These changes corresponded to a 0.1 to 0.5 mM increase in $[Mg^{++}]_i$, and were likely to be due to Mg entry through the nicotinic receptors.

M-Pos89

ADAPTIVE CONTROL OF INTRACELLULAR Ca^{2+} RELEASE IN C2C12 MOUSE MYOTUBES *((I. Györke and S. Györke))* Department of Physiology, Texas Tech University, HSC, Lubbock, TX 79430.

The spatial patterns of intracellular Ca^{2+} release were studied in the C2C12 skeletal muscle cell line using laser scanning confocal imaging. The goal was to distinguish between two schemes proposed to explain the phenomenon of "quantal" Ca^{2+} release from caffeine-sensitive Ca^{2+} stores in muscle and other tissues: (i) all-or-none (true quantal) Ca^{2+} release from functionally discrete stores that have different sensitivities to caffeine; or (ii) adaptive behavior of individual release sites, each responding transiently and repeatedly to incremental caffeine doses. In 3-5 day old myotybes, used in this study, the sarcoplasmic reticulum (SR) elements were randomly scattered and sparse, as determined by staining with rhodamine B hexyl ester. Intracellular Ca^{2+} release induced by depolarization (K^+) or caffeine occurred in discrete localized regions within the cell that correlated with SR distribution. The image areas and fluorescence intensities of some of these evoked local Ca^{2+} signals were similar to those of Ca^{2+} sparks that were observed under resting conditions and which are believed to be due to spontaneous activation of single release units. In contrast to the expectations imposed by quantal models, Ca^{2+} release triggered by incremental doses of caffeine had the same spatial patterns throughout the cell. Ca^{2+} release, at a given site, triggered by a submaximal dose of caffeine was transient and could be reactivated by addition of a higher caffeine dose, showing the same type of adaptive behavior as measured globally from larger areas of the cell. These results suggest that incremental Ca^{2+} release is accounted for by adaptive behavior of individual Ca^{2+} release sites. Supported by AHA and NIH (HL52620).

M-Pos90

ABSENCE OF A CALCIUM TRANSIENT IN SKELETAL MUSCLE CELLS FROM MUTANT MICE (CCHB1$^-$) LACKING β1 DIHYDROPYRIDINE RECEPTOR SUBUNIT. (M. Beurg, M. Sukhareva, P.A. Powers*, R.G. Gregg*, R. Coronado) Department of Physiology and Waisman Center*, University of Wisconsin, Madison, WI 53706, USA.

The DHP receptor initiates excitation-contraction coupling of skeletal muscle cells by stimulating Ca^{2+} release from the SR. We used embryonic myotubes to simultaneously measure Ca^{2+} transients and control membrane potential respectively by the Fura-2 and whole cell recording techniques. Unlike normal (●) myotubes, no Ca^{2+} transient could be detected in mutant (○) myotubes by depolarizations (50 ms to 500 ms) in the range of -30 to +50 mV (diagram). APs in mutant cells under current-clamp also failed to elicit a Ca^{2+} transient. However 5 mM caffeine induced a thapsigargin-sensitive long lasting Ca^{2+} transient. The SR of mutant cells is functional and the β1 subunit could be directly involved in the excitation - contraction coupling. *Supported by Philippe Foundation, NIH, MDA and NSF.*

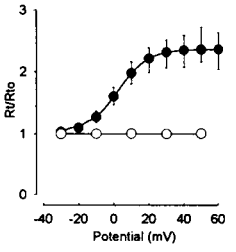

M-Pos91

INTRAMEMBRANE CHARGE MOVEMENT IN FAST SKELETAL MUSCLE FIBERS OF THE RAT. ((F. Francini, C. Bencini and R. Squecco)) Dpt. di Scienze Fisiologiche, Università di Firenze, 50134 Firenze, Italy.

Intramembrane charge movement (ICM) shows two components (Q_β and Q_γ) in normally polarized skeletal muscle fibers of the frog whereas only one component is consistently observed in mammalian fibers. The aim of this work was to investigate the ICM in skeletal muscle fibers of adult Wistar rat. Single cut fibers were mechanically dissected from extensor digitorum longus muscle and voltage clamped in a double Vaseline-gap chamber (Francini & Stefani, *J. Gen. Physiol. 94*: 953-969, 1989). All ionic currents were minimized, except for calcium current (I_{Ca}). ICM and I_{Ca} were detected at 16 °C using 153- or 1700-ms voltage pulses from a holding potential (HP) of -90 mV, in steps of 10 mV. Linear capacitive and leak currents were subtracted using appropriately scaled current in response to hyperpolarizing control pulses of 20 mV from a HP of -90 mV. I_{Ca} activation was evaluated by a multiexponential fit on I_{Ca} time course. For each voltage pulse, the time course of ICM was determined after mathematical removing of the calculated time course of I_{Ca} activation from the original current traces. ICM kinetics resulted more complex than supposed. In fact, the time integral of ICM (Q_{ICM}) vs. voltage plot showed two components (Q_1 and Q_2) described by two Boltzmann functions (with half-voltage values of -32.1 and 10.8 mV). They were further discriminated using a HP of -50 mV or a 10-ms prepulse to -50 mV from a HP of -90 mV. In both cases Q_1 was reduced in size while its voltage-dependence was slightly affected. These results agree with the presence of at least two components of ICM in mammalian muscle fibers.

Supported by grant n° 625 from Telethon-Italy.

CARDIAC MYOFIBRILS AND ENERGETICS

M-Pos92

TIME-RESOLVED X-RAY DIFFRACTION MEASUREMENTS DURING CONTRACTIONS IN SKINNED CARDIAC MUSCLE.

((A. Arner, Å. Jaworowski, R. Lagerstedt and G. Rapp*)) Dept Physiol, Lund and *EMBL Outstation, c/o DESY, Hamburg.

Time-resolved x-ray diffraction measurements were performed on chemically skinned cardiac muscle preparations from swine using synchrotron radiation at beamline X13, EMBL, c/o DESY, Hamburg. A time-resolution of 125 ms could be achieved for the equatorial 1,0 and 1,1 reflections. The ratio of 1,1/1,0 was small in the relaxed state and increased markedly in rigor. An increase in the ratio, compared to the relaxed state, was also observed in contracted fibers. The changes in ratio are consistent with previous observations (Matsubara *et al.*, 1989 J Physiol 417:555) and most likely reflect transfer of cross-bridges from thick to thin filaments. Using a protocol with BDM (Morano *et al.*, 1995; Acta Physiol Scand 154:343) a low rigor force was obtained. Photolytic release of ATP in the presence of calcium (pCa 4.3) resulted in a rapid contraction (rate about 1 s^{-1}). This was accompanied with a fast (within < 125 ms) drop in the 1,1/1,0 ratio. The fast structural change was also observed after release of ATP at low $[Ca^{2+}]$ although the rate of contraction was slower. These data suggest that the rate of detachment from rigor is sufficiently fast not to limit the rate of contraction. During the contraction phase, at high and low calcium, a second flash releasing ATP did not alter the 1,1/1,0 ratio suggesting that rigor cross-bridges are not formed during the phase of force development at either $[Ca^{2+}]$.

M-Pos93

EFFECTS OF ESSENTIAL MYOSIN LIGHT CHAIN (MLC) ISOFORMS ON FORCE-VELOCITY RELATION IN THE HUMAN HEART

[1]M. Morano, [2]M. Maier; [2]P.E. Lange, [1]I. Morano
[1]Max-Delbrück-Center for Molecular Medicine, Robert-Rössle-Straße 10, [2]German Heart Center, Berlin, Germany

We investigated force-velocity relations of chemically skinned fibers from the right ventricle of patients with congenital heart defects (CHD). Force-velocity was analyzed by the constant-load technique at maximal Ca^{2+} activation level (pCa 4.5). Velocity was analyzed between 20-70 ms after the release. MLC of the fibers were analyzed by 2D-PAGE using a pH-gradient in the first dimension of 4.5-5.4. Gels were stained with Coomassie-blue, destained, and the protein spots were analyzed densitometrically. CHD patients expressed between 0-17% atrial MLC-1 (ALC-1) of total MLC-1 in the right ventricle.

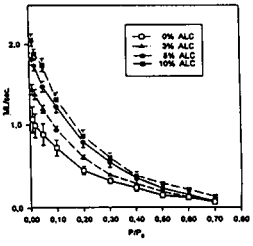

Ratios between MLC-1 and MLC-2 isoforms were around 1. MLC-2 were completely dephosphorylated. Maximal shortening velocity (Vmax) was determined by extrapolation of the force-velocity ratio to zero-load (means ± SEM, 6 fibers per patient). We found a positive correlation between ALC-1 and Vmax (see Figure). We conclude that the expression of the ALC-1 modulate cross-bridge cycling kinetics increasing maximal shortening velocity.

M-Pos94

KINETICS OF ACTIVATION AND PHOSPHATE RELEASE IN CARDIAC MYOCYTES INVESTIGATED WITH CAGED CA^{2+} AND CAGED PHOSPHATE. ((Qin Song, Alexandre Araujo and Jeffery Walker)) Department of Physiology, University of Wisconsin, Madison, WI 53706.

Ca^{2+} induced activation of tension development and phosphate (Pi) induced tension decline were measured in skinned cardiac myocytes with photolysis of caged Ca^{2+} (NP-EGTA; Ellis-Davies & Kaplan, 1994, PNAS, 91,187-191) and caged Pi (α-carboxyl-2-nitrobenzyl phosphate), respectively. Photolysis of caged Pi produced up to 3 mM Pi within the filament lattice resulting in an approximately exponential tension decline with an apparent rate constant (k_{Pi}) of about 6 s^{-1} at 1 mM Pi (pCa 4.5, pH 7, 15°C). Photolysis of caged Ca^{2+} initiated tension development with a rate constant (k_{Ca}) of about 3 s^{-1} under similar conditions. The k_{Pi} and k_{Ca} increased linearly with total Pi concentration with different slopes: 3.1 $(mM\ s)^{-1}$ for k_{Pi} and 0.8 $(mM\ s)^{-1}$ for k_{Ca}. The results suggest i) that the Pi-release step is too fast to limit the steady-state ATPase in cardiac muscle, and ii) that the tension development from a relaxed condition is both kinetically coupled to the Pi release, and influenced by steps prior to Pi release. A two state model with only the Pi release step predicts $k_{Pi} = k_{Ca}$, or $k_{Pi} < k_{Ca}$ if the forward rate constant is force dependent in the model, both of which are contradictory to the experimental results. A three state model including a crossbridge attachment step and a Pi release step accounts for both the Ca^{2+} induced tension transient, and the Pi induced tension decline reasonably well. The forward rate constants were made force dependent in a manner similar to the model of Huxley and Simmons (Nature, 1971, 233,533-8). [Supported by NIH].

M-Pos95

EFFECTS ON CROSS-BRIDGE INTERACTION WITH ACTIN DUE TO ACIDIC pH IN SINGLE CARDIAC MYOCYTES ((Joseph M. Metzger and Philip A. Wahr)) Department of Physiology, University of Michigan, Ann Arbor, MI 48109.

Acidic pH depresses maximum Ca^{2+}-activated force by a greater extent in cardiac myocytes than in skeletal muscle fibers. To gain insight into the mechanism of muscle-type differences in pH sensitivity the effects on tension and instantaneous stiffness due to acidic pH were examined in single adult cardiac myocytes and slow soleus fibers from the rat. Instantaneous stiffness (ΔP/ΔL) was determined in cardiac myocytes by applying a small amplitude (2.8 nm/hs) sinusoid length change (frequency 0.65 kHz - 1.0 kHz) and recording the resultant alteration in tension. Instantaneous stiffness was used to estimate the number of attached cross-bridges by assuming apparent myofilament compliance is similar in skeletal and cardiac muscle and unaffected by altered pH. During maximal Ca^{2+}-activation of cardiac myocytes tension decreased to 0.47 ± 0.03 (P/P_o) and stiffness to 0.65 ± 0.03 (S/S_o) upon reducing pH from 7.00 to 6.20. In comparison, acidic pH had significantly less of an effect on tension (0.73 ± 0.01 P/P_o) and stiffness (0.91 ± 0.01 S/S_o; frequency of sinusoid 1 - 3 kHz) in single soleus fibers. In cardiac myocytes the slope of the tension-stiffness relationship declined from 1.04 ± 0.04 ($n = 7$) at pH 7.00 to 0.80 ± 0.03 ($n = 6$) at pH 6.20, a result similar to that obtained in soleus fibers suggesting that acidic pH decreases force per attached cross-bridge by a similar magnitude in these two muscle types. Muscle-type differences in the magnitude of acidic pH-induced depression of maximum Ca^{2+}-activated tension may be explained by a larger decrease in the apparent number of strongly bound attached cross-bridges in cardiac myocytes compared with slow skeletal muscle fibers.

M-Pos96

ULTRASTRUCTURAL CHARACTERIZATION OF CARDIAC MYOCYTES DERIVED FROM DIFFERENTIATING EMBRYONIC STEM CELLS. ((M.V. Westfall, D.I. Yule, K. Pasyk, L.C. Samuelson, and J.M. Metzger)) Dept. of Physiology, University of Michigan, Ann Arbor, MI 48109

We examined the ultrastructure of differentiating cardiac myocytes derived from mouse D3 embryonic stem (ES) cell cultures to determine whether these myocytes exhibit characteristics similar to cardiac myocytes within the heart. Morphometric analysis was carried out on 50 individual cardiac myocytes within longitudinal sections from contracting foci of ES cell cultures. Cells exhibited the rod shaped morphology and centrally located nuclei typical of maturing cardiomyocytes, with a cell length of 58.5±14.0 μm, a cell area of 248±44 μm^2, and a cell width of 5.6±0.4 μm. Electron micrographs indicated sarcomere formation also was present in ES cell-derived cardiac myocytes. Sarcomeres developed in parallel arrays, with a sarcomere length of 2.25±0.10 μm (n=10). Sarcomere length was 2.00-2.10 μm in similarly fixed adult mouse cardiac myocytes. In addition, electron micrographs examined for gap junctions and intercellular communication, indicated gap junctions were present in foci of ES cell-derived cardiac myocytes contracting for 1-15 days. Gap junctions were also detected by indirect immunofluorescence, using a monoclonal antibody which specifically recognizes the cardiac-specific gap junction subunit, connexin 43 (CX-43). Confocal image analysis demonstrated that CX-43 immunostaining was punctate within contracting ES cell foci. Microinjection of single cardiac myocytes with Lucifer yellow (2.5 μM) resulted in the spread of fluorescence to adjacent cells within a contracting focus, an indication of functional cell-cell coupling. Together, these results indicate ES cell-derived cardiac myocytes exhibit cell morphology and sarcomeres similar to those observed in in vivo cardiac myocytes along with functional cardiac-specific gap junctions.

M-Pos97

EFFICIENT GENE TRANSFER INTO PRIMARY VENTRICULAR MYOCYTES MEDIATED BY RECOMBINANT ADENOVIRUS. ((E.M. Rust, M.V. Westfall, R. Johnston, N. Lee, and J.M. Metzger)) Dept. of Physiology, University of Michigan, Ann Arbor, MI, 48109. (Spon. by D. Dawson)

Standard transfection methods such as $CaPO_4$, DEAE-dextran, lipofection, poly-l-ornithine, and electroporation work well in transformed cell lines, but are ineffective in adult cardiac myocytes in primary culture. Recently, recombinant adenovirus vectors have been used by various groups to infect cardiac myocytes *in vivo* and *in vitro*. The aim of this study was to establish stable short-term cultures of primary ventricular myocytes which could be genetically manipulated using recombinant adenovirus. Primary ventricular myocytes were isolated from the hearts of female adult Sprague-Dawley rats by collagenase digestion and plated onto laminin-coated plates in the presence of 5% FCS for 2 hours. After 2 hours, the media was replaced with serum-free DMEM+P/S. In order to determine if the myocytes maintained their differentiated state, rod-shaped myocytes were collected at days 0-7 post-isolation and protein isoform expression determined by SDS-PAGE. Dedifferentiation would be evident by an increase in β-myosin heavy chain (MHC) expression and potentially by changes in other myofilament proteins. Laser scanning densitometry of silver-stained gels showed that the proportions of α and β MHC did not change with time in culture, nor did the stoichiometry of the myosin light chains (MLC_1 and MLC_2). Infection of the primary ventricular myocytes in primary culture with the recombinant adenovirus vector AdCMVlacZ, and subsequent staining for β-galactosidase activity showed increasing expression of *lacZ* with increasing dose of AdCMVlacZ. The efficiency of gene transfer was 50% at a dose of 4×10^8 PFU/ml, and about 90% at a dose of 10^9 PFU/ml. SDS-PAGE of the rod-shaped myocytes collected from infected cultures showed no effect of treatment on the proportions of α and β MHC, or on the stoichiometry of MLC_1 and MLC_2. In addition, rod-shaped morphology and *lacZ* expression were maintained for at least 8 days. These findings indicate that infection of primary adult ventricular myocytes with recombinant adenovirus vectors does not affect the differentiated phenotype of the myocytes. Recombinant adenovirus vectors therefore provide an efficient gene transfer system by which to genetically modify ventricular myocytes for functional studies *in vitro*.

M-Pos98

ISOFORM SPECIFIC TRANSLOCATION OF PROTEIN KINASE C (PKC) TO MYOFILAMENTS IN CARDIAC MYOCYTES. ((Xu Pei Huang and Jeffery Walker)) Department of Physiology, University of Wisconsin, Madison, WI 53706.

We investigated the effects of lipids and the phorbol ester TPA on myofilament protein phosphorylation and PKC isoform distribution in cytosol, membrane and myofilament fractions of adult rat ventricular myocytes. Using Western blot analysis with antibodies raised against α, β, δ, ε and ζ-PKC, we found that ε and δ-PKC were the predominant isoforms in isolated adult cardiomyocytes. In unstimulated cells, ε-PKC and δ-PKC had similar distributions: 55 - 75% in the cytosol, 15 - 25% in the membrane fraction and 10 - 20% in the filament fraction. TPA (100 nM) caused a 2-fold increase of ε-PKC in the membrane fraction and a 4-fold increase in the filament fraction with a concomitant decrease in cytosolic ε-PKC. TPA also induced a significant translocation of δ-PKC to membranes and filaments. Arachidonic acid (AA, 50 μM) and the sphingolipid analogue C_2-ceramide (50 μM) caused an increase of ε-PKC in the filament fraction by 3-fold with a concomitant decrease in cytosolic ε-PKC. The time course of ε-PKC translocation was faster for AA than C_2-ceramide, and in each case matched the time course of myofilament protein phosphorylation. AA and C_2-ceramide did not have a significant effect on δ-PKC translocation, and sphingosine (50 μM), another sphingolipid, had no effect on translocation of ε-PKC or δ-PKC in these cells. Our results show that ε-PKC can be specifically translocated by different lipids to cardiac myofilaments, suggesting that this isozyme mediates the myofilament protein phosphorylation induced by these lipids. [supported by NIH]

M-Pos99

MODULATORY ROLE OF THE N-TERMINAL TnC BINDING SITE OF CARDIAC TROPONIN I ON ACTIVATION OF CARDIAC MYOFILAMENT. ((Hai-ping Tang, Xiao-du Guo, Anne F. Martin and R. John Solaro)) Department of Physiology/Biophysics, College of Medicine, University of Illinois-Chicago. Chicago, IL 60612

The interaction between cardiac troponin I (cTnI) and cardiac troponin C (cTnC) in the presence of calcium is the key event responsible for the activation of cardiac myofilaments and the subsequent contraction of the muscle. Two TnC- binding domains have been identified on TnI based largely on the studies of skeletal TnI and TnC. We generated two N-terminal deletion mutants of cTnI, cTnI-d53 and cTnI-d79 by using polymerase chain reactions to examine the role of these domains on cTnI. Both of these cTnI fragments lack the proposed N-terminal cTnC binding site. Comparison of the properties of native TnI and these two mutants by TnC-affinity chromatography, TnI-induced fluorescence change of IAANS-labelled cTnC, urea alkaline gel and native polyacrylamide gel analysis demonstrated that the cTnI-d53 mutant had lost the ability to interact with cTnC. The cTnI-d79 mutant retained a reduced calcium dependent affinity for cTnC. Both mutants had the ability to inhibit rat cardiac myofibrillar ATPase activity to the same extent as native cardiac TnI. However, unlike full length cTnI, the inhibitory effect of these two mutants could not be reversed by the addtion of cTnC. Our results indicate that the N-terminal TnC binding domain on cTnI is required for the interaction of TnI with the C-terminus of TnC and the formation of a stable TnI-TnC complex. More importantly, N-terminal TnC binding site of cTnI also modulates the interaction between the inhibitory domain of cTnI and cTnC, which is responsible for calcium activation of cardiac myofilaments.

M-Pos100

DEPRESSION OF Ca^{2+}-SENSITIVITY OF SKINNED CARDIAC MUSCLE BY cAMP-DEPENDENT PROTEIN KINASE IS AMPLIFIED IN ACIDOSIS.

((*Xiao-Ling Ding, Edmund H. Sonnenblick and Jagdish Gulati*)) The Molecular Physiology Laboratory, Albert Einstein College of Medicine, Bronx, NY 10461

Myocardial inotropic response to β-adrenergic stimulation is mediated through cAMP-dependent protein kinase (PKA) system, which phosphorylates troponin I (cTnI). cTnI phosphorylation in turn causes reduced Ca-sensitivity, which may be a protective mechanism. There is evidence that the catecholamine inotropic response of intact myocardium is abolished in acidotic milieus. Thus, the question was raised whether acidosis could also augment the effect of TnI phosphorylation on Ca-sensitivity. This is investigated presently by combined influences of PKA-treatment and of pH6.2 on pCa-force relationships of rat skinned cardiotrabeculae. Under physiological conditions (pH7.0), PKA-induced shift in the midpoint of pCa-force relation (i.e., $\Delta pK = pCa50_{without\ PKA} - pCa50_{with\ PKA}$) was 0.14±0.02 pCa units (n=4). At pH6.2, the shift was doubled ($\Delta pK = 0.29 \pm 0.02$) ($P<0.01$). To rule out the possibility that such an enhancement of the PKA effect in acidotic pH might be related to the depression in peak isometric force, the maximal force levels were also compared between pH7.0 ($P_{PKA}/P_O = 0.87 \pm 0.05$, P_O & P_{PKA} are force prior to and following PKA, respectively) and pH6.2 ($P_{PKA}/P_O = 0.84 \pm 0.06$), ($P>0.05$). These findings indicate that effects of phosphorylation of serines 22 & 23 in the N-terminal overhang of cTnI are amplified in the acidotic milieu. A possible mechanism for this may be by the steric interference by the N-terminal overhang to weaken the cTnI:cTnC interaction. *(Supported by NIAMS/NIH & NY Heart Association)*

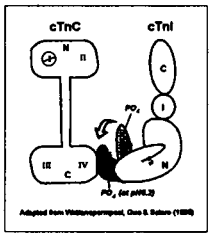

M-Pos101

EXCHANGE OF SLOW SKELETAL TROPONIN I (ssTnI) FOR CARDIAC TROPONIN I (cTnI) IN TRANSGENIC MOUSE HEARTS INCREASES MYOFILAMENT Ca^{2+} SENSITIVITY AT ACIDIC pH.

((*K. Palmiter, *R.J. Solaro, *X. Guo, ‡R. Fentzke, ‡K. Barton, ‡C. Clendenin, and ‡J.M. Leiden)) *University of Illinois at Chicago, Chicago, IL 60612 and ‡University of Chicago, Chicago, IL 60637

To test our hypothesis that expression of ssTnI in the heart decreases the effect of acidic pH on the myofilament pCa-force relation, we generated mice harboring a transgene expressing ssTnI in the adult heart. The transgene was made up of a pSPT BM21 construct containing the murine α-MHC promoter ligated to the complete coding sequence of the mouse ssTnI cDNA and its 3'UTR. An SV40 Poly A signal sequence was included to ensure correct 3' processing. Western blot analysis showed abundant activity of the transgene, with ssTnI, which is not expressed in adult heart, making up 80% of the total TnI present in the myofibrils. Compared to non-transgenic controls, detergent extracted fiber bundles from transgenic mouse hearts demonstrated a significant leftward shift of the pCa-force relation at pH 7.0 and a significantly smaller rightward shift in the pCa-force relation when the pH was dropped to 6.5 Our results demonstrate the feasibly of using a transgenic approach to exchange TnI isoforms in cardiac myofilaments, and support our hypothesis.

M-Pos102

A ROLE FOR TNI-TNC COMPLEX IN THE POSITIVE INOTROPIC EFFECT OF CGP 48506 ON CARDIAC CELLS AND MYOFILAMENTS.

((B.M. Wolska, Y. Kitada and R.J. Solaro)) Dept. of Physiol. & Biophys., Univ. of Illinois, Chicago, IL, 60612

We measured the effects of the benzodiazocine derivative, CGP 48506 (5-methyl-6-phenyl-1,3,5,6-tetrahydro-3,6-methano-1,5-benzodiazocine-2,4-dione) on contraction of intact rat myocytes and permeablized fibers of rat and guinea pig ventricular muscle. When added to isolated intact myocytes, CGP 48506 significantly increased the amplitude of cell shortening with little or no change in the Ca^{2+} transient, or diastolic length. In detergent extracted (skinned) fiber bundles, CGP 48506 increased maximum and submaximal force and shifted the pCa-force relation to the left without altering Ca^{2+}-binding to myofilament troponin C. CGP 48506 was able to reverse inhibition of contraction induced by butanedione monoxime both in intact cells and in skinned fiber bundles. These results indicate that CGP 48506 is working through a direct effect on the actin-cross-bridge reaction downstream from TnC (Wolska et al. *Am J Physiol*, In Press). Yet, its effect was significantly reduced when either cardiac TnI (cTnI) was exchanged for fast skeletal TnI (fsTnI), or when both cTnI and cTnC were exchanged with fsTnI-fsTnC. Our results indicate a unique site of action of CGP involving the reaction of TnI with other thin filament proteins that results in Ca^{2+}-sensitization with no effect on diastolic cardiac function.

M-Pos103

ALTERED MYOFILAMENT FUNCTION DURING CARDIAC ISCHEMIA CORRELATES WITH PROTEIN DEGRADATION AND IS MIMICKED BY ADDITION OF TnI INHIBITORY PEPTIDE TO CONTROL MYOFILAMENTS

((J.E. Van Eyk, K.A. Palmiter, R.M. Mraz and R.J. Solaro)) Dept. Physiol. and Biophysics, Univ. of Illinois at Chicago, Chicago, IL 60612.

We have developed a protocol for the preparation of skinned muscle fiber bundles from globally ischemic trabeculae. The rat trabeculae are tied to capillary tubes and placed in an impermeable plastic bag for 30 minutes at either 37°C (global ischemia) or on ice (control). The force developed by ischemic skinned fiber bundles is more Ca^{2+} sensitive than the control. This parallels the effect of ischemia on myofibril ATPase activity. Analysis by reversed-phase high performance liquid chromatography of the myofilament proteins extracted from ischemic myofibrils, reveals TnI and a high molecular weight protein (between 81-120 kDa) are extensively degraded during the ischemic episode. We have also shown that addition of the cardiac TnI inhibitory peptide 137-148 to control rat myofibrils is able to mimic the increased Ca^{2+} sensitivity displayed by 60 minute global ischemic myofibrils (pCa_{50} of 5.67 ± 0.04 and 6.00 ± 0.06 for the control myofibrils in the absence and presence of the peptide compared with 6.14 ± 0.07 for the ischemic myofibrils). The addition of the peptide to the global ischemic myofibrils had little effect on Ca^{2+} sensitivity (pCa_{50} of 6.00 ± 0.06 with 6.16 ± 0.11 of the control and ischemic myofibril with the peptide present). These results suggest that the presence of a degradation product of TnI which contains the inhibitory sequence would be sufficient to reproduce the myofibrillar dysfunction associated with global ischemia.

M-Pos104

CARDIAC MYOFIBRILLAR MYOSIN ATPASE DIFFERENCES IN HALOTHANE-POSITIVE AND -NEGATIVE PORCINE HEARTS.

[([1]Y.M. Liou, [2]M.C. Wu and [3]M.J. Jiang)][1]Department of Zoology, National Chung-Hsing University, Taichung;[2] Taiwan Livestock Research Institute, Tainan; [3]Department of Anatomy,National Cheng Kung University Medical College, Tainan, Taiwan.

Porcine stress syndrome, also known as malignant hyperthermia, is a stress-initiated state occurring in domestic swine in which genetically defected animals respond to halothane with skeletal muscle rigidity, hypermetabolism, and abnormal cardiac performances. In this study, we are interested in investigating contractile proteins which might lead to abnormal cardiac functions of the genetically susceptible pigs. Based on halothane contracture test and Hal-1843 DNA examination, miniature Lanyu pigs inherited with halothane-positive and -negative gene were identified and sacrificed. The effects of temperature and MgATP concentrations on the Ca^{2+}-activated ATPase activity were examined on glycerinated cardiac myofibrils obtained from the two types of pig hearts. At 30°C, there was a Ca^{2+}-activation of ATPase activity in the two types of cardiac myofibrils. The Ca^{2+}-sensitivity was abolished by raising temperature to 55°C. In addition, at 55°C, there was a greater increase in ATPase activity of the positive type than that of the negative type. When MgATP was present at the concentrations of 0.5 mM or greater, the ATPase activity of the halothane-positive hearts was higher than that of the negative hearts. The addition of Ca^{2+} further enhanced this difference. These observations suggest that the contractile machinery of the halothane-sensitive porcine hearts exhibits the higher myosin ATPase activity. This higher myosin ATPase activity might account for the abnormal cardiac functions in pigs liable to porcine stress syndrome.

M-Pos105

THE ROLE OF TITIN IN THE OPPOSING FORCE IN CARDIAC MYOCYTES

((M.H.B. Helmes & H.L. Granzier)) Washington State U. Pullman, Wa 99164-6520 (Sponsored by Miklos Kellermayer)

It is well established that when cardiac myocytes are stretched, titin develops *passive force* (figure A). We recently proposed a model in which titin can also exert *opposing force* when myocytes are below the slack length[1] (figure B). We tested this model as follows. Cardiac myocytes in suspension were allowed to shorten from their slack length (~1.85 μm sarcomere length) to about ~1.6 μm sl by putting them into rigor. Cells were relaxed by adding ATP. We found that the cells lengthened until they reached the slack length. Then we studied whether titin degradation with trypsin affects the length to which cells come back. The rigorized myocytes were incubated for 12 min. with 0.25 μg / ml trypsin (20°C). Gel electrophoresis showed that titin was completely degraded with no major changes in other proteins. After trypsin digestion rigor cells did not relengthen upon the addition of ATP. These findings support our model.

We also assessed titin's role in developing passive and opposing force by directly measuring these forces and by studying their sensitivity to trypsin. The data showed that trypsin digestion decreased both the opposing force and the passive force. These preliminary findings confirm that titin develops passive force and are consistent with the idea that titin is also responsible for the opposing force that brings myocytes back to their slack length.

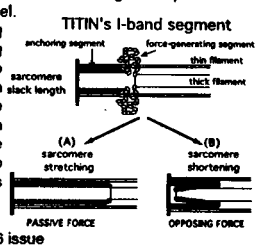

[1] Granzier et al., Biophysical Journal, January 1996 issue

M-Pos106

NON-UNIFORM ELASTICITY OF TITIN IN CARDIAC MYOCYTES.
((Trombitás, Károly & Granzier, Henk)). Washington State U., Wa 99164-6520.

In order to better understand the mechanism of passive-tension development in the heart, we investigated titin's elastic segment in cardiac myocytes using structural and mechanical techniques. Single cardiac myocytes were stretched by various amounts, immuno-labeled with monoclonal antibodies that recognize different titin epitopes, and processed for electron microscopy in the stretched state.

We found that both the A-band segment of titin and ~60% of the I-band segment are inelastic, both in sarcomeres that had been stretched and in sarcomeres that had actively shortened to below the slack length. We named the inelastic I-band segment the anchoring segment; see Fig. A. The remaining ~40% of the I-band segment of titin is elastic and, as indicated by mechanical measurements, it develops passive tension ('passive-tension segment' in Fig. A). Further, we found that in sarcomeres that are slack the passive tension segment is highly folded on top of itself (Fig. A).

We propose a two-stage mechanism of passive-tension development, in which between the slack sarcomere length (~1.85 μm) and a length of ~2.0 μm, titin's passive tension segment *straightens* (Figs. A and B) and at lengths longer than ~2.0 μm, the molecular domains that make up titin's passive tension segment *unravel*. (Fig. C). Sarcomere shortening to lengths below slack also results in straightening of the elastic titin segment (Fig. D), giving rise to a force that opposes shortening and that tends to bring sarcomeres back to their slack length.

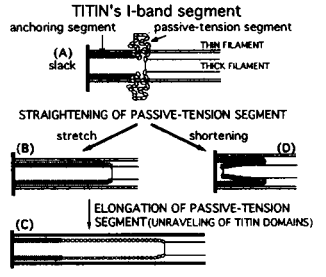

M-Pos107

INCREASED TROPONIN I PHOSPHORYLATION IN CARDIAC MYOCYTES FROM THE SPONTANEOUSLY HYPERTENSIVE RAT: EFFECT OF PHOSPHATASE INHIBITION.
((Bradley K. McConnell, Christine S. Moravec and Meredith Bond)) Dept. of Physiology & Biophysics, CWRU & Dept. of Molecular Cardiology, & Center for Anesthesiology Research, CCF, Cleveland, OH.

A decreased inotropic response to β-adrenergic stimulation is observed in hypertrophied hearts of the spontaneously hypertensive rat (SHR). We previously showed that this depressed response is associated with increased protein kinase A (PKA) dependent phosphorylation of troponin I (TnI) in SHR cardiac myocytes. This was observed either by stimulating the β-adrenergic receptor or by activating the β-adrenergic pathway upstream of PKA. Increasing TnI phosphorylation may result in decreased affinity of Ca^{2+} for troponin C and thus decreased force generation (McConnell *et al.*, submitted). The purpose of this study was to investigate the mechanism responsible for the greater increase in TnI phosphorylation in the SHR. We hypothesized that this may be due to decreased protein phosphatase activity. We used suspensions of $^{32}P_i$-labelled left ventricular (LV) cardiac myocytes, isolated from the SHR with stable hypertrophy (26 weeks), versus age-matched Wistar Kyoto rat (WKY) controls. We compared basal and β-adrenergic stimulated PKA-dependent TnI phosphorylation in response to calyculin A, an inhibitor of protein phosphatase type I and IIA. In the absence of β-adrenergic stimulation, TnI phosphorylation in both SHR and WKY myocytes increased with increasing concentrations of calyculin A and TnI phosphorylation in the SHR was also greater than in the WKY. In the presence of β-adrenergic stimulation, the increased TnI phosphorylation in the SHR was independent of calyculin A concentration, suggesting that differences in TnI phosphorylation between SHR and WKY during β-adrenergic stimulation are insensitive to phosphatase inhibition. In summary, our results indicate that the increase in PKA-dependent TnI phosphorylation in SHR, versus WKY myocytes, is not due to differences in cAMP production, cAMP breakdown, or decreased phosphatase activity, and therefore may be associated with differences in PKA activity or PKA regulatory proteins.

M-Pos108

MODEL OF LENGTH-DEPENDENT Ca^{2+} REGULATION OF TENSION IN CARDIAC MUSCLE IN STEADY STATE AND TWITCHES.
((J.J. Rice, W.C. Hunter, and R.L. Winslow)) Dept. of Biomedical Engineering, JHU, Baltimore, MD 21205. (Spon. by P. Fuchs)

We developed a model that simulates length-dependent effects from Ca^{2+} binding to force generation in cardiac muscle. First order binding of Ca^{2+} to troponin produces cooperative shifts in troponin/tropomyosin that allow crossbridges to cycle. Cooperativity is also incorporated in that: 1) strongly bound crossbridges facilitate formation of neighboring crossbridges, and 2) troponin/tropomyosin can be held in permissive state by two or more strongly bound crossbridges, even after Ca^{2+} has dissociated. Simulated F-Ca relationships (Fig. A) have half-activation and Hill coefficients that change with sarcomere length in agreement with experimental data. When the model is driven with a simulated Ca^{2+} transient (dotted trace, Fig. B), twitches are produced with realistic length-dependent amplitudes and timecourses. When coupled with existing excitation-contraction models, we can study cardiac phenomenon such as the Frank-Starling Law and mechano-electric feedback.

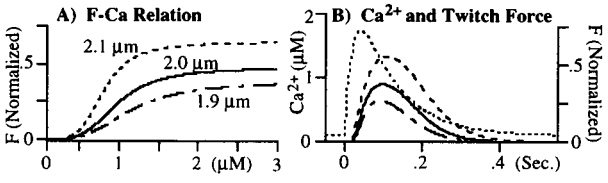

M-Pos109

EXPRESSION AND CHARACTERIZATION OF RAT CARDIAC α AND β MYOSIN SUBFRAGMENT-1 IN MAMMALIAN CELLS.
((Osha Roopnarine and Leslie A. Leinwand)) Dept of Molecular, Cellular, and Developmental Biology. Univ. of Colorado, Boulder, CO 80309.

We have previously shown that familial hypertrophic cardiomyopathy myosin missense mutations have resulted in impaired solubility and filament forming functions (Straceski et al., 1994). To assess the effect of the missense mutations on the ATPase and actin-binding properties of myosin, we have cloned rat cardiac α and β myosin subfragments-1 (S1) into mammalian expression vectors. The S1 gene fragment encodes 808 amino acids, similar to chymotryptically prepared skeletal myosin S1. A hexapeptide of histidines was cloned in at the C-terminal of S1, which allow specific binding of S1 to nickel-coupled agarose beads during purification. Monkey kidney cells (COS) were co-transfected with the cardiac S1 and rat ventricular LC1 expression plasmids. Indirect immunofluorescence of the cells showed diffuse positive staining for both S1 and LC1 in the cytoplasm of COS cells. Western blot analysis and immunoprecipitation of purified S1 showed that LC1 is associated with cardiac S1. Physiological ATPase assays of COS lysates of both S1 fragments indicates that fragments expressed in COS cells have activities similar to the tissue purified fragments.

M-Pos110

ALTERATION OF MYOSIN CROSS BRIDGES BY PHOSPHORYLATION OF MYOSIN-BINDING PROTEIN C IN CARDIAC MUSCLE.
([A. Weisberg and S. Winegrad]) Dept. of Physiology, University of Pennsylvania, Philadelphia, PA 19104

In addition to the contractile proteins, actin and myosin, contractile filaments of striated muscle contain other proteins that are important for regulating the structure and the interaction of the two force generating proteins. In the thin filaments, troponin and tropomyosin form a Ca sensitive trigger that activates normal contraction when intracellular Ca is elevated. In the thick filament there are several myosin binding proteins whose functions are unclear. Among these is the myosin binding protein C (C protein). The cardiac isoform contains 4 phosphorylation sites under the control of cAMP and calmodulin regulated kinases whereas the skeletal isoform contains fewer phosphorylation sites, suggesting that phosphorylation in cardiac muscle has a specific regulatory function . We isolated natural thick filaments from cardiac muscle and, using electron microscopy and optical diffraction, determined the effect of phosphorylation of C protein by PKA on cross bridges. Phosphorylation of the regulatory light chain was prevented by inclusion of EGTA and a calmodulin inhibitor. The thickness of the filaments that had been treated with protein kinase A was increased where cross bridges were present. No change occurred in the central bare zone that is devoid of cross bridges. The intensity of the reflections along the 43 nm layer line, which is primarily due to the helical array of cross bridges, was increased, and the distance of the first order reflection from the meridian along the 43 nm layer line was decreased. The results indicate that phosphorylation of C protein in cardiac muscle: 1) extends the cross bridges from the backbone of the filament; and 2) either increases their degree of order and/or alters their orientation. These changes could alter rate constants for attachment to and detachment from the thin filament and thereby modify force production in activated cardiac muscle.
(Supported by NIH grant HL 16010 to S.W.)

M-Pos111

REGULATION OF CROSS BRIDGE KINETICS BY ENDOTHELIN AS A MECHANISM FOR MODULATING EFFICIENCY OF ENERGY TRANSDUCTION IN CARDIAC MUSCLE.
([G. McClellan, A. Weisberg, and S. Winegrad]) Dept. of Physiology, University of Pennsylvania, Philadelphia, PA 19104.

The effect of endothelin, a powerful stimulant of contractility of cardiac muscle, has been variously attributed to increased inward Ca current, alkalization of the cytosol and increased Ca sensitivity of the contractile proteins. None of these mechanisms accounts fully for the changes in contractility of cardiac muscle that have been observed, and the physiological significance of endothelin's effects on contractility of cardiac muscle is still obscure. Here, we examine the effect of endothelin on force and actomyosin ATPase activity and the relation between the two in rat cardiac tissue. The magnitude of the effect of endothelin on force decreases as the alpha isoform of myosin heavy chain (MHC) is replaced by the slower beta isoform. The effect is nearly complete when about 20% of alpha MHC has been replaced by beta MHC. This is the same amount of replacement required to produce near maximum effect on shortening velocity (Van Buren et al 1995). It appears that the effect of endothelin on force relates to the interaction of heterogeneous cross bridges on the kinetics of cross bridge cycling. ATPase activity is always reduced at concentrations of endothelin that increase force. At very low concentrations, endothelin causes an increase in ATPase activity without altering isometric force, although the velocity of shortening of isolated myocytes is increased (Kelly et al 1990). The magnitude of the effect on ATPase activity produced by endothelin increases with resting sarcomere length of cardiac myocytes. A novel and potentially important physiological function of endothelin in cardiac muscle appears to be the regulation of efficiency in relation to force production by a mechanism that becomes progressively more active as the work load on the heart increases. As force and work are increased, the efficiency of energy transduction improves.
(Supported by NIH grant HL 16010 to S.W.)

M-Pos112

ROLE OF BOUND CREATINE KINASE IN ENERGY SUPPLY OF SR CALCIUM UPTAKE IN SKINNED RAT VENTRICULAR FIBERS. ((R. Minajeva, R. Ventura-Clapier, V. Veksler)). CJF 92-11 INSERM, Université Paris-Sud, 92 296 Châtenay-Malabry, FRANCE. (Spon. by R. Fischmeister)

MM-isoenzyme of creatine kinase (CK) in ventricular cells was found to be bound close to the sites of energy utilization. To study the role of CK in energy supply for sarcoplasmic reticulum (SR) ATPase *in situ*, saponin-permeabilized rat ventricular fibers were incubated for different times at pCa 6.5 to load the SR. Ca^{2+} release was induced by 5 mM caffeine in the presence of 0.05 mM EGTA and both ATP and phosphocreatine (PCr), and the area under isometric force (S_{force}) was measured. Free $[Ca^{2+}]$ in fibers and area under free $[Ca^{2+}]$ (S_{Ca}) during the release were estimated using steady state $[Ca^{2+}]$ /force relationship. S_{Ca} and S_{force} were plotted as a function of time of loading in different solutions. In the presence of 0.25 mM MgADP and 12 mM phosphocreatine (PCr) *i.e.* when ATP generated by the CK reaction was the only source of energy, S_{Ca} and S_{force} relationships were not significantly different from those after after loading in the presence of both ATP and PCr (control conditions). However, loading with ATP alone (3.16 mM) was considerably less efficient. After 3 min of loading, S_{force} and S_{Ca} were as low as 40 % and 45 % of their respective control values. Under these conditions, the addition of a soluble ATP regenerating system (50 IU/ml pyruvate kinase and 1 mM phosphoenolpyruvate), did not substantially improve the Ca^{2+} loading capacity. Elevation of pyruvate kinase concentration in the medium up to 100 IU/ml did not lead to any marked increase in Ca^{2+} loading. The data suggest that the Ca^{2+} uptake by SR *in situ* depends on the local ATP/ADP ratio that could be controlled mostly by bound CK rather than by a soluble ATP-regenerating system.

M-Pos113

CREATINE KINASE IS THE MAIN TARGET OF REACTIVE OXYGEN SPECIES ON CARDIAC MYOFIBRILS. ((R. Ventura-Clapier, H. Mekhfi, P.Mateo and V. Veksler)) CJF 92-11 INSERM, Univ. Paris-Sud, 92 296 Châtenay-Malabry, FRANCE.

Reactive oxygen species (ROS) have been reported to alter cardiac myofibrillar function as well as myofibrillar enzymes such as myosin ATPase and creatine kinase (CK). To understand their precise mode and site of action in myofibrils, the effects of xanthine/xanthine oxidase system (X/XO) or of hydrogen peroxide (H_2O_2) have been studied in the presence and in the absence of phosphocreatine (PCr) in Triton X-100 treated cardiac fibers. We found that XO, with or without X, induced a decrease in maximal calcium-activated tension (Tmax). We attributed this effect to a high contaminating proteolytic activity in commercial XO preparations since it could be prevented by a protease inhibitor, the phenylmethylsulfonyl fluoride (PMSF). pMgATP/rigor tension relationships have been established in the presence and in the absence of PCr in order to separate the effects of ROS on myosin ATPase and CK. In the presence of PCr, $pMgATP_{50}$, the pMgATP necessary to induce the half maximal rigor tension, was shifted from 5.03±0.17 to 4.22±0.22 after 25 min incubation in the presence of 30 mIU/ml XO and 100 µM X, or to 4.04±0.1 after incubation in the presence of 2.5 mM H_2O_2. No effect was observed on the $pMgATP_{50}$ when PCr was absent. Both incubations with X/XO system or H_2O_2 induced an increase in the calcium sensitivity of active tension and an increase in resting tension when MgATP was provided through myofibrillar CK (PCr and MgADP as substrates), but not when MgATP was directly added. In addition, myofibrillar CK but not myosin ATPase enzymatic activity was altered after incubation with either ROS. These results suggest that the main target of the ROS in myofibrils is the bound-CK and that inactivation of the enzyme induces a decrease in the local ATP/ADP ratio.

M-Pos114

NON-EQUILIBRIUM BEHAVIOR OF THE CREATINE KINASE SYSTEM NEAR MEMBRANES: A MODEL OF KINETIC COMPARTMENTATION ((D. N. Romashko, B. O'Rourke)) Johns Hopkins University, Baltimore, MD (Spons. by B. M. Ramza)

We examined a spatial reaction-diffusion model not restricted by the widely used simplifying assumption that the CK reaction is everywhere in local equilibrium. The model consists of 4 partial differential equations each describing the dynamics of ADP, ATP, Cr and PCr, respectively. CK is assumed to be soluble and uniformly distributed. The expression for reaction rate is a bilinear function of the concentrations of substrates. Boundary conditions define the rate of ATP hydrolysis and ATP/ADP translocase function on membranes surfaces and reflect the impermeability of membranes to PCr and Cr. The equations are analytically and numerically integrated in one dimension. The steady-state solution displays substrate profiles different from those predicted by "facilitated diffusion" theory [Meyer et al, 1984, Am.J.Physiol. **246**:C365]. While the bulk phase of the system approaches a local equilibrium, there are limited areas adjoining the cellular membranes where the reaction may be far from equilibrium, which is reflected in its unbalanced unidirectional rates. These layers form submembrane cellular compartments of kinetic origin. The width of the compartments weakly depends on CK activity and may be estimated to be within 0.3-0.7µM. The effect of mitochondrial inner membrane foldings dramatically decreases this size and shifts the CK reaction in this compartment towards equilibrium. The model suggests that kinetic compartmentation and local deviations from equilibrium exist near membranes and may explain experimental observations of functional coupling between CK and oxidative phosphorylation.

M-Pos115

SIMULATIONS BY A THREE COMPARTMENT MODEL OF THE CALCIUM HOMEOSTASIS IN RAT CARDIAC MYOCYTES. ((H. Salz, M.H.P. Wussling)) J. B. Insitute of Physiology, Martin Luther Univ., D-06097 Halle, Germany.

Model calculations were performed to describe calcium movements in myocardial cells. The model is based on the assumption of three compartments and simulates changes of the calcium concentration in the uptake and release compartment of the sarcoplasmic reticulum as well as in the cytosol in dependence on time.
We have simulated: (i) shape of calcium transient; (ii) calcium transient - frequency - relation (analog to force - frequency - relation); (iii) staircase phenomena; (iv) post rest calcium transients. Calcium transients of electrically stimulated rat cardiac myocytes were measured by confocal laser scanning microscopy using the Ca^{2+}-indicator fluo-3 AM. There was a good agreement between the experimental results and model calculations in case of incomplete calcium release. It is concluded that, in spite of coarse approximations, dynamic phenomena of the myocardium as observed after perturbations of the driving frequency may be well interpreted by the presented model.

FOLDING AND SELF-ASSEMBLY - DYNAMICS

M-Pos116

CONFORMATIONAL ANALYSIS OF THE B PEPTIDE OF KP6, A VIRALLY-CODED KILLER TOXIN: EVIDENCE FOR A THERMALLY-INDUCED MOLTEN GLOBULE INTERMEDIATE STATE. ((S.V. Balasubramanian[1], C.M. Park[2], J.L. Alderfer[3], J.A. Bruenn[2] and R.M. Straubinger[1])) [1] The Department of Pharmaceutics [2]The Department of Biological Sciences, University at Buffalo/State University of New York, Amherst, NY 14260 and [3]Department of Biophysics, Roswell Park Cancer Institute, Buffalo, NY 14263

Membrane insertion and translocation are essential steps in the activity of many water-soluble toxins, and these processes may be linked to their folding. KP6 is a virally-encoded killer toxin of *Ustilago maydis*, which consists of two water-soluble subunits, α and β. KP6 α may provide recognition of the toxin receptor, and combined with β, forms an ion channel in membranes. To understand KP6 membrane insertion and translocation, we investigated the conformation and folding of KP6 β, using Circular dichroism (CD) and fluorescence spectroscopy. Convex Constraint Analysis of the far UV CD spectrum suggested that in an aqueous environment, KP6 β exists predominantly in the β sheet conformation, but with detectable helical content. Upon incorporation into membranes and in non-polar solvents, the β sheet content increases and the helical content becomes negligible. Thermally-induced changes were investigated as a probe of KP6 β conformational transitions; even at higher temperatures such as 60 °C, the peptide conserves most of its secondary structural features but exhibits disordered tertiary structure, which is characteristic of molten globule intermediate states. ANS (1-anilino- 8- naphthalene sulfonate) binding experiments showed that the increase in temperature results in the exposure of hydrophobic domains. The data suggests that molten globule -like intermediate states, exposing hydrophobic domains, may be responsible for membrane insertion and translocation.

M-Pos117

THE ROLE OF PROLINE IN FOLDING STABILITY AND KINETICS OF STAPHYLOCOCCAL NUCLEASE

((Gediminas A. J. Vidugiris*, Dagmar M. Truckses⊥, John L. Markley⊥ and Catherine A. Royer*)) University of Wisconsin at Madison * - School of Pharmacy and ⊥ - Department of, Biochemistry, Madison, WI 53706

High hydrostatic pressure jump - fluorescence relaxation and pressure - fluorescence equilibrium studies were carried out on the unfolding/folding transitions of several forms of Staphylococcal Nuclease (SNase), wild type from Foggi strain, V8 strain SNase (H124L) were histidine at position 124 replaced by leucine and H124L mutants, in which proline (P) residues have been substituted by glycine (G) at positions 42, 47, 117 & 117 with 47.

Equilibrium and pressure-jump relaxation studies reveal that the stabilizing effect of P-to-G substitutions in the rank order P42G < P47G < P117G < P47G+P117G arises both from increases in the folding rate and decreases in the unfolding rate by the same magnitude. Increasing relaxation time for the unfolding/refolding transitions for SNase WT and H124L mutants is indicative of large, positive activation volumes for these processes. The activation and equilibrium volume change values are identical within error for all studied SNase proteins. The free energy difference between the folded and the transition state increases with these P-to-G substitutions, and the free energy difference between the unfolded and the transition states decreases. The most likely explanation is that each P-to-G substitution stabilizes all three of the states in the rank order unfolded state < transition state < folded state. We found that although GuHCl has a large effect on the stability of the proteins, it had no effect on the volume change values. This indicates that the volume change for binding an individual water molecule to exposed protein surface sites is similar to that of binding a molecule of GuHCl.

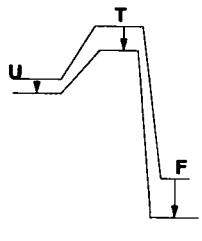

M-Pos118

ROTATIONAL AND CONFORMATIONAL DYNAMICS OF *ESCHERICHIA COLI* RIBOSOMAL PROTEIN L7/L12. ((B.D. Hamman[1,3], A.V. Oleinikov[2], G.G. Jokhadze[2], R.R. Traut[2] and D.M. Jameson[1])) [1]Dept. Biochemistry and Biophysics, Univ. of Hawaii, Honolulu, HI 96822; [2]Dept. Biological Chemistry, Univ. of California, Davis, CA 95616; [3]Dept. Medical Biochemistry and Genetics, Texas A&M Univ., College Station, TX 77843.

Fluorescence methods were utilized to study dynamic aspects of the 24 kD dimeric *E. coli* ribosomal protein L7/L12. Oligonucleotide site-directed mutagenesis was used to introduce cysteine residues at specific locations along the peptide chain, in both the C-terminal and N-terminal domains, and various sulfhydryl reactive fluorescence probes were attached to these residues. In addition to full-length proteins, a hinge-deleted variant and variants corresponding to the C-terminal fragment and the N-terminal fragment were studied. Steady-state and time-resolved fluorescence measurements were carried out and the results demonstrated that L7/L12 is not a rigid molecule. The two C-terminal domains and the dimeric N-terminal domain move freely with respect to one another. This mobility is significantly reduced in the hinge-deleted variant. The rotational relaxation time monitored by the probe depends upon its excited state lifetime. This observation implies that a hierarchy of motions exist in the L7/L12 molecule including facile relative motions of the C-terminal and N-terminal domains in addition to the overall tumbling of the protein. Upon reconstitution of labeled L7/L12 with ribosomal cores the motion associated with the N-terminal domain is greatly diminished while the facile motions of the C-terminal domains are almost unchanged. (Supported by NSF grants DMB 9005195 and MCB 9506845 (D.M.J.) and N.I.H. grant GM 17924 (R.R.T.))

M-Pos119

DIMER/MONOMER EQUILIBRIUM AND SUBUNIT EXCHANGE OF *ESCHERICHIA COLI* RIBOSOMAL PROTEIN L7/L12. ((B.D. Hamman[1,3], A.V. Oleinikov[2], G.G. Jokhadze[2], R.R. Traut[2] and D.M. Jameson[1])) [1]Dept. Biochemistry and Biophysics., Univ. of Hawaii, Honolulu, HI 96822; [2]Dept. Biological Chemistry, Univ. of California, Davis, CA 95616; [3]Dept. Medical Biochemistry and Genetics, Texas A&M Univ., College Station, TX 77843. (Spon. by I.R. Gibbons)

The dimer to monomer dissociation and subunit exchange of wild-type and cysteine variants of L7/L12 have been investigated using fluorescence spectroscopy. Steady-state polarization measurements on cysteine containing variants of L7/L12, labeled with 5-iodoacetamidofluorescein, indicated dimer/monomer dissociation constants near 30 nanomolar at 20C. When appropriate probes were attached to cysteines in the N-terminal domain (residues 12 or 33), both homo- and hetero-FRET was observed. Probes attached to cysteines in the C-terminal domains (residues 63 or 89) did not exhibit FRET. These results indicate that the intersubunit distance between specific C-terminal domain probes is, on average, greater than 85 Å. In a C-89 variant lacking 11 residues in the putative hinge region both homo- and hetero-FRET occurred suggesting that loss of the hinge region brings the two C-terminal domains closer. FRET was also observed between probes attached to a hybrid L7/L12 containing one probe in the N-terminal domain of one subunit and another probe in the C-terminal domain of the other subunit. The data thus indicate that the hinge promotes mobility of the two C-terminal domains relative to each other and relative to the N-terminal domain. Loss of homo-FRET between probes located in the N-terminal domain was used to demonstrate that labeled subunits exchange rapidly with subunits from unlabeled wild-type L7/L12. (Supported by NSF grants DMB 9005195 and MCB 9506845 (D.M.J.) and N.I.H. grant GM 17924 (R.R.T.)).

M-Pos120

A SITE-DIRECTED SPIN LABELING STUDY OF T4 LYSOZYME SOLUTION STRUCTURE ((H. Mchaourab, C.S. Fang and W.L. Hubbell)) Jules Stein Eye Institute and Department of Chemistry & Biochemistry, University of California, Los Angeles, CA 90095-7008.

The functional mechanism of many proteins involves a conformational change. The structural rearrangement can involve transitions between distinct states triggered by an interaction with the environment, or can occur as a part of a dynamic thermal equilibrium resulting from intrinsic flexibility in the protein structure. In previous work, it was shown that site-directed spin labeling (SDSL) can be used to provide a highly localized and time-resolved view of triggered structural transitions (Steinhoff et al. (1994) *Science 266*:105; Farahbakhsh et al. (1993) *Science 262*:1416). Here we report the use of SDSL to investigate equilibrium substates of T4 lysozyme apparently related to function. Although the crystal structure of T4 lysozyme is known to high resolution, there is considerable uncertainty concerning its solution structure. This is due to the observation of multiple structures related by a hinge-bending motion that effectively opens an otherwise closed active site cleft (Faber and Matthews (1990) *Nature 348*:263). To probe the structure in solution, we have introduced single nitroxides and pairs of nitroxides in relevant regions of the protein. Analysis of motional dynamics and solvent accessibilities of single nitroxides, and distances between nitroxide pairs suggests that: (1) the solution structure of the protein differs significantly from the "closed" X-ray structure, (2) there is little hinge-bending motion near helix A, although its packing with helix C is different from that observed in the X-ray structure, and (3) the data are consistent with a multi-state equilibrium that must involve a highly populated "open" state.

M-Pos121

NON-NATIVE STRUCTURE IN UNFOLDED BPTI. ((H. Pan, G. Barany and C. Woodward)) Department of Biochemistry, University of Minnesota, St. Paul, MN 55108.

Unfolded, reduced BPTI has extensive non-random, *non-native* structure (Pan et al., Biochemistry, 1995, **34**, 13974-13981). Sequential amide–amide NOEs imply that turn-like conformations are significantly populated at 18 pairs of residues. Six of these are non-native, and occur between contiguous pairs of residues in the segment 29-35, which in native BPTI constitutes a strand of extended sheet. There are also multiple non-native aromatic–aliphatic NOEs between residues which in native BPTI are in both strands of the central antiparallel β-sheet (residues 18–35). Residues 18–35 are apparently the first part of the protein to fold, as well as the most stable core of the native protein. In summary, in unfolded BPTI numerous *non-native* interactions are centered in the folding core of the protein. We suggest that these function to prevent misfolding and/or intermolecular aggregation until cooperative folding occurs. Hydrogen isotope exchange and relaxation experiments with ^{15}N-labeled, reduced BPTI are being carried out to determine if/how backbone dynamics correlate with non-native structure in unfolded BPTI.

M-Pos122

STATE TRANSITIONS IN THYLAKOIDS UNDER SHORT-TERM PHOTOREGULATORY CONDITIONS. ((R.M. Seiser, B.L. Wagner, M.F. Blackwell, and R.Wise*)) Department of Chemistry, Lawrence University, Appleton, WI 54911, *Department of Biology, University of Wisconsin-Oshkosh, Oshkosh, WI 54901.

The currently accepted model for state 1- state 2 transition includes the dephosphorylation of LHC II and its subsequent decoupling from stromal PS I and migration to granal PS II. This is thought to occur under low light conditions when the radiant intensity incident on PS II is insufficient to balance PS I activity, based on the redox level of the PQ pool [Allen et al (1981) Nature 291: 25-29]. The elevated levels of PS II activity are believed to be associated with increased appression and lateral organization of the thylakoid membrane. Compositional changes in *Spinacea oleracea* chloroplasts were observed following ten minutes of leaf shading under very low light conditions (< 2 $\mu E/m^2s$) compared to growth-chamber plants subjected to a 12-hour 100 μE light cycle. Computer-aided image analysis of electron micrographs shows an increase in the area of appressed membrane and corresponding decrease in area of non appressed stromal lamellae under shade conditions. Total area of plastoglobuli was found to decrease, suggesting the initiation of active membrane assembly. Our work suggests that membrane assembly gives rise to visible changes in thylakoid ultrastructure concomitant with LHC II migration within minutes of a change in light conditions. (Supported by HHMI 711911-529201).

M-Pos123

INVESTIGATION OF APOMYOGLOBIN KINETIC FOLDING INTERMEDIATES: ARE THESE STRUCTURES MOLTEN GLOBULES? ((J. Wyrick, J. Y. Yu, C. Yang, and A. K. Dunker)) Department of Biochemistry & Biophysics, Washington State University, Pullman, WA 99164

Hydrogen exchange pulse labeling with NMR (HX-NMR) and stopped-flow circular dichroism (SF-CD) in the far uv were used previously to suggest that the kinetic intermediates transiently observed during the folding of apomyoglobin resembled the partially unfolded equilibrium forms induced by partial destabilization, forms commonly called molten globules (Jennings and Wright, Science 262: 892-895, 1995). HX-NMR and far uv CD both probe backbone (secondary) structure, whereas molten globules have two additional characteristics - compactness and nonrigid side chain packing - that are not well-characterized by far uv CD and HX-NMR. To complete the characterization of the kinetic intermediates observed during the folding of apomyoglobin, we have been exploring methods for comparing the compactness and side chain rigidity of the kinetic and equilibrium partially unfolded forms. Our studies have focussed on the use of the probe 1-anilino-8-napthalene sulfonate (ANS), which does not seem to effect the rate of folding of apomyoglobin as judged by SF-CD with and without ANS, but which provides a very useful probe of the folding process. Fluoresence polarization of the ANS as a function of both folding time and solvent viscosity provides a means to compare the compactnesses of the equilibrium and kinetic folding intermediates and also to compare the flexibilities of the protein interiors by determining the local motions of the ANS from extrapolations of these data. The ANS fluorescence λmax, as well as the absolute and relative quenching of fluorescence by acrylamide and trichloroethanol, has also been found to provide useful data for comparing the characteristics of the hydrophobic regions of equilibrium and kinetic folding intermediates. Work in progress demonstrates the feasibility of using all these methods for comparing the kinetic and equilibrium folding intermediates of apomyoglobin.

M-Pos124

AN ALGORITHM TO COMPUTE EQUILIBRIUM VIBRATIONAL MODES OF MOTION OF MUTLIMERIC SYSTEMS ((Monique M. Tirion)) Dep't of Membrane Research and Biophysics, Weizmann Institute of Science, Rehovot 76100, Israel

An algorithm to rapidly determine equililibrium vibrations of multimeric complexes is presented. The algorithm is based on a normal mode analysis, a technique which reproduces temperature factors of X-ray scattering experiments, and reflects internal protein motions. This technique is typically applied to isolated protein systems. In a few cases additional bodies such as nucleotides and metals are included in cumbersome and inexact ways. The algorithm presented here permits analyses of multimeric systems consisting of proteins, nucleotides and metals, in a correct and analytically rigorous fashion. This algorithm also permits identification of flexibility characteristics of ensembles, providing elasticity constants for shear, stress and force deformations.
The computation proceeds using all torsional degrees of freedom for intra-molecular motions, as well as rigid-body degrees of freedom for inter-molecular motions. Introducing a simple Hookian potential for the inter-molecular interactions, a generalized eigenvalue equation is set up. The eigenfrequencies and eigen-motions that diagonalize the eigenvalue equation span all time-scales and all distance correlation lengths.
The simple Hookian potential has several advantages for systems that are extremely large and poorly resolved. It eliminates the need for costly energy minimizations, which may in any case be misleading when the structure is poorly resolved. It permits rapid and analytically exact computations of the eigenmodes. Furthermore, for large systems, slow motions with long correlation lengths are closely similar to motions obtained using more standard potentials. Results are presented showing that this software reproduces the soft modes of G-actin:ADP:Ca obtained using a more conventional energy potential. Applications within the limitations of this technique, which describes equilibrium deformations and not reaction paths, are discussed.

M-Pos125

TEMPERATURE JUMPS AND EARLY EVENTS IN PROTEIN FOLDING ((A. Gershenson*¶, C.J. Fischer*¶, J.A. Schauerte*§, P.M. Wolanin*¶, A. Gafni*§ & D.G. Steel*¶†)) *Inst. of Gerontology, §Dept. of Biological Chemistry, ¶Dept. of Physics, †Dept. of Electrical Engineering, University of Michigan, Ann Arbor, MI 48109

Initiation of protein folding or unfolding using laser based methods makes early events in protein folding (unfolding) experimentally accessible. Using a laser induced temperature jump system with a pulse width of 10 nanoseconds for studying protein folding, we have demonstrated temperature jumps in excess of 15°C which are sufficient to allow us to study either unfolding due to heat denaturation or refolding following cold denaturation using pump-probe spectroscopy. The pump beam is a near IR heating beam and the probe beam is a near UV laser beam for measurement of changes in intrinsic protein absorption and fluorescence. Initial studies focus on the heat denaturation of ribonuclease T_1 (RNase T_1), an 11 kDa protein with a well studied two state transition which displays a significant shift in both fluorescence and absorption spectra upon unfolding. Far UV circular dichroism data demonstrate that changes in absorption and fluorescence correlate with changes in secondary structure of RNase T_1. Studies of refolding following cold denaturation focus on horse muscle apomyoglobin, a protein which cold denatures, at accessible temperatures, from native to intermediate at pH 4.7 and from intermediate to denatured at pH 4 (in low salt concentrations) allowing us to study kinetics of multi-state refolding. Preliminary studies of apomyoglobin involve monitoring fluorescence shifts which reflect changes in secondary structure as detected by far UV circular dichroism. (Supported by NIA AG09761 and ONR N00014-91-J-1938)

M-Pos126

MONITORING OF FOLDING *IN VIVO* OF ALKALINE PHOSPHATASE BY ROOM TEMPERATURE PHOSPHORESCENCE ((Eric Dirnbach[1], Duncan Steel[2,3,4], Ari Gafni[2,5])) [1]Biophysics Research Division, [2]Institute of Gerontology, [3]Dept. of Physics, [4]Dept. of Electrical Engineering, [5]Dept. of Biological Chemistry, University of Michigan, Ann Arbor, MI 48109

Slow structural changes during the folding of Alkaline Phosphatase (AP) in the periplasm of E. coli are being studied using room temperature phosphorescence of the core Trp 109. This residue has a distinctive long lifetime (1.8s *in vitro*), allowing us to acquire a strong signal from intact living cells. The lifetime of the Trp phosphorescence is indicative of the environmental rigidity around the emitter and thus gives structural information of the surrounding region of the core of the protein. The phosphorescence lifetime and intensity are followed over time after induction of AP production. These data are correlated with the appearance of enzymatic activity and with protein lability as followed by the rate of denaturation by GuHCl, to examine slow "annealing" processes, as have been found *in vitro*. This non-invasive technique allows us to monitor changes during *in vivo* AP folding in real time. Using this method, there is no need for cell lysis and AP extraction, and the technique may be extended to the study of any folding protein with a long lifetime Trp emitter. (Supported by NIA AG09761 and NIH 5T32GM08270-06)

M-Pos127

PHOTODYNAMIC INACTIVATION OF GRAMICIDIN CHANNELS: A FLASH-PHOTOLYSIS STUDY. ((T.I. Rokitskaya, Yu.N. Antonenko, E.A. Kotova)) Belozersky Institute, Moscow State University 119899, Russia

Photosensitized inactivation of ionic channels formed by gramicidin in the planar bilayer lipid membrane (BLM) has been studied upon exposure of the BLM to single flashes of visible light in the presence of tetrasulphonated aluminum phthalocyanine. The gramicidin photoinactivation is inhibited by addition of unsaturated phospholipids to the membrane-forming solution as well as by the addition of azide to the bathing solution, consistent with the involvement of singlet oxygen. The characteristic time of photoinactivation (T) does not change markedly under these conditions. Moreover, T remains nearly constant upon alteration of the flash energy and the photosensitizer concentration. The value of T appears to be sensitive to the gramicidin concentration and to the factors affecting the open time of the gramicidin channels, namely the temperature and to the solvent used in the membrane-forming solution. The photoinactivation is not observed with covalent gramicidin dimers. The equations derived from the model of Bamberg and Lauger [J. Membr. Biol. (1973) 11, 177] describing the relaxation of the gramicidin-induced conductance after a sudden distortion of the dimer-monomer equilibrium are shown to explain consistently the time course of the photoinactivation provided that the damage to the gramicidin molecules leads to deviation from the equilibrium.

M-Pos128

TRYPTOPHAN FLUORESCENCE DURING CRABP FOLDING: AUTONOMOUS VERSUS ASSISTED ((Patricia L. Clark, Hwa-Ping Feng, Zhi-Ping Liu & Lila M. Gierasch)) University of Texas Southwestern Medical Center, Dallas, TX 75235 and University of Massachusetts, Amherst, MA 01003

Cellular retinoic acid binding protein (CRABP) has a predominantly β-sheet structure. The apo-protein's structure is characterized by a "clam shell" of β-strands, which wrap around a central solvent-filled cavity. The CRABP sequence contains three tryptophan residues, at positions 7, 87 and 109. Positions 7 and 87 are located towards the edges of the clam shell (W87 is partially exposed to solvent), whereas position 109 points in towards the aqueous cavity at the center of the molecule. The three tryptophan residues have been used as probes of structure formation during folding. Autonomous folding experiments indicate the rapid formation of an early (<10msec) intermediate which sequesters at least one tryptophan in an extremely hydrophobic environment. In the presence of the chaperonin GroEL, folding proceeds but with altered kinetics. Mutants with individual tryptophan residues replaced with phenylalanine give a preliminary indication of the fluorescent contributions of each tryptophan, and implicate interactions with W7 in the early intermediate. In addition, mutants containing only one of the wild-type tryptophans have been constructed. Spectral evidence suggests that the native structure of these mutants is identical to the wild-type native structure.

M-Pos129

FLUORESCENCE STUDIES OF THE KINETIC FOLDING PATHWAY OF THE *TETRAHYMENA* GROUP I INTRON. ((M.S. Rook, J.R. Williamson)) MIT, Dept. of Chemistry, Cambridge, MA, 02139

Understanding the three dimensional structures of RNA and the pathways by which these structures are formed is crucial to understanding the biological roles of RNA in the cell. The Mg^{2+} induced folding of the *Tetrahymena* group I intron has been studied in our lab using a RNase H-oligonucleotide binding competition assay. A folding pathway has been proposed that occurs on the minute timescale, and in which there is sequential folding of two domains. We have further explored the folding of the *Tetrahymena* group I intron using fluorescence spectroscopy. A fluorescent probe has been site specifically incorporated into the catalytic core of the *Tetrahymena* group I intron using a T4 DNA ligase based technique. Folding was initiated by the addition of Mg^{2+}, and the time dependent changes in fluorescence was monitored in order to obtain rate constants of folding events. Multiple kinetic phases were observed, indicating that the folding pathway is complex. Rapid kinetics, on the second timescale, were observed that could not be resolved in the previous RNase H-oligonucleotide method. Further studies will be performed using probes incorporated into different regions of the molecule, as well as studying mutants to correlate kinetic intermediates with particular structures on the folding pathway.

M-Pos130

GLOBAL ANALYSIS OF TIME-DEPENDENT FLUORESCENCE SPECTRAL CHANGES IN CHARACTERIZING FOLDING PATHWAY INTERMEDIATES. ((I.J. Ropson and P.M. Dalessio)) Dept. of Biochem. and Mol. Biol., Penn State Univ., Hershey, PA 17033. (Spon. by M. Fried)

One of the major obstacles to understanding the mechanism of protein folding is the lack of information on the nature of folding intermediates. Although large changes in the tryptophan emission spectra of proteins typically occur during folding, it has been impossible to associate these spectral changes with specific structures or with the environment of a particular tryptophan. Recent advances in stopped-flow equipment have allowed us to develop methods of observing spectral changes during folding and unfolding of rat intestinal fatty-acid binding protein. Previous studies have shown that intermediates are present during both unfolding and refolding of this protein, but little is known about the structure of the intermediates. The intermediate on the unfolding pathway has spectral characteristics similar to unfolded protein, with a maximal emission wavelength of 345 nm compared to 352 nm for unfolded protein and 330 nm for native protein. However, the signal is more intense than that of unfolded protein. The fluorescent properties of the intermediate on the folding pathway are similar to that of native protein, with a maximal wavelength of 335 nm, bit there is less intensity. The fluorescent properties of the folding intermediate are not similar to those of the "molten globule like" structure that can be obtained at low pH and high ionic strength for this protein, which has much lower intensity and a maximal wavelength of 345 nm. We have shown the fluorescence spectral characteristics of the intermediates formed during the folding and unfolding of IFABP, and can use this information to better understand the nature of the structures involved. Supported by NSF Grant MCB 94-05282.

M-Pos131

CHARACTERIZATION OF THE FOLDING INTERMEDIATES OF AN α/β BARREL PROTEIN BY TIME-RESOLVED FLUORESCENCE ANISOTROPY (O. Bilsel[1], L. Yang[2], J.M. Beechem[2] and C.R. Matthews[1]) [1]Department of Chemistry and Center for Biomolecular Structure and Function, The Pennsylvania State University, University Park PA 16802 and [2]Department of Molecular Physiology and Biophysics, Vanderbilt University, Nashville TN 37232.

Time-resolved fluorescence anisotropy of a bound extrinsic probe was studied in an effort to better characterize the intermediates along the folding pathway of the α-subunit of tryptophan synthase from *E. coli* (M.W. ~29 kD), an α/β barrel protein . Using a "double kinetic" approach [Jones, B.E., Beechem, J.M.& Matthews, C.R. (1995) *Biochemistry 34*,1867-77], the rotational relaxation time of 1-anilino-8-naphthalene-sulfonic acid bound to the protein was measured by time-correlated single photon counting at varying time delays following initiation of folding by stopped-flow techniques. Our results for the α subunit demonstrate that the rotational correlation time has a value close to that of the native state within the first 100 ms of the folding reaction. Surprisingly, this value increases approximately 20% after several seconds before subsequently decreasing to its native state value. These results, which are qualitatively similar to those obtained earlier on dihydrofolate reductase, raise the possibility that this non-monotonic change in rotational relaxation time may be a general phenomenon for globular proteins. This work was supported by NIH grants GM 23303 (CRM) and GM 45990 (JMB) and by the Lucille P. Markey Foundation (JMB).

M-Pos132

Studies on the Fluorescent Nucleotide 3-Methyl-isoxanthopterine Incorporated into Oligonucleotides. ((S. Driscoll,[1] M. Hawkins,[2] F.M. Balis,[2] W. Pfleiderer,[3] and W.R. Laws[1])) [1]Dept. of Biochemistry, Mount Sinai Sch. of Med., New York, NY 10029; [2]NCI, NIH, Bethesda, MD 20892; [3]Fakultät für Chemie, Universität Konstanz, Konstanz, Germany.

3-Methyl-isoxanthopterine (3-MI) is a fluorescent guanosine analogue (350 nm excitation; 425 nm emission) that has a high quantum yield (0.88) which is quenched in an oligonucleotide, especially by neighboring purines, and has shown potential as a probe for DNA structure and function [*Nucl. Acids Res.* **23**, 2872 (1995)]. We have incorporated 3-MI at different positions within different 21-nucleotide single-stranded oligomers. Steady-state and time-resolved fluorescence results reveal that the purine neighbor-induced quantum yield loss is due to static quenching, implying a strong purine/3-MI interaction. Acrylamide quenching studies show that the pteridine chromophore is shielded since the k_q for 3-MI is only about 10^8 $M^{-1}s^{-1}$. Incorporation of 3-MI into the oligos inhibits all acrylamide quenching regardless of the probe's position or the sequence of adjacent bases. The fluorescence anisotropy decay of single-stranded 21-mers requires two rotational correlation times for the depolarizing motions of 3-MI independent of the entire macromolecule and a third correlation time which represents an average of all 21-mer shapes in solution. Experiments on double-stranded 21-mers containing a single 3-MI probe are in progress. Supported in part by NIH grant GM39750. S. Driscoll was a 1995 Sigma Xi-Rudin Foundation Summer Fellow.

M-Pos133

FLUORESCENCE CHARACTERIZATION OF THE MIDPOINT TRANSITION OF RIBONUCLEASE T1. *(V.L. Williams, N. Silva and F.G. Prendergast) Mayo Foundation, Dept. of Biochemistry & Molecular Biology, Rochester, MN 55905*

Many of the conformational changes involved in the protein folding pathway are largely uncharacterized. Fluorescence spectroscopy offers a unique opportunity to probe localized structural changes in proteins as they unfold. In this study, we used time-resolved fluorescence techniques to monitor the unfolding pathway of ribonuclease T1. Ribonuclease T1 is an excellent model system for monitoring the unfolding pathway of a protein using fluorescence because it is one of the few single tryptophan proteins whose lifetime in the excited state can be described by a single exponential decay law. Furthermore, ribonuclease T1 has been shown to unfold by a standard two state transition, thus the changes in the population distribution of the native and denatured states of the protein can be unambiguously tracked by fluorescence properties such as the pre-exponential factors and the fluorescence lifetimes. In particular, we were interested in the fluorescence characterization at the midpoint transition of ribonuclease T1 as a function of thermal denaturation as well as of the chemical denaturants, guanidinum hydrochloride and urea. Our results show: 1) the thermodynamic parameters obtained from fluorescence measurements compare well with those parameters obtained from calorimetric data; 2) pre-exponential factors can reliably track the population distribution of the native and denatured states and 3) distinct differences exist among the conformational changes under these three denaturation conditions. *(Supported by GM34847)*

M-Pos134

CHARACTERIZATION OF THE CONFORMATIONAL STATES OF COWPEA SEVERE MOSAIC VIRUS BY USING TIME-RESOLVED FLUORESCENCE. ((A.C. Oliveira, J.E. Johnson*, J.L. Silva and A.T. Da Poian)) Depto. Bioquimica Médica - UFRJ 21941-590, RJ, Brasil. - * Scripps Research Institute-La Jolla, California (Spon. by FAPERJ, CNPq, EEC and PADCT).

Cowpea Severe Mosaic Virus (CPSMV) belongs to the Comoviridae family, a group of icosahedral plant viruses characterized by two single-stranded RNA genome encapsidated into distinct particles. Isolation of comovirus from infected plants results in a mixture of two ribonucleoprotein particles, as well as empty shells. Thus, three different particles can be separated by gradient ultracentrifugation: the top, middle and bottom components. Although these components differ in RNA content, they have the same protein composition. Hydrostatic pressure, sub-zero temperatures and urea were utilized to promote capsid dissociation and the conformational states of coat proteins were analysed by time-resolved fluorescence. For the three components, the best fits were obtained using two exponential decays. Addition of urea in crescent concentrations (from 0 to 8M) increased heterogeneity of the decay. The best fits were obtained using one-component Lorentzian distribution in the case of top component and one exponential decay and one-component Lorentzian distribution of lifetimes in the case of middle and bottom components. Completely denatured state (promoted by 8M urea) of top component coat proteins seemed to be distinct of that obtained for coat proteins of the ribonucleoprotein particles. CPSMV bottom component could be disassembled by pressures up to 2.5 kbar and coat proteins remained bound to the RNA after breakage of protein-protein contacts. At this condition, fluorescence decay was described also as two discreet lifetimes. Tryptophan lifetime measurements at lower pressures (1.2 kbar) revealed an intermediate state of coat proteins with higher heterogeneity (decay described as one distribution of lifetimes). When the temperature was decreased to -10°C under pressure, gradual increase in the width of the distribution occurred. However, coat protein conformational state at this condition seemed to be different from that completely denatured by urea.

M-Pos135

FOLDING KINETICS OF MUTANTS BPTI MUTANTS. ((R. Li and C. Woodward)) Department of Biochemistry, University of Minnesota, St. Paul, MN 55108.

Recent NMR studies of unfolded, reduced bovine pancreatic trypsin inhibitor (Pan et al., Biochemistry, 1995, **34**, 13974) and of a partially folded species which we take as an equilibrium model of BPTI early folding intermediates (Barbar et al., Biochemistry, 1995, **34**, 11423) indicate that hydrophobic interactions of Tyr23 and Tyr21 are important in initiation of BPTI folding. Tyr23, in the turn between the central antiparallel β-strands, has *local, native-like* NOEs in both unfolded BPTI and in the early folding intermediate. Tyr21 has *local, non-native* NOEs in unfolded BPTI, but has *non-local, native-like* NOEs in the early intermediate. If Tyr23 and Tyr21 are involved in initiation of BPTI folding, then this will be reflected in the folding kinetics. We have undertaken a study of the folding kinetics of nine BPTI 'mutants', all of which greatly destabilize the protein, and some of which have Tyr21 and Tyr23 replaced by alanine. Stopped-flow CD and pulsed hydrogen exchange kinetics experiments are being carried out, and preliminary results are consistent with the expectation that Tyr23, especially, is important in folding initiation.

M-Pos136

ULTRAFAST LASER INDUCED TEMPERATURE JUMP EXPERIMENTS ON PROTEINS ((C. M. Phillips and R. M. Hochstrasser)) Department of Chemistry and Regional Laser and Biotechnology Laboratories, University of Pennsylvania, Philadelphia, PA 19104-6323.

The temperature jump method that we recently developed [Phillips, et al., 1994; *Biophys. J.* **66**, A398] and used [Phillips, et al., 1995; *Biophys. J.* **68**, A131] in protein unfolding experiments has been significantly improved in both speed of data acquisition and signal-to-noise ratio. The new method incorporates a kHz pump laser and probes protein conformational changes at almost any desired infrared wavelength. In the first experiments, the results of the study on bovine pancreatic Ribonuclease A [Phillips, et al., 1995; *Proc. Natl. Acad. Sci.* **92**, 7292-7296] were confirmed and the Amide I absorption changes were more fully characterized. Infrared probing of T-jump responses associated with the structural changes in barnase, parvalbumin and green fluorescent protein are underway.

Supported by NIH grant RR 01348.

M-Pos137

FAST EVENTS IN PROTEIN FOLDING: HELIX DYNAMICS IN PROTEINS AND MODEL PEPTIDES ((R. B. Dyer,† S. Williams, † W. H. Woodruff,† R. Gilmanshin‡ and R. H. Callender‡)) †CST-4, M.S. J586, Los Alamos National Laboratory, Los Alamos, NM 87545 and ‡Physics Dept., City College of CUNY, New York 10031.

The earliest events in protein folding are critically important in determining the folding pathway, but have proved elusive to study by conventional approaches. We have developed new rapid initiation methods and structure-specific probes to interrogate the earliest events of protein folding. We have focused on the dynamics of secondary structure formation and the relative role of secondary structure in directing folding pathways and stabilizing folding intermediates. Folding or unfolding reactions are initiated on a fast timescale (50 ps or longer) using a laser induced T-jump. Laser excitation of water overtone absorbances produces a T-jump of 10 degrees or greater within 50 ps. Time-resolved observation of the infrared transient absorbances in the Amide I region reveal melting lifetimes of helices unconstrained by tertiary structure to be ca. 100 ns in a model 21-residue peptide and ca. 45 ns in "molten globule" apomyoglobin (horse, pH*3, 0.15M NaCl). A second domain in the apomyoglobin molten globule never melts, even on the long timescale (hours) of equilibrium FTIR experiments. The helix formation lifetimes, inferred from the melting rates together with the equilibrium constants, are ca. 10 and 1 ns, respectively. In "native" apomyoglobin (horse, pH*5.3, 10 mM NaCl) two helix melting lifetimes are observed and we infer that a third occurs on a timescale inaccessible to our experiment (> 1 ms). The shorter observed lifetime, as in the molten globule, is ca. 45 ns. The longer lifetime is ca. 70 μs. We suggest that the slower processes are due to helix melting that is rate-limited by the unfolding of tertiary structure. Equilibrium data suggest a lifetime of ca. 1 μs for the development of these tertiary folds.

M-Pos138

HYDROPHOBIC INTERACTIONS IN MOLECULAR DYNAMICS SIMULATIONS OF SURFACTANTS AND PROTEINS ((M.H. Alaimo and T.F. Kumosinski)) ERRC, USDA, Philadelphia, PA 19118 (spon. by H.F. Farrell, Jr.)

Hydrophobic interactions control many aspects of self-assembly and stability of macromolecular and supramolecular structures. Long-range forces between hydrophobic surfaces have been measured directly. The force between hydrophobic surfaces measured by the surface force apparatus (SFA) and atomic force microscopy (AFM) is up to several orders of magnitude larger than the expected van der Waals force. The experimental measurements of hydrophobic forces led us to consider using an effective hydrophobic force in molecular modeling and dynamics of lipid bilayers, micelles and water-in-oil microemulsions. Effective hydrophobic forces were also used in molecular dynamics simulations of the conformational changes of peptides and proteins. Results presented will show that inclusion in the force field of a simplistic approximation to hydrophobic attraction for hydrocarbon chains, provides models of self-assembled surfactant aggregates and biomacromolecular structures in good agreement with those deduced from experiment.

M-Pos139

KINETIC STUDIES ON THE REFOLDING AND MEMBRANE INSERTION OF OUTER MEMBRANE PROTEIN A (OMP A) OF E. COLI. ((J. H. Kleinschmidt and L. K. Tamm)) Dept. of Mol. Physiology and Biol. Physics, Univ. of Virginia, Charlottesville, VA 22908

OmpA is predicted to form an eight stranded β-barrel in the outer membrane of E. coli. Unfolded OmpA spontaneously inserts into lipid bilayers upon rapid dilution of the denaturant urea. OmpA binds to lipid bilayers in two forms: It is "partially inserted, adsorbed" to bilayers in the gel phase and "fully inserted, native" when bound to bilayers in the liquid-crystalline phase (1). In the present study we sought to determine if the adsorbed form could be a folding intermediate during membrane insertion of OmpA. Kinetic refolding experiments were carried out in the presence of small unilamellar vesicles of DOPC at temperatures ranging from 2 to 40 °C. At all temperatures, the tryptophan fluorescence intensity maximum shifted rapidly from 350 nm (unfolded OmpA) to 333 nm (membrane-bound OmpA). The fluorescence intensity at 333 nm then grew with kinetics that were strongly temperature dependent: At high temperatures, the fluorescence intensity reached its maximum after several minutes following a single exponential time course; at low temperatures, the kinetics were more complex and at least an order of magnitude slower. Parallel SDS-PAGE and trypsin digestion experiments showed that within the first few hours only the adsorbed form was formed at low temperatures. Even at high temperatures, the time course of the conversion to the native form as determined by SDS-PAGE was slower than the tryptophan insertion kinetics. When adsorbed OmpA was subjected to a temperature shift from 2 to 40 °C, it was rapidly converted into the native form, as judged from the kinetics and fluorescence characteristics which precisely paralleled those of OmpA that was directly inserted at the higher temperature. We interpret these results as evidence that the adsorbed form can be converted into the native form and, therefore, is a folding intermediate during membrane insertion of OmpA.
(1) Rodionova et al., 1995, Biochemistry, 34, 1921-1929).

M-Pos140

PROTEIN FOLDING KINETICS STUDIED BY ULTRAFAST MIXING. (C-K. Chan*, Y. Hu*, S. Takahashi[1], D. L. Rousseau[1], W. A. Eaton*, and J. Hofrichter*) *Laboratory of Chemical Physics, NIDDK, NIH, Bethesda, MD and [1]AT&T Bell Laboratories, Murray Hill, NJ

A rapid mixing, continuous flow method has been developed to study submillisecond processes in protein folding. Turbulent flow created by pumping solutions through a narrow gap into a small orifice produces complete mixing in less than 100 microseconds. We have used this method to study the collapse of cytochrome *c* from the chemically-denatured state. Collapse is monitored by measuring the fluorescence of tryptophan-59, which is completely quenched by energy transfer to the heme in the native state. At acid pH, where protonation of histidines inhibits binding of non-native heme ligands, the kinetics are highly nonexponential, extending from tens of microseconds to seconds. In terms of energy landscape theory[1], the kinetics might be interpreted as a "downhill run" toward the native structure. The extended time course would then result from a decrease in the effective diffusion coefficient, due to the increased roughness of the landscape, as the protein becomes more compact.

(1) J. D. Bryngelson, J. N. Onuchic, N. D. Socci, P. G. Wolynes, *Proteins* **21**, 167-195 (1995).

M-Pos141

PROTEIN FOLDING INITIATED BY LASER T-JUMP (P. A. Thompson, W. A. Eaton, and J. Hofrichter) Laboratory of Chemical Physics, NIDDK, NIH, Bethesda, MD 20892-0520 (Spon. by H. R. Sunshine).

Conventional methods for investigating protein folding kinetics are limited to the study of processes at times longer than a few milliseconds, the dead time of stopped flow mixers. Many proteins, however, fold much faster. To study protein folding in the submillisecond time regime we are developing a laser temperature-jump instrument. The instrument uses the fundamental of a Q-switched Nd:YAG laser, Raman shifted to about 1.5 μm, to directly heat water by vibrational excitation. The spatial and temporal profile of the temperature rise have been characterized by observing the change of tryptophan fluorescence and by measuring the UV absorption accompanying the proton transfer reaction between tyrosinate and TRIS. The probe for these measurements is an intracavity-doubled argon ion laser. With this instrument uniform temperature increases of at least 30 degrees can be achieved in less than 10 nanoseconds. The temperature decays approximately exponentially with a time-constant of 100 milliseconds. Measurements of protein folding from the cold-denatured state using this technique are in progress.

M-Pos142

DIFFUSIONAL DYNAMICS OF AN UNFOLDED PROTEIN. ((S.J. Hagen, J. Hofrichter, and W.A. Eaton)) Laboratory of Chemical Physics, NIDDK, NIH, Bethesda, MD 20892-0520 (Spon. by D. R. Davies).

The formation of native and non-native contacts within a random coil polypeptide must represent one of the earliest steps in protein refolding from the chemically denatured state. Jones *et al.* optically triggered the refolding of cytochrome *c* in guanidine hydrochloride (*Proc. Natl. Acad. Sci. USA* 90, 11860 (1993)), and found that the methionine residues at positions 65 and 80 bind ten times more quickly to the heme at position 18 than do the histidine residues which are much closer at positions 33 and 26. What accounts for this difference in rate? To establish the contribution from chemical bond formation (*i.e.* the geminate binding) to these rates we have used nanosecond-resolved absorption spectroscopy to measure the bimolecular rates for free methionine and histidine binding to the hemepeptide of cytochrome *c* under the (near theta) solvent conditions of Jones *et al.* We calculate the geminate rate for methionine to be $k^M \geq 6\times10^{10}$/s, much faster than that for histidine, $k^H \approx 1.3\times10^8$/s. The rate of H33 (and H26) binding to the heme of the complete polypeptide is most likely limited by k^H and by the equilibrium probability that the required loop will form spontaneously. From our data we can estimate this probability, yielding Flory's ratio *C*, which characterizes the statistical properties of the intervening segment of polypeptide. By contrast, the binding of M65 and M80 is rate-limited by the diffusion of the polypeptide chain to form an encounter complex. Assuming a Gaussian distribution of heme-residue distances, we estimate the time constant to be 35-40 microseconds. This may represent the minimum time for the collapse of the polypeptide chain under folding conditions.

M-Pos143

RAPID, PHOTO-INDUCED PROTON TRANSFER: DEPENDENCE ON ACCEPTOR SIZE, SHAPE AND CONCENTRATION.

((S. Abbruzzetti, L. Masino, C. Viappiani, A. Vecli, L.J. Libertini, E.W. Small, R. Nandagopal, R. McRae and J.R. Small)) Università di Parma, 43100 Parma, Italy; Quantum Northwest, Inc., Spokane, WA 99223; Eastern Washington University, Cheney, WA 99004 (viappiani@vaxpr.pr.infn.it, 75603.3012@compuserve.com, jsmall@ewu.edu)

Photolabile caged proton (2-hydroxyphenyl 2-nitrophenylethyl phosphate, sodium salt) has been used to induce a fast pH jump in aqueous solution by pulsing the sample with a nitrogen-pumped dye laser operating at 366.6 nm. Time-resolved, volumetric photoacoustic measurements with a 1.0-MHz transducer at the β=0 temperature (in the 0 to 4 °C range, depending on solvent) indicate solution volume changes arising from the fast release of protons and from their subsequent binding to acceptors. A series of acceptors has been studied, including simple buffers, propylamine, lysine monomers, lysine derivatives with blocked α-amino groups, and poly-L-lysine polymers ranging from 1000 to 375,000 MW. Concentration, solvent, and incident laser pulse energy parameters were varied. Data are interpreted in terms of decomposition of the photolabile caged compound, interactions between released protons and solvent, protonation of acceptors, and conformational transitions in the polymeric acceptors induced by proton binding.

Supported by CNR, Italy (CV), DMI-9362206 and GM51147 (EWS), and an EWU Faculty Research Grant (JRS).

M-Pos144

AN UNUSUALLY STABILE DNA STRUCTURE

((E Protozanova & RB Macgregor*)) Faculty of Pharmacy
University of Toronto, Toronto, Ontario M5S 2S2

DNA sequences containing runs of consecutive dG residues form tetraplex structures in the presence of certain inorganic cations. Similar sequences have also been found in teleomeric regions of chromosomes and are implicated in cellular senescence.

We have found that the single stranded oligomer $(dA)_{15}(dG)_{15}$ exhibits interesting behaviour under a variety of experimental conditions. A solution of this oligomer containing 50% formamide, heated to 90 °C for 5 min and electrophoresed on a denaturing polyacrylamide gel (7 M urea) at 50 °C resolves into several discrete bands. The most rapidly migrating band is at the position expected for the monomer. A semilogarthmic plot of the relative mobility of slower-migrating, higher molecular weigh species is linear with respect to integer values presumably reflecting the number of strands in each complex. The proportion of higher molecular weight species increases with the concentration of oligomer. Similar results are found on native polyacrylamide gels run at 10 °C. Addition of the complementary strand to the solution prior to the heat denaturation step inhibited formation of the high molecular weight species under the conditions of denaturing gels. On native gels, addition of the complementary strand at various mole ratios led to formation of duplex and RRY triplexes. In the presence of the complementary third Y strand, RYY triplexes were formed. A similar sequence with six random bases at both ends did not exhibit any of these properties.

M-Pos145

BIOPHYSICAL PERSPECTIVES OF PROTEIN PRECIPITATION-COPRECIPITATION. Rex Lovrien and Daumantas Matulis, Biochemistry Department, Univ. of Minnesota, St. Paul, MN 55108

Protein precipitation (and crystallization) is an end result of several kinds of subreactions. New kinds of precipitating and coprecipitating agents (matrix ligands), very old kinds like ammonium sulfate (salting out) studied in new ways, may be able to overhaul and perhaps upgrade some of our perspectives. Our observations are that protein precipitation may be pushed (raising the chemical potential of proteins in solution), or pulled (increase the stability of the product) or a combination of both. The trigger for precipitation-coprecipitation most frequently is electrostatic (charged protein, charged ligands, polarizability of ligands). But the overall drive to carry it through often sharply depends on how water has to get shifted, and on strengths of hydrophobic reactions between protein molecules and between organic ligand tails when matrix ligands are used. Very dilute detergents (SDS) are good protein precipitating agents in narrow windows of parameters such as (protein charge) x (ligand charge), and degree of site filling. There exists about eight common ways to precipitatively protect protein activity. Probably two of these are "pure" ways, exclusively pulling (matrix ligand method) or exclusively pushing (sulfate kosmotropicity-exclusion). The remainder are hybrids of more than one basic mechanism. When protein conformation tightening, ordering, squeezeout of water occurs, coprecipitation can evolve into cocrystallization. Inorganic sulfate still is supreme in cocrystallization. However matrix ligands have potential to compete with it. Protein precipitation has been avoided in many cases, being regarded as an inconvenience or as evidence for denaturation. However it is due for renewed interest because of what it may show about protein-ligand behavior in solution.

M-Pos146

DIRECT AND SPINODAL-PROMOTED GELATION OF AQUEOUS SOLUTIONS OF BOVINE SERUM ALBUMIN

((D. Bulone ^, A. Emanuele*, V. Martorana^, P.L. San Biagio*^, and M.U. Palma*)), ^ CNR Institute for Interdisciplinary Applications of Physics and * Dept. of Physics, University of Palermo, Via Archirafi 36, I-90123 Palermo, Italy.

The following well known aspects of gel self-assembly cover high practical interest: I) the dependence of the gel structure and texture upon the condition of gelation and ii) the possibility for gelation to occur, in many cases, at polymer concentrations much lower then those predicted by random percolation theories. The conceptual background common to these different aspects can be found by unraveling the nature of the initial spontaneous break of symmetry and the time sequence of kinetic processes which bring to gelation. This also covers a marked theoretical interest because kinetic and diffusional aspects are hardly taken into account in current theories of gelation/percolation. Here we present gelation kinetic studies of Bovine Serum Albumin (BSA) aqueous solutions. Recent work showed that BSA unfolding causes the appearance of an instability region of the sol not observed for native BSA. For concentration below the threshold of random cross-links percolation, the thermodynamic phase transition corresponding to spinodal demixing is the determinative symmetry breaking step allowing the subsequent occurrence of (correlated) cross-linking and its progress up to the topological phase transition of gelation. The structure function (S(q)) of the gel obtained in this case is seen to be similar to that generated in the sol by spinodal demixing. For higher BSA concentrations no sign of spinodal demixing is observed. The occurrence of direct gelation yields a less structured S(q).

M-Pos147

PROTEIN FOLDING AND INFORMATION THEORY. ((T.G. Dewey and B.J. Strait)) Department of Chemistry, University of Denver, Denver CO 80208.

A number of information theoretical parameters are calculated for protein sequences, solvent accessibility profiles and hydrophilicity profiles. The Shannon entropy is calculated from a k-tuplet analysis of sequences from a "representative" data set of 155 proteins. Using a fundamental theorem of information theory, this parameter is used to calculate the total number of probable protein sequences. The total number of probable protein sequences is over 10^9 times less than the total number of possible sequences. This indicates that only small regions of sequence space are populated by viable proteins, suggesting that shows that considerable sequence editing occurs throughout evolution. The Shannon entropy and mutual information entropy can likewise be calculated for the hydrophilicity and solvent accessibility profiles. The mutual information between these two profiles is low, indicating that only a small fraction of the information contained in the hydrophilicity profile is transmitted to the final structure as represented by solvent accessibility. In this conceptualization, the hydrophilicity can be viewed as the "message sent" and the solvent accessibility is the "message received". The folding process is the "communication channel". Adopting this view, it is seen that the transmission of information by the folding process does not have a high fidelity. This, in part, reflects a lack of sequence stringency in the folding process.

M-Pos148

19F-NMR SPECTROSCOPIC STUDY OF THE UNFOLDING OF D-LACTATE DEHYDROGENASE OF E. COLI ((Z.-Y. Sun, S. R. Dowd, and C. Ho)) Dept. of Biol. Sci., Carnegie Mellon Univ., Pittsburgh, PA 15213.

D-Lactate dehydrogenase (D-LDH) of *E. coli* is an FAD containing, 65 kD membrane-associated protein. The ^{19}F-NMR spectra of 5F-Trp-labeled D-LDH unfolded by guadinine hydrochloride (Gdn.HCl) show that, in the presence of detergent, the protein unfolds in several steps. At lower Gdn.HCl concentrations, the 5 native Trps of the unfolded protein give rise to 5 narrow NMR peaks. Experimental results suggest that the unfolded protein at this stage may have lost the FAD cofactor but contains a large degree of secondary structure. The ^{19}F-NMR spectra also show that the 5 resonances from the native Trps in the unfolded protein can be divided into two groups, with the 3 resonances in the upfield group subject to more changes with increasing denaturant concentrations. Circular dichroism studies suggest that the main unfolding transition occurs at 2.9M Gdn.HCl, while a subsequent conformational change indicated by ^{19}F-NMR studies occurs at 4.3M Gdn.HCl. Thus, ^{19}F-NMR spectroscopy is a useful tool in monitoring the unfolding behavior of small domains of large proteins. ^{19}F-NMR results also show that detergent help stabilize the unfolding intermediates of D-LDH and prevent them from aggregating. The ^{19}F-NMR spectrum of a mutant D-LDH, T79W, which lost the FAD cofactor, is similar to the spectrum of unfolded D-LDH at 2.5M Gdn.HCl, agreeing with the conclusion that the first unfolding intermediate may be the apoenzyme. [This work is supported by NIH grant GM-26874].

INTRACELLULAR COMMUNICATION

M-Pos149

TEMPERATURE-DEPENDENT BLOCK OF THE CALCIUM-RELEASE-ACTIVATED-CURRENT (I_{CRAC}) IN KU812, A HUMAN LEUKAEMIC CELL LINE. ((Baggi Somasundaram, M. P. Mahaut-Smith & R. Andres Floto)) The Physiological Laboratory, Downing Street, Cambridge, CB2 3EG, U.K.(Spon. by R.D. Keynes)

The mechanism whereby depletion of intracellular Ca^{2+} stores is coupled to the activation of I_{CRAC} is not understood. We recently showed that primaquine, an inhibitor of vesicular transport, blocks I_{CRAC} in rat megakaryocytes, thus providing evidence that the CRAC channel may be recruited to the plasma membrane by vesicular transport following store depletion (Somasundaram et al, 1995). It is well established that vesicular transport is temperature sensitive and is blocked below temperatures ranging from 16-18°C. Therefore, we have tested the effect of temperature on the activation and maintenance of I_{CRAC} in KU812, a human leukaemic cell line. I_{CRAC} was measured as described previously for rat megakaryocytes (Somasundaram et al,1995). Activation of I_{CRAC} by thapsigargin was temperature-sensitive showing a transition at 20-22°C and complete inhibition at 17°C (see Fig). Once activated, I_{CRAC} also displayed a transition reduction at 20-22°C, but was not completely blocked by lower temperatures, down to 15°C. Fura-2 measurements of $[Ca^{2+}]_i$ suggested that these effects were not an indirect effect of temperature on the ability of thapsigargin to release stored Ca^{2+}. These temperature effects were reversible and are consistent with the actions of temperature on vesicular transport. However, other temperature effects have to be considered such as ATP hydrolysis or direct effects on the CRAC pathway by changes in membrane lipid viscosity.

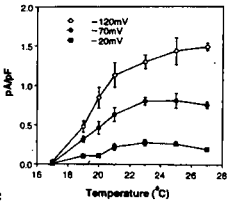

Somasundaram B., Norman J.C. & Mahaut-Smith M.P. (1995) Biochem. J. 309, 725-729.

M-Pos150

STORE-MEDIATED Ca^{2+} INFLUX IN THE HUMAN LEUKAEMIC CELL LINE KU-812, IS BLOCKED BELOW 18°C. ((R.Andres Floto, M.P.Mahaut-Smith & Baggi Somasundaram)) The Physiological Laboratory, Downing Street, Cambridge, CB2 3EG,U.K.(Spon. by T.Tiffert)

We have investigated the effect of temperature (10-37°C) on the activation and maintenance of store-mediated Ca^{2+} influx (SMCI) in fura2-loaded KU-812 cells. Using cuvette fluorimetry at the isosbestic excitation wavelength (360 nm), we measured the difference in the rate of Mn^{2+} photoquench (ΔQ) between store-depleted (thapsigargin 100 nM, 6 min) and control cells at different temperatures. We find a temperature-dependent reduction in SMCI, which is completely blocked at 18°C. A similar temperature relationship is found if SMCI is activated at 37°C and the temperature then changed. This is consistent with a temperature-dependent block primarily of the influx pathway rather than of the activation process. Measurements of cytosolic ATP concentrations (by luciferin-luciferase assay) in cells at different temperatures suggest this block is not due to ATP depletion. These results are consistent with temperature-dependent changes in lipid membrane viscosity affecting either vesicular transport or transmembrane protein conformational changes.

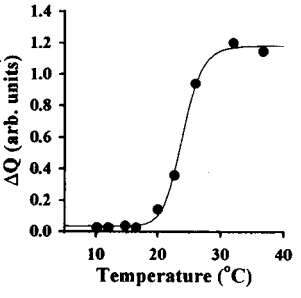

M-Pos151

CO-LOCALIZATION OF SARCOLEMMA, SARCOPLASMIC RETICULUM, AND LOCALIZED Ca^{2+} GRADIENTS IN CORONARY SMOOTH MUSCLE CELLS ((M. Sturek)) Vascular Biology Laboratory, Dalton Cardiovascular Res. Center and Dept. of Physiol., Univ. of Missouri, Columbia, MO 65211. (Spon.: H.-D. Kim)

The morphological association of sarcoplasmic reticulum (SR) with the sarcolemma and intracellular free Ca^{2+} (Ca_i) gradients was studied with confocal microscopy. Coronary artery cells were loaded by incubation with SR marker 3,3'-dihexyloxacarbocyanine iodide (DiOC), the sarcolemmal marker di-8 ANEPPS (Di8), and the Ca_i indicators fluo-3 or fura red. Optical sections were obtained at 1 μm intervals in the z-axis to observe SR and sarcolemmal morphology while measuring Ca_i simultaneously. Maximal release of Ca^{2+} from the SR with $5x10^{-3}$ M caffeine was associated with localized sites of high Ca_i near areas of superficial SR, i.e. Ca_i was localized in a subsarcolemmal compartment (Ca_s) before Ca_i increased in the bulk myoplasm (Ca_m). Three-dimensional reconstruction of optical sections of di8-loaded cells confirmed large infoldings of the sarcolemma 1-2 μm wide and 1-6 μm deep into the interior of the cell, which I previously found using membrane impermeant dyes in the bathing solution. These data strongly indicate functional and structural colocalization of the SR and sarcolemma and the usefulness of these membrane markers in living cells. (Support: NIH HL52490, RCDA HL02872, AHA 93011900)

M-Pos152

MULTIPLE CONDUCTANCE LEVELS IN NEONATAL MOUSE AND RAT LIVER NUCLEI. ((R. Tonini, F. Bertaso, and M. Mazzanti)) Dipartimento di Fisiologia e Biochimica Generali, Laboratorio di Elettrofisiologia, via Celoria 26, I-20133, Milano, ITALY.

In the last five years several authors, working on isolated nuclei from different cell types, have demonstrated ionic permeabilities on the nuclear membrane. In addition to channels present also on the endoplasmic reticulum, such as the Ca release IP_3-sensitive channel, there are many K and Cl pathways whose precise function is not yet known. One hypothesis suggests that some of the ionic channels revealed on the nucleus surface are part of the pore complex. During electrophysiological recordings using a conventional patch-clamp pipette, the probability of including a pore in the area isolated by the patch electrode is very high. Therefore, if the hypothesis is valid, it should be possible to find a correspondence between number of conductance levels recorded in nucleus-attached experiments and nuclear pore density obtained from freeze-fracture assessment. Our study shows that, in particular conditions, it is possible to record a high number of current levels equally spaced. According to the latest nuclear pore structure model, eight peripheral aqueous pathways are associated with each complex. We use isolated liver nuclei from neonatal rats and/or mice in which the density of nuclear pore complexes is lower than in the adult. Our patch-clamp single-channel data show a reasonable number of current sublevels compared with nuclear pore density.

M-Pos153

EFFECT OF CYTOSOLIC FREE CALCIUM UPON THE INOSITOL(1,4,5) TRISPHOSPHATE RECEPTOR AT THE SINGLE CHANNEL LEVEL.

((Thrower, E., Lea, E.J.A. and Dawson, A.P.)) School of Biological Sciences, University of East Anglia, Norwich NR4 7TJ., UK.

Cytosolic free calcium has been shown to have both activating and inhibitory effects upon the inositol (1,4,5) trisphosphate receptor (IP_3 R) during intracellular calcium release. The effects of cytosolic free calcium on IP_3 R have already been monitored using cerebellar microsomes (containing IP_3R) incorporated into planar lipid bilayers [Bezprozvanny et al 1991. *Nature* 351:751-754]. In these experiments the open probability of the channel exhibited a "bell-shaped Ca dependence". However this has only been seen when the receptor is in the presence of its native membrane (eg. microsomal vesicles).

Using solubilized, purified IP_3R incorporated into planar lipid bilayers using the dip-tip technique, we set out to see if the same effect is seen in the absence of its native membrane. Channel activity was observed in the presence of 4μM IP_3 and 200nM free Ca. Mean single channel current was approximately 2.4pA and more than one population of lifetimes was observed. Two populations had mean open times of approximately 20ms and 110ms. With 2μM free Ca, the mean single channel current remained virtually unchanged, but the lifetimes were found to have increased to approximately 30 ms and 500 ms respectively. Increasing the free Ca concentration to 4μ M did not significantly affect mean single channel current although mean open times increased further. At 10μM free Ca no channel activity was observed.

Thus, with purified receptor in artificial bilayers, free [Ca] on the cytosolic face of the receptor has major effects on channel behaviour, particularly on channel closure, although inhibition of channel activity is not seen until very high free [Ca] is reached.

M-Pos154

RECIPROCAL RELATION BETWEEN RATE AND DURATION OF $InsP_3$ EVOKED Ca^{2+} RELEASE IN PURKINJE, ENDOTHELIAL AND LIVER CELLS.

((D.Ogden, T.Carter & T.Capiod)) NIMR, Mill Hill, London NW7 1AA, UK.

$InsP_3$ evoked Ca^{2+} release shows large kinetic differences between cerebellar Purkinje neurones, pig vascular endothelia and guinea pig hepatocytes. Following a pulse of high $InsP_3$ concentration the maximum Ca^{2+} flux into unit cytosolic volume, $d[Ca^{2+}]/dt$, was much greater in Purkinje neurones (<1400 $\mu M/s$) than endothelia (<150 $\mu M/s$) and hepatocytes (<40 $\mu M/s$), and terminates abruptly in each case. The duration of the Ca^{2+} flux was brief in Purkinje neurones (7-25ms) compared with endothelia (40-1000ms) and hepatocytes (200-2000ms). The relation between $d[Ca^{2+}]/dt$ and duration was investigated by varying $InsP_3$ concentration and utilising the differences in maximum $d[Ca^{2+}]/dt$ between cell types. The rate of termination of Ca^{2+} flux was measured as reciprocal of the 10-90% risetime of $d[Ca^{2+}]/dt$. A linear correlation was found between the rate of termination and $d[Ca^{2+}]/dt$ within each cell type and also for the pooled data from the three cell types over the range of $d[Ca^{2+}]/dt$ from 0.5 to 1400 $\mu M/s$. Two mechanisms may contribute to the abrupt termination of Ca^{2+} release. The simplest explanation is depletion of Ca^{2+} from stores, giving short durations at high $d[Ca^{2+}]/dt$ as observed. However, if closed $InsP_3$ receptors are inactivated by high $[Ca^{2+}]$ adjacent to Ca^{2+} release sites then the rate of termination would increase as $d[Ca^{2+}]/dt$, ie Ca^{2+} flux, increases. Evidence favoring this latter mechanism is the strong inhibition of $d[Ca^{2+}]/dt$ by elevated cytosolic $[Ca^{2+}]$ following Ca^{2+} influx through the plasmalemma of Purkinje neurones.

M-Pos155

THE LYSOSOMAL Ca^{2+}-POOL CAN BE RELEASED BY $InsP_3$-DEPENDENT AGONISTS OR THAPSIGARGIN, BUT DOES NOT ACTIVATE STORE-OPERATED Ca^{2+} ENTRY.

((T. Haller, H. Völkl and P. Dietl)) Dept. of Physiology, Univ. of Innsbruck, A-6020 Innsbruck.

In MDCK cells, cleavage of glycyl-L-phenylalanine-β-naphtylamide (GPN) by lysosomal cathepsin C caused osmotic swelling of lysosomes followed by a release of endocytosed low molecular weight dyes and a dissipation of the lysosomal pH-gradient, consistent with a reversible permeabilization of lysosomal membranes. This permeabilization was accompanied by a transient rise of the cytoplasmic Ca^{2+} concentration ($[Ca^{2+}]_i$) as measured by fura-2 fluorescence, reflecting release of Ca^{2+} from lysosomes. This effect of GPN was unaffected by pretreatment with U-73,122, a phospholipase C inhibitor, or with caffein and ruthenium red, suggesting that Ca^{2+} release by GPN indeed originated from permeabilized lysosomes. Accordingly, activation of phospholipase C by extracellular ATP subsequent to GPN still resulted in intracellular Ca^{2+} release, indicating that the $InsP_3$-sensitive pool was largely unaffected by prior lysosomal Ca^{2+} depletion. Conversely, however, GPN did not cause an elevation of $[Ca^{2+}]_i$ subsequent to the Ca^{2+} release by ATP or thapsigargin, suggesting that Ca^{2+} release from the $InsP_3$- and thapsigargin-sensitive pool also decreased lysosomal Ca^{2+} content, either via functional coupling of intracellular Ca^{2+} stores or via direct lysosomal Ca^{2+} release through lysosomal $InsP_3$ receptors. This suggests an involvement of the lysosomal pool in $InsP_3$-mediated Ca^{2+} signaling. Whereas $InsP_3$-induced Ca^{2+} release activates store-operated Ca^{2+} entry via a store-operated cation current (Delles *et al.*, J. Physiol. 486:557-569, 1995), this was not activated by GPN-induced Ca^{2+} release. Hence, agonists could modulate store-operated Ca^{2+} entry by targeting different intracellular Ca^{2+} pools. (Supported by FWF, grant P10963-MED).

M-Pos156

GIGA-OHM SEALS ON INTRACELLULAR MEMBRANES: A POTENTIAL TECHNIQUE FOR CHARACTERIZING INSULIN-SENSITIVE CA2+ STORES IN APLYSIA NEURONS?

((E.A. Jonas, R.J. Knox, J.A. Connor, and L.K. Kaczmarek)) Dept. of Pharm., Yale Univ. Sch. of Med., New Haven, CT 06520 and Roche Inst. of Molec. Bio., Nutley, NJ, 07110. (Spon. by L.K. Kaczmarek)

Monitoring of Ca^{2+} in fura-2 loaded bag cell neurons has shown that activation of plasma membrane insulin receptors stimulates the release of Ca^{2+} from an apparently novel intracellular Ca^{2+} source (Jonas et al., 1993). In cells pre-injected with heparin, a known inhibitor of Ca^{2+} release through the IP3-sensitive intracellular channel, insulin continues to cause release of Ca^{2+} from an intracellular source. A response to insulin can also be detected after treatment of the cells with thapsigargin, an agent that depletes Ca^{2+} from most known endoplasmic reticulum stores. In order to characterize further the differences in the insulin-sensitive store from other intracellular Ca^{2+} stores, we developed a technique to form giga-ohm seals on presumed intracellular membranes. In this technique, a patch pipette is inserted into a larger intracellular microelectrode, which is used to penetrate the cell. The protective outer electrode is then withdrawn, leaving the patch pipette within the cell. Using this technique, seals are made successfully in approximately 60% of attempts, and usually follow whole cell recordings in which typical bag cell neuron currents are elicited using the intracellular patch electrode. Further studies will be aimed at identifying the insulin-sensitive intracellular Ca^{2+} release channel, and characterizing the electrophysiological properties of various types of intracellular membranes.

M-Pos157

SPECIFIC REGULATION OF Ca^{2+} POOLS AND CELL GROWTH BY CYTOCHROME P-450 METABOLITES OF ARACHIDONIC ACID

((M.N. Graber, A. Alfonso, and D.L. Gill)) The University of Maryland School of Medicine, Baltimore, MD 21201

The inositol 1,4,5-trisphosphate ($InsP_3$)-sensitive Ca^{2+} pools of DDT_1MF-2 smooth muscle cells empty after inhibition of the intracellular Ca^{2+}-ATPase by thapsigargin. Pool emptying causes cells to cease division and enter a stable, quiescent G_0-like state. High serum treatment of these pool-depleted quiescent cells induces synthesis of new Ca^{2+} pump protein, refilling of $InsP_3$-sensitive Ca^{2+} pools, and re-entry of cells into the cell cycle. Here we reveal that this re-entry into the cell cycle is mediated by specific lipid metabolites, namely eicosanoids. The essential fatty acids linolenic acid, linoleic acid, and arachidonic acid (AA) each induced recovery of Ca^{2+} pools and re-entry of cells into the cell cycle. Each essential fatty acid induced recovery with an EC_{50} of 5 μM; the action of each was dependent on protein synthesis. All non-essential fatty acids and growth factors tested did not promote recovery. Inhibitors of the prostanoid and lipoxygenase metabolism pathways had no effect on essential fatty acid-induced Ca^{2+} pool or growth recovery. However, the cytochrome P-450 inhibitors SKF-525A, metyrapone, and nordihydroguaiaretic acid each prevented the action of AA. Importantly, treatment of quiescent cells with either of 8,9- or 11,12-epoxyeicosatrienoic acid (EET), two of the four regiospecific cytochrome P-450 metabolites of arachidonic acid, also induced recovery. However, the dihydroxyeicosatrienoic acid metabolites of these EET's were unable to induce recovery. Preliminary results suggest that the mechanism of action of these EET's is via an increase in cAMP levels. These results are important in understanding the role of cytochrome P-450 derived eicosanoids in cellular regulation and the relationship between pool emptying and cell cycle control. (Supported by NIH grant NS19304 and NSF grant MCB9307746.)

M-Pos158

Ca^{2+} INFLUX STIMULATED BY EXTRACELLULAR ATP IN MOUSE THYMOCYTES.

((Paul E. Ross and Michael D. Cahalan)) Department of Physiology and Biophysics, UC Irvine, CA 92717. (Spon. by R.K Josephson)

Extracellular ATP ($[ATP]_o$) elevated the concentration of intracellular Ca^{2+} ($[Ca^{2+}]_i$) in fura-2-loaded single mouse thymocytes. Most thymocytes (≈ 80% exposed to $[ATP]_o$ exhibited a biphasic rise in $[Ca^{2+}]_i$; $[Ca^{2+}]_i$ rose slowly a first, then increased rapidly. A slowly declining plateau which lasted for a perio of minutes was established after $[Ca^{2+}]_i$ peaked at μM levels. Extracellular Ca^{2+} removal attenuated the rise in $[Ca^{2+}]_i$, suggesting that Ca^{2+} influx, rather tha the release of stored Ca^{2+}, is stimulated by $[ATP]_o$. Phenotyping experiment illustrate that both immature ($CD4^-CD8^-$, $CD4^+CD8^+$) and mature ($CD4^+CD8^-$ $CD4^-CD8^+$) thymocyte populations respond to ATP. Peripheral lymphocyte isolated from mouse spleen also respond to $[ATP]_o$. The $[ATP]_o$-mediated Ca^{2+} influx was sensitive to the concentration of extracellular Mg^{2+} ($[Mg^{2+}]_o$). 35% of thymocytes responded to $[ATP]_o$ in 2 mM $[Mg^{2+}]_o$, while an additional 48% exhibited a rise in $[Ca^{2+}]_i$ when the $[Mg^{2+}]_o$ was halved to 1 mM. This suggest that ATP^{4-} is the active agonis form. In the absence of $[Mg^{2+}]_o$ 3'-O-(4-benzoyl)ben-zoyl-ATP (BzATP) proved to be the mos effective agonist. The order o potency for adenine nucleotide was $BzATP^{4-}$>ATP^{4-}>$MgATP^{2-}$ >ADP^{3-}, suggesting purino receptors of the P_{2Z} class mediat the $[ATP]_o$ response in mous thymocytes. Supported by NI grants NS14609 and GM41514.

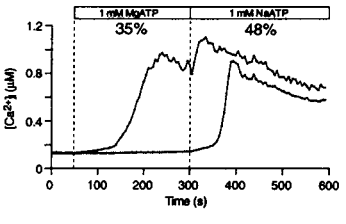

M-Pos159

SIMULTANEOUS MONITORING OF CYTOSOLIC AND MITOCHONDRIAL $[Ca^{2+}]$ IN SINGLE CELLS. ((D.F. Babcock, J. Herrington and B. Hille)) Dept. of Physiology & Biophysics, Univ. of Washington, Seattle WA 98195-7290.

The $[Ca^{2+}]$ probe Rhod-2 is generated preferentially in mitochondria of cells exposed to the permeant cation ester precursor Rhod-2AM. This compartmental localization is evident in confocal images of rat adrenal chromaffin cells and supported by resistance of dye to loss during whole-cell dialysis. Dual excitation, dual emission wavelength photometry allows simultaneous quantitative monitoring of Ca^{2+} signals from Rhod-2 and Calcium Green in single cells coloaded with the esters of both. Identification of these signals as reporters of $[Ca^{2+}]$ in mitochondria (Ca_m) and cytosol (Ca_c) respectively, is supported by responses to protonophore CCCP. CCCP elevates indicated Ca_c but lowers Ca_m from similar resting values (~150nM). With entry of external Ca^{2+} evoked by brief depolarizations (DP), the rise in Ca_m is slower (inset), smaller, and less extensive, but more prolonged than the transient rise in Ca_c. An intermediate plateau phase of Ca_c recovery coincides with the slow decline in Ca_m.

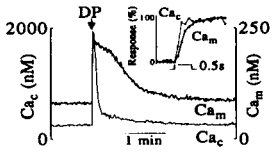

CCCP severely blunts the rise of Ca_m but not of Ca_c. Mobilization of internal Ca^{2+} stores by bradykinin or muscarine also transiently increases both Ca_m and Ca_c. These results provide direct support for the hypothesis that mitochondrial uptake and release modulate cytosolic Ca^{2+} signaling.

Supported by AR17803, HD07878 and the W.M. Keck Foundation

M-Pos160

INTERDEPENDENCE OF MITOCHONDRIA AND CRAC CHANNELS IN CALCIUM SIGNALLING IN T CELLS. ((Markus Hoth, Christopher M. Fanger, Alexandra B. Nelson and Richard S. Lewis)) Dept. Mol. & Cell. Physiol., Stanford Univ. School Med., Stanford, CA 94305-5426.

Prolonged Ca^{2+} influx through highly selective, Ca^{2+} release-activated Ca^{2+} (CRAC) channels is an essential signal for the activation of T lymphocytes by antigen. After maximal depletion of thapsigargin-sensitive stores in the absence of Ca^{2+}, readdition of 2 mM Ca^{2+} elevates cytosolic Ca^{2+} in Jurkat T cells to a plateau level of ~1000 nM lasting tens of minutes. Blockade of mitochondrial Ca^{2+} uptake with a protonophore (3 μM CCCP), or inhibition of Ca^{2+} release from mitochondria by intracellular Na^+ depletion, renders the Ca^{2+} response transient and reduces the steady state Ca^{2+} plateau to ~400 nM. Thus, long lasting Ca^{2+} plateaus are contingent upon active mitochondrial uptake and release. Probing the mitochondrial store content with ionomycin revealed that the threshold for uptake is about 400 nM cytosolic Ca^{2+} and that the uptake is not saturated at $[Ca^{2+}]_i$ as high as 1500 nM; thus, the store is both sensitive and has a large capacity. Based on these results, we conclude that (1) mitochondria take up and release Ca^{2+} that enters the cell through CRAC channels, and (2) mitochondria may prolong Ca^{2+} elevation by acting as a high capacity Ca^{2+} source from which Ca^{2+} is slowly released, by taking Ca^{2+} away from plasma membrane Ca^{2+} pumps, and/or by reducing Ca^{2+} induced inactivation of CRAC channels.

M-Pos161

POTENTIATION OF CYTOPLASMIC Ca^{2+} REMOVAL BY CAFFEINE IN FROG SYMPATHETIC NEURONS ((Z. Cseresnyés, A.I. Bustamante, M.G. Klein, and M.F. Schneider)) Department of Biological Chemistry, University of Maryland School of Medicine, Baltimore, MD 21201

Ca^{2+} release and reuptake were studied in neurons from frog sympathetic ganglia (*Rana pipiens*), lightly loaded with fura-2-AM (2 μM, 15-20 min, 20 °C). Total cellular fluorescence was recorded at 380 and 358 nm. Elevation of extracellular K^+ to 50 mM causes a rise in intracellular Ca^{2+} which persists for the duration of the 50-K^+ exposure and is dependent on extracellular Ca^{2+}. Caffeine (10 mM) causes a rapid and transient rise in $[Ca^{2+}]_i$ due to release from internal stores (Friel and Tsien, J. Physiol. 450: 217, 1992). The decline of $[Ca^{2+}]_i$ after 50-K^+ exposure is 5-fold slower than the decline during caffeine. After a cell is exposed to 50-K^+ and $[Ca^{2+}]_i$ is recovering relatively slowly, exposure to caffeine causes a rapid rise in $[Ca^{2+}]_i$ and then a rapid recovery to the pre-50K^+ $[Ca^{2+}]_i$ level. Thus the rate of removal of the elevated $[Ca^{2+}]_i$ appears to be potentiated; caffeine exposure results in rapid removal of the $[Ca^{2+}]_i$ elevated by both 50-K^+ and caffeine. The recovery always follows the faster time-course of the caffeine exposure. This effect can be observed at any time during the relatively slow decline of $[Ca^{2+}]_i$ after exposure to 50-K^+, regardless of the level of Ca^{2+} prior to the caffeine exposure. The effect is not due simply to caffeine, but depends either on the elevation of $[Ca^{2+}]_i$ by caffeine, the release of Ca^{2+} by caffeine or on loaded stores since depletion of the stores by 10 μM ryanodine eliminates the caffeine potentiation of the rate of removal. Elevation of $[Ca^{2+}]_i$ by 50-K^+ itself does not activate the potentiation mechanism. Neither thapsigargin (20-100 nM) nor DBHQ (2 - 60 μM) slowed the rapid decline of $[Ca^{2+}]_i$ caused by caffeine when the stores were not yet depleted. If the cell is exposed to 50-K^+ within ca. 1 min *after* 10 mM caffeine, the resulting elevation of $[Ca^{2+}]_i$ decays rapidly and is attenuated by 60-80%, which is much more than can be accounted for by depletion of the caffeine-sensitive store. This effect recovers in about 5 minutes and is also consistent with potentiation of the rate of cytoplasmic Ca^{2+} removal after exposure to caffeine.

M-Pos162

IDENTIFICATION AND FUNCTIONAL CONSEQUENCES OF OXIDATIVE MODIFICATION TO CALMODULIN ASSOCIATED WITH NORMAL BIOLOGICAL AGING. ((Jun Gao*, D. Yin*, Y. Yao*, A. Hühmer†, T. Williams♦, M. Michaelis*, Ch. Schöneich‡, D. Bigelow*, and T. Squier*)) Departments of Biochemistry*, Pharmacology and Toxicology*, Pharmaceutical Chemistry†, and Mass Spectrometry Laboratory♦, University of Kansas, Lawrence, KS 66045-2106.

We have examined calmodulin (CaM) as a potential target of aging in the brain, comparing its functional properties and primary structure with those resulting from in-vitro oxidative modification. In both in-vitro oxidatively modified CaM and for CaM isolated from the brains of Fischer 344 rats, we find a reduced capability to activate the plasma membrane Ca-ATPase from either erythrocyte ghosts or neuronal plasma membranes relative to unoxidized CaM obtained from young brains. Expression levels of CaM from aged brains are not significantly altered as evidenced by immunoassays of brain homogenates. Neither do the yields of purified CaM vary significantly with age, indicating that any structural changes do not affect the isolation of this protein. Using FAB-mass spectroscopy subsequent to the proteolytic digestion of CaM, and the separation of the resulting peptides by reversed-phase HPLC we find extensive oxidative modification of the majority of the methionines in CaM to the corresponding sulfoxides. The resulting oxidation products are analogous to those observed using in-vitro methods of oxidative modification, and represent the first identifiable modification to the primary structure of a protein associated with aging. The observed oxidative modification to CaM isolated from aged brain provides a molecular mechanism for the elevated cytoplasmic calcium levels and extended calcium transients associated with excitable cells during aging.

PROTEIN STRUCTURE PREDICTION

M-Pos163

THE COMPOSITION OF TRANSMEMBRANE SEGMENTS OF HUMAN TYPE I INTEGRAL MEMBRANE PROTEINS THAT SPAN THE MEMBRANE ONCE. ((G. Saberwal and O. S. Andersen)) Dept. Physiol. Biophys., Cornell Univ. Med. Coll., New York, NY, 10021. (Spon. by E. E. Windhager).

We examine putative single transmembrane (TM) helices in 163 human Type I proteins. The TM segments were defined using membrane-solution interface delimiter rules and characterized in terms of the distribution of hydrophobicity of the segments, and the distribution and positional preferences of each residue. We also analyzed the distributions of groups of residues (hydrophobic, non-aromatic polar, β-branched, aromatic), the distribution of runs of members of a group, and the relative distributions of two residues (or groups) within individual segments. The results show that the β-branched residues are surprisingly well represented. They can form runs that are seven residues long, and can account for two-thirds of a TM helix. Whereas Gly cannot occur in stretches of more than three residues, it can outnumber Leu or Leu *cum* Ala in individual segments. As expected Pro is poorly represented. We formulate rules that govern the distributions of residues in the TM helices of single-span Type I proteins. We also show that these rules apply to other single and multi-span transmembrane proteins.

M-Pos164

FORM BIREFRINGENCE CALCULATIONS USING THE FINITE ELEMENT METHOD ((Zorica Pantic-Tanner and Don Eden*)) School of Engineering and *Department of Chemistry and Biochemistry, San Francisco State University, San Francisco, CA 94132.

An approach based on the finite element method (FEM) is employed to calculate the form birefringence of protein solutions. The solutions are treated as suspensions of arbitrarily shaped particles in a solvent. It is assumed that the suspended particles are small compared to the wavelength of light. Accordingly, a quasi-static approximation for the refractive index is used, i.e., it is equal to the square root of the dielectric constant of the mixture. The average dielectric constant of the mixture has to be calculated for two separate cases. The uniform external electric field is parallel to and normal to the principal axis of the suspended particles. The FEM is a very powerful numerical technique that has been used widely in civil, mechanical and electrical engineering. We propose to extend its application to birefringence calculations. The advantage of the FEM over analytical and some other numerical methods is that it can treat inhomogeneous, arbitrarily shaped and oriented particles. The suspended particles, as well as the solvent, can be isotropic or anisotropic. This approach has been tested for ellipsoidal particles and good agreement is obtained. Some numerical results for small arbitrarily shaped proteins, such as the motor domains of kinesin and ncd, will be presented.
(Supported in part by grant NIH 1R15-AR42751 to DE.)

M-Pos165

DETERMINATIONS OF A MEDIUM RESOLUTION MATRIX DESCRIPTOR OF PROTEIN SECONDARY STRUCTURE USING OPTICAL SPECTROSCOPY-- ((Timothy A. Keiderling and Petr Pancoska)) Department of Chemistry, University of Illinois at Chicago, 845 W. Taylor St., Chicago IL 60607-7061

Optical spectra of proteins have traditionally been used to estimate average fractional contribution of secondary structure types to the overall conformation. We have shown that improved data collection and combination of information from different spectral techniques (eg. CD, IR, and vibrational CD) together with improved mathematical methods for empirical spectral analyses can provide a more detailed view of protein structures. Selective multiple regressions using the principal component method of factor analysis and a complete search over the the spectral components show that optimal prediction algorithms for fractional secondary structure parameters use only part of the observable spectral features. Neural network algorithms can then be used to extract a more detailed, distributed secondary structure representation of the protein encoded in a novel matrix descriptor. The structure is represented by segments of a continuous type of secondary structure, and by their interconnectivities, resulting in a matrix. This higher level structural descriptor can be predicted with an error comparable to the simpler fractional structure parameters. Correlation to the sequence offers a way of using optical spectral experimental data to distribute the secondary structure and move toward determination of the fold.

M-Pos166

PREDICTING THE STRUCTURE OF THE LIGHT HARVESTING COMPLEX II OF *RHODOSPIRILLUM MOLISCHIANUM*

((Xiche Hu[1], Dong Xu[1], Klaus Schulten[1], Juergen Koepke[2] and Hartmut Michel[2])) [1]Beckman Inst., UIUC, Urbana, IL 61801; [2]Max Planck Inst. for Biophys., Frankfurt, Germany (Spon. by S. H. White)

Presently, prediction of tertiary structure is only of practical use when the structure of a homologous protein is already known. We attempted to develop a structure prediction protocol in case that a highly homologous structure is not available. The protocol was applied to predict the structure of the light-harvesting complex II (LH-II) of *Rhodospirillum molischianum* which is an integral membrane protein of sixteen independent polypeptides, eight α-apoproteins and eight β-apoproteins, aggregating and binding to 24 bacteriochlorophyll a's and 8-12 lycopenes. A consensus assignment for the secondary structure was derived from hydropathy analysis and multiple sequence alignment propensity analyses, which were independently verified and improved by homology modeling. Three-dimensional structures for the α- and the β-apoprotein were built by means of comparative modeling. The resulting tertiary structures were combined into an αβ dimer pair with bacteriochlorophyll a's attached under constraints provided by site directed mutagenesis and spectral data. The αβ dimer pairs were then aggregated into a quaternary structure through further molecular dynamics simulations and energy minimization. Available diffraction data of a crystal of the protein served to screen the predicted structures in the framework of the molecular replacement method. The *ab initial* predicted structures of LH-II were significantly accurate to successfully probe the position of the unknown protein in the unit cell, which is promising since it is well-known that the radius of convergence of the molecular replacement method is very narrow.

M-Pos167

PREDICTING TRANSMEMBRANE HELICAL DOMAINS AND TOPOLOGY IN PROTEINS WITH NEURAL NETWORKS. ((P. Fariselli and R.Casadio)) Dept.of Biology, University of Bologna, Italy.

An Helical-Transmembrane-Predictor (HTP), based on feed forward neural networks, which does not require multiple sequence alignment and can run on microcomputers is described. The predictor is trained on the few membrane proteins known at atomic resolution, locates the helical transmembrane segments of proteins and predicts their orientation with respect to the membrane bilayer. HTP discriminates between membrane and globular proteins with high reliability (3% of false classifications). The performance of HTP in the testing phase reaches 91 %. In order to evaluate the confidence of the prediction, the HTP output shows the predicted helical transmembrane segments along the protein sequence together with the reliability index for each residue within the domain.

The overall topology of the protein is evaluated by computing the propensity of its loops from the frequency of the residues to be respectively in outside or inside loops. By this, the orientation of 52 out of 58 proteins of known membrane topology is correctly assigned, irrespectively of the protein source.

M-Pos168

COMPARING NMR AND X-RAY PROTEIN STRUCTURES USING INFORMATION PARAMETERS. ((B.J. Strait and T.G. Dewey)) Department of Chemistry, University of Denver, Denver CO 80208.

Protein structures derived from NMR and X-ray crystallograpy are compared using three different information theoretical parameters. The Shannon information entropy of the solvent accessibility profile of X-ray and NMR structures of ten different proteins are calculated. This provides information on the number of binary digits required to express the respective profiles. These values run from 1.7-4.7 bits per amino acid. The NMR and X-ray structures are compared using the mutual information entropy, the relative information entropy and the Rényi information dimensions. The mutual information provides a measure of the information content that is shared between the X-ray and the NMR accessibility profiles. This information measure is usually quite low and is typically 1.4 bits per amino acid. However, cases with mutual information as high as 3.1 bits per amino acid are observed. The relative information entropy of the NMR and X-ray accessibilities provide a measure of the "distance" that the two distributions are apart. This value can run from 0 to infinity and a low value indicates that the distibutions are very close to each other. This comparison shows X-ray and NMR structures to be similar with values for the relative information being less than 1 bit per amino acid. The Rényi information dimensions provide a spectrum of exponents based on a moment expansion of the probability distribution. This spectra shows considerable difference between X-ray and NMR results.

M-Pos169

MODELING OF AMINERGIC G-PROTEIN COUPLED RECEPTORS FROM EXPERIMENTAL DATA BY RULE-BASED AUTOMATED PROCEDURE ((P. Herzyk and R.E. Hubbard)) Department of Chemistry, University of York, Heslington, York, YO1 5DD, UK.

We have developed a rule-based automated method for modeling the structures of the 7 trans-membrane helices in G-protein-coupled receptors. The structures are generated using a simulated annealing Monte Carlo procedure which positions and orients rigid helices to satisfy structural restraints. The restraints are derived from analysis of experimental information from biophysical studies on native and mutant proteins, from analysis of sequences of related proteins, from theoretical considerations of protein structure, and from 2-D projection map of bovine rhodopsin. The methodology was validated through calculations using appropriate information for bacteriorhodopsin which produced a model structure with a root mean square deviation of 1.9Å from structure determined by electron microscopy. Here we present application of this methodology to the aminergic G-protein-coupled receptors. Several models of different types of receptors are presented and their properties discussed.

M-Pos170

CLONING AND EXPRESSION OF HUMAN Ca^{2+} CHANNEL β SUBUNITS. ((P. Lory, T. Collin, S. Lemaire and J. Nargeot)) CRBM CNRS, BP 5051, 34033 Montpellier cedex (Spon. by J. C.R. Randle).

The interaction between the α_1 and β subunits determines the basic properties of voltage-dependent Ca^{2+} channels. In other words, the β subunit is a potent regulator of the Ca^{2+} channel activity. We are interested in determining the molecular properties of the human isoforms of the β subunit and, in a recent study, we have characterized the human β_3 subunit *(Collin et al. Eur. J. Biochem. 220, 257-262, 1994)*. We have now identified two novel cDNAs encoding for the human β_2 and β_4 isoforms. We have studied their functional properties using *Xenopus* oocytes. Overexpression of any of the human β isoforms (β_1, β_2, β_3 and β_4) results in a 5 to 8 fold increase in endogenous oocyte Ba^{2+} current. The β isoforms differentially affect the inactivation properties of Ba^{2+} current. Overexpression of the β_2 isoform, by contrast with β_1, β_3 and β_4, markedly slow down inactivation kinetics. Using RT-PCR, we were able to identify transcripts for β_1, β_2 and β_3, but not β_4, isoforms in whole human heart. However, the expression of the β_2 isoform tends to be restricted to coronaries in human. Altogether, our results indicate that the human β isoforms behave similarly to their animal counterparts, and that an interesting feature distinguishing human from animal (i.e. rat or rabbit) β isoforms may reside in their expression profile in heart.

M-Pos171

CHARACTERIZATION OF AN ARGININE TO HISTIDINE MUTATION IN II/S4 OF THE CARDIAC L-TYPE CALCIUM CHANNEL. ((H. Lerche[2], N. Klugbauer[1], F. Lehmann-Horn[2], F. Hofmann[1], W. Melzer[2])) [1] Dept. of Pharmacology and Toxicology, Technical University of Munich, D-80802 Munich and [2]Dept. of Applied Physiology, University of Ulm, D-89069 Ulm. (Spons. by R.H.A. Fink)

The mutation R528H in segment II/S4 of the skeletal muscle dihydropyridine (DHP) receptor α_1 subunit causes the human skeletal muscle disease hypokalaemic periodic paralysis (HypoPP). This mutation has been reported to shift voltage-dependent inactivation of L-type Ca channels in myotubes from HypoPP patients by -40 mV (Sipos et al. 1995, J. Physiol. 483: 299-306). We introduced the corresponding mutation (R650H) in the homologous polypeptide of the rabbit cardiac α_1 subunit which was functionally expressed in HEK293 cells together with other L-type channel subunits (β_2 or β_1, α_2-δ, γ). R650H produced a small (-5 mV) shift of both the steady-state activation and inactivation curves of L-type Ca inward currents. The difference between wild type (WT) and R650H was neither enhanced by increasing the pH of the bathing solution from 7.4 to 8.4 to favour neutralization of the histidine residue, nor by cotransfection of skeletal muscle specific subunits (β_1, γ). A selective effect on inactivation as in HypoPP myotubes could not be found. Thus, R650 may play a different role in the cardiac L-type Ca channel than the corresponding residue in the human skeletal muscle homologue.

M-Pos172

THE FULL-LENGTH ISOFORM OF THE ALPHA1 SUBUNIT OF THE SKELETAL MUSCLE CALCIUM CHANNEL IS PRESENT IN THE SARCOLEMMA AND DECLINES IN ABUNDANCE DURING DEVELOPMENT ((D.Shulman, S.R.Levinson*, N.Chaudhari and K.Beam)) Colorado State University, Fort Collins, CO 80523 and *University of Colorado, HSC, Denver, CO 80262

Two isoforms of the skeletal calcium channel α_1 subunit have been identified, α_1-200 and α_1-175. The α_1-200 is thought to represent the full-length translation product and α_1-175 to be generated by proteolytic cleavage of the carboxyl terminus of α1-200. α_1-175 is the predominant form in adult muscle. We have examined the expression of α_1 isoforms during muscle development. The proportions of α_1-200 and α_1-175 were determined by Western blot analysis followed by scanning densitometry. Identity of the α_1-200 as the full-length translation product was confirmed by immunoprecipitation with an antibody directed distal to the truncation site on the carboxyl terminus and recognized on Western blot with an antibody to the pore region of the alpha$_1$ subunit. The immunoprecipitated α_1-200 was shown to be associated with the β subunit by probe of Wetern blot with an anti-β antibody and with the α2 subunit by co-purification with the α_2 on lectin beads. At postnatal day 1 (P1) α_1-200 comprised 30% of the total α_1 subunit, declining to 16% by P6 and to the adult level of 6% by P24. A qualitatively similar pattern was seen during in vitro development of cultured myotubes. After 3 days in culture (time of fusion), 43% of the total α_1 subunit is long form decreasing to 28% by day 7 and 24% by day 10. Cell surface label of membrane proteins in myotubes at days 3, 7 and 10 indicated that the α_1-200 is inserted into the sarcolemma. Taken together, this raises the possibility that the full-length α_1 isoform may be functional and may be of importance in developing muscle. Supported by NIH NS 24444 to KGB.

M-Pos173

PARTIAL GENOMIC STRUCTURE OF α_{1E} SUBUNIT FROM VOLTAGE GATED CALCIUM CHANNELS.
((T. Schneider, A. Pereverzev, R. Vajna, J. Hescheler)) Institute of Neurophysiology, University of Cologne, Robert-Koch-Str. 39, D-50931 Cologne, Germany. (Spon. by T. Schneider)

Six different ion conducting subunits (α_{1S}, α_{1C}, α_{1D}, α_{1A}, α_{1B}, and α_{1E}) of voltage operated Ca^{2+} channels have been identified by cloning their cDNA. Purified Ca^{2+} channels are heteromultimeric complexes containing additional auxiliary subunits ($\alpha_2\delta$, ß, γ, p95). Identified structures and functional entities (L-, P/Q-, N-, or R-type channel Ca^{2+} channel) are not yet linked unequivocally. Coexpression of individual subunits in heterologous systems is misleading, as long as the native subunit makeup of a channel type is unknown. The selective knockout of the murine α_{1E} subunit will be used to understand the function of this neuronal Ca^{2+} channel subunit.
Using the human α_{1E} cDNA as a probe, a genomic library from mouse strain 129SVJ was screened. Thirteen clones containing homologous sequences were identified and sequenced. The sequences selected for the knockout and the logic of the gene inactivation will be reported.

M-Pos174

INFLUENCE OF AUXILIARY Ca CHANNEL SUBUNITS ON VOLTAGE-DEPENDENT ACTIVATION OF RECOMBINANT α_{1E} Ca CHANNELS
((L.P. Jones and D.T. Yue)) Johns Hopkins Univ., Baltimore, MD 21205

The main α_1 component of voltage-dependent Ca channels forms an operational channel, but coexpression of α_2 and β subunits may profoundly change expression and function. Prior reports conflict as to subunit interactions, and mainly focus on the cardiac α_{1C} channel. We now determine subunit effects on a different class of Ca channel, exploiting exceptional expression of a neuronal α_{1E} construct (Soong et al., *Science*, 1993) in HEK 293 cells to obtain high-resolution ionic and gating currents. G-V curves, derived from tail currents (B, inset), quantify activation of ionic current (B, n=8-11 cells). Q-V curves, calculated from on transients of gating currents (A, inset), characterize underlying voltage sensor movement (A, n=4-15 cells). We find that although β_{2a} coexpression yields >10-fold larger currents than α_{1E} alone; auxillary subunits have little effect on the voltage dependence of activation (A, B). Boltzmann fits of G-V curves reveal indistinguishable $V_{1/2}$ (-15.6 to -19 mV), and a slightly diminished z_G of α_{1E} alone (2.6 vs. 3.7, p<.05). Q-V curves shows no appreciable differences for z_Q (2.7-3.0), and only a slight, but statistically unresolved right-shift of $V_{1/2}$ for α_{1E} alone (-21.7 vs. -29 mV). Coupling efficiency between opening and voltage sensor movement (G_{max}/Q_{max}) changes little with subunit composition (110-160 pS/nF), contrasting with a large increase in G_{max}/Q_{max} produced by β coexpression with α_{1C} (Neely et al., *Science*, 1993). The role of auxillary subunits may therefore differ substantially among the various classes of Ca channels.

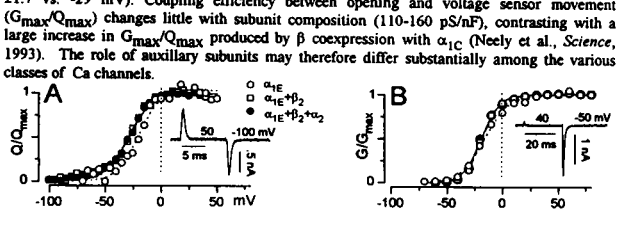

M-Pos175

SIMILARITY OF BIOPHYSICAL PROPERTIES OF Ca^{2+} CURRENTS IN α_{1C} AND α_{1C}/β_{2a} TRANSFECTED MAMMALIAN CELLS. ((R.Shirokov, G.Ferreira, J.Yi, J.Zhou, A.Chien, M.Hosey and E.Ríos)) Rush Univ., Northwestern Univ., Chicago, IL 60612.

The effects of β_{2a} subunit on currents through α_{1C} Ca^{2+} channels were studied in transiently transfected HEK 293 and tsA 201 cells.

Ca^{2+} and Ba^{2+} (I_{Ca} and I_{Ba}) currents in cotransfected (α_1/β) cells were nearly 5 times greater than in cells transfected with α_{1C} alone. The voltage dependence of activation was not significantly different between α_1 and α_1/β cells.

I_{Ba} in α_1 and α_1/β cells decayed in 5 s long pulses with similar rates: 753 ± 60 ms, n = 6 and 720 ± 88 ms, n = 7, respectively. Steady state inactivation curves of I_{Ba} in α_1 and α_1/β cells had similar steepness and transition voltage. Surprisingly, the minimal availability was significantly greater in α_1 cells (40 ± 5%, n = 7 in α_1 *vs.* 16 ± 5%, n = 14 in α_1/β).

The extent of inactivation of I_{Ca} after 120 ms (I_{peak}-I_{120})/I_{peak}) was a good measure of fast calcium dependent inactivation (CDI) since it was negligible for I_{Ba}. The extent of CDI was less in α_1 cells. To study the role of the β subunit in CDI, the extent was determined 40-50 hrs posttransfection in cells with different molar ratios of β_{2a} and α_{1C} cDNAs. Extent of CDI increased with the amount of β_{2a} cDNA. Scatter plot of the extent of CDI *vs.* maximal current density showed a weak correlation ($r^2 = 0.46$, n = 75). At the same time, correlation between average values of the extent of CDI and current density in groups of cells transfected with different β_{2a}/α_{1C} cDNA molar ratio was high ($r^2 = 0.9$), suggesting that current density is one of several variables that can enhance CDI.

Density of maximal I_{Ca} and maximal intramembrane charge (Q_{max}) correlated strongly ($r^2 = 0.8$). As Q_{max} is expected to be proportional to density of channels, we propose that β subunit increases I_{Ca} density mainly by increasing the number of α_1 subunits in the membrane (targeting function).

Therefore, one way in which β cotransfection increases extent of CDI is secondarily to increase in number of channels in the membrane. The similarity in biophysical properties of currents in α_1 and α_1/β cells can be explained by the presence of endogenous β subunit in the α_1 cells, *necessary for* targeting α_1 subunits in mammalian cells.

(Supported by AHA-MC and NIH).

M-Pos176

THE MEMBRANE-LOCALIZED β_{2a} SUBUNIT OF L-TYPE CA CHANNELS IS PALMITOYLATED THROUGH A BASE-SENSITIVE THIOESTER LINKAGE.

((Andy J. Chien, Tipu S. Puri, and M. Marlene Hosey)) Dept. of Mol. Pharm. and Biol. Chem., Northwestern University Medical School, Chicago IL, 60611.

The β_{2a} subunit of L-type Ca channels was recently shown to be membrane localized when heterologously expressed in HEK293 cells (Chien et al., in press) and in Sf9 insect cells (Puri and Hosey, unpublished observation). The β_{2a} subunit contains no known consensus sites for lipid modifications such as prenylation or myristoylation. In contrast, there is no known consensus site for palmitoylation, a reversible post-translational modification which is thought to play a role in the membrane localization of many proteins including G proteins and the *src* family of tyrosine kinases. This modification involves the attachment of an acyl group to a cysteine residue via a base-sensitive thioester linkage. Upon metabolic labeling with [^{3}H]-palmitic acid, the expressed β_{2a} subunit was shown to incorporate an acyl group through a hydroxylamine-sensitive linkage. Base hydrolysis of the attached lipid group, followed by HPLC analysis, revealed that the acyl group was palmitic acid. Studies on the solubilization of metabolically-labeled β_{2a} membranes revealed that palmitoylated β_{2a} could only be solubilized with detergents. In contrast, salt was able to solubilize a population devoid of palmitoylated β_{2a} subunits. Palmitoylation also occurred upon co-expression with α_{1C}. The reversible nature of palmitoylation introduces the possibility of its role in the dynamic regulation of channel complexes.

M-Pos177

TWO SEPARATE DOMAINS OF THE β SUBUNIT MODULATE VOLTAGE DEPENDENT INACTIVATION OF α_{1E} Ca^{++} CHANNEL.

((R. Olcese, N. Qin, J. Zhou, L. Birnbaumer, E. Stefani)) Dept. of Anesthesiology UCLA School of Medicine, Los Angeles, CA 90095-1778

We recently reported that the regulation of voltage dependence of the inactivation and activation in α1E are separable functions and that the N-terminus of Ca^{++} channel β subunits sets the rate of channel inactivation (Olcese et al., Neuron 1994). In the present work N-terminal deletions (ΔN) of different β subunits ($\Delta N\beta_{1b}$, $\Delta N\beta_{2a}$ and $\Delta N\beta_3$) were coexpressed in *Xenopus* oocytes with α1E and their effects on the current inactivation were studied. While the N-terminal deletion of β_{1b} and β_3 ($\Delta N\beta_{1b}$, $\Delta N\beta_3$) no longer strongly modified the voltage dependent inactivation, the equivalent deletion $\Delta N\beta_{2a}$ still maintained the property of the wild-type β_{2a} subunit. The half inactivation potentials ($V_{1/2}$) from steady state inactivation curves were (mV): α_{1E} alone = -34.37 ± 0.8; β_{1b} = -53.8 ± 0.7; $\Delta N\beta_{1b}$ = -39.5 ± 1.0; β3 = - 49.9 ± 0.7; $\Delta N\beta_3$ = - 41.0 ± 0.6; β_{2a} = -23.5 ± 1.6; $\Delta N\beta_{2a}$= -27.6 ± 0.9). These results suggest the existence of a secondary domain involved in the modulation of inactivation. The major structural difference between $\Delta N\beta_{2a}$, and both ΔNβ1b and ΔNβ3, lies in a region (domain 3) which exists in two forms of different length, each encoded in a separate exon (7 amino acids in β_{1b} and β_3, 52 in B_{2a}). We constructed a chimeric $\Delta N\beta_{2a}$ with the short form of domain 3 ($\Delta N\beta_{2a}$Short). When coexpressed with α_{1E}, $\Delta N\beta_{2a}$Short was ineffective on slowing the voltage dependent inactivation (($\Delta N\beta_{2a}$Short) $V_{1/2}$ = -39.7 ± 1.2 mV). We conclude that the long form of domain 3 of β subunits can modulate the voltage dependent inactivation of α_{1E} and its effect is recessive to the one of the N-terminus. All the β subunit tested (wild-type and chimeric) had similar effect on the activation, increasing the proportion of the steeper first component of the G-V curves. Supported by NIH grants AR-43411 to L.B. and AR-38970 to E.S.

M-Pos178

MODULATION OF THE HUMAN α_{1E} CALCIUM CHANNEL BY NEURONAL β AND α_2 AUXILIARY SUBUNITS.

((T. Rodriguez, T. Schneider*, L. Parent)) Dept Molecular Physiology & Biophysics, Baylor College Medicine, Houston, TX 77030 and *Dept Neurophysiology, University of Cologne, Cologne, Germany.

The human brain α_{1E} Ca^{2+} channel subunit was cloned and functionally expressed in *Xenopus* oocytes (Schneider et al., 1994). Whole-cell currents were measured with the two-electrode voltage clamp method following intracellular injection of 10 mM Bapta. Expression of large Ba^{2+} inward currents revealed voltage-dependent activation and inactivation. At 0 mV, Ba^{2+} inactivation can be described by a sum of 2 exponential functions with τ_1 = 34 ± 9 ms and τ_2 = 177 ± 21 ms (n=5) not significantly different than τ_1 = 25 ± 5 ms and τ_2 = 155 ± 13 ms measured with Ca^{2+}. Steady-state inactivation was investigated using 5s-prepulses. $E_{0.5}$ = -54 mV (10 Ba^{2+}) and -52 mV (10 Ca^{2+}) were computed from single Boltzmann fits to the inactivation curves. Coinjection with the cardiac/brain β_{2a} and the neuronal α_{2b} subunits stimulated whole-cell Ba^{2+} currents from 1.3 μA (α_{1E}) to 15 μA ($\alpha_{1E}/\beta_{2a}/\alpha_{2b}$) although coinjection with either β_{2a} or α_{2b} failed to increase α_{1E} peak currents. Coexpression with β_{2a} strongly reduced Ba^{2+} inactivation, eliminating the fast τ_1 and increasing τ_2 to 655 ± 53 ms (n=3). Coexpression with α_{2b} shifted the Ba^{2+} peak current from 0 to +10 mV and slightly decreased the rate of Ba^{2+} inactivation. Steady-state inactivation data were best fitted with $E_{0.5}$ = -54 mV (α_{1E}); -47 mV (α_{1E}/α_{2b}); and -36 mV (α_{1E}/β_{2a}). Coexpression with β_{2a} and α_{2b} yielded Ba^{2+} currents with inactivation kinetics similar to the β_{2a} induced currents. This result indicates that the neuronal α_{2b} subunit does not reverse the effect of β subunits on α_{1E} kinetics, unlike previously reported for the skeletal α_{2a} subunit (Wakamori et al., 1994). Supported by AHA-Texas 94G-195 to L. Parent.

M-Pos179

A Ca^{2+} CHANNEL MODEL WITHOUT IONIC INTERACTION.

((Thieu Dang and Ed McCleskey)) Vollum Institute, Portland, OR 97201

Voltage-gated Ca^{2+} channels choose Ca^{2+} over Na^+ by means of an intrapore, high affinity binding site (K_d = 1 μM Ca^{2+}). The maximum off-rate from such a site is about 100 times less than observed single channel current. All theories that explain how this high current might pass through such a sticky pore assume that the binding of one Ca^{2+} ion diminishes the affinity of the pore for another Ca^{2+} ion; in other words, Ca^{2+} flux occurs only when the pore's affinity for Ca^{2+} is transiently diminished. We now describe a model that quantitatively fits all key features of Ca^{2+} channel permeation without allowing one ion to alter binding of another. The model has a single high affinity Ca^{2+} binding site flanked by a low affinity site on either side. The low affinity sites provide steps of potential energy that speed the exit of a Ca^{2+} ion off the selectivity site. Such steps are a common means of accelerating chemical reactions and they provide another general mechanism for obtaining high fluxes in ion channels that select by affinity.

M-Pos180

ARE ALL THE MEASURED CHARGES PER CHANNEL COUPLED TO PORE OPENING IN VOLTAGE-DEPENDENT CHANNELS?

((F. Noceti, L. Toro, and E. Stefani)) Depts. of Anesthesiology and Physiology, UCLA School of Medicine, Los Angeles, CA 90095-1778.

The number of equivalent electronic charges *z* per channel can be inferred from the limiting slope method (Almers, 1978) or from the ratio in the same patch between the integral of the gating current and the number of channels obtained from ionic current fluctuations (Schoppa et al., 1992). Both methods have intrinsic limitations. The limiting slope method is valid to a strictly sequential model of activation and tends to underestimate the number of charges due to the difficulty in attaining the limiting slope of the conductance-voltage (G-V) curve (Bezanilla and Stefani, 1994). The variance analysis may overestimate the number of charges if a constant fraction of channels can undergo voltage dependent transitions eliciting gating current without reaching the final open state, thus being silent for the ionic current fluctuation measurements. We have compared the number of charges per channel with both methods in voltage dependent K^+ and Ca^{2+} channels. We used the cut open oocyte and giant patch experiments on K^+ (Shaker H4IR and DRK1) and Ca^{2+} channel clones (α_{1E} and $\alpha_{1E}\beta_{1b}$) expressed in *Xenopus* oocytes. For the limiting slope method we increased the resolution by using voltage ramps and small pulse increments (0.2 mV). For K^+ channels both methods gave equivalent results (H4IR *z* = 12-14 and DRK1 *z* = 6-8). This suggests that all the channels that gate can open and that all the measured charge is coupled to pore opening in a strictly sequential kinetic model. For both Ca^{2+} channel clones the variance analysis gave larger values (10-12 charges per channel) than the limiting slope method (7-9 charges per channel). This difference may be due to either the intrinsic difficulty to resolve the limiting slope or to the fact that in α_{1E} and $\alpha_{1E}\beta_{1b}$ a set of charges are not coupled to pore opening, for example by moving in a parallel path. Null traces in single Ca^{2+} channel experiments support this second hypothesis. Thus, channels in the "null" mode will not contribute to the ionic current fluctuations, but would elicit gating currents. (Supported by NIH grants).

M-Pos181

ENANTIOMERIC SEPARATION OF THE SITES FOR DHP AGONIST AND ANTAGONIST ACTION ON THE VOLTAGE-DEPENDENT CALCIUM CHANNEL α_1 SUBUNIT.

((M. He, M. Wakamori and A. Schwartz)) Inst. of Mol. Pharm. and Biophys., Univ. of Cincinnati Coll. of Med., Cincinnati, OH 45267

The L-type voltage-dependent Ca^{2+} channel (VDCC) is a complex of five subunits, α_1, α_2/δ, β, and γ. The α_1 subunit is the major functional component both pharmacologically and electrophysiologically. Dihydropyridines (DHPs) are one of the three major classes of L-type VDCC modulators. We have shown that part of SS2-S6 of motif IV is involved in DHP agonist action (Neuron 11:1, 1993). In order to specifically identify regions that are responsible for DHP effects, chimeric Ca^{2+} channel α_1 subunits were constructed. These were made by replacing various regions of motif III S5-S6 of the DHP-sensitive rabbit cardiac Ca^{2+} channel α_1 subunit with the corresponding regions of the DHP-insensitive brain BI Ca^{2+} channel α_1 subunit. The chimeric α_1 subunits were coexpressed with α_2 and β subunits in *Xenopus* oocytes, and the effects of DHP agonists and antagonists were studied using electrophysiological methods. The results revealed that the chimeras with the S5-S6 of motif III replacement, lost both DHP agonist and antagonist sensitivity, while the chimera with the S6 replacement lost only antagonist sensitivity. These data suggest that S5-SS1 of motif III and SS2-S6 of motif IV interact with DHP agonists, while S6 of motif III is important for DHP antagonist action.

M-Pos182

CGP 48506. A NOVEL BENZODIAZOCINE DERIVATIVE, ACTIVATES CARDIAC CALCIUM CHANNELS BY INCREASING "MODE 2" ACTIVITY.
((S. Herzig)) Department of Pharmacology, University of Cologne, 50924 Cologne, Germany

CGP 48506 is the (+)-enantiomer of 5-methyl-6-phenyl-1,3,5,6,-tetrahydro-3.6,-methano-1,5-benzodiazocine-2.4-dione. It has been identified as a novel type of positive inotropic agent, possessing stereoselective calcium-sensitizing properties (Herold et al., 1995, J. Med. Chem. 38, 2946). We found that CGP 48506, at a positive inotropic concentration of 10^{-4} mol/l, increased L-type calcium channel activity in guinea-pig ventricular myocytes (by 77±10%, n=7, 2mmol/l Ca^{2+}, physiological solutions, whole cell configuration). To investigate the mechanism of channel stimulation, studies where done under conditions which minimize K^+ current contamination and Ca^{2+}-dependent inactivation. Here, it became apparent that CGP 48506 markedly slowed the kinetics of activation and deactivation: for instance, tail currents at -20mV deactivated with a time constant of 10.7±0.9ms (control: 3.8±0.3ms, n=7). The basis of this effect was resolved at the single channel level. CGP 48506 (10^{-4}mol/l) increased the ensemble average current from 14.2±4.6 to 36.3±11.5fA (n=5). This effect was entirely due to an increase in the mean open time of the channel (from 0.44±0.06ms to 1.11±0.15ms). Clearly, open times were distributed biexponentially in the presence of CGP 48506, with 20% of openings forming the second component with a slow τ of 3.3ms. These long openings were found to be grouped in "mode 2"-like sweeps. Interestingly, channel availability remained unaffected by the drug. Therefore, the functional pattern of effects of CGP 48506 on L-type channels is reminiscent of that of dihydropyridine agonists or FPL 64176. In conclusion, CGP 48506 represents a new type of calcium channel agonist.

M-Pos183

MODULATION OF CLASS A CA^{2+} CHANNELS BY G-PROTEIN βγ SUBUNITS
((S. Herlitze, T. Scheuer and W.A. Catterall)) Dept. of Pharmacology, U. of Washington, Seattle, WA 98195. (Spon. by D. Teller)

Voltage-sensitive transmitter-mediated reduction of high-voltage-activated Ca^{2+} currents occurs in a variety of cell types. Such modulation is proposed to occur by direct binding of G-protein subunits to the Ca^{2+} channel, leading to a positively shifted voltage-dependence of activation. G-protein interaction is destabilized by strong depolarization, resulting in G-protein unbinding and facilitation of the Ca^{2+} current. G-protein subunits causing this Ca^{2+} channel modulation were identified by transiently transfecting tsA201 cells with Ca^{2+} channel α_{1A}, β_{1b} and $\alpha_2\delta$ subunits as well as with appropriate G-protein subunits. Activation of endogenous G-proteins by including GTPγS in a whole cell recording pipette caused activation curves to shift to more positive voltages and become less steep. Tail currents were facilitated by prepulses to strongly depolarized potentials. Effects of GTPγS were blocked by peptides corresponding to the Gβγ interaction site of adenylate cyclase or an analogous site in α_{1A}. In the absence of GTPγS, cotransfection of G-protein β_2 and γ_3 subunits resulted in a positively-shifted and shallow voltage-dependent activation in the absence of GTPγS and the currents could be facilitated by depolarizing prepulses. These effects were not seen after cotransfection with $G\alpha_{i1}$, $G\alpha_{i2}$, $G\alpha_{i3}$ or $G\alpha_o$. $G\beta_2$ alone, but not $G\gamma_3$, caused similar effects as the $G\beta_2\gamma_3$ combination. These results argue that G-protein β subunits (in this case $G\beta_2$), but not pertussis toxin-sensitive α subunits are responsible for the positive shift in voltage-dependence and for facilitation caused by neurotransmitter modulation of Ca^{2+} currents and are likely to bind to the Ca^{2+} channel α subunit.
Supported by Deutsche Forschungsgemeinschaft.

M-Pos184

Role of drug and channel structure in Ca^{2+} channel block by phenylalkylamines.
((B.D. Johnson, G.H. Hockerman, T. Scheuer and W.A. Catterall)) Dept. of Pharmacology, U. of Washington, Seattle, WA 98195-7280. (Spon. by L. Byerly)

The phenylalkylamines (-)D888, verapamil (VER), and D600, cause voltage- and use-dependent block of L-type Ca^{2+} channels. A mutant Ca^{2+} channel α_{1c} subunit containing mutations Y1463A, A1467S, and I1470A (mutant YAI) in transmembrane segment S6 of domain IV (IVS6) disrupted block of resting and depolarized channels by (-)D888 when cotransfected with β_{1b} and $\alpha_2\delta$ subunits in tsA201 cells. Surprisingly, affinities for block by VER or D600 were unaffected. Despite the specific effect on affinity, recovery from block after long depolarizations was accelerated 4-20 fold for all 3 drugs in YAI. Also, block of depolarized YAI channels was accelerated for VER and D600. Thus, effects on affinity were (-)D888-specific whereas effects on block kinetics were not. Since effects of mutant Y1463A were qualitatively similar to those of YAI, other substitutions for Y1463 were introduced. Y1463F, which eliminates an -OH, reduced (-)D888 affinity as effectively as Y1463A without affecting affinity for block by VER. Unlike Y1463A, unblock rates for Y1463F were not accelerated. Conversely, effects of Y1463T were similar to Y1463A. Thus, (-)D888 affinity is sensitive to the hydroxyl group of Y1463 whereas effects on recovery kinetics require larger changes, perhaps related to residue size. (-)D888 differs from VER and D600 in having fewer methoxy groups on its terminal phenyl rings and it blocks WT channels with far higher affinity. The selective effect on affinity of (-) D888 block suggests that these mutations disrupt an interaction specific to high affinity binding of (-)D888, as well as interactions which determine the rates of binding and dissociation of all phenylalkylamines.

M-Pos185

A MAJOR ROLE FOR G-PROTEIN BETA AND GAMMA SUBUNITS IN CALCIUM CHANNEL INHIBITION.
((D.E. Garcia*, K. Mackie, S. Herlitze, W.A. Catterall, and B. Hille.)) University of Washington, Seattle, WA 98195 and *UNAM Mexico D.F.

The role of G protein subunits in inhibition of neuronal N-type calcium current (I_{Ca}) was examined by injection of purified G-βγ subunits or cRNA encoding for G-α_o, β_2, and γ_3 into cultured rat superior cervical ganglion neurons. Control I_{Ca} was measured in 5 mM Ca2+ solutions between 5 and 6 ms during a 10 ms depolarization to 10 mV with no prepulse. The same pulse protocol was used with a preceding 25 ms depolarization to 125 mV to measure facilitated I_{Ca}. Prepulse facilitation is taken as evidence for voltage-dependent inhibition. Vehicle injected cells showed only 10% facilitation. Injection of G-βγ subunits purified from bovine brain increased facilitation to 100% and reduced inhibition of control I_{Ca} by 10 μM norepinephrine (NE) by 30%. Injection and overnight incubation with G-β_2 or β_2/γ_3 cRNA markedly increased facilitation (to 200-400%) and reduced inhibition of control I_{Ca} by NE by 40%. Injection of G-γ_3 or α_o cRNA had little effect on facilitation or on the ability of NE to inhibit control I_{Ca}. The relative amplitude of *facilitated* I_{Ca} is taken as a measure of voltage-independent modulation. In contrast to inhibition of control I_{Ca} by NE, inhibition of *facilitated* I_{Ca} was reduced by 30% in the G-γ_3 and β_2/γ_3 cRNA injected cells but was preserved in cells injected with G-β_2 and α_o cRNA. Taken together, these results support the hypothesis that G-protein βγ subunits play a major role in I_{Ca} modulation by G protein-coupled receptors. Taken literally they also suggest a greater role of β_2 in voltage-dependent and γ_3 in voltage-independent inhibition.
Supported by an Alexander von Humboldt and DFG Fellowships, the Keck Foundation, D6APA UNAM IN203293, NIDA, and NINDS.

M-Pos186

LEAD IS A POTENT BLOCKER OF CARDIAC L-TYPE CALCIUM CHANNELS.
((J. Bernal[1], J.-H. Lee[2] and E. Perez-Reyes[2])). [1] Centro Biomédico, Universidad Autonoma de Aguascalientes, C.P. 20100, AGS., México and [2] Loyola University Medical Center, Maywood IL., USA

It has been proposed that lead modulates ionic Ca^{2+} permeability in several cell types. However, it is not known if lead modulates cardiac Ca^{2+} channels. The objective of this work is to evaluate the effects of lead (Pb^{2+}) and 2-3-dimercapto-1-propanesulfonic acid (DMPS), a putative lead antidote, on the ionic permeability of cardiac L-type Ca^{2+} channels in ventricular myocytes, and using Ca^{2+} channels expressed in *Xenopus laevis* oocytes. The cRNA of the α_1 subunit of the rabbit cardiac L-type Ca^{2+} channel was injected into *Xenopus* oocytes. For some experiments, a beta (β_2 or β_4) and a α_2 subunit were also co-injected. It was found that Pb^{2+} at concentrations in the range of 0.001 - 100 μM decreased the magnitude of the inward Ba^{2+} current, IC_{50}=0.4 μM. When cells were exposed to lead, DMPS, a putative chelating agent for heavy metals, reverted the effects initially produced by lead. DMPS alone did not have any effect on control Ca^{2+} currents. These results provide experimental evidence that support the hypothesis that lead is a high threshold cardiac calcium channel blocker and it acts in a reversible and dose-dependent manner. In addition these results support the use of DMPS as a putative lead antidote.

M-Pos187

MOLECULAR DETERMINANTS CRITICAL FOR THE HIGH AFFINITY AND ALLOSTERIC MODULATION OF DIHYDROPYRIDINE BINDING TO L-TYPE CALCIUM CHANNELS
((Blaise Z. Peterson, Timothy N. Tanada and William A. Catterall)) Department of Pharmacology, University of Washington, Box 357280, Seattle, WA 98195-7280, USA.

L-type Ca^{2+} channel function is pharmacologically modulated by Ca^{2+} antagonists, such as dihydropyridines (DHPs), by an unknown mechanism. In this study, site-directed mutagenesis and radioligand binding were utilized to identify individual amino acids that account for the differences in DHP sensitivity observed between L-type (DHP-sensitive) and non L-type (DHP-insensitive) Ca^{2+} channels. Amino acids within five distinct peptide segments of the L-type Ca^{2+} channel α_1 subunit in domains III and IV were identified as being critical for conferring DHP sensitivity. Three of these peptide segments near the extracellular ends of the S5 and S6 transmembrane helices in domains III and IV contain amino acid residues which are required for high affinity DHP binding at optimal Ca^{2+} concentration. These amino acid residues may form part of the DHP receptor site. The other two segments lie within the ion-selective pore between transmembrane segments S5 and S6 of domains III and IV where Ca^{2+} selectivity and permeability are determined by conserved Ca^{2+}-binding glutamate residues within these segments. High affinity Ca^{2+} binding to these glutamate residues in domains III and IV stabilizes the DHP receptor site in its high affinity state. DHP antagonists may block Ca^{2+} channel function by stabilizing a high affinity Ca^{2+}-blocked state through allosteric interactions with Ca^{2+}-binding sites within the pore.

M-Pos188

IN VITRO PHOSPHORYLATION OF SUBUNITS OF CARDIAC L-TYPE Ca CHANNELS BY PROTEIN KINASE A AND PROTEIN KINASE C

((B. Gerhardstein[1]. T. Puri[1], X. -L. Zhao[2], and M. Hosey[1])) [1]Dept. of Mol. Pharmacology and Biol. Chemistry, Northwestern University Medical School, Chicago, IL 60611. [2]Dept. of Pharmacology, University of California at San Diego, La Jolla, CA 92093.

We have characterized the phosphorylation of two subunits of L-type Ca channels in *in vitro* studies with purified protein kinases. The α_{1C} and β_{2a} subunits, believed to be essential components of L-type Ca channels in heart and brain, were heterologously expressed in Sf9 insect cells by infection with recombinant baculoviruses. The expressed α_{1C} and β_{2a} proteins were identified by subunit specific antibodies as membrane proteins of ~240 and ~68 kDa, respectively. Crude membrane fractions were isolated and used in protein phosphorylation assays with [γ-^{32}P]ATP and purified preparations of the catalytic subunit of cAMP-dependent protein kinase (PKA) and protein kinase C (PKC). The β_{2a} subunit was readily studied in the membrane fraction due to its high level of expression (~0.2 nmols/mg protein as assessed by metabolic labelling with ^{35}S-methionine). The β_{2a} subunit underwent rapid phosphorylation by both PKA and PKC. The stoichiometry of phosphorylation was calculated using ^{35}S/^{32}P-labelled proteins and found to be ~2 mols phosphate/mol protein for both protein kinases. Peptide mapping indicated that similar domains of the protein were phosphorylated by PKA and PKC. The α_{1C} subunit was also found to be a protein kinase substrate *in vitro*. The stoichiometry of phosphorylation by PKA was assessed after immunoprecipitation of ^{35}S/^{32}P labelled protein and found to be 1-3 mols P/mol protein. The phosphorylation of these subunits may play a role in the receptor mediated regulation of L-type channels in cardiac and neuronal cells.

M-Pos189

Ca^{2+}-INDUCED INACTIVATION OF NATIVE AND CLONED SINGLE L-TYPE Ca^{2+} CHANNELS

((G. Höfer, W. Baumgartner, M. Sulzbacher, K. Hohenthanner, A. Koplin, N. Klugbauer*, F. Hofmann* and C. Romanin)) Institute for Biophysics, University of Linz, Austria; *Institute of Pharmacology and Toxicology, TU Munich, Germany

Cardiac L-type Ca^{2+} currents show inactivation with Ca^{2+} as charge carrier, which is markedly reduced when Ba^{2+} is substituted for Ca^{2+}. This phenomenon termed Ca^{2+}-induced inactivation was investigated at the single channel level with native and cloned Ca^{2+} channels employing the inside-out patch configuration. Run-down of channel activity was prevented by calpastatin and ATP. Ba^{2+} currents through native L-type Ca^{2+} channels were subjected to µM concentrations of Ca^{2+} at the cytoplasmic side of the membrane patch leading to a progressive reduction in peak current concomitant to an enhancement of the inactivation rate as evaluated from ensemble average currents. The nature of inactivation was further studied on a sweep to sweep basis in experiments employing a rapid perfusion system enabling solution change in the ms time range. Recovery from inactivation is apparently accelerated by a voltage-dependent step. An involvement of the sarcoplasmic reticulum which might indirectly affect Ca^{2+} channels by a Ca^{2+}-induced Ca^{2+} release was excluded by experiments showing a similar Ca^{2+}-induced inactivation in the presence of ryanodine. In experiments with cloned Ca^{2+} channels where the $\alpha_{1c\text{-}a}$ and β_3 subunits are stably coexpressed in CHO-cells, stabilization of Ca^{2+} channel activity was similarly achieved by calpastatin + ATP in the excised patch. Preliminary data suggest that the Ca^{2+}-induced inactivation of cloned Ca^{2+} channels might occur at higher concentrations than that of native Ca^{2+} channels. (Supported by Austrian Research Funds S06606, S06607)

M-Pos190

TRANSFERRING Ca^{2+} DEPENDENT INACTIVATION PROPERTY FROM CARDIAC TO NEURONAL Ca^{2+} CHANNELS

((R. Olcese, J. Zhou, N. Qin, L. Birnbaumer, E. Stefani)) Dept. of Anesthesiology UCLA School of Medicine, Los Angeles, CA 90095-1778

The ionic current flowing through the L-type Ca^{2+} channels rapidly inactivates when the charge carrier is Ca^{2+}. This process, known as Ca^{2+} dependent inactivation is present in the cardiac α1C clone expressed in oocytes and it is absent in the neuronal α_{1E} Ca^{2+} channel. The C-terminus of the α_{1C} has been shown to be involved in the Ca^{2+} dependent process. (M. de Leon et al., 1995). We constructed chimeric Ca^{2+} channels by swapping domains between α_{1C} and α_{1E} C-termini in order to define the molecular domains participating in Ca^{2+} dependent inactivation. The cut-open oocyte voltage clamp technique was used to measure Ca^{2+} and Ba^{2+} currents from BAPTA injected *Xenopus* oocytes. The Ca^{2+} inactivation process was encoded in the C- terminus domain. The function was lost in α_{1C} with α_{1E} C-terminus, and conversely, the Ca^{2+} inactivation function was gained in α_{1E} with the α_{1C} C-terminus. The transfer of the putative E-F hand Ca^{2+} binding motif from α_{1C} C-terminus into the corresponding region of α1E failed to confer Ca^{2+} dependent inactivation. α_{1E} did not gain Ca^{2+} inactivation unless a large region downstream to the N-terminal part of the C-terminus was transposed into α_{1E} (see Figure). Supported by NIH grants AR-43411 to L.B. and AR-38970 to E.S.

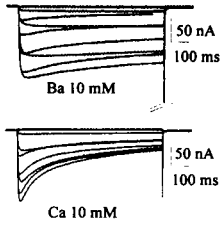

Ca^{2+} dependent inactivation in α_{1E} with α_{1C} sequences.

M-Pos191

SILENT CALCIUM CHANNELS GENERATE EXCESSIVE TAIL CURRENTS AND FACILITATION OF Ca^{2+} CURRENTS IN RAT SKELETAL MYOBALLS

((Andrea Fleig and Reinhold Penner)) Max-Planck-Institute for biophysical Chemistry, Göttingen, Germany.

L-type calcium channels of skeletal muscle are subject to voltage- and time-dependent facilitation so that calcium currents following strong and long-lasting depolarizations are markedly augmented. Previous work suggested the involvement of phosphorylation by cAMP-dependent protein kinase in facilitation. Recent evidence indicates that a large subset of calcium channels remain silent during depolarizations but are primed by strong and long-lasting depolarizations to conduct calcium ions upon repolarization, generating excessive tail currents. We present evidence that recruitment of excessive tail currents and facilitation occur in parallel and that ryanodine and caffeine selectively inhibit both tail currents and facilitation. We propose that facilitation of calcium currents and excessive tail currents are consequences of a common mechanism linked to ryanodine receptors.

M-Pos192

PRE-PULSE FACILITATION OF THE CARDIAC α_{1C} CALCIUM CHANNEL IS ALTERED BY DIFFERENT β SUBUNITS AND UNAFFECTED BY MUTATION OF PUTATIVE PKA SITES ON THE α_1 SUBUNIT.

((J.L. Costantin, N. Qin, X. Wei, L. Birnbaumer, E. Stefani)) Dept. of Anesthesiology, UCLA, Los Angeles CA 90095-1778

Pre-pulse facilitation (2-4 fold increase) of neuronal α_{1C} calcium channel currents occurs in the presence of the β_1 or β_3 subunit and is reduced by inhibitors of protein kinase A (PKA) (Bourinet *et al.*, EMBO J. 1994). We have found a 1.5-2.5 fold pre-pulse facilitation in the magnitude of currents through the rabbit cardiac α_{1C} subunit coexpressed with either the β_1 or β_3 subunit in Xenopus oocytes. This large facilitation is not present when the α_1 subunit is expressed alone or when the β_2 subunit is coexpressed. Pertussis toxin does not affect the facilitation while inhibitors of PKA (Rp cAMP) cause ≈50% reduction. Identical values for facilitation are found when these β subunits are coexpressed with an α_{1C} channel in which six consensus sites for PKA phosphorylation have been mutated to alanines. The β subunit specificity and the evidence of a role for PKA suggest that phosphorylation sites on the β subunit may play a role, or that the β subunits that promote facilitation may expose sites on the α_1 subunit that are not the putative sites we mutated. Facilitation of α_{1C}+β_1 channels is shown in the Figure. Prepulses are delivered to voltages every 20 mV between the holding potential of -90 mV and +150 mV. The magnitude of the second pulse begins to increase at prepulse values near +30 mV and increases as the prepulse becomes more positive. Facilitation is not caused by the prepulse current itself as the increase occurs independently of whether inward or outward current is elicited. Recovery from facilitation caused by a single prepulse to 150 mV, decays with two exponentials (τ_1= 3 seconds, τ_2=20 seconds). (Supported by N.I.H. grants AR-38970 to E.S. & AR-43411 to LB.)

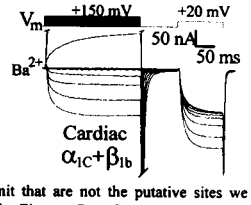

M-Pos193

CHARACTERIZATION OF A T-TYPE VOLTAGE-GATED Ca^{2+} CURRENT IN PRIMARY SPERMATOCYTES FROM ADULT TESTIS.

((C. Santi, A. Darszon, and A. Hernández-Cruz)). Instituto de Fisiología Celular, UNAM, México City, D.F., and Instituto de Biotecnología, UNAM, Cuernavaca. México.

The kinetic properties of a Ca^{2+} current present in acutely dissociated mouse primary spermatocytes were examined using the whole-cell patch-clamp technique. Recording solutions contained (in mM): pipette: 110 CsMe, 10 CsF, 15 CsCl, 2 Cs-BAPTA, 4 ATP-Mg, 10 Phosphocreatine, 5 Cs-HEPES; bath: 130 NaCl, 3 KCl, 2 $MgCl_2$, 1 $NaHCO_3$, 0.5 NaH_2PO_4, 5 Na-HEPES, 5 Glucose, 10 $CaCl_2$ pH 7.35. Ca^{2+} currents begin to activate at ≈ -60 mV and peaked ≈ -25 mV. Peak Ca^{2+} current density was 6.5 ± 0.6 µA/cm^2 (mean ± SEM, n=16). Currents inactivate with a single exponential time course (τ_i = 8.7 ms at -20 mV). Both time to peak and time constant of inactivation were strongly voltage dependent and decayed monotonically between -40 and +10 mV, approaching a minimum of 11 ms and 7 ms respectively. Activation occurs between -65 and -10 mV with half-activation voltage $Va_{i/2}$ =-47.3 ± 2.1 (mean ± SEM) and steepness parameter ka = 6.9 ± 0.3 mV (mean ± SEM); n=9. Steady state inactivation occurs between -90 and -40 mV with half inactivation $Vi_{i/2}$ = -63.9 ± 1.7 (mean ± SEM) and ki = 6.4 ± 0.5 mV (mean ± SEM); n=12. Ca^{2+} current tails could be fitted with single exponentials with time constants approaching 0.9 ms at -100 mV. Ni^{2+} 100-200 µM reduced Ca^{2+} current peak amplitude by 40%-75% and amiloride 500 µM by 62%. Nifedipine (5-10 µM), a specific blocker of L-type Ca^{2+} channels also reduced Ca^{2+} current peak amplitude by 38-53%. It is concluded that these cells apparently possess only T-type voltage-gated Ca^{2+} channels. Since these Ca^{2+} channels are the primary pathway for voltage-gated Ca^{2+} entry, they could play a significant role in regulating meiotic cell division and sperm differentiation.

This work was supported by grants from DGAPA, CONACyT (México) and Howard Hughes Medical Institute.

M-Pos194

IDENTIFICATION OF PKA PHOSPHORYLATION SITES IN THE CARBOXYL TERMINUS OF CLASS C,D AND S CALCIUM CHANNEL α_1 SUBUNITS BY SITE DIRECTED MUTAGENESIS. ((J. Mitterdorfer, M. Froschmayr, M. Grabner, H. Glossmann and J. Striessnig)) Institut für Biochemische Pharmakologie, Universität Innsbruck, Peter Mayr Str. 1, A-6020 Innsbruck, Austria.

Full length L-type Ca^{2+} channel α_1 subunits are rapidly phosphorylated by protein kinase A (PKA) *in vitro* and *in vivo* at sites located in their long C-terminal tails. In skeletal muscle, heart and brain the majority of biochemically isolated α_1 subunits lack these phosphorylation sites due to post-translational proteolytic truncation of the C-terminus. Truncation may therefore modify the regulation of channel activity by PKA. We investigated the extent to which putative cAMP-dependent phosphorylation sites in the C-terminus of α_1 subunits α_{1S} from rabbit and carp skeletal muscle, α_{1C} from rabbit heart and α_{1D} from rat neuroendocrine tissue are phosphorylated *in vitro* by combining site directed mutagenesis and heterologous expression. Wild type and mutant Ca^{2+} channel α_1 subunits were expressed in *Saccharomyces cerevisiae* to obtain high yields of the full length size form. Like in intact cells (1), the rabbit skeletal muscle α_1 C-terminus was phosphorylated at Ser_{1754} and Ser_{1857}. In the carboxyl terminus of α_{1S} from carp skeletal muscle and α_{1C} from rabbit heart single residues (Ser_{1739} and Ser_{1928}, respectively) were phosphorylated by PKA. In contrast, the C-terminus of α_{1D} was phosphorylated at more than one site. Employing deletion mutants, most of the phosphorylation (>70%) was found to occur between amino acid residues 1782 and 1972. (Supported by FWF grants S6601-med (H.G.) and S6602-med (J.S.))

(1) Rotman et al., JBC *270*, 16371-16377 (1995).

K CHANNELS I

M-Pos195

TEMPERATURE-DEPENDENT FUNCTIONAL EXPRESSION OF SQUID KV1.1 CHANNELS IN AN INSECT CELL LINE. ((M.W. Brock, A.W. DeTomaso, J.J.C. Rosenthal, Z.N. Lebaric, and W.F. Gilly)) Department of Biology, Hopkins Marine Station, Stanford University, Pacific Grove, CA 93950.

Squid (Sq) Kv1.1 (=KZ4) is a cDNA cloned from a stellate ganglion/giant fiber lobe (GFL) library (Biophys. J. 66:A105) that we propose corresponds to the gene encoding "delayed rectifier" K^+ channels in giant axons and GFL cell bodies: 1.) SqKv1.1 mRNA is selectively expressed in GFL neurons at high level. 2.) Polyclonal antisera to SqKv1.1 peptide sequence specifically recognize protein in cleaned giant axon and GFL preparations using Western blots. 3.) Injection of SqKv1.1 cRNA into *Xenopus* oocytes produces single channel and macroscopic I_K with properties similar to those described for giant axons and GFL neurons (Biophys. J. 68:A270). We have incorporated this cDNA into a recombinant baculovirus for expression in Sf9 cells. Virtually all cells in infected cultures were positive for SqKv1.1 protein (as assayed by immunofluorescence) regardless of culture temperature (27°C vs. 18°C). Expression of I_K as assayed by whole cell patch clamp, however, was dependent on temperature. If Sf9 cells were infected and maintained at 27°C prior to recording, I_K was essentially nonexistent. If cells were maintained at 18°C after an initial 12-24 hour infection/incubation period at 27°C, I_K was identifiable within several days. After 4-5 days in at 18°C, approximately 50% of the cells displayed I_K of 1-20 nA (at +60 mV) with properties similar to those of native I_K in axons and GFL neurons. Under these conditions, infected cultures contain viable cells expressing SqKv1.1 I_K for least 20 days. This system will be valuable for biophysical analyses of channel function and for cell biological investigations of assembly and trafficking. Supported by NIH NS-17510.

M-Pos196

EXPRESSION OF THE KV1.1 RAT BRAIN K CHANNELS IN MAMMALIAN CELLS: TEMPERATURE EFFECTS ((Oscar Moran and Franco Conti)) Istituto di Cibernetica e Biofisica, C.N.R. Via De Marini, 6. I-16149 Genova, Italy

We studied the currents mediated by K channels Kv1.1 cloned from rat brain expressed by permanent transfection in the cell line 292er. Voltage-gated no-inactivating outward currents, with a reversal potential near to the Nernst potential for K, were elicited by depolarising pulses. The amplitude of the current measured at room temperature (≈ 18°C) for V_m=+20 mV ranged between 0.8 and 5.5 nA. The activation kinetics at this potential, evaluated as the time to one half of the maximum amplitude, $t_{1/2}$, was less that 2 ms. The deactivation time constant τ_d, was less than 2 ms at –120 mV. The activation curve was fitted with a simple Boltzman function, yielding a V_{half}=–25.0±1.8 mV, and the maximum exponential slope, V_a=3.8±0.7 mV. The voltage-dependence and the kinetic properties are similar to those expressed in frog oocytes injected with cRNA coding the same Kv1.1

Properties of the currents were studied at different temperatures between 13°C and 27°C. A decrease in temperature results in a reversible reduction of the amplitude of the current and a slowing of its kinetics. The Q_{10} of the peak current evoked by $V_m \geq +20$ mV was between 1.3 and 2.5. The kinetic constants τ_d (–120 mV) and $t_{1/2}$ (+20 mV) showed temperature dependence coefficients of Q_{10}= 2.8 and a Q_{10} = 2.6 respectively. A reduction of temperature from 24°C to 14°C produced a positive shift of ≈7.5 mV in the half activation potential, i.e. channels activate at more positive potentials at low temperature than at high temperature. We conclude that in Kv1.1 channels the closed states are associated with more ordered structure of the channel protein than the open state.

This work was partially supported by P.F. Ingegneria Genetica – CNR

M-Pos197

EXPRESSION OF A NOVEL *SHAKER*-RELATED K^+ CHANNEL, Kv1.7, IMPLICATED IN DIABETES.
((K. Kalman, J. Tseng-Crank*, I.D. Dukes*, G. Chandy, J. Aiyar, G. Gutman+, K.G. Chandy)) Depts. of Physiol. & Biophys., and Microbiol. & Mol. Genet.+, Univ. California, Irvine, CA., and Glaxo Research, Research Triangle Park, Durham NC.

Non insulin-dependent diabetes mellitus is a metabolic disease of unknown etiology, typified by defects in insulin secretion and insulin action. Ion channels in the pancreatic islet β-cell represent the primary elements coupling nutrient signals to the regulation of insulin secretion, and drugs against these molecules are used for the therapeutic mangement of NIDDM. We report the expression and characterisation of a novel K^+ channel, mouse Kv1.7, which shows an increased level of expression in diabetic *db/db* islets, and is unique among mammalian Shaker-related genes in having a coding region made up of at least two exons. We generated a Kv1.3/Kv1.7 chimera in a pBSTA expression vector, containing the first 45 residues of rKv1.3, and 501 amino acids of mkv1.7 (beginning 181 residues upstream of the S1 segment). This chimera allowed us to test the functionality of Kv1.7 even though we have not yet identified the 5'-terminus of the coding region. In particular, we were able to evaluate the conduction and pharmacological properties generally associated with the hydrophobic core of Kv proteins. The Kv1.3/Kv1.7 chimera under the control of the T7 promoter was transcribed *in-vitro* and cRNA injected into RBL cells. Patch clamp recording of injected cells revealed a voltage-dependent, rapidly-activating, use-dependent K-selective current that is insensitive to both TEA (Kd = 86mM), and ChTX (Kd = 690nM), but sensitive to 4-aminopyridine (Kd = 200nM), tedisamil (Kd = 18μM), resiniferatoxin (Kd = 18μM), nifedipine (Kd = 13μM), diltiazem (Kd = 66μM), clofilium (Kd = 47μM), and capsaicin (Kd = 24μM). The channel has a single channel conductance of 20 pS.

M-Pos198

CLONING AND FUNCTIONAL EXPRESSION OF Kv1.5 FROM FERRET ATRIUM. ((T. Schwegel, J. Wang, N.K. Jurkiewicz, K.L. Folander, R. J. Swanson, J.J. Salata and B. Fermini.)) Merck Research Laboratories, West Point PA 19486.

Northern blots of cardiac atrial and ventricular mRNAs demonstrated that, as in the human heart, the steady-state level of mRNA encoding the K^+ channel Kv1.5 is much higher in the atria than the ventricle. cDNAs encoding this channel were isolated from ferret atrium. The deduced amino acid sequence of the protein is 86-93% identical to the 5 other cloned species variants of Kv1.5. Ferret Kv1.5 was expressed in *Xenopus* oocytes and its properties assessed by the two microelectrode voltage-clamp technique. Depolarizing voltage steps from a holding potential of -80mV elicited rapidly activating (τ_a : 7.2 ± 0.3ms at +30mV, n=9), slowly inactivating (τ_i : 1606 ± 175ms at +30mV, n=8), time and voltage-dependent currents and outward tail currents upon return to -30mV. The current was carried largely by K^+; the reversal potential (E_{rev}) shifted 52.0 ± 0.6mV per decade change in extracellular K^+ (from 3-100 mM, n=4). Activation and inactivation curves were fit to a Boltzman function and had midpoints ($V_{\frac{1}{2}}$) and slope factors (k) of -15.5 ± 0.8mV, 8.3 ± 0.5mV, -25.3 ± 1.7mV and 6.0 ± 0.6mV, respectively. At potentials > 0mV the current inactivated slowly and incompletely over 3s (24.3 ± 1.9% decrease at +30mV, n=8). Recovery from inactivation was very rapid; 97% of Kv1.5 recovered after a paired pulse interval of 5ms (150ms pulses to +50mV, n=4). Kv1.5 was inhibited by 4-AP (IC_{50} 127.5 ± 23.7μM at +30mV, n=6) and verapamil (50μM, 85.6 ± 1.8% block at +30mV, n=5). We conclude that, consistent with the strong sequence conservation, the biophysical and pharmacological properties of ferret Kv1.5 are very similar to those of the human channel, and other species variants.

M-Pos199

SIMILAR POTASSIUM CHANNEL INACTIVATION KINETICS EXIST IN SQUID GIANT AXON AND GIANT FIBER LOBE CELL BODIES.
((C. Mathes, J.J.C. Rosenthal, C. M. Armstrong and W.F. Gilly))
Hopkins Marine Station of Stanford University, Pacific Grove, CA 93950 and Marine Biological Laboratory, Woods Hole, MA.

We have compared inactivation properties of potassium conductance (g_K) in perfused giant axons (GA) of *Loligo pealei* and in somata of giant fiber lobe (GFL) neurons of *L. opalescens*. GA measurements were carried out with an axial wire voltage clamp by pulsing to V_K (~ -10 mV in 50-70 mM external K) for a variable time and then assaying available g_K with a strong, brief test pulse. GFL cells were studied with whole-cell patch clamp using the same pulse procedure and with long depolarizations for comparison. Under our experimental conditions (12-18°C; 4 mM internal Mg·ATP) a large fraction of g_K inactivates within 250 msec at -10 mV in both preparations (0.3 to 0.9). This fraction tends to be larger in GFL cells than in axons but substantial overlap between the data sets exists. For depolarizations less than 1 sec in duration, inactivation in GA and GFL cells shows two kinetic components, the faster of which is more temperature sensitive and becomes more prominent at 18°C. We also find that inactivation is sensitive to external K concentration, the presence of internal ATP, and the application of intracellular protease. [Supported by NS-17510].

M-Pos200

DELAYED RECTIFIER CURRENTS IN BULLFROG SYMPATHETIC NEURONS WITH INTRACELLULAR Cs^+. ((Brian M. Block and Stephen W. Jones)) Departments of Neurosciences and Physiology & Biophysics, Case Western Reserve University, Cleveland, OH 44106.

Bullfrog delayed rectifier K^+ channels can carry inward Cs^+ current even in the presence of intracellular K^+ (88 mM) (Block and Jones, Biophys. J. 68:A42, 1995). Replacement of Na^+ and K^+ with Cs^+ (120 mM Cs^+_o, 100 mM Cs^+_i) gave large whole cell currents. Tail currents contained 2 exponential components, with the larger (~85%) and faster component (τ ~10 at -80 mV) blocked 91 ± 3% (mean ± SEM, n=4) by 40 mM TEA (K_D ~2 mM, comparable to TEA block of this delayed rectifier in K^+ solutions). The slow component was unaffected by TEA. Comparing 120 mM Cs^+_o to K^+_o (with Cs^+_i), the current sensitive to 10 mM TEA had a permeability ratio (P_{Cs}/P_K) of 0.12 ± 0.001 (n=3). From chord conductances measured 40 mV negative to reversal, K^+_o carried ~4 fold more inward current than Cs^+_o. The TEA-sensitive current showed a strong anomalous mole fraction effect in mixtures of $Cs^+_o + K^+_o$ ($G_{25K/95Cs}/G_{120Cs} = 0.37 \pm 0.02$, n=3). Based on the TEA sensitivity, this current is likely to be the delayed rectifier. Although it is selective for K^+ over Cs^+, Cs^+ can carry substantial inward and outward currents. Replacement of intracellular K^+ by Cs^+ may not be sufficient for isolation of Ca^{2+} and Na^+ currents.

M-Pos201

CHARACTERIZATION OF THREE TYPES OF DELAYED RECTIFIER POTASSIUM CHANNELS IN CANINE PULMONARY ARTERY SMOOTH MUSCLE CELLS. ((R.I. Jabr, D.S. Ahn and J.R. Hume)) Department of Physiology and Cell Biology, University of Nevada, Reno, NV 89557.

Hypoxic pulmonary vasoconstriction may be caused by inhibition of 4-aminopyridine (4-AP) sensitive delayed rectifier K^+ currents (I_{Kdr}) (Circ. Res. 77:131-139,1995) leading to membrane depolarization and subsequent Ca^{2+} entry. So far, it is not clear how many types of delayed rectifier K^+ channels may exist in pulmonary artery smooth muscle cells (PASMC) and which exhibit 4-AP sensitivity. In perforated whole-cell voltage clamp experiments, I_{Kdr} recorded from canine PASMC in Ca^{2+}-free solutions showed fast activation followed by slow inactivation. The peak and steady state currents recorded at +30 mV were significantly decreased with 4-AP (5mM) by 80.5 ± 3.9 and 70.8 ± 1.8 % respectively (n=3). Whether whole-cell 4-AP sensitive I_{Kdr} is mediated by more than one type of K^+ channel was investigated in inside-out membrane patches. In presence of charybdotoxin (200 nM; an inhibitor of Ca^{2+}-activated K^+ channels) in the pipette, three types of K^+ channels could be identified during voltage steps based upon differences in unitary conductance: 9 ± 0.3 pS (n=13), 12.7 ± 0.2 pS (n=4) and 34.7 ± 1.7 pS (n=7). These channels were detected in less than 10 % of the patches examined. Channels with conductances of 9 and 13 pS were sensitive to bath applied 4-AP (10 mM). These results suggest that more than one type of K^+ channel may be responsible for macroscopic I_{Kdr} in canine PASMC. (Supported by NIH HL49254 and AHA Nevada Affiliate).

M-Pos202

DELAYED RECTIFIER CHANNEL OPEN PROBABILITY DURING DIASTOLIC DEPOLARIZATION IN SINOATRIAL NODE CELLS. ((M.W. Veldkamp, A.C.G. van Ginneken and L.N. Bouman)) Department of Physiology, University of Amsterdam, Amsterdam, The Netherlands. (Spon. by B. van Duijn)

Various types of currents are thought to be involved in the diastolic depolarization of sinoatrial node (SAN) cells. The decay of the delayed rectifier (I_K) current in conjunction with an inward current is considered to be a major cause of the initiation of diastolic depolarization. With the patch clamp technique, we studied the behaviour of I_K channels during the process of diastolic depolarization in rabbit SAN cells. Two electrodes were used on the same spontaneous beating cell, one for whole-cell recording of action potentials and one for cell-attached patch recording of single I_K channel activity. Both electrodes were filled with a high potassium solution. Under these conditions we observed a 14 pS K^+ channel that showed channel openings during the repolarization phase of the action potential and during the diastolic depolarization phase. During repolarization of the action potential, channel open probability (P_o) was initially very low, but rapidly increased towards final repolarization and reached a maximum at the time of the maximum diastolic potential. Next, P_o slowly decayed again during the subsequent diastolic depolarization. P_o varied between 0.08 and 0.23. Increasing evidence suggests that the rapidly activating delayed rectifier current exhibits inactivation at depolarized potentials. In this light, the increase in channel open probability during final repolarization might be the result of recovery from inactivation, whereas the slow decay of channel activity most probably reflects the deactivation process.

M-Pos203

ELECTRO-ELASTIC CAPACITATIVE COUPLING IS A POSSIBLE MECHANISM FOR VOLTAGE GATING. ((M.B. Partenskii, V. Dorman and P.C. Jordan)) Dept. of Chemistry, Brandeis University, Waltham, MA 02254-9110.

One of the central puzzles in the functioning of voltage gated ion channels is their extreme sensitivity to a very small change of the transmembrane potential. An elastic capacitor model (J. Chem. Phys., 99, 2992 [1993]) suitably generalized to account for coupling between the surface charge at the solvent/channel former interface and the "gating assembly" represented by an internal "capacitor" with elastically coupled sheets of charge (of constant charge density) is described. This model has features highly reminiscent of voltage gated channels. The system undergoes a "phase transition" (the equivalent of a conformational change) at low transmembrane voltages. As long as the gating capacitor is highly charged (e.g., the S4 region of Shaker) the transition requires only small conformational changes in this capacitor, which need not be near the ionic pathway; the role of the gating capacitor is to initiate the instability which then permits conductance. We also discuss hysteresis and the possibility of "cooperativity" between neighboring channels.

M-Pos204

HODGKIN-HUXLEY AND PARTIALLY COUPLED MODELS OF INACTIVATION PREDICT DIFFERENT VOLTAGE DEPENDENCE OF BLOCK. ((Shuguang Liu and Randall L. Rasmusson)) Duke U. Med. Ctr., Durham, NC (Spon. M. Lieberman)

Potassium channel blockers have been shown to exhibit complex time- and voltage-dependent effects on cardiac K^+ currents measured under voltage clamp conditions. Modeling and simulation of these effects have been an important component in furthering our understanding of the mechanism of block. While much attention has been focused on the state-dependence of K^+ channel block, how a particular channel model can alter the predicted time- and voltage-dependence of channel block remains unexplored. We compared the effects of a theoretical open-state specific channel blocker on macroscopic currents using two different model formalisms for the same I_{to} channel. Model 1 is a Hodgkin-Huxley like model in which inactivation is an intrinsically voltage dependent process and occurs independently of activation. It is similar to those commonly employed in cardiac action potential simulations. Model 2 is a "partially coupled" model in which inactivation is intrinsically voltage insensitive but requires channel activation before it can proceed. In the absence of drug (blocking agent), the two models reproduce the macroscopic current data within the limitations of experimental observations. In the presence of open channel blocking agent, both models predict the same degree of reduction of peak current in response to a single step from -70mV to +50 mV. However, once depolarized the fraction of bound vs. inactivated channels begins to differ substantially for the two models with Model 1 displaying much less block than Model 2 due to the strong voltage-dependent absorbing inactivation of Model 1 . The result is that recovery of peak current in Model 2 occurs on an order of magnitude more slowly than in Model 1. Thus, choice of model formalism may be extremely important for quantitative analysis of state specific drug-channel interactions and will be essential for computer models which attempt reconstruction of pharmacological effects on action potential morphology and more complex electrophysiological properties.

M-Pos205

SPECULATION ABOUT THE MECHANISM OF ACTIVATION IN SHAKER K+ CHANNELS. ((D.M. Papazian, S.K. Tiwari-Woodruff, S.-A. Seoh, W.R. Silverman, D. Sigg, and F. Bezanilla)) Department of Physiology, UCLA School of Medicine, Los Angeles, CA 90095-1751.

Neutralizing E293 (S2), R368 (S4), and R371 (S4) in Shaker channels reduces the number of gating charges per channel (Seoh et al., this volume), suggesting that these residues undergo voltage-dependent conformational changes during activation. However, the charge/channel is reduced, at least in part, by indirect effects on residues other than the mutated one. Neutralizing nearby residues E283 (S2), R365 (S4) and K374 (S4) does not reduce the charge/channel. Likely short range interactions between S2, S3, and S4 have been identified and incorporated into a packing model (Tiwari-Woodruff et al., and Silverman et al., this volume). It postulates that S2, S3, and S4 form an interacting set of α-helices, with S2 and S4 tilted relative to S3. The functional and structural results are complementary and may have implications for the mechanism of activation. 1) The biochemical results suggest that charged residues in S2, S3, and S4 interact electrostatically, which could account for the indirect effects of neutralization mutations on the charge/channel. 2) Reducing the angle of tilt of S2 (with 283 fixed) and S4 (with 374 fixed) in response to a depolarization could account for the differential contribution of nearby residues to the charge/channel; 293, 368, and 371 would move in the expected directions, but 283 and 374 would not move relative to the field. This cannot account for all of the charge movement that accompanies activation, however, if the field spans the whole membrane. Alternatively, 283 and 374 may be out of the transmembrane field. This may be less likely because they appear to interact at short range with residues that, by their contribution to the charge/channel, are within the field.

M-Pos206

EFFECT OF CHEMICAL MODIFICATION ON THE GATING AND IONIC CURRENTS OF THE *SHAKER* POTASSIUM CHANNEL. ((S. Eskandari, L. Toro and E. Stefani)) Dept. of Anesthesiology, UCLA School of Medicine, Los Angeles, CA 90095

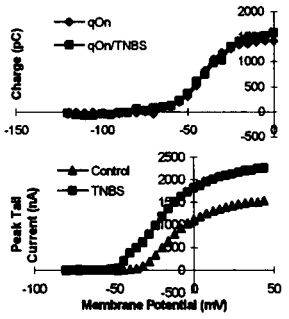

The cut-open oocyte vaseline gap technique was used to investigate the effect of an amino modifying reagent (trinitrobenzene sulfonic acid, TNBS) on the coupling between charge movement and pore opening in *Shaker* K^+ channels (inactivation removed conducting *Sh*H4-IR, and non-conducting *Sh*H4-IR W434F). TNBS covalently neutralizes the positive charge of the ε-amino group of lysine residues and has been shown to potentiate squid native K^+ currents (Spires and Begenisich, 1992). A 10-minute treatment of the *Sh*H4-IR W434F K^+ channel with an external solution of 5 mM TNBS at pH 9.0, while the membrane was continuously pulsed from negative to positive potentials, resulted in no apparent change in the amount of charge movement during the gating process of the channel. In contrast, an equivalent treatment of the *Sh*H4-IR K^+ channel greatly increased K^+ currents with a shift to more negative potentials of the g-V curve. We conclude that TNBS leads to modification of residues that do not significantly contribute to charge movement but may regulate the weakly voltage-dependent transition between the last closed and the open state of the channel. Supported by NIH grants.

M-Pos207

VOLTAGE-INSENSITIVE GATING IN *SHAKER* B S4 MUTANTS. ((H.Bao, A.Hakeem, K.McCormack‡, M. Rayner, J.Starkus)) Békésy Lab, PBRC., Univ. Hawaii, Honolulu, HI 96822, and ‡Dept of Genetics, U. of Wisconsin, Madison, WI 53706.

Neutralizations of the 2nd or 4th charges in the *Shaker* B S4 segment have previously been described as left-shifting the G(V) curve, and destabilizing the closed state of the channel (see Sigworth, *Q. Rev Biophys.*, 1993). We show here that neutralization of both 2nd and 4th charges, appears to decouple channel gating from the voltage sensor. In these mutants, single channel records show a low NPO (10 to 20%) which remains approximately constant from -160 to +80 mV. Channels continue to open and close with normal selectivity, but in a voltage-insensitive manner. Closed time distributions demonstrate brief closed intervals, similar to the shortest intervals seen in control channels, as well as long closed intervals which are also seen in control *Shaker* channels. We conclude that normal voltage sensor coupling is mediated primarily via the intermediate closed state.

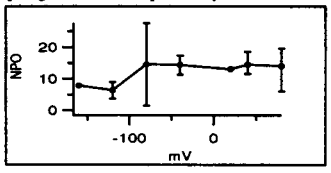

M-Pos208

THE RISING PHASE OF IgOFF IN *SHAKER* B GATING CURRENTS. ((J.Starkus, A.Hakeem, M.Rayner)) Békésy Lab, Pac. Biomed. Res. Ctr., Univ. Hawaii, Honolulu, HI 96822

OFF gating currents, in inactivation-removed mutants of both conducting and non-conducting *Shaker* B channels, show a well-documented slow rising phase (Stefani et al., *Biophys.J.* 66, 1994). However, comparison of these gating currents with tail currents obtained in conducting versions of the same channels (see below) clarifies that channels close in a voltage-sensitive manner during the rising phase of the IgOFF. Mutants, which alter the affinity of the inactivation binding site in inactivation-intact Shaker channels, also affect the rising phase of IgOFF. We suggest that this rising phase may be determined by the rate of recovery from gating charge immobilization, induced by permeant ions binding to the inactivation binding site in "ball-deleted" Shaker channels. "Knock-on" effects may limit such binding in conducting channels.

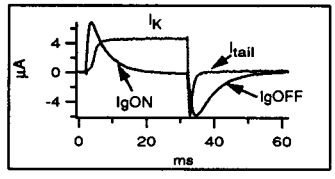

M-Pos209

STABILIZATION OF THE OPEN STATE IN *SHAKER* B CHANNELS. ((M.Andres, H.Bao, M.Henteleff, M.Hermosura, J.Lu, M.Rayner, and J.Starkus)) Békésy Lab, Pac. Biomed. Res. Ctr., Univ. Hawaii, Honolulu, HI 96822

Previous work has shown that both the L1 and L2 heptad leucines affect open state stability (see review by Sigworth, *Q. Rev. Biophys.* 27, 1993). Using thermodynamic analysis of a defined first order reaction, which leads into and out of the open state (see Rayner et al.,1996 *Biophys J, Abstr.*), we note well-defined changes in reaction parameters in a series of L1 mutants. These changes are consistent with previous findings, and clarify that this defined reaction is crucial for the control of open state stability. We show that this reaction determines both mean open time and the intermediate closed duration, but not the fast or slow closed times. For mutations of L1 to F, Y, V, A, S and T we note apparent changes in folding probability (as previously reported for the L2 site) and also changes in well-to-barrier heights for the back (deactivation) reaction. However, there are only minor changes in forward (reactivation) reaction parameters, further clarifying that these mutants specifically affect open state stability. On the other hand, we detect that there are consistent effects on barrier position and on the apparent reaction valence, suggesting that hydrophobic interactions are also important in localizing the steep region of the transmembrane field.

(Supported by PHS grant #NS-21151, and NIH RCMI grant #RR-03061)

M-Pos210

STABILIZATION OF THE C-INACTIVATED STATE BY THE FAST INACTIVATION PARTICLE IN NON-CONDUCTING *SHAKER* H4 W434F POTASSIUM CHANNELS. ((M.J. Roux, R. Olcese, L. Toro, E. Stefani)) Department of Anesthesiology, UCLA School of Medicine, Los Angeles, CA 90095-1778.

Shaker H4 channels are fast-inactivating (A-type) potassium channels, with a multi-exponential decay of the ionic currents. The fast component (N-type) (3-5 ms) is due to the blocking of the pore by the N-terminal cytoplasmic domain (Hoshi et al, 1990). The slow component (C-type) (~500 ms), is still present in the Δ6-46 deletion mutant removing fast inactivation (Hoshi et al., 1990), though with a slower time constant (~5 s), suggesting a coupling between the two mechanisms (Hoshi et al., 1991). C-type inactivation, induced by prolonged depolarization at 0 mV, has been shown to induce a shift in the voltage dependency of the gating charge return in the non-inactivating non-conducting *Shaker* H4 IR W434F channels (Olcese et al, Biophys.Soc.Abs). We report here that this shift is more important in the non-conducting mutant *Shaker* H4 W434F, indicating that the two types of inactivation are indeed coupled, the presence of the inactivation particle in its binding site increasing the stability of the C-inactivated state.

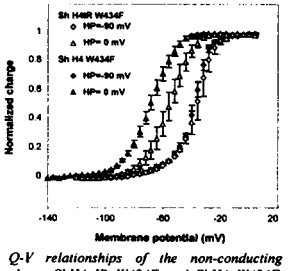

Q-V relationships of the non-conducting clones ShH4 IR W434F and ShH4 W434F. held at least 1 minute at either -90 or 0 mV.

Supported by NIH grants

M-Pos211

AMINO ACID RESIDUES INVOLVED IN EXTERNAL BARIUM BLOCK OF THE SHAKER POTASSIUM CHANNEL EXPRESSED IN *XENOPUS* OOCYTES. ((R. S. Hurst, L. Toro and E. Stefani)) UCLA, Dept. of Anesthesiology, Los Angeles, CA 90095.

Barium ions block a wide variety of K^+ selective ion channels. It has been proposed, based on crystal dimensions, that Ba^{2+} blocks these channels by binding at a K^+ site within the conduction pathway (Standen and Stanfield, 1978; Armstrong and Taylor, 1980; Eaton and Brodwick, 1980; Vergara and Latorre, 1983). We recently reported that external Ba^{2+} block of the non-inactivating *Shaker* K^+ channel (*Sh*H4-IR) is comprised of a fast and slow component and proposed that each component represented a separate binding site. In an attempt to identify these binding sites, amino acid substitutions were made at two positions (T^{449} and D^{447}) within the putative pore forming region. Substitution of T^{449} by either A or V slightly increased the apparent dissociation constant for the slow component (K_s) while substitution by either Y or H had a much more marked effect; for T^{449}, K_s = 1.5 ± 0.9 (n = 5); for T449A, K_s = 3.5 ± 1.2 (n = 8); for T449V, K_s = 6.1 ± 3.0 (n = 5); K_s for T449Y and T449H could not be determined. According to a sequential two site model, the main effect of these mutations was to decrease the binding rate of the slow component while the unbinding rate was much less affected. None of these mutations significantly altered the fast component of block ($K_f \approx 22$ mM). The charge neutralization D447N, two positions deeper in the pore, completely abolished the ionic current but left the gating charge movement intact (see also Seoh et al., this meeting). Therefore, we compared the effects of Ba^{2+} on the movement of gating charge in two non-conducting mutants, W434F and D447N. External Ba^{2+} increased the rate of gating charge return of W434F but only following depolarizations to potentials more positive than about -45 mV (see Hurst et al., this meeting). The single mutation D447N alone or when introduced into the background of W434F markedly reduced this affect of Ba^{2+}. Together, these results suggest that D^{447} contributes to an external Ba^{2+} binding site while the residue at position 449 imposes an energy barrier to the access of this site. (Supported by NIH grant GM50550)

M-Pos212

THE LIMITING SLOPE OF Kv. 2.1 CHANNELS SHOWS A GATING CHARGE OF ABOUT 12e_o. ((Leon D. Islas and Fred J. Sigworth)), Dept. Cell. and Molec. Physiology, Yale School of Medicine, New Haven , CT , 06510.

DRK1 potassium channels have two fewer positive charges than *Shaker* in the S4 region and are thought to have less voltage sensitivity. We have used the method of Patlak et al. (*Biophys. J. 68 : A156, 1995*) to measure the channel open probability (P_O) in patches containing thousands of channels, down to values as low as 10^{-8}. High expression was obtained with a toxin-sensitive DRK1 construct (provided by S. Aggarwal) and with incubation of oocytes in CTx . At the lowest values, the open probability increases approximately 10-fold per 5 mV, corresponding to a total charge of 12 to 13 e_o, similar to the value for *Shaker* channels. Even in the range of $P_O = 10^{-4}$ to 10^{-2} the slope is very steep, corresponding to ~9e_o .

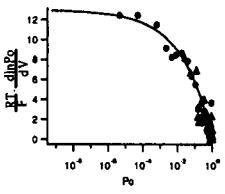

M-Pos213

HOW DOES W434F BLOCK SHAKER CHANNEL CURRENT? ((Y. Yan, Y. Yang, F. J. Sigworth)) Dept. Cellular and Molecular Physiology, Yale University, New Haven CT 06520.

The *Shaker* channel mutant W434F is useful in gating current studies because it has no measurable ion conductance. We constructed tandem tetrameric constructs of N-terminal-truncated wild-type (W) and mutant (F) subunits. Constructs containing one (FWWW) and two (FWFW) mutant protomers showed increased C-type inactivation, as evidenced by sensitivity to external cations, but no changes in selectivity. Although the exact stoichiometry of the channels expressed from the tetramers is unknown, the results suggest that W434F channels are permanently locked in the C-inactivated state. The figure shows normalized whole-oocyte currents at +40 mV in 20 mM external K^+.

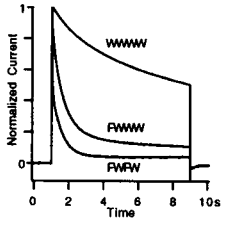

M-Pos214

SUB-CONDUCTANCE STATES OF A MUTANT *SHAKER* CHANNEL ((J. Zheng and F. J. Sigworth)) Dept. of Cellular and Molecular Physiology, Yale Univ. School of Medicine, New Haven, CT 06520

The mutation T442S which is very close to the presumed selectivity filter dramatically slows the deactivation process without changing ion selectivity (Heginbotham, et al., Biophys. J. 66:1061, 1994) and has effects on inactivation (Yool and Schwartz, Biophys. J. 68:448, 1995). We have introduced T442S into a Shaker/NGK2-S6 chimera (Lopez, Jan & Jan, Nature 367:179, 1994). This new construct retains the slow deactivation property. In addition, it shows at least two subconductance levels (about 37% and 70% of the full open channel conductance) which appear during channel activation and deactivation and have voltage dependent dwell times. The trace shows activation at -70mV and deactivation at -140mV in symmetrical 140mM K^+. On activation the 37% conductance substate is often skipped when the channel opens, but the 70% conductance substate (arrows) is traversed in more than 90% of the traces.

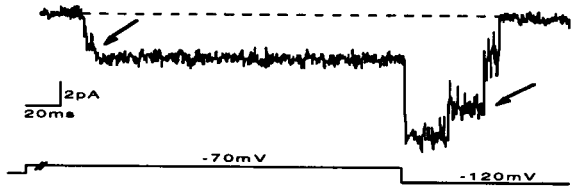

M-Pos215

D447N AND W434F MUTATIONS IN THE PORE REGION OF SHAKER B K^+ CHANNELS PREVENT ION CONDUCTION BUT RESTORE CONDUCTING STATES BY COMBINED MUTATION WITH T449Y. ((S.-A. Seoh, D. Starace, D.M. Papazian, E. Stefani and F. Bezanilla)) Departments of Physiology and Anesthesiology, UCLA School of Medicine, Los Angeles, CA 90095-1751

We have reported that the D447E-IR has very fast C-type inactivation with a time constant of 2-3 ms. Increase of external K^+ or TEA^+ increases current amplitude in D447E-IR. These effects are not seen in D447N-IR (Seoh *et al.*, A35, Biophysical J., 1995). Further study of the characteristics of D447N-IR channels provides evidence that the channel has only gating current and not ionic current. The parameters of the two Boltzmann fit for the gating charge vs. membrane potential curve (Q-V) are similar to those of W434F-IR. External TEA^+ does not affect ON- and OFF-gating currents, whereas internal TEA^+ immobilizes the OFF-gating current without affecting the ON-gating current. When holding the membrane potential at 0 mV and pulsing toward negative membrane potentials, the Q-V curve shows a 20-30 mV shift to more negative potentials as compared to the Q-V while holding at -90 mV. This result suggests that the failure of this mutant to conduct may result from the removal of an ion binding site necessary for ion conduction rather than C-type inactivation of the channel. As expected, the combined mutant channel, W434F+D447N-IR, does not conduct and shows only gating current. In contrast, other combined mutant channels, D447N+T449Y-IR, W434F+T449Y-IR, and W434F+T449V-IR, but not D447N+T449V-IR, restore ion conduction. Although the single mutant channels, T449V-IR and T449Y-IR, have markedly slower C-type inactivation compared to the control inactivation-removed, IR (Lopez-Barneo *et al.* Receptors and Channels, 1:61, 1993), the combined mutants, W434F+T449Y-IR and D447N+T449Y-IR have significantly accelerated C-type inactivation. In contrast, the inactivation rate of W434F+T449V-IR (measured with ionic currents) and D447N+T449V-IR (measured with gating currents) is similar to that of IR. Supported by NIH GM30376.

M-Pos216

STRUCTURAL IMPLICATIONS OF NOVEL METAL BINDING SITES INTRODUCED INTO A POTASSIUM CHANNEL PORE. ((H.S. Krovetz, H.M.A. VanDongen and A.M.J. VanDongen)) Department of Pharmacology, Duke University Medical Center, PO BOX 3813, Durham, NC 27710. (Spon. by A.M.J. VanDongen)

Potassium channels consist of four subunits, each containing six putative transmembrane segments, S1-S6. The narrow part of the pore and the external vestibule are formed by the segment linking S5 and S6. The highly conserved P-region in the S5-S6 linker forms a hairpin structure and defines conductance and selectivity. We have used cysteine substitution mutagenesis of the *drk1* channel (K_v2.1) to probe the surface accessibility of amino acids in the external vestibule and mouth of the channel. Six of the seven functional mutations resulted in an increased sensitivity to block by divalent cations. Two consecutive residues on either side of the pore were found to be exposed. These results are inconsistent with the antiparallel beta barrel model of the pore. Dose-response curves of the two most sensitive mutants and their dimeric constructs indicate that divalent cations bind to four individual sites in the Y380C mutant but not in the I379C mutant.

M-Pos217

STABLE EXPRESSION OF A TRANSIENT OUTWARD K^+ CHANNEL IN MAMMALIAN CELLS AND MODULATION BY DIVALENT CATIONS

((♥H. Masaki, *S. Green, ♥L. K. Lane *, ♥S. Yamamoto, ♦J. Heiny and ♥A. Yatani)) ♥Dept. of Pharmacol., ♦Dept. of Physiol. and *Dept. of Medicine (Pulmonary), Univ. of Cincinnati, Cincinnati, OH 45267.

The transient outward K^+ current (I_{to}) plays an important role in the function of cardiac cells and is regulated by neurotransmitters and second messengers through G-protein coupled receptors. To study the regulation of this channel in a system suitable for biophysical and biochemical analysis, we stably transfected Chinese hamster fibroblast (CHW) cells with a K^+ channel cDNA cloned from rat heart (Kv1.4) and determined the electrophysiological properties. Untransfected CHW cells showed no endogenous I_{to} under whole-cell clamp conditions. Cells transfected with Kv1.4 exhibited a voltage-dependent, 4-aminopyridine-sensitive current with characteristics similar to cardiac I_{to}. Cell-attached patches revealed a single-channel conductance of ≈10 pS, and yielded ensembles showing rapid activation and inactivation. The addition of divalent cations blocked the current. The rank order of IC_{50} values was $Zn^{2+} < Ni^{2+} \cong Cd^{2+} << Ba^{2+} \cong Mn^{2+}$. The voltage-dependence of activation and inactivation was shifted to positive potentials by these ions. Preliminary data show that external application of phorbol ester reduced the expressed I_{to}. Compared to the oocyte expression system, this cell line has cellular components that more closely resemble native myocytes (Masaki et al., 1994) and will be a useful cell model for studying the cellular processes involved in the regulation of this channel. (Supported by NSFCAA and AHA93012860).

M-Pos218

PI1 A NEW SCORPION TOXIN AGAINST K^+ CHANNELS. BLOCK OF *SHAKER* B K^+ CHANNELS.

((F. Gómez-Lagunas., Olamendi-Portugal, T., and L. D. Possani)) IBT, UNAM. Cuernavaca, Mor. 62210 Mexico. Financed by DGAPA IN206994 (Spon by M. Hiriart)

Scorpion toxins against K^+ channels are known to be built around a common scheme: they are short (32 to 39 aminoacids) basic peptides, cross-linked by 3 disulfide bridges.

We have isolated a novel peptide (Pi1), from the venom of the scorpion *Pandinus imperator*, whose structure departs from the classical scheme: 35 aminoacids, cross-linked by 4 disulfide bridges. Pi1 added to the external solution blocks *Shaker* B K^+ channels, under whole-cell patch clamp. The extent of block does not depends on the voltage. Pi1 binds to the channels with a 1:1 stoichiometry with a Kd of 62 nM in 0 K^+ (Na^+ external solution). Pi1 block is quite insensitive to the external pH (5.5 to 8.1), but it is strongly reduced by the addition of K^+, Rb^+, and Cs^+, with an order of potency: $Cs^+ > K^+ \sim Rb^+ >> NH_4^+ \sim Na^+$. This sequence is different from the one at site 449 (T^{449}), regarding the C-type inactivation of the channels. Therefore this suggests that another residue plays a critical role for the binding of this new toxin.

M-Pos219

COASSEMBLY OF SYNTHETIC PEPTIDES CORRESPONDING TO TRANSMEMBRANE DOMAINS OF THE SHAKER K^+ CHANNEL.

((1Hadas Peled, 2Isaiah T. Arkin, 2Donald M. Engelman and 1Yechiel Shai)). 1Department of Membrane Research and Biophysics, Weizmann Institute of Science, Rehovot, 76100 Israel, and 2Department of Molecular Biophysics & Biochemistry, Yale University School of Medicine, New Haven, CT, 06510, U.S.A. (Spon. by K. Rosenheck)

Interactions between membrane-embedded segments of integral proteins are receiving a growing amount of attention. Such interactions are likely to contribute to the folding and oligomerization of integral proteins, and can vary in their degree of specificity. We have used synthetic peptides corresponding to the S2, S3, and S4 segments from the hydrophobic core of the *Shaker* potassium channel to study mutual interactions between membrane-embedded segments. Secondary structure measurements revealed that the predicted helical S2, S3 and S4 segments indeed contain different percentages of α-helical structure. The peptides bind strongly to zwitterionic phospholipids, with partition coefficients in the order of 10^4 M^{-1}-10^5 M^{-1}. ATR-FTIR studies showed that while the S4 peptide is oriented parallel to the membrane surface, S3 tends to a more transmembranal orientation. The ability of the peptides to interact with each other was assessed by RET studies in high lipid/peptide molar ratios. Although neither S3 nor S4 are able to self assemble, they can coassemble with the S2 segment and with each other. Furthermore, S3 does not interact with the homologous S4 region from the first repeat of the eel sodium channel, demonstrating specificity in the interactions. These results are in line with data indicating that functionally important interactions exist between the negatively charged S2 and S3 regions and the positively charged S4 region [Papazian et al., (1995) *Neuron 14*, 1293-1301].

M-Pos220

MUTATIONS IN THE S6 SEGMENT OF SHAKER CHANNELS ALLOW SODIUM PERMEATION IN THE ABSENCE OF POTASSIUM

((E.M. Ogielska, and R. W. Aldrich)). Dept. of Mol. and Cell Physiol., HHMI, Stanford University School of Medicine, Stanford CA 94305

Under physiological conditions potassium channels are extraordinarily selective for potassium regardless of the other ions present. In the absence of potassium the Kv2.1 channel, but not Kv1.5, is able to conduct sodium ions appreciably (Ikeda & Korn, Science 269,410-412,1995). The Shaker channel, like its homologue Kv1.5, allows for little if any Na^+ permeation under these ionic conditions. Simultaneously mutating three amino acids in the sixth membrane spanning region (S6) of Shaker to their corresponding residues from Kv2.1 allows for Na^+ permeation in the Shaker channel upon the removal of all K^+. The activation gating of the S460G:A463C:T469V mutant is not significantly different from wild-type under physiological conditions although the mutations do greatly slow the C-type inactivation process. Unlike wild-type, the mutant channel conducts significant Na^+ current in the absence of K^+. In equimolar Na^+ solutions the channel conducts current outward more efficiently than inward. Maximal outward currents are observed with external NMG^+ and internal Na^+. When Na^+ is the charge carrying species the activation range of the channel is shifted to more positive voltages and the deactivation kinetics are altered. The observed currents in the S460G:A463C:T469V mutant are blocked by nanomolar concentrations of Agitoxin (kindly provided by S. Aggarwal). Agitoxin is a specific blocker of Shaker channels indicating that the observed currents must be due to Na^+ conduction through the Shaker potassium channels. We plan to determine whether a subset of these mutations could account for the observed permeation changes.

M-Pos221

Channels from purified mouce Kv1.3 K^+ channel protein reconstituted in lipid bilayers have most of the biophysical properties found *in vivo*.

((Yuri Sokolov, Robert Spencer*, Bruce Takenaka, K. George Chandy and James E. Hall.)) Departments of Physiology and Microbiology & Molecular Genetics, UC Irvine, Irvine CA 92717.

Kv1.3 potassium channel protein was overexpressed in mammalian cells using a *vaccinia* virus system, purified to homogeneity using column chromatography (Biophys. J A343, 1994) and reconstituted into small unilamellar vesicles. These protein-containing vesicles were fused with planar lipid bilayers resulting in appearance of single-channel currents under standard voltage-clamp conditions. The voltage dependence of the reconstituted channels, which turn on at hyperpolarizing voltages and inactivate at depolarizing voltages, suggested that external side of the channel was located on the side of bilayer to which vesicles were added. The reversal potential measured in asymmetric solutions demonstrated high selectivity of the channel for K^+ over Na^+. Two peptide toxins, margatoxin and stichodactyla toxin, that bind to Kv1.3 with high affinity, blocked reconstituted channels at nanomolar concentrations. These results suggest that reconstituted Kv1.3 protein retains most of its important biophysical characteristics following the purification procedure. (Supported by grants from Pfizer, Inc).

M-Pos222

CHANGES IN INTRACELLULAR FREE CALCIUM AND ACTIVATION OF CALCIUM-ACTIVATED K^+ CHANNELS INDUCED BY ACETYLCHOLINE APPLICATION AT THE ENDPLATE OF ISOLATED MOUSE SKELETAL MUSCLE FIBERS.

((B. Allard, J.C. Bernengo*, O. Rougier and V. Jacquemond)). Physiologie des Eléments Excitables, CNRS URA 180, Université Claude Bernard Lyon I, Villeurbanne, France. *INSERM U.121, Bron, France.

Calcium entry through the endplate nicotinic receptors can produce intracellular calcium signals, the role of which has been questioned. Experiments were performed on enzymatically isolated skeletal muscle fibers to investigate the effects of applying acetylcholine (ACh) onto the endplate area, on intracellular free calcium [Ca^{++}], measured using the indicator indo-1 (fluorescence was detected from a 40 μm portion of fiber), and single channel activity using the patch clamp technique. With a 140 mM KCl, 2.5 mM $CaCl_2$ containing solution as extracellular medium, ACh (0.1 mM, 1s) induced a slow transient rise in [Ca^{++}], from a mean (± s.e.m.) resting value of 55 ± 10 nM to 220 ± 20 nM (n=33 from 16 cells). Using the same extracellular solution, in cell-attached membrane patches on the endplate membrane (with Tyrode in the pipette), application of ACh (0.1 mM) induced reversible opening of channels carrying an outward current of about 4.5 pA amplitude at 0 mV. These channels were suspected to be Ca-activated potassium (KCa) channels on the basis of (i) their high single channel conductance which was similar to the one observed in excised patches (220 pS with symmetrical [K^+]), and (ii) on the basis of the dependence of their activity upon the presence of calcium at the cytoplamic membrane face after patch excision. In inside-out patches at 0 mV, the channels presented a half-maximum activation when internal [Ca^{++}] was close to 3 μM. The channels showed a typical voltage-dependence characterized by an increase in the channel activity at depolarized membrane potentials. In outside-out patches these channels were fully blocked by bath application of 0.1 μM charybdotoxin. These results suggest that the inward flux of calcium due to the opening of the endplate nicotinic receptors could give rise to a high enough local increase of the subsarcolemmal [Ca^{++}] to activate the KCa channels.

M-Pos223

DIFFERENTIAL EFFECT OF VOLTAGE ON THE OPEN CHANNEL CONDUCTANCE LEVEL AND THE Ba^{2+}-INDUCED SUBCONDUCTANCE LEVEL IN CA^{2+}-ACTIVATED K^+ (BK) CHANNELS FROM RAT SKELETAL MUSCLE. ((R. A. Bello and K. L. Magleby)) Department of Physiology and Biophysics, University of Miami School of Medicine, Miami, FL 33101-6430.

Ba^{2+} can block the passage of K^+ through BK channels with high affinity (K_d=1 μM) by binding in the pore of the channel (Vergara and Latorre, 1983). After a mean block of 1-5 seconds the channel becomes unblocked and the current either proceeds to the full open channel level or to a subconductance level (Ferguson *et al.*, 1994). To investigate the voltage dependence of the conductance of the sub-level and full open level, outward single-channel currents were recorded from BK channels in excised inside-out patches of muscle membrane held at +10 mV to +90 mV. The pipette contained 150 mM NMDG and the internal solution contained 500 mM KCl and 10 μM Ba^{2+}. Both solutions contained 5 mM TES (pH=7.0). High Ca^{2+}_i (100 μM) maintained a high open probability so that the majority of long shut intervals could be identified as Ba^{2+} blocks. The relative conductance of the subconductance level with respect to that of the full open conductance level did not remain constant over the range of potentials tested. At +10 mV (inside positive) the subconductance current was 24 ± 2% that of the full open current, whereas at +90 mV the subconductance current was 40 ± 1% that of the full open current. A linear fit of data from five experiments gave a relative change in the conductance of the subconductance level with respect to that of the full conductance level of 0.17% per millivolt. Thus, voltage has a differential effect on the conductance of the two states. Possible mechanisms for the shift in relative conductance with voltage include differential effects on the rectification properties, the shape of the pore/vestibule, or the ionic environment near the mouth of the channel during the two states. Supported by grants from the NIH and Muscular Dystrophy Association to K.L.M.

M-Pos224

THE DEPENDENCE OF RECOVERY FROM INACTIVATION OF BK CHANNELS IN RAT CHROMAFFIN CELLS ON CALCIUM AND VOLTAGE (J.P. Ding, C.R. Solaro, C.J.Lingle#)) Dept. of Anesthesiology, #Dept. of Anatomy and Neurobiology, Washington University School of Medicine, St. Louis, MO 63110.

Most rat chromaffin cells express inactivating Ca^{2+} and voltage-dependent BK channels [Solaro et al., (1995) J. Neurosci. 15:6110]. Inactivation is favored by channel opening and is removed by brief cytosolic applications of trypsin [Solaro & Lingle, (1992), Science 257:1694]. Using both ensemble currents generated from excised patches and macroscopic currents recorded from cells dialyzed with defined $[Ca^{2+}]_i$, we have examined the dependence of recovery from inactivation on $[Ca^{2+}]_i$ and recovery potential. Recovery from inactivation is described by two exponential components [τ_{fast} (~60%) ~5-25 ms; τ_{slow} ~ 150-400 ms] over $[Ca^{2+}]_i$ from 1 to 20 μM and recovery potentials from -40 to -100 mV. The duration of the inactivating command step (to +90 mV) has no effect on the relative amplitude or rates of the two recovery components. More elevated $[Ca^{2+}]_i$ and more positive recovery potentials decrease the rates of both fast and slow components of recovery with no effect on their relative amplitudes. Slowing of recovery from inactivation at more elevated $[Ca^{2+}]_i$ and more positive recovery potentials may reflect the Ca^{2+}- and voltage-dependent reopening and subsequent reinactivation of channels following an initial recovery from inactivation.

M-Pos225

APPROXIMATELY 10-20% OF BK CHANNELS IN RAT CHROMAFFIN CELLS ARE MAXIMALLY ACTIVATED DURING SHORT CA^{2+} INFLUX STEPS ((M. Prakriya, T. Kerwin, and C.J. Lingle)) Department. of Anesthesiology, Washington University School of Medicine, St. Louis, MO 63110.

BK channels in rat chromaffin cells were used to assay submembrane Ca^{2+} elevations arising from Ca^{2+} influx through voltage-gated Ca^{2+} channels. During short (5 ms) depolarizations to -9 mV, it was found that while most of the BK channels in the cell are not activated at all, 10-20% of the BK channels are driven to maximal open probabilities. Fractional activation of BK current at various voltages and $[Ca^{2+}]_i$ was determined to estimate the $[Ca^{2+}]_i$ seen by these BK channels. The results indicate that BK channels maximally activated during Ca^{2+} influx are exposed to $[Ca^{2+}]_i$ of at least 60 μM. Simulations were performed to test if random arrangement of BK and Ca^{2+} channels in the cell membrane could account for the high $[Ca^{2+}]_i$ seen by some BK channels. We varied the numbers of BK and Ca^{2+} channels, and, based on assumptions of single-channel Ca^{2+} current and cell buffering characteristics, determined the $[Ca^{2+}]_i$ seen by BK channels. Simulations to date suggest that random distribution of BK and Ca^{2+} channels may be insufficient to account for 10-20% of BK channels detecting $[Ca^{2+}]_i$ of 60 μM or higher.

M-Pos226

Grouped Calcium Titration Curves: Gating Components of the Calcium-activated K^+ Channels May Be Heterotetramerous. ((Jin V. Wu, Trevor J. Shuttleworth, and Per Stampe)) Dept. of Physiology, Univ. of Rochester School of Medicine, Rochester, NY 14642-8642.

Calcium-activated potassium channels (maxi K^+ channels) were isolated from avian nasal salt gland cells and reconstituted into lipid bilayers. Characterizing this 266 pS channel, we find that it is discretely blocked by nanomolar concentrations of charybdotoxin from the external side and by micromolar concentrations of Ba^{2+} from the cytosolic side. Tetraethylammonium (TEA) blocks the channel from either side of the membrane. The fast blocking events by TEA are seen as an apparent reduction of the unitary currents. Calculated from the residual current in the presence of the blocker, the TEA binding affinity is 0.16 mM for the external blockade and 37 mM for the internal blockade. The overall properties of this channel resemble those of maxi K^+ channels found in other epithelia. The calcium sensitivity of the channel is variable from channel to channel over a wide range of concentrations from 1 to 1000 μM. By plotting all 28 titration curves in one graph, we find that they are grouped into five clusters, and that the probability distribution of the clusters matches a binomial distribution. The titration curves distributed in this fashion suggest that the gating components and the calcium binding sites of the maxi K^+ channels are heterotetramerous and this may result from the random mixing of two different subunits, one with high and another with low calcium sensitivity.

M-Pos227

MULTI-ION BARIUM BLOCKADE OF A MAXI K^+ CHANNEL FROM HUMAN VAS DEFERENS EPITHELIAL CELLS. ((Y.Sohma, A.Harris*, C.J.C.Wardle*, B.E.Argent, M.A.Gray)) Dept Physiol. Sci., Univ. Med. Sch., Newcastle upon Tyne NE2 4HH, U.K.; *Inst. Mole. Med., John Radcliffe Hosp., Oxford OX3 9DU, U.K.

Our previous experiments have shown that the maxi-K^+ channel from human vas deferens epithelial cells has at least two Ba^{2+} binding sites accessible from the extracellular side; a "flickering" binding site located deep within the channel pore and a "slow" site located close to extracellular mouth of the pore (Biophys.J.66(2):A329,1994). However this two-site model couldn't explain the unusual voltage-dependence of the "slow" blockade, which showed both voltage-dependent and independent properties. In order to clarify this we have compared the properties of slow Ba^{2+} blockade from the cytoplasmic surface to the slow block from the extracellular side. The characteristics of cytoplasmic Ba^{2+} blockade were basically consistent with those of other maxi-K^+ channels, although on careful analysis we did observe a fast flickering blockade, in addition to the characteristic slow form of block. However, using conditions where the slow extracellular site is occupied by K^+, cytoplasmic Ba^{2+} still caused slow block. This implies that the cytoplasmic Ba^{2+} binding site is not identical to the "slow" extracellular Ba^{2+} site, and suggests that a "third" Ba^{2+} site is involved. We have incorporated this information into a model consisting of a 4-state cyclic equilibrium of Ba^{2+} binding to a open channel. This model includes two single occupancy Ba^{2+} sites, connected to a double occupancy state. The voltage-dependent slow form of block is only observed when both sites are occupied, since the Ba^{2+} dissociation rate is decreased under double occupancy.

M-Pos228

CALCIUM ACTIVATED POTASSIUM CHANNELS IN HUMAN BLADDER TUMOR CELLS. ((Scott H. Monen and Robert Wondergem)) Department of Physiology, Quillen College of Medicine, East Tennessee State University, Johnson City, TN 37614-0576.

HTB-9 cells derive from a human bladder carcinoma, and various K^+ channel blockers inhibit their growth in vitro (Schmidt, et al., J. Gen. Physiol. *105*: 39a, 1995). The aim of this study was to determine whether intracellular Ca^{2+} activates an outward K^+ current. HTB-9 cells (ATCC) were superfused at room temperature with external medium in which gluconate was substituted for Cl^-. Fire polished micropipettes were filled with either external medium or an internal medium with the same anion substitution. Giga seals of micropipette to plasma membrane were obtained in non-mitotic cells, and currents were measured in either the whole-cell clamp, the inside-out patch, or the outside-out patch mode. Whole-cell outward currents of cells dialyzed with 0.01 μM Ca^{2+} were activated by depolarization, and the specific conductance ranged from 0.57 ± 0.13 nS/pF at -70 mV holding potential to 3.10 ± 0.15 nS/pF at 30 mV holding potential. In contrast, activation of outward current by depolarization did not occur in cells dialyzed with medium containing 11 mM EGTA and no added Ca^{2+}. This Ca^{2+}- and voltage-dependent outward conductance was inhibited completely by 50 nM iberiotoxin (IbTx) added to the bath, and inhibited two-thirds by 50 nM charybdotoxin (ChTx) added to the bath. Voltage ramps from -100 to 60 mV (pipette potential) were applied to inside-out patches to determine a K^+ channel conductance of 214 ± 3.9 pS. Channel open probability (P_o) increased together with $[Ca^{2+}] \geq 1$ μM and with membrane depolarization beginning at 20 mV (pipette potential). Positive pipette potentials evoked channel activity in outside-out patches. This was inhibited by either IbTx or ChTx, and the activity returned after washout. We conclude that the predominant outward current in HTB-9 cells results from voltage- & Ca^{2+}-dependent maxi-K channels. SHM supported by a TN-SBR scholarship.

M-Pos229

HETEROLOGOUS SUBUNITS OF DSLO CHANNELS INDENTIFIED BY AN INTERACTIVE TRAP GENETIC SCREEN. ((X.M. Xia, M. Forte, S. Smolik, M. Kohler, A. Lagrutta, J.P Adelman)) Vollum Institute, Oregon Health Science University, Portland, OR 97201.

Drosophila and mammalian BK channels (*Slo* channels) are formed by the association of four alpha subunits, encoded by a single genetic locus, and functional diversity is generated at least in part, by alternative splicing of one primary transcript. A second, beta subunit has been identified in mammalian organisms and coexpression studies demonstrate that the presence of the beta subunit shifts the calcium dose-response to lower concentrations. However, no beta subunits have yet been identified from *Drosophila*. We employed a genetic screen in yeast, the interactive trap, to search for heterologous proteins which touch the alpha subunit of d*Slo* channels. The constant region within the C-terminal domain of d*Slo* was used as 'bait' (amino acids 665-1164) to screen for 'prey' within a *Drosophila* head cDNA library. Three distinct clones have been identified which pass all primary and secondary genetic tests. Database searches and sequence analyses demonstrates that these clones are novel, and without obvious homology to known proteins. Using salivary chromosome squashes, one clone (2H6) was mapped to region 102C-D on the fourth chromosome. In situ hybridizations using d*Slo* and Y2H6 demonstrate that Y2H6 mRNA is present in every cell which expresses d*Slo* mRNA, and that both mRNAs are expressed throughout the *Drosophila* nervous system. In addition, several splice variants of Y2H6 have been identified. Biochemical analyses and functional coexpression studies will be presented. These results indicate that native d*Slo* channel complexes may contain several heterologous proteins.

M-Pos230

TRANSFORMATION OF *hSlo* BK (Maxi-K) CHANNEL CHARACTERISTICS BY CO-EXPRESSION OF A HUMAN β-SUBUNIT. ((V.K. Gribkoff, C.G. Boissard, J.T. Lum-Ragan, M.C. McKay, D.J. Post-Munson, J.T. Trojnacki and S.I. Dworetzky)) Central Nervous System Drug Discovery, Bristol-Myers Squibb Company, 5 Research Parkway, Wallingford, Connecticut 06492

Expression of the human (*hSlo*) large-conductance Ca^{2+}-activated K^+ (BK or maxi-K) channel in *Xenopus* oocytes or HEK 293 cells produced rapidly-activating channels that were very sensitive to the peptidyl BK blocker iberiotoxin (IbTX). In addition, BK currents were relatively insensitive to the alkaloidal BK blocker tetrandrine, and P_{open} was increased by application of the catalytic subunit of cyclic AMP-dependent protein kinase (PKA). We recently cloned a human BK ß-subunit, and co-expressed this construct with *hSlo* channels. Several characteristics of the resultant channels (*hSlo*-ß) and whole-cell currents were altered. The activation kinetics of *hSlo*-ß was significantly slower than *hSlo*; this was observed in whole-cell currents and ensemble average currents. In addition, the sensitivity of *hSlo*-ß currents to IbTX was greatly reduced; the potency of the peptide was reduced, but the efficacy was unchanged. Tetrandrine was much more potent on *hSlo*-ß mediated currents, and exacerbated the slower activation kinetics. A majority of *hSlo*-ß channels tested were insensitive to PKA. Previous data, obtained using mouse BK channels co-expressed with the bovine ß-subunit, demonstrated an increase in Ca^{2+} sensitivity. Our results, obtained using human constructs, suggest additional effects of co-expression. Native BK channels in neurons have been previously grouped into Type I and Type II BK channels based on their blocker sensitivities, kinetics, and their response to phosphorylation. Type I BK channels are fast-activating, IbTX-sensitive, and activated by cAMP-dependent protein phosphorylation, while Type II BK channels are slow-activating, IbTX-insensitive, tetrandrine-sensitive, and not activated or inactivated by PKA-dependent protein phosphorylation. These results suggest that one factor which may contribute to these phenotypic archetypes is the presence or absence of the regulatory ß-subunit.

M-Pos231

CHARGE MOVEMENT IN A VOLTAGE AND Ca^{2+} SENSITIVE POTASSIUM CHANNEL (*hSlo*). ((M. Ottolia, F. Noceti, R. Olcese, M. Wallner, R. Latorre, E. Stefani and L. Toro)) Dept. of Anesthesiology, UCLA, Los Angeles , CA 90095-1778 and CECS, Chile.

A voltage- and Ca^{2+}- sensitive potassium channel cloned from human myometrium (*hslo*) was expressed alone and in combination with the β subunit in *Xenopus* oocytes. To achieve high expression levels necessary to detect gating currents, we have modified the 5' untranslated region of *hslo*. The electrical properties of the channel protein were characterized using giant patches and the cut-open oocyte techniques. Ionic current was recorded in isotonic K-MES, while gating currents were isolated using TEA-MES or NMG-MES in presence of 100 µM ouabain. Gating currents were recorded as fast transient currents at the beginning and end of voltage pulses. They were not detected in control oocytes and their size correlated with the expression level of *hslo* ionic currents. As expected for charge movement, the same amount of charge moved at the ON and the OFF of voltage pulses. Moreover, their time course of decay was slowed down by lowering the temperature. Both ionic currents and charge movement had a similar voltage range for activation, but gating currents preceded in time the activation of ionic currents. The position in the voltage axis of the conductance (G-V) and charge (Q-V) to voltage relationships was shifted to more negative potentials by raising internal Ca^{2+}. The small separation between Q-V and G-V curves in *hslo* is in contrast with other voltage dependent K^+ channels, and suggests that a large part of the charge moves in transitions close to the open states. In addition, when depolarizing pulses were delivered from very negative holding potentials, the ionic current activation had a brief but clear time delay. In agreement with the presence of few closed states preceding channel opening , this delay was shortened with short depolarizing prepulses. Supported by HL54970 and GM52203 grants.

M-Pos232

GENOMIC ANALYSIS OF THE HUMAN BETA SUBUNIT OF THE MAXI K_{Ca} CHANNEL COMPLEX. ((Z. Jiang, Wallner, M., Meera, P., and L. Toro)). Dept. of Anesthesiology. UCLA, Los Angeles, CA 90095-1778.

We have cloned the human homologue of the bovine β subunit (Knaus *et al, JBC*, 269:17274, 1994) from a cDNA library of human uterus (GenBank U25138). The human β subunit modulates the human pore-forming α subunit (*hslo*) in a similar manner as the one previously isolated from bovine trachea (Wallner et al., Receptors and Channels, in press). The β subunit increases the apparent Ca^{2+} sensitivity of the α subunit and makes *hslo* susceptible of regulation by dehydrosoyasaponin I. Northern blot analysis was performed in RNA isolated from human tissues. Strong signals were obtained in smooth muscle (uterus, small intestine, colon). The β subunit RNA was also present in considerable amounts in lung, prostate, testis, and ovary. Consistent with a low calcium sensitivity of skeletal muscle K_{Ca} channels, skeletal muscle RNA gave a weak signal. Other tissues showing weak signals were: brain cortex, cerebellum, thalamus, kidney, pancreas, spleen, thymus, and leukocytes. Interestingly, human ventricle and atrium total RNA gave strong signals when probed with the β subunit. We have previously shown that the α subunit RNA seems to be absent in rat heart consistent with electrophysiological studies showing that maxi K_{Ca} channels are not detectable in this tissue. Thus, it is possible that the β subunit modulates other K channels. We have isolated genomic DNA from a human placenta λ phage library, and identified four exons spanning a region of about 11 kb. The first exon consists of 5'-untranslated region of the β gene. The second and fourth exons encode the two putative transmembrane regions. The fourth exon also encodes for part of the putative extracellular loop and the 3'-untranslated region. The size of exons 1-3 is about 160 bp, whereas exon 4 is about 800 bp. The isolation of the β gene will be useful to study the regulation of expression of this modulatory protein. Supported by NIH HL54970.

M-Pos233

MUTATION R207Q IN THE S4 SEGMENT INCREASES Ca^{2+} SENSITIVITY OF A CLONED MAXI K^+ CHANNEL (*hslo*). ((L.F. Diaz, M. Wallner, E. Stefani, L. Toro, and R. Latorre)). Univ. of Chile, CECS, Santiago, Chile and Dept. of Anesthesiology, UCLA Sch.of Med., Los Angeles, CA 90095-1778.

At difference from other voltage-dependent channels, the S4 segment of h*slo* channels contains four basic and one negatively charged residues. In voltage-dependent channels the S4 domain has been postulated to be the voltage sensor. Mutations of positively charged residues within S4 alter gating of Na^+ and *Shaker*-type K^+ channels. Here, we examine the contribution of individual charged residues to the voltage-dependence and Ca^{2+} sensitivity of h*slo* channels. In order to accomplish this goal we have mutated an arginine at position 207 to glutamine (R207Q) and the glutamate 219 to glutamine (E219Q). R207 is equivalent to R368 in *Shaker*-type K^+ channels. Neutralization of R368 in *Shaker*-type K^+ channels induces a large reduction of the limiting gating valence (z_g) of the channel (Papazian et al. 1991. *Nature* **349**:305). The R207Q mutation causes a large shift of the conductance-voltage (g-V) curve to the left along the voltage axis. In cell-attached patches, wild-type h*slo* g-V curve can be fitted by a single Boltzmann distribution with a $V_{0.5}$ ~ 200 mV and an apparent gating valence z = 1.76. In contrast, the g-V of the R207Q mutant is well described with a $V_{0.5}$ = 7.5 mV and a z = 0.92. However, at very low values of activation ($P_o < 0.001$), z_g is similar for both the wild-type and the R207Q mutant (z_g = 3-4). The mutation E219Q induces K^+ currents with Ca^{2+}- and voltage dependencies almost identical to that of wild-type h*slo* channels. We conclude that R207Q mutant dramatically increases the Ca^{2+} sensitivity with minor effects on the limiting gating valence of the channel and that E219 residue does not play a functional role in h*slo* channel activation. Supported by NIH HL 54970, GM 52203 and FNI 2950028 and 94-0227 grants.

M-Pos234

THE ACTIVITY OF LARGE CONDUCTANCE, Ca^{++}-ACTIVATED K^+ CHANNELS (*mslo* AND *dslo*) EXPRESSED IN *XENOPUS* OOCYTES IS INCREASED BY ETHANOL. ((Alejandro M. Dopico, Vellareddy Anantharam and Steven N. Treistman)) Dept. Pharmacol. & Mol. Toxicol., UMass. Med. Sch., Worcester, MA 01655.

We previously reported that 10-100 mM ethanol (EtOH) activates large conductance, Ca^{++}-activated K^+ (BK) channels in both neurohypophysial terminals and PC12 cells. To establish functional-structural relationships, we studied the effects of EtOH on the activity (NPo) of mouse (*mslo*) and *Drosophila* (*dslo*) cloned BK channels expressed in *Xenopus* oocytes. These clones possess a "core" domain, underlying ion permeation and voltage sensitivity and a "tail" domain, underlying Ca^{++}-sensitivity. EtOH (10-200 mM) reversibly increased NPo of both *mslo* and *dslo* channels when applied to the cytosolic surface of inside-out patches, plateauing at 100-200 mM. Activation was due to EtOH-induced changes in channel gating. The unitary conductance (245 and 209 pS, *mslo* and *dslo*) and the zero current potential (0 mV) in symmetric 145 mM K^+, and the voltage-sensitivity of the channel (21 mV and 28 mV per e-fold change in NPo, *mslo* and *dslo*) were unchanged by EtOH. These data indicate that EtOH does not alter functions associated with the core domain. EtOH decreased the Ca^{++}-sensitivity of *mslo* channels, probably reflecting an interaction with the tail domain. This interaction, however, would not explain the activation of the channel by EtOH. Support: ABMRF grant (AMD) and NIH grant AA08003 (SNT).

M-Pos235

FUNCTIONAL ANALYSIS OF THE C-TERMINUS OF THE HUMAN BK CHANNEL. ((T.D. Tsai, L.S. Wood and G. Vogeli)) Cardiovascular Pharmacology, The Upjohn Company, Kalamazoo, MI 49001.

To test the function of the cytoplasmic C-terminus of the human BK channel (hBK), we deleted 170 aa beyond transmembrane segment 10. A large outward K^+ current was recorded at +80 mV from *Xenopus* oocytes two days after the injection of cRNA (66.7 ± 6.6 μA ,n=4 with 22 ng cRNA or 35.3 ± 2.7 μA ,n=2 with 2 ng of cRNA). Iberiotoxin blocked the current in the nM range. At 10 nM and +80 mV, the current was 89.6 ± 1.3% (n=2) and with 100 nM it was 36.4 ± 0.8% (n=4) of the current in ND96 alone. NS004 increased the current in the μM range. At 50 μM and +60 mV, it was 153.0 ± 7.3% (n=2) of the control value. To change the intracellular Ca^{2+} concentration we treated the oocyte with the divalent cation ionophore A23187 (5 μM). With 5 mM Ca^{2+} in the ND96 bath solution, the current increased almost 6 fold (5.7 ± 0.4, n=3) at +20 mV compared to the current in Ca^{2+} free ND96. All above-mentioned effects could be washed out easily. In conclusion, our results show that the last 170 aa of hBK are not responsible for the action of IBTX, NS004, nor for the Ca^{2+} sensitivity of hBK.

M-Pos236

Using Green Fluorescent Protein (GFP) as a Reporter Gene for Expression of Recombinant Maxi-K^+ Channels in a Mammalian Cell Line ((Michael Myers and Per Stampe)) Department of Physiology, University of Rochester School of Medicine and Dentistry, Rochester, NY 14642-8642.

Complementary RNAs (cRNAs), transcribed from a complex mouse gene, *mSlo*, have been shown to encode a calcium-activated potassium channel (maxi-K^+ channel) when injected into *Xenopus* oocytes. We have studied the Ca^{2+} activation, Ba^{2+} block and CTX block of *mSlo* channels expressed in a mammalian cell line, COS-7, and reconstituted into lipid bilayers. A plasmid probe was constructed using the jellyfish green fluorescent protein (GFP) as a reporter gene to estimate the relative levels of *mSlo* expression. This probe facilitates optimized expression of channels. When GFP is expressed alone in our cloning vehicle pMT3, or in combination (coexpressed) with *mSlo* in pMT3, COS-7 cells fluoresce ten-fold above background. Construction of a second, chimeric GFP probe containing the cloning vehicle, GFP, as well as *mSlo*, has further optimized expression. Transfection levels as high as 50% have been achieved using the optimized conditions and has resulted in recordings of functional maxi-K^+ channels. The chimeric GFP probe will be refined to create a fusion protein representing a "tagged" channel. These fluorescent probes may prove to be a powerful tool in the study of ion channel expression, localization, and processing.

CHANNELS: TOXINS, PEPTIDES

M-Pos237

KINETICS OF FLUORESCENCE QUENCHING OF FITC-C9 UPON ASSEMBLY IN MEMBRANE ATTACK COMPLEX REPORTS MEMBRANE INSERTION.((J.F. McDonald and G.L. Nelsestuen)) Dept. of Biochemistry, U. of Minnesota, St. Paul, MN 55108.

Complement C9 labeled with fluorescein isothiocyanate (FITC-C9) exhibited fluorescence quenching upon assembly in the membrane attack complex (MAC) with phospholipid vesicles. Stopped-flow kinetics of this event at 25 ° C revealed single exponential kinetics that was consistent with the reporting of a rate-limiting transition ($k = 0.11\ sec^{-1}$) following rapid association. Temperature dependence of the rate constant resulted in determination of an activation energy (32 kcal/mole) that corresponded well with previous values determined by the rate of C9 polymerization and by hemolysis. Fluid phase assembly (ie. in the absence of membranes) resulted in a 3-fold lower rate ($k = 0.033\ sec^{-1}$), indicating phospholipid interactions can promote the membrane insertion of C9. The positional dependence of FITC-C9 assembly in the MAC was examined with preassembled unlabeled C9 polymers. Assembly of FITC-C9 with a complex containing one preassembled C9 molecule occurred at a rate greater than twice that observed for its assembly as the first subunit ($k = 0.26\ sec^{-1}$), and exhibited a lower activation energy (24 kcal/mole). As more C9 subunits were inserted, the observed rate of assembly of FITC-C9 was progressively reduced. These results confirmed the sequential nature of the assembly of the C9 polymer. The kinetics of FITC-C9 fluorescence quenching can be used to determine the relationship of membrane composition and structure to cytolytic activity. (Supported in part by grant HL 15728 from NIH).

M-Pos238

CONFORMATIONAL CHANGES IN A. ACTINOMYCETEMCOMITANS LEUKOTOXIN DETECTED BY TRYPTOPHAN FLUORESCENCE ((D.Karakelian, U.G.Furblur, J.D.Lear, E.T.Lally, J.C.Tanaka)) University of Pennsylvania, School of Dental Medicine, Philadelphia, PA 19104

Actinobacillus actinomycetemcomitans (Aa) leukotoxin is a soluble 116 kDa protein which kills susceptible cells by creating large membrane pores. The fluorescence of the five Trp residues in the toxin was used to follow conformational changes upon the addition of Guanidinium HCl (GnHCl), octyl β-D-glucoside, and temperature in order to monitor the stability of the protein. At 30°C, the spectrum shows a characteristic Trp shape with a λmax of ~326 nm (λex of 280 nm). Addition of GnHCl or octylglucoside, or increasing temperature produces changes in the emission spectrum. With each, the spectra initially decrease in intensity with little or no shift in λmax. This behavior is observed between 0.38 and 2 M GnHCl, 0.01 and 0.03 % octylglucoside, and 30 to 65°C. Further increases in GnHCl concentration produce significant spectral changes consistent with the protein unfolding in 7 M GnHCl. Increasing octylglucoside concentration above 0.03% results in a blue-shifted λmax, suggestive of a change in conformation but not necessarily an unfolded state. At 65°C, where the biological activity of Aa toxin irreversibly inactivates, the intensity is ~65% of that at 30°C with little change in λmax. The fluorescence indicates that at least some elements of the toxin molecule structure, in aqueous buffer at 30°C, are readily subject to perturbations by changes in the molecule's environment and may be relevant to the mechanism of toxin insertion into target cell membranes.

M-Pos239

THE INFLUENCE OF STEROL AND PHOSPHOLIPID STRUCTURE ON THE PROPERTIES OF SYRINGOMYCIN E-INDUCED CHANNELS. (L.V. Schagina[1], A.M.Feigin[2], J.Y.Takemoto[3], J.H.Teeter[2,4], J.G.Brand[2,4]) [1]Inst.Cytol.Russ.Acad.Sci., St.Petersburg,Russia; [2]Monell Chem. Senses Ctr, Phila.,PA19104; [3]Utah State Univ., Logan, UT84322; [4]Uv.Penn., Phila, PA19104

We demonstrate that the properties of channels induced by the addition of the lipodepsipeptide antibiotic, syringomycin E (SR) at one (*cis*) side of the bilayer, depend on the structure of phospholipid and sterol that are used to form the bilayer. With DOPC bilayers a change of voltage from positive to negative value resulted neither in an abrupt increase in the single channel conductance nor in a closing of these channels, the typical of membranes formed from DOPS. Also, the conductance of channels induced in DOPC bilayers increased with voltage in any direction (negative or positive), while the channel conductance in DOPS bilayers increased only with an increase in negative voltage. The properties of the channels induced by addition of SR to ergosterol- or cholesterol-containing bilayers formed from DOPS were similar to those observed in sterol-free bilayers (activation and inactivation in a voltage-dependent manner) although the channel conductance at each particular voltage was smaller compared with the conductance of channels induced in sterol-free membranes. The influence of sterols and phospholipids on the channel properties suggests a possibility that sterols and phospholipids directly participate in formation of channels induced by SR.

M-Pos240

VOLTAGE-GATED ION CHANNELS FORMED BY SYRINGOMYCIN E IN PLANAR LIPID BILAYERS (A.M.Feigin[1], J.Y.Takemoto[2], R.Wangspa[2], J.H.Teeter[1,3], and J.G.Brand[1,3]) [1]Monell Chem. Senses Ctr, Phila., PA 19104; [2]Utah State Univ., Logan, UT 84322; [3]Univ. of Pennsylv., Phila , PA19104

We demonstrate that the lipodepsipeptide antibiotic, syringomycin E, forms voltage-sensitive ion channels of weak anion selectivity in planar bilayers made from dioleoylglycerophosphatidylserine. The formation of channels in bilayers doped with syringomycin E at one side (1-40 μg/ml) was greatly affected by *cis*-positive voltage. A change of voltage from a positive to a negative value resulted in 1) an abrupt increase in the single channel conductance (the rate of increase was voltage dependent) simultaneous with 2) a closing of these channels and an exponential decrease in macroscopic conductance over time. The strong voltage dependence of multichannel steady state conductance, the single channel conductance, the rate of opening of channels at positive voltages and closing them at negative voltages, as well as the observed abrupt increase of single channel conductance after voltage sign reversal suggest that the change of the transmembrane field induces a significant rearrangement of syringomycin E channels, including a change in the spacing of charged groups that function as voltage sensors. The conductance induced by syringomycin E increased with the sixth power of syringomycin E concentration suggesting that at least six monomers are required for channel formation.

M-Pos241

***MANDUCA SEXTA* MIDGUT RECEPTORS FOR *BACILLUS THURINGIENSIS (Bt)* TOXINS AFFECT ION CHANNELS FORMED BY THE INSECTICIDAL PROTEINS IN PLANAR LIPID BILAYERS.**

((J.L. Schwartz[1,2], Y.J. Lu[3], P. Soehnlein[1], R. Brousseau[1], L. Masson[1], R. Laprade[2] and M. Adang[3])) [1]BRI, National Research Council, Montreal, [2]GRTM, Université de Montréal, Que, Canada and [3]Department of Entomology, University of Georgia, Athens, GA, USA.

Current work in our laboratory demonstrates that trypsin-activated CryIA(a) (Grochulski *et al.*, J. Mol. Biol., in press), CryIA(c) and CryIC (Schwartz *et al.*, J. Memb. Biol.(1993)132:53-62) toxins partition in planar lipid bilayers (PLBs) in the absence of receptor proteins and at doses in excess of 5μg/ml. Purified, GPI-linked receptor complex isolated from *M. sexta* midguts (Sangadala *et al.*, J. Biol. Chem.(1994)269:10088-10092) were incorporated in liposomes and fused to PLBs. Under these conditions, the three toxins formed channels at much lower doses (20-100 ng/ml) than in a receptor-free system. Channels formed by CryIA(c) in the presence of the receptor complex displayed a rectifying conductance, while CryIA(a) and CryIC exhibited linear current-voltage relations similar to those observed for CryIA(a), CryIA(c) and CryIC incorporated in PLBs at higher doses and without receptor proteins. These results indicate that channel formation is facilitated by receptors incorporated in PLBs and that the channels formed by CryIA(c), the most potent *Bt* toxin against *M. sexta* larvae, possess altered biophysical properties when the protein is bound to its receptor.

M-Pos242

TETANUS TOXIN CHANNELS IN CULTURED NEURONS STUDIED BY THE PATCH-CLAMP TECHNIQUE ((A. Carpaneto, M. Pisciotta and F. Gambale)) CNR-Istituto di Cibernetica e Biofisica, Genova, Italy 16149 (Spon. by C. Frediani)

The effects induced by tetanus toxin (TeTx) on the plasma membrane of the cultured cell line N2A were studied by the patch-clamp technique. It was already shown (Hoch et al., 1985) that TeTx is able to increase the ionic permeability of model membranes by the formation of ion permeable channels. By previous inhibition of endogenous channels present in our cell line, we were able to isolate and identify channels induced by μM TeTx concentrations in neuron membrane-patches. Single channel recordings, obtained in standard physiological solutions at neutral pH, were compared with data recorded in planar lipid bilayers. In both systems (BLM and neuron-patches) TeTx induced single channel openings which were gathered in current bursts and which displayed high frequency transitions between two main states. Noise analysis of single channel traces displayed power spectra presenting a double Lorentzian distribution characterized by cut-off frequencies in the order of 20 and 500 Hz, respectively.

- Hoch DH, Romero-Mira M, Ehrlich A, Finkelstein A, DasGupta BR and Simpson LL. 1985 Proc. Natl. Acad. Sci. USA. 82:1692-1696

M-Pos243

CHARACTERIZATION OF RECOMBINANTLY-EXPRESSED α-BUNGAROTOXIN AND MUTANT ANALYSIS. ((J.A. Rosenthal, B. Chang and E. Hawrot)) Dept. of Molecular Pharmacology and Biotechnology, Division of Biology and Medicine, Brown University, Providence, RI 02912.

In order to study the structural features involved in the macromolecular recognition of protein complexes, we have focused on the interaction of α-bungarotoxin (Bgtx) with the nicotinic acetylcholine receptor (nAChR). We have previously shown the production of recombinantly-expressed Bgtx as a fusion protein containing a 7-residue histidine-tag that allows for rapid purification using nickel affinity chromatography. The toxin is liberated from its fusion partner by thrombin digestion and biologically active fractions are isolated by cation-exchange chromatography. We have been successful in producing ~600 μg of active toxin/L of starting LB shaker culture. Yields can be increased to > 1 mg of active toxin/L of LB culture by utilizing a benchtop fermentor as an alternative to the shaker culture. This toxin has been shown to be fully active through solid-phase competition assays using nAChR-enriched *Torpedo* electric organ membranes. We have further demonstrated that the histidine-tagged recombinant Bgtx (H_2Bgtx) is capable of blocking ACh-evoked currents in both *Xenopus* oocyte-expressed mouse muscle nAChR receptors and in chick α_7 neuronal receptors using voltage-clamp techniques. In both instances the toxin was as effective as native toxin in blocking ACh-evoked responses.

We have now begun investigating which residues within the toxin sequence are involved in functional contacts with the nAChR. Substitution of K26A shows a 10-fold reduction in IC_{50} values compared to that of native toxin in the solid-phase assay. Similarly, only a modest 15-fold decrease in binding is seen with the removal of the last 7 amino acid carboxy-terminal tail representing nearly 10% of the Bgtx sequence. The most dramatic effect was seen when R36 was substituted with alanine resulting in up to a 100-fold reduction in binding. No effect was observed when the two residues Q and R are switched at positions 72 and 73. We are continuing to characterize the mutant proteins and to assess the physiological effects of these mutant toxins on nAChRs heterologously-expressed in oocytes.

(Supported by NIH-GM32629).

M-Pos244

RESISTANCE TO α-BUNGAROTOXIN IN COBRA IS MEDIATED BY A DISCRETE SEGMENT OF THE ACh RECEPTOR α-SUBUNITS. ((Z. TAKACS*, K. WILHELMSEN† & S. SOROTA*)) *Dept of Pharmacology, Columbia Univ, New York, NY 10032, †Dept of Neurology, UCSF, San Francisco, CA, 94110.

Evolution of potent and specific animal toxins required a strategy preventing their actions in the individual producing them. Venoms of the cobra snakes, *Naja* spp., contain α-neurotoxins, such as α-bungarotoxin (α-BTX) targeted against the nicotinic acetylcholine receptor (nAChR). These toxins remain without effect in conspecific neuromuscular preparations. The peptide fragments of the cobra, *N. naja*, ligand binding region do not bind α-neurotoxin *in vitro*. Substituting mouse residue 189 with the corresponding *Naja* residue will lower the affinity for α-BTX in binding assays. The effect of cobra residues on α-BTX interactions with ionic currents through functional nAChR has not been studied. We cloned the ligand binding region of *N. haje* nAChR α subunit and constructed a mouse/154-195cobra chimeric α subunit. The α mouse/cobra chimera and the β, γ and δ wild type mouse cRNAs were coinjected into *Xenopus* oocytes and assayed with two-microelectrode voltage-clamp. The dose-response relationship to ACh of the chimera (EC_{50} 1.4 μM) was similar to the wild type (EC_{50} 2.7 μM) receptor. However, while the wild type receptor (•) was inhibited upon 15 min exposure to α-BTX with an IC_{50} of ~7 nM, the chimera (○) was little affected by 1 μM α-BTX. We conclude that α-neurotoxin resistance in *Naja* is mediated by the presence of a unique sequence in their nAChR α subunit which binds ACh physiologically but prevents its recognition by the toxin.

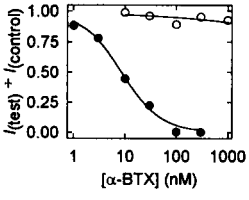

M-Pos245

PHYSICO-CHEMICAL CHARACTERIZATION OF THE ACTION OF THE ANTIMICROBIAL PEPTIDE NISIN WITH LIPOSOMES FROM *LISTERIA MONOCYTOGENES*, A FOODBORNE PATHOGEN ((K. Winkowski, R. D. Ludescher and T. J. Montville)) Department of Food Science, Rutgers-The State University of New Jersey, New Brunswick, NJ 08903-0231

Small cationic amphiphilic antimicrobial peptides are produced by organisms ranging from bacteria to insects, to frogs, to humans. One of these peptides, nisin, is produced by *Lactococcus lactis* and has activity against *Listeria monocytogenes*, a foodborne pathogen that grows at refrigerated temperatures. This study gained mechanistic information about nisin's antilisterial action by examining the efflux of carboxyfluorescein from *Listeria monocytogenes*-derived liposomes. The initial leakage rate (% efflux/min) of the entrapped dye was dependent on both nisin and lipid concentrations. Isotherms for the binding of nisin to liposomes were constructed on the basis of the Langmuir isotherm and gave an apparent binding constant of $6.2 \times 10^2 M^{-1}$ at pH 6.0. The critical number of nisin molecules required to induce efflux from liposomes at pH 6.0 was ≈7000 molecules per liposome. The pH affected the carboxyfluorescein leakage rates, with higher pH values resulting in higher leakage rates. The increased leakage observed at higher pH values was not due to an increase in the binding affinity of the nisin molecules towards the liposomal membrane. Rather, the critical number of nisin molecules required to induce activity was decreased (≈ 1000 nisin molecules/liposome at pH 7.0). These data are consistent with a poration mechanism in which the ionization state of histidine residues in nisin plays an important role in membrane permeabilization.

M-Pos246

AMYLIN INDUCES ION CHANNELS IN PHOSPHOLIPID MEMBRANES. ((Tajib A. Mirzabekov[1], Meng-chin Lin[1], and Bruce L. Kagan[1,2]) [1]Neuropsychiatric Institute of UCLA Medical School and [1,2]West Los Angeles Veterans Administration Medical Center, Los Angeles, CA 90024.

Amylin is a 37-amino acid cytotoxic constituent of amyloid deposits found in the pancreatic islets of Langerhans of patients with type II diabetes. Extracellular accumulation of this peptide results in damage to insulin-producing beta cell membranes and cell death. We report here that amylin forms voltage dependent, relatively nonselective, ion permeable channels (7-8 pS in 10 mM KCl) in planar phospholipid bilayer membranes. At cytotoxic concentrations (1-10 μM) human amylin dramatically (10^3-10^4 times) increased the conductance of bilayer membranes. At identical concentrations non-amyloidogenic and non-cytotoxic rat amylin produced no change in membrane conductance. The amylin-induced conductance showed asymmetric voltage-dependence. It was stable and maximal at negative voltages and turned off at positive voltages. At + 60-70 mV the residual conductance was less than 20-30% of its initial level. The dependence of membrane conductance on the concentration of amylin in the aqueous solution was linear. The channel forming activity of amylin in salt solutions composed of 10 mM KCl was more than 100 times higher than that in 1 M KCl. Amylin, which has net charge of +5, exhibited the highest activity in the negatively charged (40%) membranes (PC/PS/PA = 3/1/1, w/w/w) whereas membranes carrying no net surface charge (DPPC) were only slightly sensitive to amylin. We suggest that channel formation may be the mechanism of cytotoxicity of human amylin.